



National Library
of Canada

Bibliothèque nationale
du Canada

Canadian Theses Service

Services des thèses canadiennes

Ottawa, Canada
K1A 0N4

CANADIAN THESES

NOTICE

The quality of this microfiche is heavily dependent upon the quality of the original thesis submitted for microfilming. Every effort has been made to ensure the highest quality of reproduction possible.

If pages are missing, contact the university which granted the degree.

Some pages may have indistinct print especially if the original pages were typed with a poor typewriter ribbon or if the university sent us an inferior photocopy.

Previously copyrighted materials (journal articles, published tests, etc.) are not filmed.

Reproduction in full or in part of this film is governed by the Canadian Copyright Act, R.S.C. 1970, c. C-30.

**THIS DISSERTATION
HAS BEEN MICROFILMED
EXACTLY AS RECEIVED**

THÈSES CANADIENNES

AVIS

La qualité de cette microfiche dépend grandement de la qualité de la thèse soumise au microfilmage. Nous avons tout fait pour assurer une qualité supérieure de reproduction.

S'il manque des pages, veuillez communiquer avec l'université qui a conféré le grade.

La qualité d'impression de certaines pages peut laisser à désirer, surtout si les pages originales ont été dactylographiées à l'aide d'un ruban usé ou si l'université nous a fait parvenir une photocopie de qualité inférieure.

Les documents qui font déjà l'objet d'un droit d'auteur (articles de revue, examens publiés, etc.) ne sont pas microfilmés.

La reproduction, même partielle, de ce microfilm est soumise à la Loi canadienne sur le droit d'auteur, SRC 1970, c. C-30.

**LA THÈSE A ÉTÉ
MICROFILMÉE TELLE QUE
NOUS L'AVONS REÇUE**

THE UNIVERSITY OF ALBERTA

"PLEISTOCENE VALLEY GLACIER SEDIMENTOLOGY AND STRATIGRAPHY
IN THE BANFF-CANMORE AREA OF ALBERTA, CANADA"

by

(C) GREGORY BYRON MANDRYK

A THESIS

SUBMITTED TO THE FACULTY OF GRADUATE STUDIES AND RESEARCH
IN PARTIAL FULFILMENT OF THE REQUIREMENTS FOR THE DEGREE
OF MASTER OF SCIENCE

DEPARTMENT OF GEOLOGY

EDMONTON, ALBERTA

FALL, 1986

Permission has been granted to the National Library of Canada to microfilm this thesis and to lend or sell copies of the film.

The author (copyright owner) has reserved other publication rights, and neither the thesis nor extensive extracts from it may be printed or otherwise reproduced without his/her written permission.

L'autorisation a été accordée à la Bibliothèque nationale du Canada de microfilmer cette thèse et de prêter ou de vendre des exemplaires du film.

L'auteur (titulaire du droit d'auteur) se réserve les autres droits de publication; ni la thèse ni de longs extraits de celle-ci ne doivent être imprimés ou autrement reproduits sans son autorisation écrite.

ISBN 0-315-32389-2

THE UNIVERSITY OF ALBERTA

RELEASE FORM

NAME OF AUTHOR: GREGORY BYRON MANDRYK

TITLE OF THESIS: "PLEISTOCENE VALLEY GLACIER
SEDIMENTOLOGY AND STRATIGRAPHY IN THE
BANFF-CANMORE AREA OF ALBERTA, CANADA"

DEGREE: MASTER OF SCIENCE

YEAR THIS DEGREE GRANTED: FALL, 1986

Permission is hereby granted to THE UNIVERSITY OF ALBERTA LIBRARY to reproduce single copies of this thesis and to lend or sell such copies for private, scholarly or scientific research purposes only.

The author reserves other publication rights, and neither the thesis nor extensive extracts from it may be printed or otherwise reproduced without the author's written permission.

(SIGNED) *G. B. Mandryk*

PERMANENT ADDRESS:

11006-76 ST
EDMONTON, ALBERTA
T5B 2L6

DATE: OCTOBER 10, 1986

THE UNIVERSITY OF ALBERTA

FACULTY OF GRADUATE STUDIES AND RESEARCH

The undersigned certify that they have read, and recommend to the Faculty of Graduate Studies and Research, for acceptance, a thesis entitled "PLEISTOCENE VALLEY GLACIER SEDIMENTOLOGY AND STRATIGRAPHY IN THE BANFF-CANMORE AREA OF ALBERTA, CANADA" submitted by GREGORY BYRON MANDRYK in partial fulfilment of the requirements for the degree of MASTER OF SCIENCE.

[Signature]
.....
Supervisor
Philippe Robit
.....
J. L. K.
.....
W. J. Dundas
.....

Date: *Oct. 9, 1985*

Abstract

This study was conducted in the glaciated Bow River valley, located in the Canadian Rocky Mountains. Unconsolidated valley-fill sediments consisting of diamicton and sorted sediments were examined in the Banff and Canmore region of Alberta. The study was undertaken in this particular area so that recent advances in glacial sedimentology, made since some of the deposits were previously studied, could be applied and thus result in a more comprehensive understanding of the region's glacial history.

Seven facies were recognised. Facies 1 consists of a diamicton with numerous sorted sediment filled lenses; many of the lenses are inclined. Facies 1 is interpreted to be basal melt-out till. Facies 2 consists of a diamicton that has numerous elongated, thin gravel layers. Facies 2 is interpreted to be lodgement till. Facies 3 consists of a massive diamicton with very few, sorted sediment-filled lenses. Facies 3 is interpreted to be lodgement till. Facies 4 consists of a diamicton with numerous, generally horizontal lenses filled with sorted sediment. Facies 4 is interpreted to be basal melt-out till. Facies 5 consists of mainly an interfingering, interbedded sequence of poorly sorted gravels, diamicton lenses and blocks. Some poorly sorted gravels are also present. Facies 5 is interpreted to be proglacially

deposited glacial mudflow complexes, dissected till plains, and glacial outwash channel-fill deposits. Facies 6 consists of mainly horizontal, interbedded, interfingering lens-shaped gravel horizons. Facies 6 is interpreted to be braided glacial outwash deposits with a minor amount of alluvial fan deposits. Facies 7 consists of mainly interbedded gravel and sand layers. Facies 7 is interpreted to be ice proximal, proglacial outwash sediments.

Three major, glacially related sedimentation events are recognized in the Banff-Canmore area. The first major event is marked by the formation of a sandur in front of a retreating valley glacier. The second major event is defined by the advance of a valley glacier which also deposited a thick basal till. The third major event began with a glacial advance just into the study area, this advance deposited a proglacial mudflow complex. The glacier then retreated slightly and then readvanced completely through the study area. This final glacial advance deposited basal till. The final glaciation was 2-10 times shorter than the event 2 glacial advance. The final deglaciation of the Banff and Canmore area featured a debris-free glacier occupying the Bow River valley, gradually melting away.

Acknowledgments

This thesis was completed with the help of numerous people, my appreciation is extended to them. Carole Mandryk, Kim Martman, and Peter Bobrowsky went unarmed into bear country to assist in the field work. George Mandryk provided very comfortable field accommodation for the field season. Harry and Alex Mandryk supported and provided a field vehicle. Major funding was provided by Nathaniel Rutter through his NSERC grant; additional financial aid came from Sigma Xi, The Scientific Research Society. Carole Mandryk and Peter Bobrowsky edited early drafts of the thesis. Thanks go to Nathaniel Rutter and the Quaternary Research Group for discussion and advice.

Table of contents

Chapter	Page
I. INTRODUCTION.....	1
A. OBJECTIVES.....	1
B. LITERATURE REVIEW.....	1
INTRODUCTION.....	3
DEBRIS FLOWS.....	6
BRAIDED RIVER, GLACIOFLUVIAL, AND SANDUR	
DEPOSITS.....	10
ALLUVIAL FANS.....	11
GLACIAL SYSTEMS.....	14
II. SETTING, PREVIOUS WORK, AND METHODOLOGY.....	44
A. PHYSIOGRAPHY.....	44
B. BEDROCK GEOLOGY.....	45
C. PREVIOUS WORK.....	45
D. FIELD METHODS.....	48
E. LABORATORY METHODS.....	51
III. GLACIER FLOW-LINES AND FLOW-CELLS.....	54
A. INTRODUCTION AND DEFINITION.....	54
B. GLACIER FLOW-LINE AND FLOW-CELL	
RECONSTRUCTION.....	55
IV. FACIES DESCRIPTIONS, INTERPRETATIONS,	
AND DISCUSSIONS.....	58
A. FACIES 1.....	59
FACIES 1 DESCRIPTION.....	59
FACIES 1 INTERPRETATION.....	64
FACIES 1 DISCUSSION.....	72
B. FACIES 2.....	84
FACIES 2 DESCRIPTION.....	84
FACIES 2 INTERPRETATION.....	90
FACIES 2 DISCUSSION.....	96
C. FACIES 3.....	101
FACIES 3 DESCRIPTION.....	101
FACIES 3 INTERPRETATION.....	109
FACIES 3 DISCUSSION.....	113
D. FACIES 4.....	122
FACIES 4 DESCRIPTION.....	122
FACIES 4 INTERPRETATION.....	139
FACIES 4 DISCUSSION.....	144
E. FACIES 5.....	154
FACIES 5 DESCRIPTION.....	154
FACIES 5 INTERPRETATION.....	165
FACIES 5 DISCUSSION.....	177

F.	FACIES 6.....	179
	FACIES 6 DESCRIPTION.....	179
	FACIES 6 INTERPRETATION AND DISCUSSION.....	187
G.	FACIES 7.....	199
	FACIES 7 DESCRIPTION.....	199
	FACIES 7 INTERPRETATION.....	211
	FACIES 7 DISCUSSION.....	217
V.	GEOLOGICAL-SEDIMENTATION HISTORY AND CONCLUDING DISCUSSION.....	220
A.	GEOLOGICAL-SEDIMENTATION HISTORY.....	220
	EVENT 1.....	220
	EVENT 2.....	226
	DEGLACIATION OF EVENT 2.....	234
	EVENT 2b.....	236
	EVENT 3a.....	236
	EVENT 3b.....	239
	EVENT 3c.....	239
	DEGLACIATION OF EVENT 3c.....	246
B.	RELATIVE LENGTHS OF GLACIATIONS.....	247
C.	METHODS EVALUATION.....	249
D.	CONCLUSIONS.....	250
VI.	REFERENCES.....	252
VII.	APPENDICES.....	265
A.	SAND, SILT, AND CLAY PERCENTAGES OF DIAMICTON SAMPLES.....	265
B.	GRAINSIZE PHI VALUES AT VARIOUS CUMULATIVE PERCENTAGES.....	268
C.	GRAPHIC STATISTICAL PARAMETERS.....	272
D.	ROUNDNESS VALUES OF EACH SAMPLE.....	278
E.	PETROLOGICAL COMPOSITION OF EACH SAMPLE.....	281
F.	FACIES LOCATIONS THROUGHOUT STUDY AREA.....	285
G.	DIAMICTON PEBBLE FABRIC PLUNGES.....	286

Tables

TABLE 1:	BASAL DEBRIS LAYER THICKNESS.....	20
TABLE 2:	DENSITY OF BASAL DEBRIS.....	21
TABLE 3:	LODGE MENT TILL PROPERTIES.....	24
TABLE 4:	MELT-OUT TILL PROPERTIES.....	30
TABLE 5:	MUDFLOW COMPLEX PROPERTIES.....	37
TABLE 6:	RANGES AND AVERAGE DIMENSIONS OF UNITS AND CLAST SIZES IN SORTED SEDIMENT PORTION OF FACIES 5.....	160
TABLE 7:	COMPARISON OF DIAMICTON PROPERTIES BETWEEN FACIES 1 TO 4 AND FACIES 5.....	167
TABLE 8:	ORIENTATION OF BEDS IN FACIES 7.....	210
TABLE 9:	SUMMARY OF THE FACIES PROPERTIES AND INTERPRETATIONS.....	222
TABLE 10:	SUMMARY GEOLOGICAL HISTORY OF THE BANFF-CANMORE AREA.....	223
TABLE 11:	COMPARISON OF RUTTER'S (1972) AND MANDRYK'S (THIS STUDY) CHRONOLOGY.....	225

Figures

FIGURE 1:	LOCATION OF STUDY AREA.....	2
FIGURE 2:	MAPS OF STUDY AREA.....	4
FIGURE 3:	BEDROCK GEOLOGY OF THE BOW RIVER VALLEY.....	46
FIGURE 4:	GLACIER FLOW LINES.....	56
FIGURE 5a:	NORTH FIRESIDE SECTION.....	60
FIGURE 5b:	SOUTH FIRESIDE SECTION.....	61
FIGURE 6:	FACIES 1, 2, 3, AND 4 DIAMICTON MATRIX CUMULATIVE GRAIN SIZE CURVES.....	65
FIGURE 7:	ROUNDNESS OF GRAINS IN DIAMICTONS.....	67
FIGURE 8:	PETROLOGICAL CONTENT OF DIAMICTONS.....	68
FIGURE 9:	FACIES 1 DIAMICTON FABRICS.....	69
FIGURE 10:	FACIES 2, 3, AND 4 DIAMICTON FABRICS.....	70
FIGURE 11:	FACIES 1 GRAIN SIZE COLUMN.....	73
FIGURE 12:	FACIES 1 ROUNDNESS COLUMN.....	73
FIGURE 13:	FACIES 1 PETROLOGY COLUMN.....	76
FIGURE 14:	SKETCH OF FACIES 1 FORMATION.....	78
FIGURE 15:	POWERHOUSE SECTION.....	85
FIGURE 16:	ANTHRACITE SECTION.....	87
FIGURE 17a:	FACIES 2 DIAMICTON MATRIX CUMULATIVE GRAIN SIZE CURVES.....	93
FIGURE 17b:	FACIES 2 GRAIN SIZE COLUMN.....	93
FIGURE 18:	FACIES 2 PETROLOGY COLUMN.....	94
FIGURE 19:	FACIES 2 ROUNDNESS COLUMN.....	94
FIGURE 20:	SKETCH OF FACIES 2 FORMATION.....	97
FIGURE 21:	FACIES 2 DIAMICTON FABRICS.....	100
FIGURE 22:	CASCADE RIVER SECTION C1.....	102
FIGURE 23:	CASCADE RIVER SECTION C2.....	103
FIGURE 24:	CASCADE RIVER SECTION C3.....	104
FIGURE 25:	JOHNSON LAKE SECTION JL-3.....	105
FIGURE 26:	JOHNSON LAKE SECTION JL-4.....	106
FIGURE 27:	JOHNSON LAKE SECTION JL-5.....	107
FIGURE 28:	FACIES 3 PETROLOGY COLUMN.....	112
FIGURE 29a:	FACIES 3 DIAMICTON MATRIX CUMULATIVE GRAIN SIZE CURVES.....	115
FIGURE 29b:	FACIES 3 GRAIN SIZE COLUMN.....	115
FIGURE 30:	FACIES 3 ROUNDNESS COLUMN.....	116
FIGURE 31:	SKETCH OF FACIES 3 FORMATION.....	118
FIGURE 32:	FACIES 3 DIAMICTON FABRICS.....	121
FIGURE 33:	CARROT CREEK SECTION.....	123
FIGURE 34:	CANMORE SECTION.....	126
FIGURE 35:	CASCADE RIVER SECTION C6.....	128
FIGURE 36:	CASCADE RIVER SECTION C7.....	129
FIGURE 37:	CASCADE RIVER SECTION C8.....	130
FIGURE 38:	COUGAR CREEK SECTION.....	131
FIGURE 39:	JOHNSON LAKE SECTION JL-1.....	132
FIGURE 40:	JOHNSON LAKE SECTION JL-2.....	133
FIGURE 41:	JOHNSON LAKE SECTION JL-6.....	134

FIGURE 42:	FACIES 4 PETROLOGY.....	141
FIGURE 43:	ROUNDNESS AND PETROLOGY COLUMNS OF FACIES 1 TO 4.....	142
FIGURE 44a:	FACIES 4 DIAMICTON MATRIX CUMULATIVE GRAIN SIZE CURVES.....	145
FIGURE 44b:	FACIES 4 GRAIN SIZE COLUMN.....	145
FIGURE 45:	FACIES 4 ROUNDNESS COLUMN.....	146
FIGURE 46:	SKETCH OF FACIES 4 FORMATION.....	147
FIGURE 47:	FACIES 4 DIAMICTON FABRICS.....	152
FIGURE 48:	FACIES 5 DIAMICTON MATRIX CUMULATIVE GRAIN SIZE CURVES.....	156
FIGURE 49:	FACIES 5 GRAVELS CUMULATIVE GRAIN SIZE CURVES.....	159
FIGURE 50:	FACIES 5 CUMULATIVE GRAIN SIZE CURVES OF SAND LENSES WITHIN GRAVELS.....	162
FIGURE 51:	LAMINATED MATRIX OF FACIES 5 GRAVELS.....	164
FIGURE 52:	SKETCH OF FACIES 5 FORMATION.....	166
FIGURE 53:	PETROLOGICAL TERNARY PLOT OF FACIES 1 TO 5.....	168
FIGURE 54:	ROUNDNESS OF FACIES 1-4 (DIAMICTON), FACIES 5 (GRAVEL) AND FACIES 6 (GRAVEL).....	173
FIGURE 55:	FACIES 5 AND FABRICS.....	175
FIGURE 56:	FACIES 6 CUMULATIVE GRAIN SIZE CURVES.....	182
FIGURE 57:	PETROLOGICAL TERNARY PLOT OF FACIES 6.....	188
FIGURE 58:	FACIES 6 GEOGRAPHICAL DISTRIBUTION.....	190
FIGURE 59:	PETROLOGICAL TERNARY PLOT OF FACIES 6.....	192
FIGURE 60:	PETROLOGICAL TERNARY PLOT OF DIAMICTON UNITS (FACIES 1-5) AND FACIES 6.....	195
FIGURE 61:	PLOT TO DETERMINE THE DISTANCE BETWEEN THE SEDIMENT SOURCE AND THE DEPOSITIONAL SITE.....	198
FIGURE 62:	ANTHRACITE SECTION A1.....	200
FIGURE 63:	COMPOSITE GEOLOGICAL COLUMN AND HISTORY OF FACIES 7 DEPOSITION.....	212
FIGURE 64:	FACIES 7 AND ADJACENT FABRIC IN FACIES 3.....	214
FIGURE 65:	SEDIMENTATION FILLING EVENTS AT ANTHRACITE SUBSECTION A1.....	216
FIGURE 66:	SEDIMENT FILLING DIRECTIONS OF THE CHANNEL AT ANTHRACITE SUBSECTION A1.....	218
FIGURE 67:	COMPOSITE GEOLOGICAL SECTION.....	221
FIGURE 68:	EVENT 1 SEDIMENT DISTRIBUTION.....	224
FIGURE 69:	EVENT 2 SEDIMENT DISTRIBUTION.....	227
FIGURE 70:	EVENT 2 AND 3c CORRELATION CHART.....	229
FIGURE 71:	EVENT 2 LATERAL TILL FACIES CHANGES.....	232
FIGURE 72:	ATHABASCA VALLEY GLACIER TRANSVERSE TO FLOW SECTION.....	235
FIGURE 73:	EVENT 2b SEDIMENT DISTRIBUTION.....	237
FIGURE 74:	EVENT 3a SEDIMENT DISTRIBUTION.....	238
FIGURE 75:	EVENT 3b SEDIMENT DISTRIBUTION.....	240
FIGURE 76:	EVENT 3c TILL DISTRIBUTION.....	242
FIGURE 77:	EVENT 3c LATERAL TILL FACIES CHANGES.....	244

Plates

PLATE 1:	Airphoto of facies 1 and the bedrock protuberance.....	80
PLATE 2:	Folded silt-filled lens in facies 1.....	83
PLATE 3:	Elongated gravel bands in facies 2 at the Powerhouse P2 subsection.....	89
PLATE 4:	Airphotos of drumlinized topography in the Powerhouse vicinity.....	91
PLATE 5:	Deformed sand-filled lens in the diamicton of facies 3.....	120
PLATE 6:	Curved joints with striated surfaces in facies 4.....	185
PLATE 7:	Facies 5.....	170
PLATE 8:	Facies 5.....	171
PLATE 9:	Proglacial stream eroding basal till.....	178
PLATE 10:	Facies 6.....	181
PLATE 11:	Facies 6, large diameter clasts.....	184
PLATE 12:	Facies 7.....	201
PLATE 13:	Subfacies 7f.....	208

I. INTRODUCTION

A. OBJECTIVES

Although modern valley glacier sedimentary environments have been studied by several researchers including Boulton (1967, 1970a, 1970b), Lawson (1979, 1981a, 1982), and Mills (1977, 1978); few studies have used a sedimentological approach in the analysis of ancient valley glacier sediments. The traditional approach to the study of ancient glacial deposits has focused more on stratigraphy. The traditional approach has also had fewer modern sedimentological studies to use as a reference. The sedimentological approach, on the other hand, is a valuable tool that can be used for understanding the dynamic interacting processes of glaciers and their deposits. In this study the sedimentological approach was used in the description and interpretation of ancient valley glacier sediments in the Banff-Canmore area of Alberta (Figure 1). This area, originally studied in detail by Rutter (1965a), was chosen because it contains substantial Quaternary deposits accessible for study.

Major objectives of the study:

1. To refine the Quaternary stratigraphy and Quaternary glacial history of the Banff-Canmore

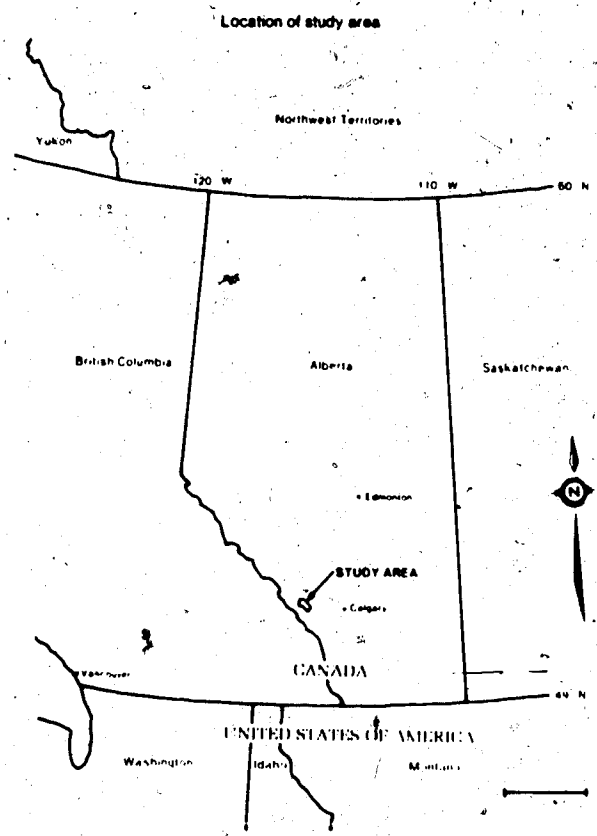


Figure 1. Location of study area.

area of Alberta.

2. To determine the sedimentological genesis of the Quaternary deposits in the Banff-Canmore area.
3. To contribute to the understanding of valley glacier sedimentation processes.

B. LITERATURE REVIEW

INTRODUCTION

The sediments investigated in this study are located in the Bow River valley (Figures 2a, 2b). These sediments are unconsolidated deposits which unconformably overlie older rocks. This spatial relationship suggests the unconsolidated sediments were deposited as valley-fill sediments within the mountains. The four types of sediments commonly deposited in mountainous settings and which also have characteristics similar to the sediments in the Banff-Canmore area are debris flow deposits, fluvial deposits, alluvial fan deposits, and glacial deposits.

The depositional processes and characteristics of the four types of deposits will be reviewed below. One aim of the review is to present information on the depositional processes responsible for each type of deposit since in many cases the differing processes result in deposits with practically indistinguishable characteristics.

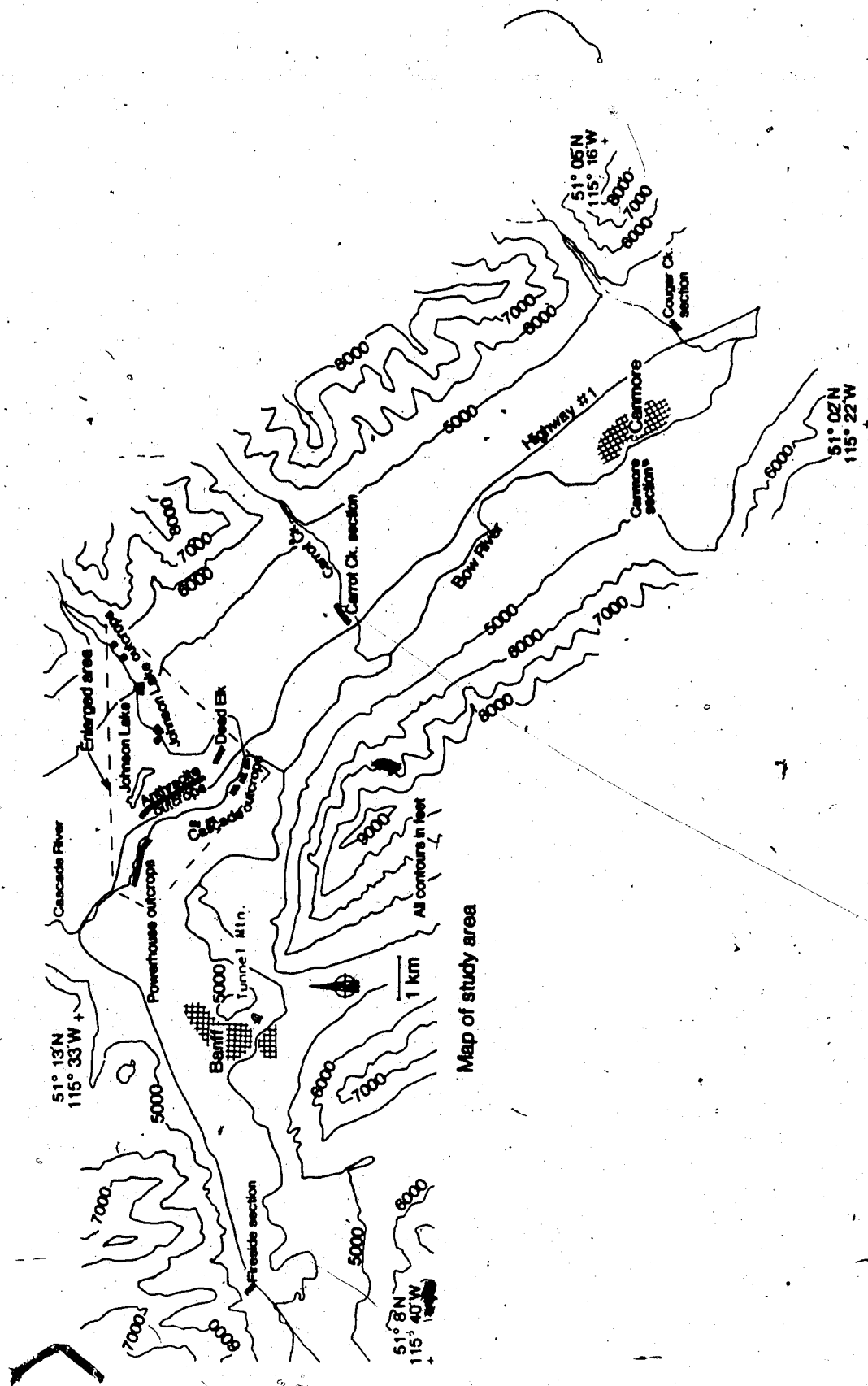


Figure 2a. Map of study area with locations of outcrops studied.

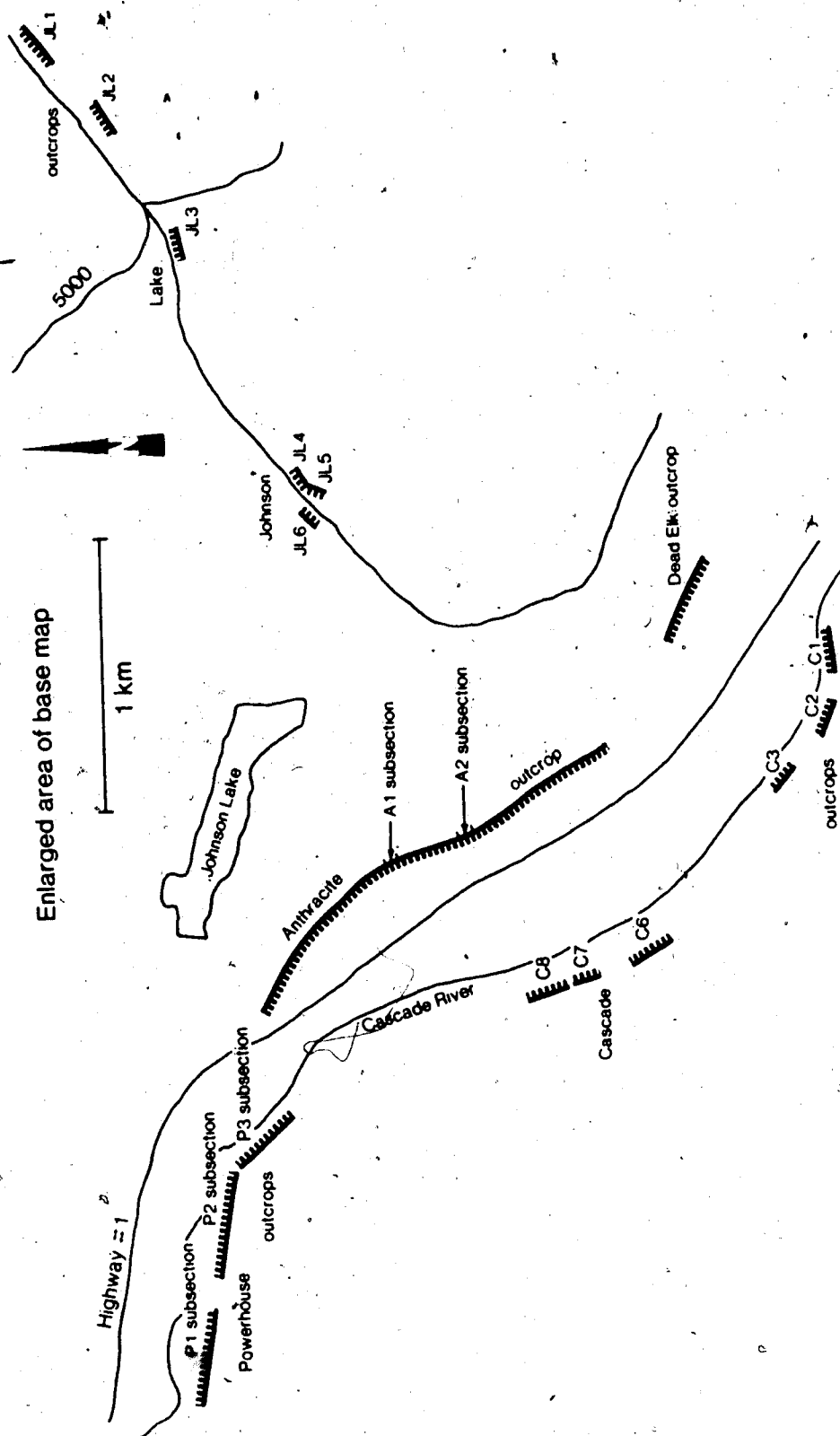


Figure 2b. Enlarged portion of figure 2a.

DEBRIS FLOWS

Debris flows are sediment gravity flows in which a sediment mass, consisting of clasts suspended in a finer grained matrix, flows downslope usually under the influence of gravity and also sometimes by dispersion within the mass (Enos 1977; Lowe 1979). Debris flows are bingham substances (Lowe 1979). Bingham substances have strength, and flow with constant viscosity once the substance's yield strength is exceeded (Fisher 1971).

Macroscopic processes of debris flow initiation, movement, and flow termination (deposition), have been observed. Two mechanisms of debris flow initiation pertinent to this study are, (i) by rainwater or floodwater mixing with unconsolidated sediment with the resulting water-sediment mass flowing (Fryxell and Horberg 1943; Pierson 1981; Clague et al. 1985) and, (ii) by water saturated debris on glacier ice attaining a state of excess pore pressure and then flowing (Boulton 1968; Lawson 1982).

Once initiated, debris flows can move along slopes with as little as $1-2^\circ$ slope (Middleton and Hampton 1976).

Debris flow movement is by one of three mechanisms (Pierson 1981; Lawson 1982).

(i) Laminar flow. In laminar flow the entire debris flow is undergoing laminar deformation and clasts are homogeneously distributed. Lowe (1979) attributes the clast distribution to dispersive pressure forcing colliding gravel-sized clasts apart. Clast support is provided by the yield

strength of the finer grained matrix in which the clasts are dispersed (Johnson 1970; Fisher 1971; Middleton and Hampton 1976).

(ii) Rigid-plug flow mechanism. Movement occurs with a rigid, non-deforming plug of sediment rafted above a basal zone of laminar shear (Carter 1975).

(iii) Turbulent debris flow. This is a stage of peak flow. Cobbles and boulders are forced out from the body of the flow and towards the flow's edge by turbulent and dispersive pressure (Pierson 1981). Turbulent flow has only been observed to occur when the mass is totally confined within a channel.

Debris flows observed within incised channels are usually preceded and followed by the flow of stream-water. The body of the debris flow has a boulder-rich front; behind the front are fewer boulders. Increased mud and pebble-sized fragments in laminar flow usually make up the remainder of the upstream end of the flow (Johnson 1970; Morton and Campbell 1974).

Debris flows cease moving by the following mechanisms. For example, when sediment input to the flow diminishes (Carter 1975), when water in the debris flow is lost to underlying sediments (usually gravel) (Hooke 1967; Lawson 1982), when bed slope decreases (Lawson 1982), and when the thickness of the flow decreases (Carter 1975; Lawson 1982). Any one, or combination of the above changes causes the

applied shear stress acting on the debris-flow mass to drop below the yield strength of the debris (Hooke 1967; Fisher 1971; Lowe 1979). This drop in applied shear stress causes the flow's motion to stop or "freeze". As the applied shear stress is decreasing, the thickness of the rigid plug, if present, increases in a downwards direction until the entire debris mass is non-shearing (Carter 1975). Laminar debris flows can freeze from the top or the bottom (Hooke 1967; Lowe 1979; Carter 1975).

As the debris flow stops flowing, and even after, cobbles and boulders may settle out of suspension if the debris cohesion is too low to support the larger clasts (Pierson 1980). Pierson (1980) observed that rocks composing lateral levees sank into the frozen debris flow mass. In other instances, the boulders and cobbles along the front portions of debris flows did not sink into the debris flow deposit (Curry 1966; Pierson 1980).

Muddy water often emerges from the frozen debris flow deposit to wash away fine-grained sediment on the deposit's surface (Pierson 1980). Rain- and stream-water also remove fine-grained sediment from the upper surface of flow deposits.

Characteristics of debris flow deposits

Debris flows range in thickness from a few centimeters to 6 meters. An individual debris flow deposit usually has a sheet-like geometry of uniform thickness (Pierson 1980) although channelized shapes do exist (Morton and Campbell 1974).

Internally, debris flow deposits are poorly sorted and consist of randomly distributed rock fragments supported in a finer-grained matrix (Hooke 1967; Johnson 1970; Fisher 1971; Ehos 1977; Nardin et al. 1979). The presence and nature of stratification varies amongst deposits; in general most are massive (Fryxell and Horberg 1943; Hooke 1967; Fisher 1971; Nardin et al. 1979). Some deposits have internal sedimentary structures interpreted to be the result of flowage (Nardin et al. 1979). Inverse grading or poorly developed inverse grading is sometimes observed either throughout a deposit (Fisher 1971; Nardin et al. 1979) or only in the basal zone of the deposit (Nardin et al. 1979). Lowe (1979) and Pierson (1980) have observed debris flow deposits that have large cobble- and boulder-sized blocks or clasts concentrated along the base of the deposit. Many deposits have the coarsest sediments, cobbles and boulders, situated along the deposit's sides

and front portions (Curry 1966; Hooke 1967; Johnson 1970; Morton and Campbell 1974; Pierson 1980). In some instances the surfaces of some gravel-sized clasts are abraded (Hooke 1967) or are marked by 5 cm long, randomly oriented striae.

Debris flow deposits do not have a characteristic pebble fabric pattern although within shear zones fabric develops either parallel to flow (Enos 1977; Nardin et al. 1979) or perpendicular to flow (Enos 1977). The imbrication of the clasts may be inclined up- or down-flow (Nardin et al. 1979). Clast orientations are random within zones of non-shear, including inside a rigid non-deforming plug.

Debris flow deposits often have sharp, conformable lower contacts (Hooke 1967; Fisher 1971) which are either horizontal or U-shaped (Rodine and Johnson 1976).

BRAIDED RIVER, GLACIOFLUVIAL, AND SANDUR DEPOSITS

Depositional processes and sediment characteristics of braided river, glaciofluvial, and sandur deposits will not be reviewed because the basic processes are generally well understood.

Some useful braided river references are in Price and Howarth (1970), Church (1972), Smith (1974), Church and Gilbert (1975), Miall (1978), Boothroyd and Nummedal (1978), Rust and Koster (1984), and Smith (1985). Useful

references on glaciofluvial and ice contact rivers are in Shaw (1972), McDonald and Shilts (1975), and Allen (1982).

ALLUVIAL FANS

An alluvial fan is defined by Bull (1972, p.63) as, "a deposit whose surface forms a segment of a cone that radiates downslope from the point where the stream leaves the mountains." Alluvial fans are composed of sediments that have a wide range of both grain sizes and sorting, ranging from sorted-silt, -sand, and -gravels (water-laid sediments) to diamictons¹ (mudflows) (Bull 1960).

Alluvial fans form where a single trunk stream exits a side valley and enters a larger valley (Bull 1972). These streams are often ephemeral and when flowing contain clear water to viscous mud (Bull 1963). The sediment deposition which initially forms and then maintains an alluvial fan is usually induced by a decrease in stream gradient (Bull 1963). This change in gradient may result from a base level fall in the main valley caused, for example, by valley

¹Diamicton is referred to throughout this thesis. Diamicton is a descriptive term used when referring to, "any nonsorted or poorly sorted terrigenous sediment that consists of sand and/or larger particles in a muddy matrix. Size distribution is commonly bimodal or polymodal, with one or more modes in the coarse grain range and one or more in the silt-clay sizes," (Flint *et al.* 1960a, p.509 1960b). Frakes (1978) notes that the clasts in a diamicton may or may not be in contact with one another.

glacier erosion (Bull 1977). Bull (1963) observed that alluvial fans also formed from mud flows which freeze upon entering the main valley because of a decrease in flow depth and velocity. Sediment is distributed across a fan's surface by a network of braided streams which continually fill with sediment and change location (Bull 1963; Kochel and Johnson 1984), and also by debris flows exiting channels and spreading sediment over the fan surface (Bull 1963; Hooke 1967; Pierson 1980).

Characteristics of alluvial fan deposits²

The cross-sectional shape of an alluvial fan, profiled from the valley side to the valley center, is a wedge which thins away from the mountains (Bull 1972). The gross geometry of the beds within a fan are sheet-like beds (Bull 1972) which vary in thickness. Bedding is not usually visible within fans composed solely of gravel. Individual beds extend for many meters in cross-sections parallel to the fan's surface slope, cut and fill bedding relationships are seldom observed (Bull 1972). In sections parallel to an alluvial fan's topographic contours numerous cut and fill structures exist (Bull 1972).

²A table of alluvial fan characteristics is located in Kochel and Johnson (1984).

Alluvial fans are composed of sediment types which range (i) from well sorted, cross bedded, laminated, or structureless silt-sized grains to sorted gravel-sized clasts which were transported by braided distributary channels (Bull 1963, 1972), to (ii) diamictites deposited by sediment gravity mudflow processes (Bull 1963; Pierson 1980), to (iii) sieve deposits formed when fine grained sediments (clay- to sand-sized) are blocked upstream of a coarser lobe of gravel-sized sediment (Hooke 1967).

The alluvial fan depositional environment cannot be identified or characterized by a particular grain size (Bull 1972; 1977). The mean grain size of an alluvial fan is a function of the source region (Hooke 1967). In general, grain-size decreases downslope in modern arid-climate alluvial fans (Bull 1977). Grain size and sorting differs markedly between individual beds within an alluvial fan (Bull 1972).

Gravel clasts, in sediments interpreted as alluvial fan deposits, are more angular than nearby river deposited clasts (Ryder 1971). In the same study Ryder observed alluvial fan gravels have less lithologic variation than river gravels, a function of the source area's lithologic composition. Hooke (1967) noticed that clasts within an alluvial fan are abraded.

GLACIAL SYSTEMS

1.1. GLACIAL DEBRIS INCORPORATION

Valley glaciers incorporate clastic material subglacially (from below the glacier) and supraglacially (from above the glacier) (Shaw 1985). Any debris on a glacier's surface in the accumulation area is supraglacially incorporated into an englacial position by snow burial or by direct inception into a crevasse. Material which falls onto a glacier in the ablation area will remain on the glacier's surface unless it enters a crevasse. Basal incorporation of material in subpolar glaciers is by the process of regelation (Boulton 1970a) and also basal freeze-on (Weertman 1961). Polar glaciers are thought to basally incorporate material by overriding frontal aprons (Shaw 1977).

Sediment incorporated by a glacier is classified as glacial debris (Dreimanis 1982). Glacial debris is defined by Dreimanis (1982, p. 16) as, "material being transported by a glacier in contact with glacier ice. In most cases it is disaggregated, except for clasts of various sizes, including large rafts."

Glacial debris is transported by the glacier in one of

three possible positions, supraglacial (on the glacier), englacial (within the glacier), and subglacial (basally or in the lower, basal portions of the glacier) (Reheis 1975). Glacial debris is unlikely to remain in one transport position and will usually change transport positions. Attributes acquired by debris in one transport zone may be retained once another zone is entered.

Flow lines in the accumulation area of a glacier are directed downwards and as a result supraglacial and englacial debris in the accumulation areas are transported to a basal position (Boulton and Eyles 1979). Basal melting in temperate glaciers is another method of transferring englacial debris to the basal transport zone (Boulton 1978).

Englacial debris can also move upwards and become exposed supraglacially in areas of dominant surface melting (Sharp 1949). Upward transport of basal debris along inclined shear planes or thrust faults will also elevate basal debris into an englacial position. Shear planes develop in many valley glacier settings. For example, (1) when a valley glacier is overridden by a tributary ice stream (Eyles and Rogerson 1977), (2) when merging tributary valley glaciers move basal debris into an englacial position along the mutual boundary of the two glaciers (Boulton 1978), (3) basal debris follows an upwards path when a subglacial knob is crossed (Eyles and

Rogerson 1978; Boulton 1978), and (4) compression and thrust faulting happen at a valley glacier's terminus where the glacier's base is frozen to the ground or impeded by stagnant ice (Boulton 1968). This differential movement also causes basal debris-rich ice to be carried into an englacial and then into a supraglacial position (Clayton 1964; Boulton 1970a).

2. CHARACTERISTICS OF GLACIALLY TRANSPORTED DEBRIS

2a. SUPRAGLACIALLY TRANSPORTED DEBRIS

An airphoto survey of valley glaciers (conducted by the author) reveals that most modern valley glaciers are largely free of supraglacial debris. If supraglacial debris is present on the ice it is concentrated above lateral and medial moraines. This surficial debris ranges in thickness from a few to 50 centimeters (Small et al. 1979).

(Supraglacial debris which has been deposited is called "supraglacial morainic till" by Eyles (1979)).

a. Grain size

Relative to debris in the basal transport zone, supraglacial debris has less fine-grained sediment (less than 15% clay and silt) (Sharp 1949; Boulton and Eyles

1979). Supraglacial debris therefore has a coarser mean grain size and also better sorting (Boulton and Eyles 1979). The clay and silt content increases downwards in a vertical section of supraglacial debris (Boulton and Eyles 1979). Some clay and silt may be concentrated in strata which represent former supraglacial ponds (Sharp 1949). Clast diameters range up to 1 meter in diameter in supraglacial exposures of medial moraines (Small and Clark 1974); clasts much larger than this could conceivably be carried onto glaciers by avalanches.

b. Fabric

Clasts within supraglacial debris have no preferred orientation (Eyles 1979).

c. Petrology

Supraglacial debris is often composed of distantly derived lithologies, a result of derivation from mountain sides situated far up-valley; the lithology of the debris therefore has a component reflecting this distant source (Dreimanis 1976).

d. Roundness

Supraglacial debris is usually composed of only angular clasts (Sharp 1949; Small and Clark 1974). Angularity is maintained because processes which round the clasts are

generally lacking; in fact frost shattering enhances angularity (Sharp 1949; Dreimanis 1976). Some rounded clasts are present, a product of supraglacial stream transport (Sharp 1949).

2b. ENGLACIALLY TRANSPORTED DEBRIS

Englacial debris is transported in a non-abrasive environment as is demonstrated by the lack of grainsize or roundness alteration (Boulton 1978) along the englacial transport path. Weathering and erosion processes, which mainly affect supraglacial and subglacial debris respectively, do not affect englacially transported material (Lawson 1979). Because of this, grain size and roundness properties attained by debris prior to entering the englacial realm are retained. Clast fabric is one property not retained.

Englacial debris generally consists of scattered debris within the ice, although some debris may be concentrated into bands (Lawson 1979) or as englacial stream sediments (Boulton 1972a). Englacial debris concentration by volume ranges from 0.002% to 25% (Lawson 1979); the mean being closer to the former value. Englacially and supraglacially transported debris accounts for about 3% of the debris load of the Matanuska Glacier (Lawson 1979), this suggests most debris is basally transported.

a. Grain size

Englacial debris is composed of a wide range of grain sizes and generally has poor sorting. Englacial stream sediments are better sorted and consist mainly of gravels and sands (Boulton 1972a). Bedding of this latter sediment is mostly planar; high angle cross beds are rare (Boulton 1972a).

b. Fabric

Englacial clast fabric is generally parallel to ice flow (Humlum 1981). In zones of compressive flow, including zones of thrusting, transverse pebble fabrics develop (Dreimanis 1976).

c. Roundness

Clasts generally have low roundness (Boulton 1978; Small and Gomez 1981).

2c. BASALLY TRANSPORTED DEBRIS

The lowermost, basal portions of a glacier transport up to 97% of a glacier's debris load (Reheis 1975; Lawson 1979). Basal glacial-debris consists of unsorted clay- to gravel-sized material (Boulton 1967; Gow et al. 1979).

concentrated into 1 cm to 10 cm thick bands (Clapperton 1975; Shaw 1977). These bands alternate with layers of cleaner ice which are a few centimeters thick (Clapperton 1975; Shaw 1977) or with unstratified debris containing interstitial ice (Lawson 1979).

The amount of basal debris in transport and the thickness of the basal debris layer is a function of the glacier's temperature regime. The basal debris layer is thicker in polar type glaciers (Tables 1 and 2) and thinner in temperate-type glaciers.

Table 1. Basal debris layer thickness

<u>Type of glacier</u>	<u>Thickness range</u>
temperate	up to 15 m (1) but generally less than 1 m (2)
subpolar	up to 16 m (3)
polar	<5 to 60 m (4)

(1) Lawson 1979

(2) Boulton 1972b

(3) Herron and Langway 1979

(4) Boulton 1972b; Shaw 1977.

Table 2. Density of basal debris
(% debris by volume of ice)

<u>type of glacier</u>	<u>average</u>	<u>range</u>
temperate	40% (1)	<4-75% (2)
subpolar	-	0-15% (3)
polar	-	5-50% (4)

(1) Mickelson 1973; Boulton et al. 1974;
Boulton 1975; Clapperton 1975; Reheis 1975; Lawson
1979; Humlum 1981

(2) Lawson 1979; Boulton 1975; Mickelson 1973

(3) Boulton 1967; Gow et al. 1979

(4) Boulton 1972b; Shaw 1977.

a. Grain size

Basally transported debris makes frequent contact both with neighbouring particles, also in transport, and with the stationary subglacial substrate. Any contact results in the abrasion and crushing of debris. This increases the finer-grained fraction of the basal debris (Boulton 1972a). Basal debris is thus enriched in fine-grained fractions and depleted in coarser-grained fractions relative to debris in higher levels of glacier transport, such as supraglacial transport (Boulton 1978; Boulton and Eyles 1979).

b. fabric

Basal-debris pebble fabrics are usually oriented parallel to the direction of ice flow (Lawson 1979; Humlum

1981) albeit less pronounced than englacial pebble fabrics (Humlum 1981). Lawson (1979) found that basal-debris pebble fabrics have a mean divergence of 12° from the actual ice-flow direction and the plunge of the primary fabric trend is parallel to debris stratification (Lawson 1979).

c. Roundness

Clasts are generally subangular to subrounded (Reheis 1975; Dreimanis 1976). Lawson (1979) found roundness varies according to the basal debris density.

3. GLACIAL-DEBRIS DEPOSITION

3a. THE TRANSFORMATION OF GLACIAL DEBRIS TO TILL

Glacial debris that has been deposited by glacier ice is till. In this thesis I use Lawson's (1979, p. 28) definition of till, i.e. "till is defined as sediment, deposited directly from glacier ice, which has not undergone subsequent disaggregation and resedimentation."

This definition is adopted because it only defines one main process, the direct deposition of debris from ice.

Dreimanis' (1982) definition of till, which is widely used, includes sediment gravity flow as one formative process of till. Since sediment gravity flow often follows

the release of glacial debris from ice (Boulton 1972a; Dreimanis 1982; Shaw 1982; Dreimanis and Lundqvist 1984) the flow process is an intervening, distinct process in some instances of glacial debris deposition. I believe a definition of till that includes the sediment gravity flow process is counter productive because one goal of glacial sedimentology is to distinguish flow deposits from tills. Using a till definition which includes additional processes makes such a task even more difficult.

3b. DEBRIS DEPOSITION FROM A BASAL ICE POSITION

LODGEMENT TILL

Processes of lodgement till deposition

Lodgement till is deposited beneath an actively sliding warm-based (temperate) glacier (Boulton 1972a; Kruger 1979; Shaw 1983). If the basal ice temperature is not above the freezing point of water (i.e. cold-based), pressure on the basal glacial-debris and -ice may depress the melting temperature of the ice and induce the warm-based conditions required for lodgement processes to operate (Dreimanis 1982).

Lodgement till forms when glacial debris in basal transport (Boulton 1975, 1976b) makes contact with an underlying, stationary substrate. If the resulting friction between the glacial debris and the substrate is greater than the strength holding the debris into the glacier the result is the glacial debris becoming pried- or sheared-off the glacier and being lodged into or against the substrate (Boulton 1972a; Boulton 1975; Shaw 1982; Muller 1983a). Muller (1983a) also proposes that lodgement till may be deposited by accretion of entire layers of basal debris instead of by the deposition of individual particles.

Characteristics of lodgement till

The characteristics of lodgement till are listed by author in Table 3.

Table 3. Lodgement till properties

Boulton 1972a (modern)

- massive, no stratified horizons
- may have drumlins on surface

Boulton et al. 1974 (modern)

- wisps of soft clasts
- reduced number of grains in 4 phi to 1 phi range

Rose 1974 (ancient)

- fabrics parallel to ice flow, low angle of dip

Marcussen 1975 (ancient)

- hard, dense till
- horizontal and sub-horizontal jointing
- few lenses of sorted sediments
- flutes or drumlins parallel to ice flow
- fabrics parallel to ice flow
- limited association with sorted sediment

Dreimanis 1976 (review)

- high compactness
- fissility or foliation
- shear planes which rise down glacier marked by sand or silt
- boulder pavements may be present
- fabrics parallel to ice flow, a-axes plunge up glacier
- also transverse fabrics
- local lithologies dominate

Boulton 1976b (review)

- may have isoclinal folds with flat lying axial planes
- jointing parallel to surface
- shear banding may be present
- may have boulder clusters
- no sedimentary banding
- may be any thickness, average may be large
- fluted or drumlinoid surface aligned in direction of ice movement
- strong parallel fabric, up glacier plunge, may also have transverse fabric
- small grain size
- located at base of sequence

Lawson 1979 (modern)

- till forms up-glacier of terminus

Broster et al. 1979 (ancient)

- well developed fissility in some places
- fissility, shear planes
- some pebble rich zones
- fabric parallel to ice flow or bimodal

Kruger 1979 (modern and ancient)

- compact, clayey till
- platy structure
- lenses consisting of boulders lodged against each other
- smudges, soft clasts of limestone smeared out
- some ellipical sand lenses
- fabric strongly developed parallel to ice flow
- smoothed pebbles with minor breakage
- consistent striation of clasts

Boulton and Deynoux 1981 (review)

- may be folded
- may be jointed
- boulder clusters
- no sedimentary stratification
- any thickness
- fabrics: strong, parallel to flow peaks with upglacier imbrication; may have transverse peaks

Eyles and Sladen 1981 (ancient)

- upper surfaces of fluvially deposited units are sheared off, some are folded and slickensided
- streamlined low relief surface, drumlinized
- fabric: preferentially oriented axes

Haldorsen 1982 (ancient)

- fissility
- fabric: strong a-axis orientation
- high proportion of fine grained material
- abraded (rounded) clasts
- bullet nose boulders

Dreimanis 1982 (review)

- less distantly derived material

Shaw 1982 (ancient)

- parallel to flow sole marks on base of till

Eyles et al. 1982 (ancient)

- sheared-out stringers
- smudges of coal and shale
- sand bodies below till have flat tops and concave bottoms
- drumlinoid upper surface
- streamlined boulders

Muller 1983a (ancient and review)

- fissility
- silt films on horizontal fracture surfaces
- lineation-like slickensiding on horizontal fracture surfaces
- thin layers of sorted sediment
- sorted layers drape clasts

Kruger 1984 (ancient)

- clasts with double stoss-lee form

Lodgement: till generally appears as a massive, hard, dense till (Boulton 1972a; Marcussen 1975; Kruger 1979)

with a wide range of thicknesses (Boulton 1976a). Lodgement till may contain isoclinal folds with flat lying axial planes (Boulton 1976b). Horizontal or sub-horizontal joints are often present in lodgement till (Marcussen 1975; Boulton 1976b). Other features related to joints are former shear planes marked by sand or silt which may rise down valley (Dreimanis 1976), fissility and foliation (Dreimanis 1976; Broster et al. 1979; Haldorsen 1981; Muller 1983a), or a platy structure (Kruger 1979).

Boulders within lodgement till often make contact with other boulders, thus forming horizontal planes of boulders (Boulton 1976b; Dreimanis 1976; Kruger 1979) termed boulder clusters (Boulton 1976b) or boulder pavements (Dreimanis 1976). Pebble-rich zones have also been observed in what is interpreted as lodgement till (Broster et al. 1979). Softer clasts of, for example, limestone, shale, and coal often appear as smudges or wisps drawn-out in the ice flow direction (Boulton et al. 1974; Kruger 1979; Eyles et al. 1982).

Lodgement till may contain a few lenses filled with sorted sediment (Marcussen 1975; Kruger 1979). Aside from such lenses, sedimentary banding (Boulton 1976b), major stratified horizons (Boulton 1972a), or internal stratigraphy (Boulton and Deynoux 1981) is not observed.

A lodgement till deposit has a surface expression of

low relief (Eyles and Sladen 1981) with drumlins or flutes aligned parallel to the former ice flow direction (Boulton 1972a; Marcussen 1975; Boulton 1976b; Eyles and Sladen 1981; Eyles et al. 1982).

Pebble fabrics are generally strongly oriented parallel to the former ice flow direction (Rose 1974; Marcussen 1975; Boulton 1976b), the predominant orientation usually plunges at a low angle up-valley (Rose 1974; Boulton 1976b; Dreimanis 1976). Fabric patterns transverse to former ice flow direction (Boulton 1976b; Dreimanis 1976) and bimodal fabrics (Broster et al. 1979) are less commonly observed.

Lodgement tills are described as clayey (Kruger 1979). This is a reflection of the high proportion of fine-grained sediment in the till (Boulton 1976b; Haldorsen 1982).

Pebbles in lodgement till are generally smooth or rounded (Kruger 1979; Haldorsen 1982) with only a minority broken (Kruger 1979). Numerous striated (Kruger 1979) and streamlined boulders are also present (Eyles et al. 1982; Haldorsen 1982). Most clasts are of locally derived lithologies (Dreimanis 1976; Dreimanis 1982).

Lodgement till is thought to be deposited upglacier from the glacier's terminus (Lawson 1979); as a result the till has only a limited temporal association with sorted sediments (Marcussen 1975). Lodgement till is also most likely to be located at the base of a vertical sequence of temporally related glacial deposits (Boulton 1976b).

The lower till surface may have ~~sole~~ marks parallel to the former ice flow direction (Shaw 1982). Fluvially deposited sand and gravel units directly below lodgement till often have flat upper surfaces and concave bases. The flat, upper surface is interpreted to result from shearing caused by an overriding glacier (Eyles and Sladen 1981; Eyles et al. 1982).

MELT-OUT TILL

Process of melt-out till formation

Melt-out till is formed from glacial debris released during either top- or bottom-melting of debris-rich ice (Boulton 1970b; Lawson 1979) which is neither sliding nor deforming internally in the area of debris release (Shaw 1983). Bottom melting of stagnant glacial ice results in subglacial melt-out till forming (Boulton and Deynoux 1981). This bottom melting can also occur under the base of a piece of stationary debris-rich ice which lies beneath a moving glacier (Boulton 1970b; Lawson 1981a). Surface melting of stagnant glacial ice also releases debris; if this sediment remains immobile it forms supraglacial melt-out till (Boulton 1970b; Boulton and Deynoux 1981). A confining force, such as overlying sediment, is needed if this debris is to remain immobile (Lawson 1981a).

The process of melt-out till formation is non-destructive, that is, the till retains the texture and fabric of the parental glacial debris (Boulton 1978; Lawson 1981a). Also retained intact during deposition are lenses of texturally and structurally distinct material, such as sand lenses (Lawson 1981a). Sand lenses are products of streams which carried meltwater through basal ice (Shaw 1979; Haldorsen and Shaw 1982).

During melt-out till formation interstitial ice within glacial debris melts and releases the debris. The fabrics and structures of this debris are more likely to be preserved in melt-out till when the ratio of glacial debris to interstitial ice is high (Lawson 1979).

Characteristics of melt-out till

The characteristics of melt-out till are listed by author in Table 4.

Table 4. Melt-out till properties

Boulton 1970b (modern)

- transverse fabrics in regions of compressive flow

Dreimanis 1976 (review)

- lower compactness than lodgement till
- laminae of silt or sand, approximately parallel to depositional surface
- parallel or perpendicular fabrics
- more distantly transported lithologies

Boulton 1976b (review)

- thin, likely less than 2 m
- no banding
- no folding, no faulting, rarely jointed
- parallel or perpendicular fabrics, major axes parallel to bed
- small grain size- and spatial-variation
- always overlain by overburden
- never exposed at surface
- directly above lodgement till or eroded surface

Boulton 1978 (review)

- multidirectional striae on clasts

Lawson 1979 (modern)

- basal melt-out till is very dense and impenetratable
- supraglacial melt-out till is loose and readily disaggregates
- generally massive appearance, with possible discontinuous layers, lenses, pods of texturally distinct material
- tabular geometry, meters thick, km long
- lacks distinct, continuous internal contacts
- strongly defined pebble fabric, minor scatter, low angle of dip
- primary mechanism of till formation near glacier's terminus

Kemmis 1981 (ancient)

- no vertical grainsize variation

Boulton and Deynoux 1981 (ancient)

- unlikely to exceed 2 m thick
- massive bedding
- internal folding rare
- rarely jointed
- sediment infillings of englacial tunnels
- most fabrics flow parallel, also flow perpendicular
- fabrics likely have large scale areal consistency

Broster and Dreimanis 1981 (ancient)

- silt laminae in till
- silt coatings around clasts

Lawson 1981a (modern)

- structureless to banded
- may have sub-horizontal or dipping planes of differing composition, texture, or color
- generally lacks concentrated zones of pebbles or larger sized clasts
- preferential systematic alignment of clasts into a regional pattern

Dreimanis 1982 (review)

- more englacially transported material than lodgement

Shaw 1982 (ancient and modern)

- incorporated clasts of unconsolidated subglacial sediment
- intrabeds of stratified material within till
- plano-convex lenses of gravel at base of till and stratified lens deposits within till
- fabrics unidirectional, parallel to ice flow

Haldorsen and Shaw 1982 (ancient and modern)

- unlithified, sorted and stratified sediment within till
- fabrics may be parallel to flow
- lithological and textural properties of englacial debris

Melt-out till is generally massive (Lawson 1979), although banded melt-out till has also been observed (Lawson 1981a). Melt-out till will often contain discontinuous laminae, layers, and lenses of texturally or compositionally distinct material preserved from the glacier ice (Dreimanis 1976; Lawson 1979; Lawson 1981a). Basal melt-out till is very dense and impenetrable relative to supraglacial melt-out till; supraglacial melt-out till is loose and disaggregates easily (Lawson 1979). In general, melt-out till is less compact than lodgement till (Dreimanis 1976).

Melt-out till does not contain fault displacements or internal folds and is rarely jointed (Boulton 1976b).

1 Concentrated zones of pebbles or boulders which are commonly observed in lodgement till are seldom seen in melt-out till (Lawson 1981b). Any concentration of stones

in melt-out till is a relict feature preserved from glacier ice and is not a product of lodgement processes (Lawson 1981b).

Melt-out till contains two types of inclusions or lenses composed of unconsolidated sediment. More commonly observed in melt-out till are lenses or intrabeds of unlithified, sorted, and stratified sediment (Haldorsen and Shaw 1982; Shaw 1982). These represent in-fillings of englacial tunnels (Boulton and Deynoux 1981). Less commonly observed are pieces of unconsolidated subglacial sediment originally incorporated by the glacier and now preserved within till (Shaw 1982).

Pebble fabrics of melt-out till usually have a unidirectional, strongly defined orientation parallel to the ice flow direction (Boulton 1976b; Dreimanis 1976; Boulton and Deynoux 1981; Haldorsen and Shaw 1982). The axis of major fabric orientation is either parallel to the base of the glacier or has a low angle of dip (Boulton 1976b; Lawson 1979). Some pebble fabric trends are oriented normal to the ice flow direction in regions of compressive flow (Boulton 1970b; Dreimanis 1976; Haldorsen and Shaw 1982). Regardless of a particular fabric site's alignment, groups of sites have a regional consistency (Boulton and Deynoux 1981; Lawson 1981a).

The grainsize of melt-out till also has a regional consistency with no (Kemmis 1981) or little spatial variation (Boulton 1976b) in the generally fine-grained till (Boulton 1976b). Melt-out till usually reflects more of the properties of englacial debris than lodgement till does (Dreimanis 1982). Because englacial debris is often derived far up-valley the textural and petrological composition of melt-out till also reflects the up-valley compositions of the source material (Dreimanis 1976; Haldorsen and Shaw 1982).

A deposit of melt-out till has a tabular geometry (Lawson 1979). A single deposit will most likely be less than two meters thick (Boulton 1976b; Boulton and Deynoux 1981) and can have a lateral exposure up to kilometers in length (Lawson 1979). Melt-out till is often observed to have the following field relationships with other types of deposits; the till may lie, directly above lodgement till (Boulton 1976b), above an eroded surface (Boulton 1976b), or above planar-based, concave upwards lenses filled with sand and gravel (Shaw 1982).

3c. DEBRIS DEPOSITION FROM A SUPRAGLACIAL ICE POSITION

Process of mudflow complex formation

Glacial mudflow complexes are here defined as interbedded glacial mudflows and glacial outwash sands and gravels. The mudflows originated from glacial debris released from ice. I propose this definition should replace Eyles' (1979) term "till complexes" on the basis that Eyles' definition of till is incompatible with the definition of till being used in this thesis.

The first stage in the formation of a glacial mudflow complex is the supraglacial release of glacial debris. This commonly occurs at the glacier's terminus (Lawson 1982) when upturned debris bands in temperate or sub-polar glaciers melt out of the ice (Boulton 1967; Boulton 1968; Kruger 1979). These upturned bands result from compressive ice flow thrusting basal debris upwards (Lawson 1982).

Another source of sediment for mudflows is glacial debris released from the high level of transport in polar or subpolar glaciers (Boulton 1978; Boulton and Deynoux 1981).

Glacial debris released at a glacier's terminus will remain stationary if the ice slope is small; in such a case, supraglacial melt-out till may form (Boulton 1970b). In addition, hummocky terrain may result (Boulton and Eyles 1979) if the glacier is already covered with supraglacial

debris. This scenario forms till variously referred to as lowered till (Lawson 1981a), supraglacial morainic till, or supra-till (Boulton and Deynoux 1981).

The developing hummocks may then provide enough topographic relief and slope to allow sediment gravity flow movement off of the hummocks (Kruger 1979; Boulton and Eyles 1979). Supraglacial debris released at a steep glacier terminus will definitely flow off the ice (Hartshorn 1958; Boulton 1967; Boulton 1968) and possibly onto ice situated at a lower elevation (Boulton 1972a). When this now buried-ice melts, folds and faults will develop in the overlying assemblage of debris-flow deposits (Boulton 1972a).

Debris flows at the glacier terminus usually flow onto proglacial outwash areas (Boulton 1968; Boulton 1976b; Boulton and Eyles 1979) and into topographic hollows (Boulton 1967). Diamicton which flows onto outwash areas will become sorted by meltwater streams (Boulton and Eyles 1979) and likely buried by the same meltwater stream's deposits (Eyles 1979; Boulton and Deynoux 1981). Subsequent debris flow and meltwater deposition produces a complex, interbedded sequence of the two deposits (Boulton and Deynoux 1981), termed glacial mudflow complexes in this thesis or till complexes by Eyles (1979) and Boulton and Deynoux (1981). These complexes are preserved when major outwash streams are situated at an elevation below mudflow

deposition (Boulton 1972a; Eyles 1979).

Glacial mudflow complexes account for only a small percentage of the total debris deposited by a glacier. Boulton (1978) estimates 30 to 100 times more material is released basally, upglacier from the terminus; although at ice margins, debris flows produce 50-75% of the deposits (Lawson 1982).

Mudflow complex characteristics

The characteristics of mudflow complexes are listed by author in Table 5.

Table 5. Mudflow complex properties

Hartshorn 1958 (ancient)

- till as lenses, wider than thick, lenticular beds
- voids in till
- till overlies sand and gravel or is intrastratified with sand and gravel

Boulton 1967 (modern)

- diamictos and gravels are interbedded
- may have interdigitations of diamictos and bedded clays and silts
- diamictos have isoclinally folded internal stratification
- diamicton bands have planar internal bedding
- complex internal structures when debris is let down on hummocky topography
- flows may be depleted in gravel

Boulton 1968 (modern)

- complex interdigitation of till and bedded silts, sand, gravel
- diamicton may contain wisps of sand which form flat lying isoclinal folds

- parallel or perpendicular fabrics depending on location within flow (diamicton)
- fabric oriented in direction of greatest surface slope
- sharp, planar interfaces between diamictons and stratified sediments
- associated with stratified deposits (meltwater stream deposits)
- complex overlies melt-out till

Boulton 1970b (modern)

- diamicton-flows overlie proglacial or ice marginal outwash sediments and lake sediments
- complex overlies till

Boulton 1972a (modern)

- beds folded when overlie glacial ice
- high angle reverse and normal faults when overlies ice
- planar and distinct contacts between diamictons and gravels
- complex overlies supraglacial melt-out till.

Marcussen 1973 (ancient)

- diamicton contains silt stringers and flat lying pebbles

Marcussen 1975 (ancient)

- diamicton and sand-gravel interbedded
- "loose, incoherent character"
- sedimentary structures indicative of slumping
- irregular surface topography
- irregularly shaped fabric diagrams

Boulton 1976b (review)


- intraformational folding
- may have parallel to surface jointing
- high angle faulting
- sedimentary banding present
- variable thickness, from very thin to very thick
- surface expression: slightly irregular or irregular hummocky ridges
- parallel or perpendicular fabrics, large within site variability
- considerable grain size variation throughout complex
- located top-most in a sequence of tills, often above outwash

Lawson 1979 (modern)

- sedimentary units have varied geometry, orientation, and dimensions; units often deformed
- laterally discontinuous strata
- diamictons may have sorted sediment cap

- massive to graded diamictons, may have gravel rich bases
- dimensions of complex, 2 m or less thick and less than 100's meters long
- rapid lateral and vertical texture variations
- upper and lower contacts of diamictons very distinct

Eyles 1979 (modern)

- 
- blocks and lenses of diamicton interbedded with outwash
 - massive structureless sand units present
 - faults observed
 - deformed stringers and lenses of fine grained sediment in diamicton
 - maximum observed thickness of complexes is 3 m

Kruger 1979 (ancient and modern)

- many layers and irregular lenses of variable composition
- loose, sandy diamicton
- irregular concentrations of boulders
- weakly developed, inconsistent fabrics
- large clasts oriented randomly relative to ice flow direction
- most pebbles are angular and broken

Boulton and Eyles 1979 (modern)

- diamicton interbedded with planar, matrix-supported outwash beds
- may contain deformed mud lenses
- association: rests on basal till, usually lodgement

Lawson 1981a (modern)

- desiccation cracks may be on top surface of diamictons
- graded, inverse to normally
- restricted dimensions
- polymodal fabrics, widely dispersed orientations about a poorly defined mean
- internal variation in coarser particle size fractions within diamictons
- most basal contacts non-erosional

Lawson 1981b (modern)

- flow induced deformation features may be present in diamictons
- clasts may be concentrated into layers, usually at base of a unit
- laminated silts and sands separate some of the diamicton units
- may have no aligned fabrics

Haldorsen 1982 (ancient)

- some areas of diffuse stratification in diamicton
- irregular lenses of fine sand in diamicton
- fabric trend parallel to local surface slope

Lawson 1982 (modern)

- diamictons may have sorted tops.
- gravel may be concentrated at base of diamicton units
- gravel concentration may vary lengthwise in diamictons
- fabrics range from no preferred alignment to parallel or perpendicular alignment

Haldorsen and Shaw 1982 (ancient and modern)

- clast orientations not systematically related to ice flow directions

Dejong and Rappol 1983 (ancient)

- interbedded diamictons, gravels, sands
- graded or ungraded diamictons
- poorly developed fabrics
- between and within fabric site variability is large
- variable sorting of matrix
- flat upper bed contacts, with lower gullied contacts

Mudflow complexes mainly consist of interbedded layers and lenticular-shaped lenses of diamicton and fluvially deposited sand and gravel (Hartshorn 1958; Boulton 1967; Boulton 1968; Marcussen 1975; Dejong and Rappol 1983). The layers and lenses are laterally discontinuous (Lawson 1979) and much wider than thick (Hartshorn 1958). Some of the lenses are deformed (Lawson 1979). Blocks of diamicton also occur amongst the interbedded deposits (Eyles 1979).

Deposition occurs in a dynamically active environment. This is reflected in the total folding of some beds (Boulton 1972a) and in high angle reverse and normal faults displacing a number of beds or lenses (Boulton 1972a; Boulton 1976b; Eyles 1979).

The internal character of diamicton units varies substantially depending on the exact flow mechanisms which deposited a particular unit. Internally, the diamicton units may be massive, bedded, graded, folded, or have small voids (Hartshorn 1958).

Bedding within diamicton layers includes planar internal bedding (Boulton 1967). The uppermost portions of some diamicton units are comprised of stratified sediments (Lawson 1979). Graded units may be inverse or normally graded (Lawson 1979). Folding is manifest by isoclinal folding of internal stratification (Boulton 1967). Disrupted internal stratigraphy of the diamicton units are often caused by let-down over buried ice in hummocky terrain (Boulton 1967).

Within diamicton units are lenses and smaller stringers filled with clay- to sand-sized sediment (Boulton 1968; Marcussen 1973; Boulton and Eyles 1979; Haldorsen 1982). These lenses and stringers are almost always deformed; deformation ranges from minor (Eyles 1979; Haldorsen 1982) to recumbent folds (Boulton 1968).

The dimensions of individual diamicton and sand-gravel units are variable (Boulton 1976b; Lawson 1979). Lawson (1979) found the general thickness of glacial mudflow complexes as a whole are 2 meters or less and the overall length is less than hundreds of meters. Eyles (1979) reports the maximum observed thickness is 3 m. The surface topography of recent mudflow complexes is irregularly-shaped hummocks or ridges (Marcussen 1975; Boulton 1976b).

Pebble fabrics of diamicton units usually have a poorly defined mean orientation (Lawson 1979; Kruger 1979; Lawson 1981a; Dejong and Rappol 1983) aligned parallel or perpendicular to the direction of debris flowage (Boulton 1968; Boulton 1976b; Lawson 1979; Lawson 1982). The fabrics can also have maximum orientations aligned parallel to the depositional surface (Boulton 1978; Lawson 1981a). Since this surface is not necessarily related to the direction of ice flow the pebble fabrics have a random relationship with respect to the ice flow direction (Kruger 1979; Haldorsen and Shaw 1982). Pebble inclination ranges from flat lying (Marcussen 1973) to vertical (Lawson 1981a). Pebble fabrics have large within (Boulton 1976b) and between (Dejong and Rappol 1983) site variability.

Glacial mudflow complexes have rapid lateral and vertical grainsize variations (Boulton 1976b; Lawson 1979). Gravel-sized material may be depleted within the diamicton

members (Boulton 1967) or vary in concentration throughout (Lawson 1982). Diamicton units may also have clasts concentrated along the base of the unit (Kruger 1979; Lawson 1979; Lawson 1981a; Lawson 1982).

The contacts between diamicton units and sand-gravel units are sharp, distinct, and planar when viewed at a macroscopic scale (Boulton 1968; Boulton 1972a; Lawson 1979). The upper contacts are usually flat (Dejong and Rappol 1983) and the lower contacts non-erosional (Lawson 1981a) or sometimes gullied (Dejong and Rappol 1983). Viewed at a more microscopic scale the contacts between diamictons and bedded clays and silts are interdigitated (Boulton 1967).

Glacial mudflow complexes are usually the top-most deposit in a sequence of tills (Boulton 1976b) and are directly associated with meltwater stream deposits (Boulton 1968). The complexes have been observed to directly overlie the following types of deposits; basally deposited till (melt-out till) (Boulton 1968) or lodgement till (Boulton and Eyles 1979); fluvially deposited sand and gravels (Hartshorn 1958) and lake sediments (Boulton 1970b) in a proximal glacial environment; and supraglacial melt-out till (Boulton 1972a).

II. SETTING, PREVIOUS WORK, AND METHODOLOGY

In this section the setting of the study area will be presented, including the physiography and bedrock geology of the area. The previous research in the Banff-Canmore area will also be reviewed. This is followed by a summary of the field and lab methods used in this study.

A. PHYSIOGRAPHY

The study area is located within the 4 km wide, mountain bound, broad, U-shaped, Bow River valley (Figure 1). The mountain peaks are at approximately 2750 meters elevation above sea level and the valley floor is at about 1400 meters above sea level.

Rutter (1972) determined that the Bow River valley was glaciated and that the glaciers flowed entirely within the valley. Postglacial erosion by the Bow and Cascade Rivers has removed quite a volume of what Rutter (1972) interprets as Quaternary-period sediments. These sediments, which outcrop in the Banff-Canmore portion of the Bow River valley, are studied in this thesis. Outcrops exposing the Quaternary sediments are situated along the Bow and Cascade Rivers, and also along the numerous tributary streams which enter the Bow River (Figure 2).

B. BEDROCK GEOLOGY

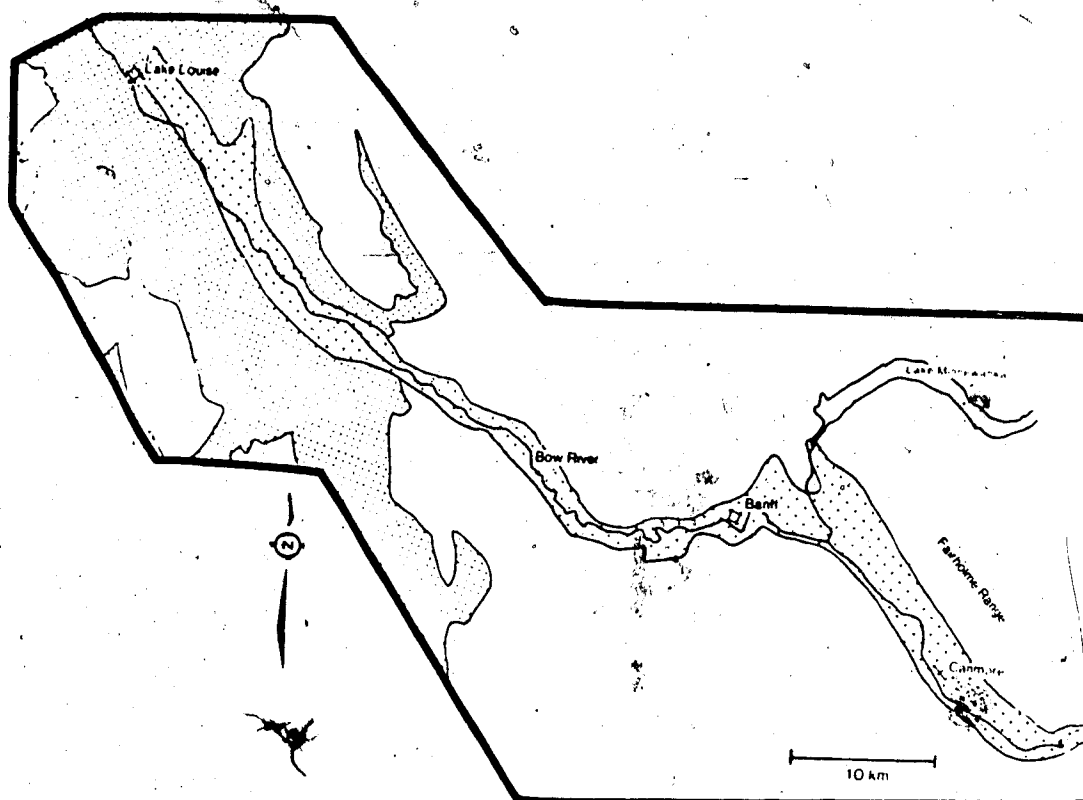
The bedrock exposed in the study area is dominated by Paleozoic-era carbonate rocks (Figure 3). Less extensive outcrops of sedimentary rocks ranging up to Lower Cretaceous in age also appear. Approximately 20 km upstream of the study area, along the Bow River Valley, are large outcrops of generally quartzitic Devonian and Precambrian rocks of the Gog and Miette groups, respectively (Figure 3). These quartzitic outcrops continue up-valley along the Bow river valley.

Relative to the study area's location, a more distant lithology refers to quartzite, and a local lithology refers to carbonates (limestone and dolomite). The distribution of the rock types in the Bow valley and in the tills within the Banff-Canmore area is very important with respect to the petrological analyses performed in this study.

C. PREVIOUS WORK

Only Rutter (1965a, 1972) has previously undertaken detailed studies of the unconsolidated sediments in the Banff to Canmore portion of the Bow and Cascade River valleys. (See Rutter 1965a for references to very early general studies of the area.) Rutter's study included the

Bedrock geology of the Bow River valley



LEGEND

- Quartzite-dominant bedrock. Precambrian and Cambrian.
- Carbonate-, sandstone-, chert-, shale-, siltstone-, and coal-dominant bedrock. Middle Paleozoic and Mesozoic.
- Un lithified sediments. Quaternary.

Figure 3. Bedrock geology of the Bow River valley between the towns of Lake Louise and Canmore (after Wit 1975).

Powerhouse and Carrot Creek sections. Based on observations at these and other outcrops he established the Quaternary stratigraphy and presented a glacial geological history for the Banff-Canmore area.

Rutter (1972) recognised a 30 meter thick till overtop of at least 11 meters of well sorted gravels at the Powerhouse section (Figure 2). At the Carrot Creek section (Figure 2) he observed a thinner till (1.5 m) overlying 2.8 meters of what may be mudflows. Gravels were observed along the base of the Carrot Creek section. Finally, he also recognised surface landforms above the Powerhouse section in the form of drumlins parallel to the inferred direction of glacial flow.

Rutter (1972) proposed a Quaternary geological history for the Banff-Canmore area of Alberta based on his observation of the area's stratigraphy and sedimentary deposits. He interprets the lower gravels at the Powerhouse section as representing glacial outwash deposited from a retreating valley glacier. The earlier advance of the retreating glacier, which was responsible for the lower Powerhouse section gravels, is termed the pre-Bow Valley advance. The till at the Powerhouse section is interpreted to represent a major glacial advance down the Bow Valley and is termed the Bow Valley advance. Apparently, the glacier which deposited the Bow Valley till then retreated up-valley to the Powerhouse section area, based on the fact

that only one till occurs there. At some time following this retreat and standstill of the glacier's snout, the glacier re-advanced down the valley and deposited a thin layer of till. Rutter calls this final ice advance into the Banff-Canmore area the Canmore advance.

D. FIELD METHODS

Field work was performed during June to August, 1983 and in June and August, 1984. A variety of techniques were employed to collect the field data. One of the first steps was to locate pertinent outcrops. Rutter's (1965a) study gives the location of the Powerhouse and Carrot Creek sections, other sections were spotted from highway 1. Airphotos were also used to locate additional outcrops.

Once outcrops were located in the field they were mapped by laying a metered grid line along either the top or bottom of the outcrop, thereby establishing a horizontal scale. The exposure's dimensions were then drawn to scale on square-ruled graph paper. The outcrop's sedimentary units were identified and drawn on outcrop maps, as were contacts between units and all pertinent features of the units. The compass orientations of the contacts and features were also recorded.

While examining an outcrop in detail, written

descriptions were made of all observations. The outcrop's shape, orientation, composition, and sedimentary structures were described. Also described were features such as sediment-filled lenses within diamicton or diamicton blocks within a sorted-sediment matrix.

The contacts between sedimentary units were described in detail. Noted were the contact's orientation, sharpness, and distinction. The contacts were also excavated to see if any sedimentary structures such as flutes were present on the contact's surface. In addition, pebbles which intersected the contacts were examined for facets or striations as their presence may indicate relative movement along the contact.

Sediment was sampled for laboratory analysis. Materials sampled included diamicton matrix, the sediment fill of lenses or inclusions within the diamicton, and sediment from distinct units composed of sand and gravel. Individual sample volumes were about 0.5 liters. Samples were collected in order to determine the sediment's grain size distribution and to determine the roundness and petrology of certain size fractions. Samples were collected in vertical increments up an exposure and in horizontal increments along an exposure so that analysis could reveal if changes in the sediment occurred throughout an outcrop. Weathered sediment was scraped away from the outcrop prior to sample collection to ensure only unaltered

sediment was obtained. Sample locations were marked on the outcrop sketch and on the airphoto of the outcrop.

Pebble fabrics were measured on pebble-sized clasts (Wentworth scale) within the diamicton units. Fabrics provide information about the genesis of the diamicton. Pebble fabrics were measured at numerous sites along an exposure to reveal any horizontal changes in the diamicton's fabric. At outcrops where the diamicton is thick, fabrics were measured in a vertical succession at numerous locations; fabric sites were usually located near the top, middle, and bottom of the unit. Two fabric sites were selected at thinner exposures at locations about one-third and two-thirds above the unit's base. The fabric sites' locations were also marked on outcrop sketch maps and airphotos.

Pebble fabrics were recorded by measuring the trend and plunge of the long axis of the first 50 pebbles meeting selection criteria. To meet the criteria a pebble had to have a ratio of longest-: intermediate-: shortest-axis of 2:1:1. The pebble orientation was measured using a Silva (brand name) compass with a built in dip meter. Rose histograms were plotted and eigenvectors and eigenvalues were calculated for each fabric site with a computer program provided by Dr. H.A.K. Charlesworth of the Department of Geology, University of Alberta.

E. LABORATORY METHODS

Laboratory analysis consisted of analyzing sediment samples collected in the field as a means to yield additional data.

Granulometric analysis was performed on diamicton matrix samples (less than 2 mm fraction) and also on sand and gravel samples. Grain size analysis of the diamicton matrix was undertaken to help quantify the diamicton matrix. The resulting grain size parameters can aid interpretation of the diamicton's genesis. Size analysis of the sand and gravel units was done mainly to determine the samples' mean grain size for classification purposes.

The American Society for Testing Materials (ASTM) (1964) procedures were followed in performing the diamicton-matrix grain size analysis (hydrometer method). The procedure utilized in this study deviated slightly from ASTM (1964) methodology. The temperature of the control cylinder during each hydrometer reading was used in conjunction with ASTM (1964) temperature correction factors to compensate for the lack of a constant temperature water bath. The sand, silt, and clay percentages of the diamicton samples are listed in Appendix A.

Grain size analysis of the sand and gravel samples was performed by passing the samples through standardized wire mesh sieves. A Ro-Tap machine was used to shake each stack

of sieves for approximately 15 to 20 minutes.

Calculation of graphic statistics required grain size phi values at various cumulative percentages, (Folk and Ward 1957). This data (Appendix B) was read off of the cumulative grain size curves. The graphic statistical parameters calculated were Graphic Mean (Mz), Inclusive Graphic Standard Deviation (SDI), Inclusive Graphic Skewness (SKI), and Kurtosis (KG) (Appendix C). All the formulae used are from Folk and Ward (1957).

Calculation of the graphic statistics required all phi percentile values to be read directly from the cumulative curves with the exceptions of some phi values for $\phi 5$, $\phi 85$, and $\phi 95$. About 20% of $\phi 5$ and $\phi 85$, and 75% of the $\phi 95$ values had to be determined by extrapolation from the cumulative curve itself. This was necessary because in some cases the portion of the curve based on laboratory data did not extend to the ordinates of $\phi 5$, $\phi 85$, and $\phi 95$.

Roundness values of each sample were used to characterize and aid in establishing genetic interpretations of the facies the samples represent. Roundness of the 1-2 mm carbonate grain size fraction was determined as follows.

For diamicton samples the 1-2 mm size fraction remaining after wet sieving the hydrometer fraction was used. For sand and gravel samples the 1-2 mm size fraction following dry sieving was used. The 1-2 mm fraction of

grains was quartered until about 75 to 100 grains comprised each quarter. The first fifty carbonate grains encountered were then picked from the pile. These 50 grains were placed one at a time under a binocular microscope and visually compared to Krumbein's (1941a) roundness chart. The grain's roundness was recorded and the procedure repeated until all 50 grains were assigned a roundness value. A roundness value for the sample is the average roundness of the 50 grains. Smaller roundness values are more angular than larger numbers. The roundness value of each sample is listed in Appendix D.

Petrology was used to characterize and help correlate units. Petrology of the very coarse sand fraction was determined by staining a sample's 1 to 2 mm grain size fraction with an Alarazine-red carbonate stain. The stained and dried fraction was quartered. Every grain's petrology within the quarter was identified under a binocular microscope; this usually consisted of 150 to 200 grains. Identification was aided because carbonate grains acquired a red stain. The petrological composition of each sample is listed in Appendix E.

III. GLACIER FLOW-LINES AND FLOW CELLS

This chapter introduces the concept of glacier flow-lines and flow-cells. This concept is discussed here because flow-lines and flow-cells are referred to many times throughout the remainder of the thesis.

A. INTRODUCTION AND DEFINITION

An explanation of the concept of glacier flow-lines is presented at this point so that the reader will be familiar with the concept when it is referred to in the following sections. A glacier flow-line is defined here as the path delineated or traced by a point in glacier transport. In this thesis flow-lines will be considered primarily in map view. Map views are two-dimensional projections of the glacier's flow in the horizontal plane.

Glacier flow-lines are useful in two ways. First, they provide a reference-line or trend for measured diamicton fabric orientations. A reference line is needed to determine if a fabric trend is related to either the former ice flow trend, a relation expected in tills, or if the fabric trend is totally unrelated to ice flow directions as is expected in debris flow fabrics. Secondly, glacier flow lines establish the glacier flow-cell boundaries in a valley glacier. Flow-cells (reconstructed) are defined here

as regions of equal flow behavior. These reconstructed flow-cells are delineated by reconstructed flow-lines which have the same trends, but not the same locations, as the reconstructed flow-lines shown in Figure 4. This is an idealistic, simplified definition of flow within a glacier undergoing extending flow.

The following section describes how the flow lines and flow cells were reconstructed.

B. GLACIER FLOW-LINE AND FLOW-CELL RECONSTRUCTION

The direction of extending flow in valley glaciers is mainly parallel to the bounding valley walls (Raymond 1971; Robin and Millar 1982). As a result, the flow-lines of glaciers with extending flow have smooth paths down the valley. Extending glacial flow is hypothesized to have existed during glaciation throughout most of the study area. This is based on the large scale bedrock-controlled topography of the valley and the lack of any major obstructions downstream of Tunnel mountain which could have prevented extending, valley-trend-parallel ice flow.

Former glacial flow lines are reconstructed as follows. A central valley flow-line is drawn by joining all points which bisect valley-normal lines joining bedrock topographic contours of equal elevation on opposite sides

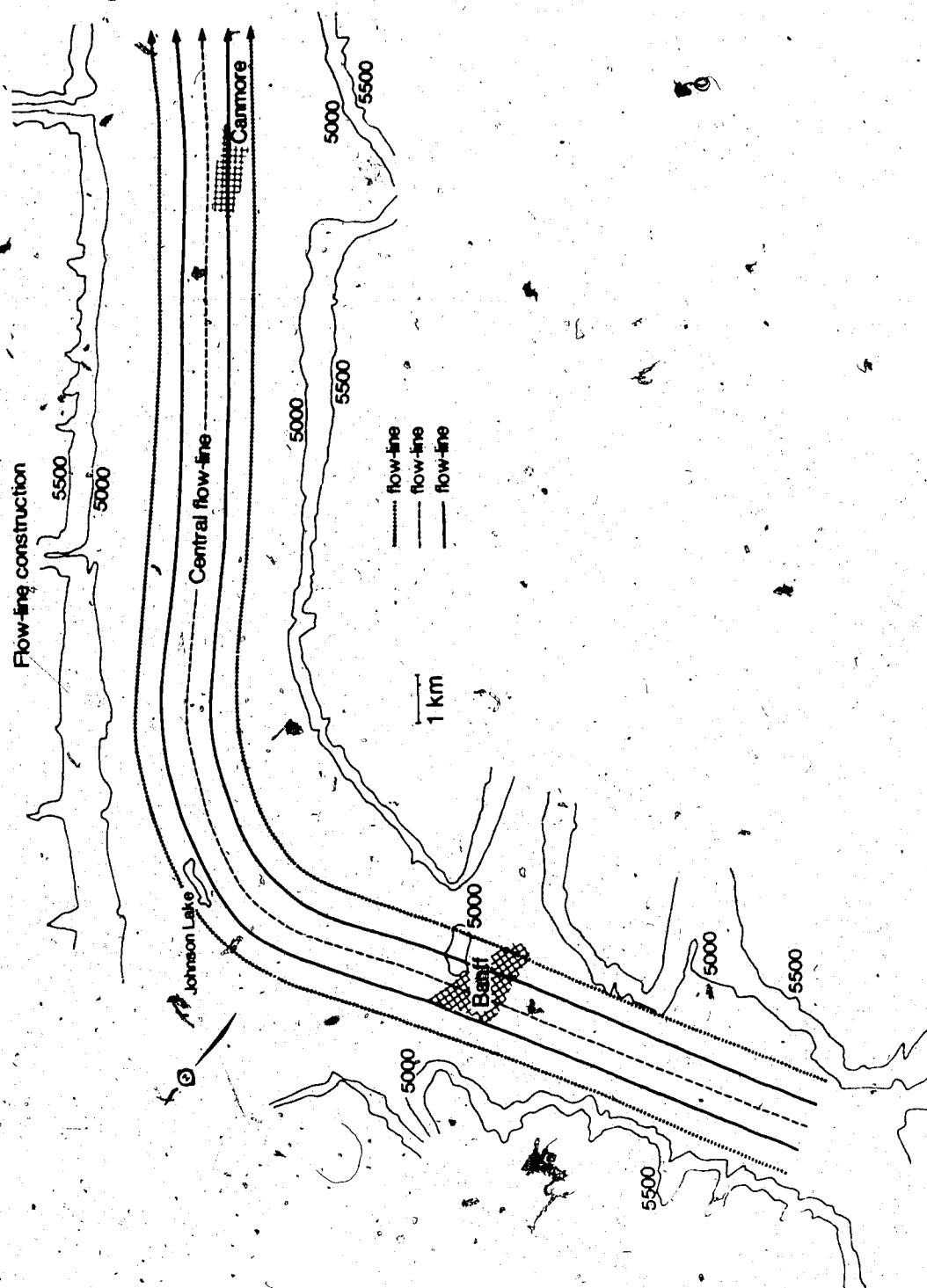


Figure 4. Reconstructed glacier flow lines.

of the valley (Figure 4). Additional flow-lines are then reconstructed by subdividing these valley-normal lines into different proportions and joining the equal points along the valley's length.

IV. FACIES DESCRIPTIONS, INTERPRETATIONS, AND DISCUSSIONS

Observations and descriptions of the sedimentary deposits in the Banff-Canmore area are presented in a facies-type format. Facies is "the aspect, appearance, and characteristics" (Bates and Jackson 1980, p. 220) of the sedimentary units' field characteristics alone (Middleton 1978, p. 323). Facies are utilized in this thesis to impart simplicity to the great variety of deposits observed and to also aid formulating genetic interpretations of these deposits.

Each individual facies consists of sediment that has the same general characteristics. This results in outcrops which consist of only a few facies. Facies in this study are therefore large-scale features.

Facies boundaries are mainly defined by drastic property changes across horizontal unconformities. Some lateral facies changes also have been recognised. These are more subtle and are usually based on changes in sand-lens abundance or gravel-layer abundance.

Seven major facies are recognised in the study area. In this chapter each facies is described, interpreted, and discussed. In chapter V the seven facies will be considered together.

A. FACIES 1

FACIES 1 DESCRIPTION

The outcrops where facies 1 is exposed are illustrated in Figures 5a and 5b. (Appendix F lists the locations of the various facies in the study area.)

Facies 1 consists mainly of diamicton (defined on page 11) which is at least 10 meters thick. The diamicton is matrix supported, with many irregularly-shaped voids throughout the matrix averaging $1-2 \text{ mm}^3$ in volume.

The distribution of the less than 10-20 cm diameter cobbles is homogenous throughout the diamicton. Clasts with larger diameters are more abundant in the southeast portion of the facies exposure. The maximum projection planes of the larger elongated clasts often dip up to 45° . Small (<6 cm diameter) undeformed clasts of very soft brown shale also occur.

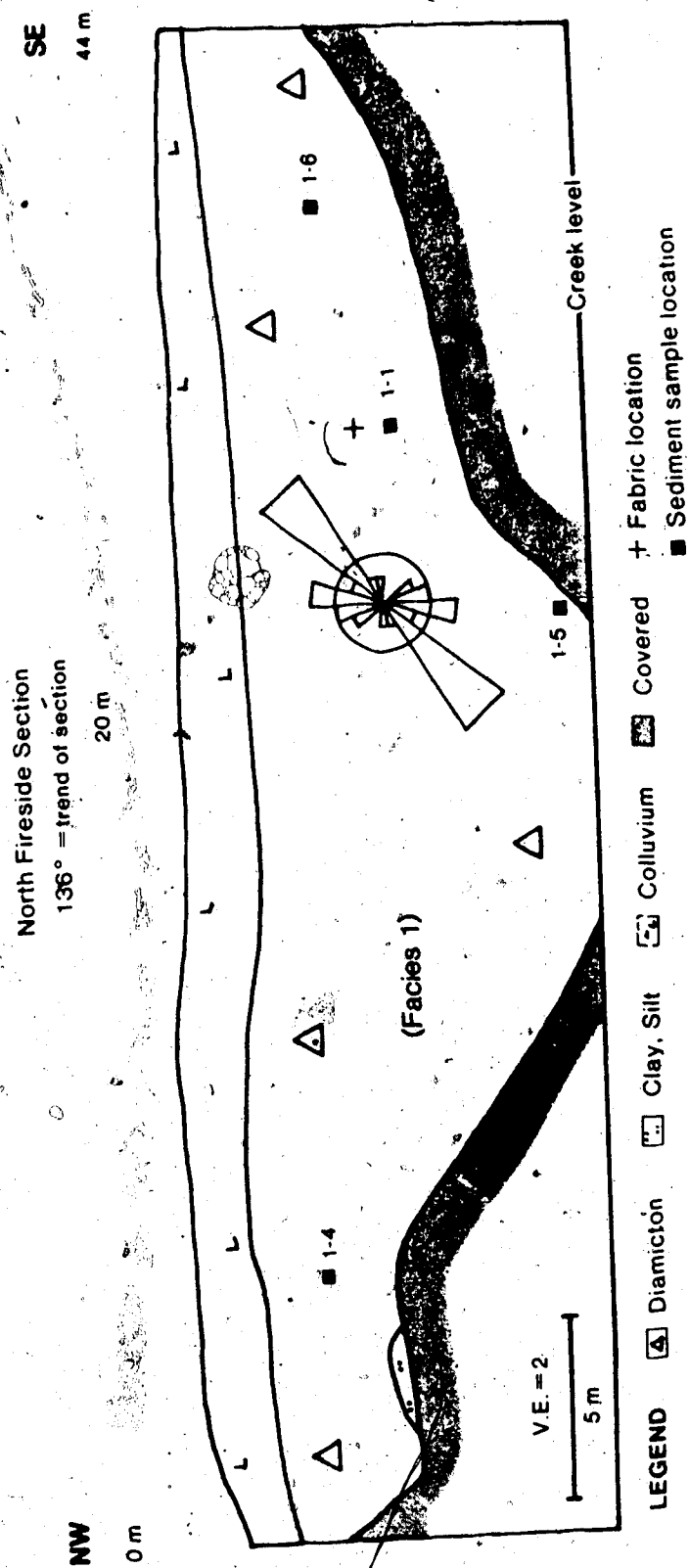


Figure 5a. North Fireside section.

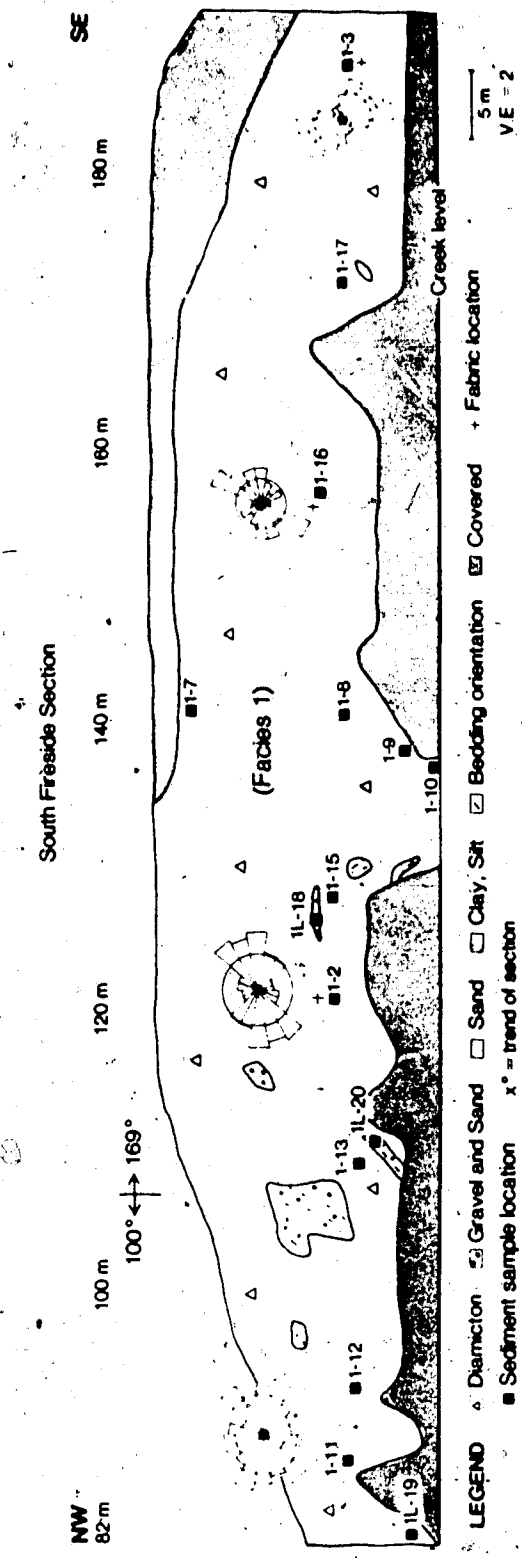


Figure 5b. South Fireside section.

Description of lenses within diamicton

Sediment-filled lenses, all enclosed within the diamicton, have a variable distribution. More lenses are present in the northwest half of the facies exposure. In this area about one lens is present per 3 m² area. The southeast portion of the facies outcropping contains one lens per 100 m² of area. The contact between the enclosing diamicton and lenses is sharp and distinct.

Most lenses are mainly sand-filled and have equidimensional or elongated-tabular shapes. Sand-filled lenses are generally larger than clay- and silt-filled lenses. Many sand-filled lenses cover about 75 cm²; some larger lenses have a range of dimensions of 50 cm X 100 cm to 5 cm X 400 cm. Sand-filled lenses are usually horizontally oriented with some lenses dipping up to 30°. Many of the sand-filled lenses contain medium sand and have matrix supported pebbles sporadically throughout. Pebble diameters range from 0.5 cm to 5 cm. A minority of sand-filled lens contain laminations of rippled clay; these same lenses also have 1 to 4 cm diameter pebbles randomly throughout.

Lenses filled with clay and silt are less abundant. These lenses have a variety of two-dimensional outcrop shapes, but most are round or elongated tabular. The majority of the elongated lenses dip 15° on average (range: 0°-50°). Dimensions of the clay- and

silt-filled lenses' two-dimensional exposures vary from about 1.5 cm X 1.5 cm to 20 cm X 100 cm (height X length). These lenses have compositions varying from massive clay, to clay with silt laminations, to silty clay with granule-sized clasts randomly spaced throughout. Some lenses have 1-3 mm thick rippled sand laminae set in a silty clay matrix.

A few larger lenses have dimensions up to 4 m X 3 m. Grain size within the larger lenses varies from clay to gravel. The largest lens (4 X 3 m) has a bed of open-work gravel near its base. The upper half is composed of, (i) massive sand with matrix supported pebbles (average pebble diameter is 4 cm) in one area and, (ii) bedded sand and fine gravel in another area. Within the upper part of this same lens rectangular-shaped blocks composed of silty clay are randomly throughout the bedded sand. These chunks have faint parallel laminations and nearly right-angled corners. Bedding in the lens is defined by slight grain size changes in regions composed of sand and gravel. Overall, bedding in the two largest lenses dips at about 25° away from the valley center.

FACIES 1 INTERPRETATION

This section explains how facies 1 formed. The general interpretation of facies 1 is the same as the general interpretation for facies 2, 3, and 4.

The following general interpretation of facies 1 contains three parts. Firstly it will be demonstrated that the sediment composing facies 1 originated from glacial debris; secondly, that the glacial debris was deposited directly from ice without undergoing resedimentation; and thirdly, that the deposition occurred basally (below ice). These three steps lead to the general interpretation that facies 1 is basal till.

PART 1: INTERPRETATION THAT FACIES 1 ORIGINATED FROM GLACIAL DEBRIS

Four characteristics of the sediments composing facies 1 lead to the interpretation that the sediment was transported as glacial debris into the study area by glaciers flowing down the Bow River valley. The four characteristics are: (i) Facies 1 is composed dominantly of diamicton (Figure 6). This suggests glacial derivation since Mills (1977) found that modern glaciers upvalley of the Banff region also transport and deposit diamicton. (ii) Carbonate clasts within the diamicton are usually striated

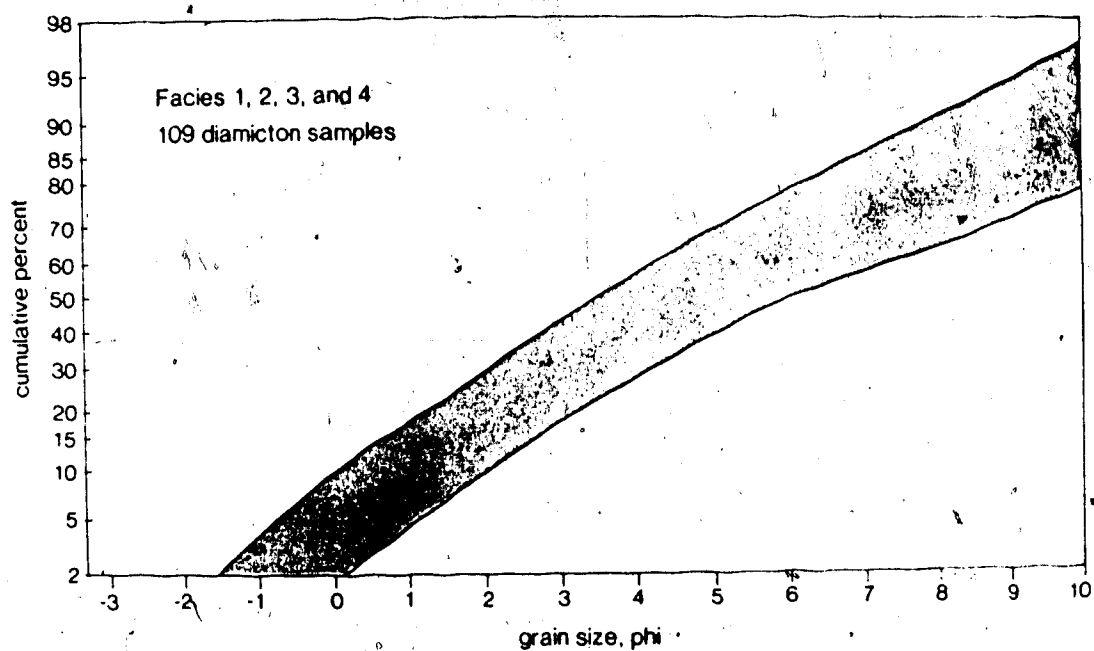


Figure 6. Facies 1, 2, 3, and 4 diamicton matrix (less than 2 mm) cumulative curves. Shaded area represents 109 curves.

in a consistent direction. Striated diamicton clasts are a direct product of glacial transport (Boulton 1978; Kruger 1979). (iii) The 1-2 mm grains in the diamictons are more angular than other sediments in the study area, for example the sorted sediments of facies 6 (Figure 7). Angular grains in a diamicton are usually a direct result of abrasion and crushing during glacial transport (Drake 1972). (iv) Quartzite grains are present in the diamicton (Figure 8) even though quartzitic bedrock is not present in the study area; quartzite does outcrop 22 km upvalley of the study area (Figure 3). Glacial ice is interpreted to have incorporated the quartzite grains upvalley of the study area and then transported the quartzite into the study area.

PART 2: INTERPRETATION THAT FACIES 1 WAS DEPOSITED DIRECTLY FROM GLACIAL ICE WITHOUT RESEDIMENTATION

Four characteristics lead to the interpretation that facies 1 was deposited directly from glacial ice without subsequent re sedimentation, thus forming till. The four characteristics are: (i) The diamicton pebble fabric orientations are generally aligned parallel, and less often perpendicular, to the reconstructed glacier ice flow-lines in the Bow Valley (Figure 9; Figure 10 shows facies 2, 3, and 4). This alignment implies the clasts were directly deposited from ice and not deposited by re sedimentation

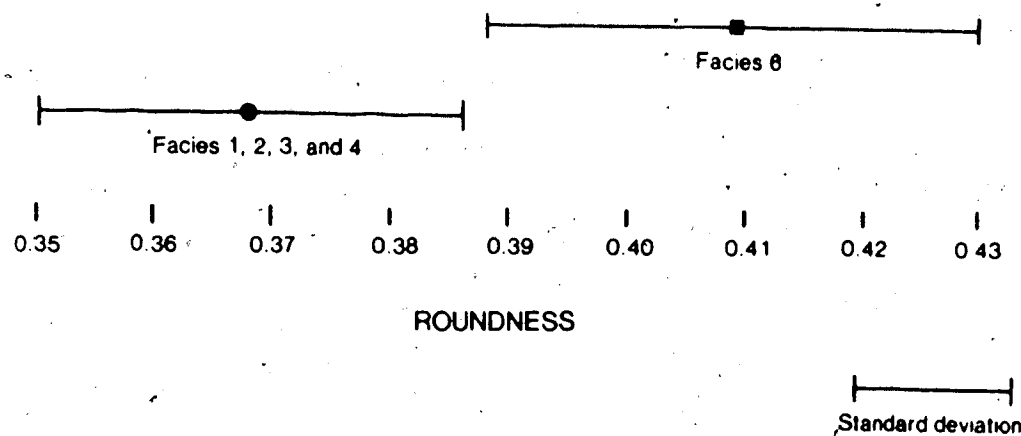


Figure 7. Roundness of the 1-2 mm carbonate grains in the diamicton matrix of facies 1, 2, 3, and 4 versus facies 6.

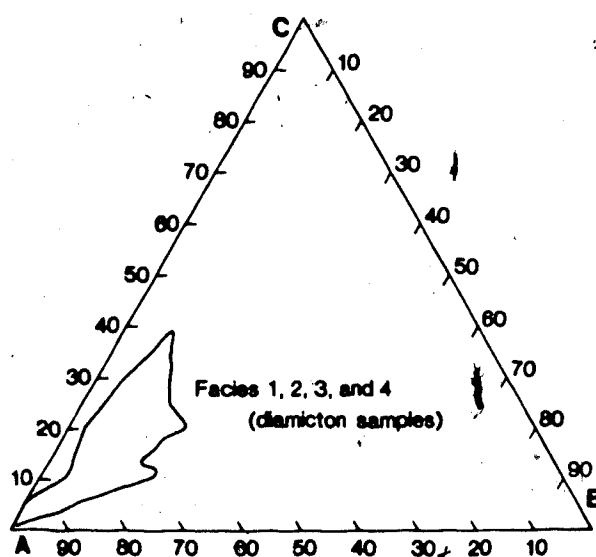


Figure 8. Ternary plot of facies 1, 2, 3, and 4 (diamicton samples). A=carbonates, cherty limestone; B=quartzite; C=chert, sandstone, siltstone, shale, and coal.

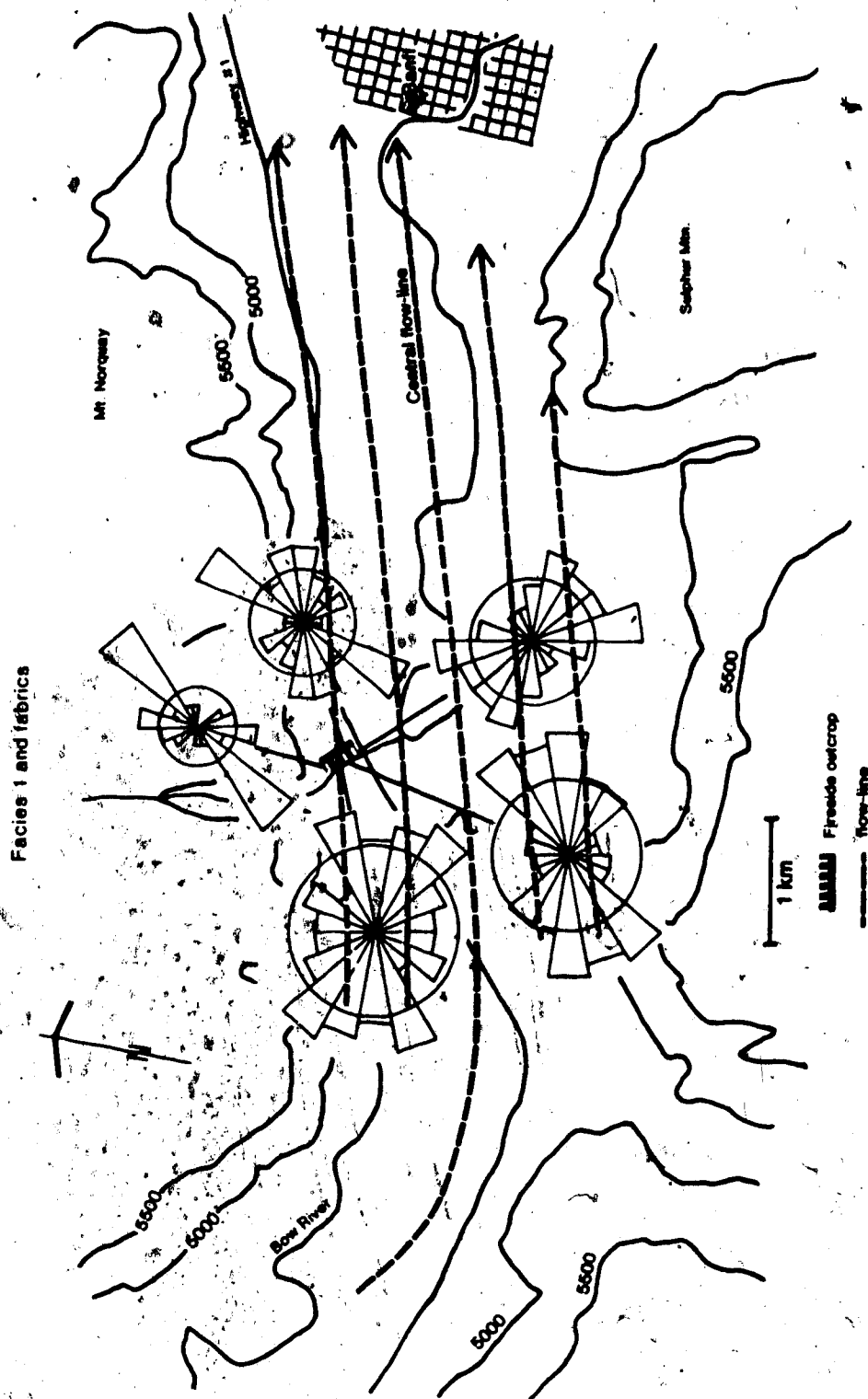


Figure 9. Diamicton pebble fabrics of facies 4 relative to reconstructed glacier flow lines.

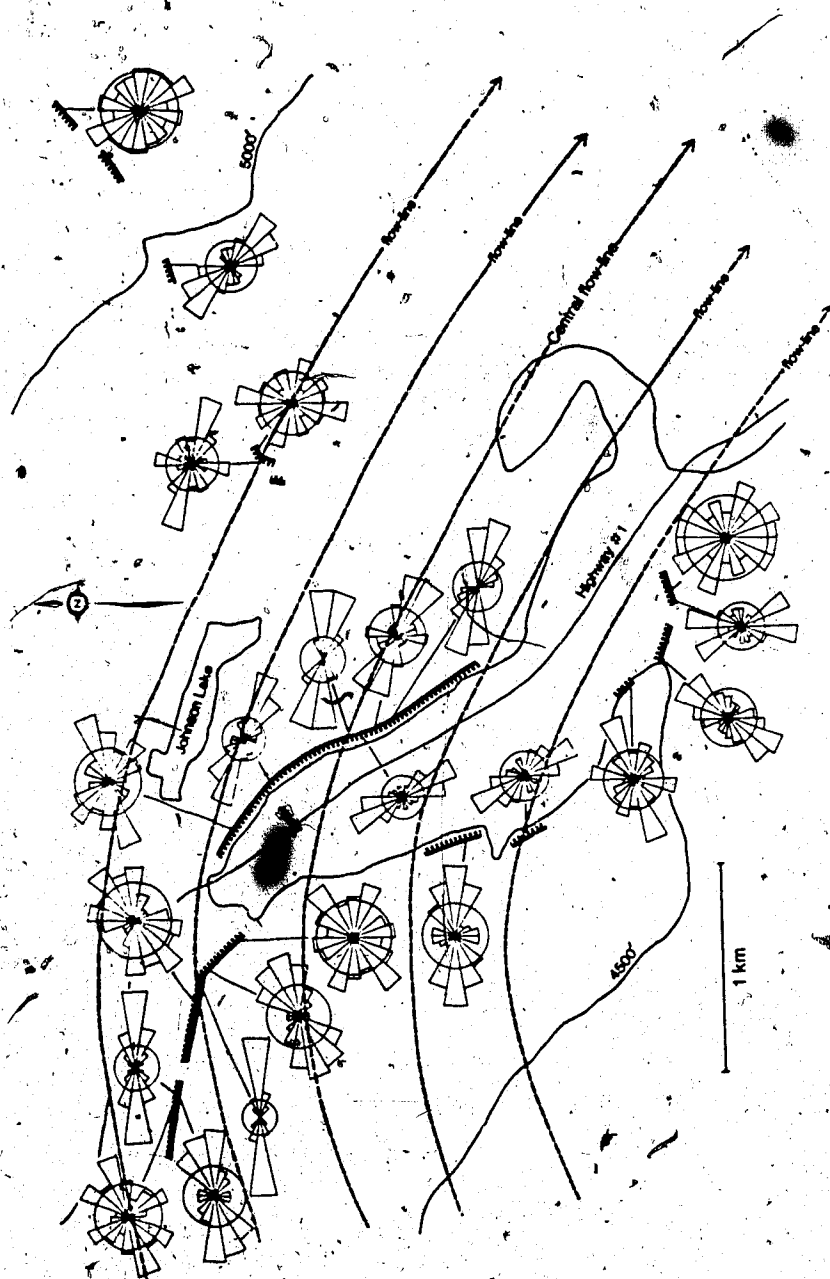


Figure 10. Diamicton pebble fabrics of facies 2, 3, and 4 relative to reconstructed glacier flow lines.

processes such as debris flows (Lawson 1981b). (ii) Facies 1 has a tabular geometry (Figures 5a and 5b), this is consistent with the geometry of glacially deposited diamictons (Lawson 1979). Alluvial fans constructed of diamicton debris-flows would have conical geometries (Bull 1972) related to side-valley streams. Debris flows from side valleys would also have a petrological composition of entirely carbonate clasts (the local lithology in the study area) without the observed upvalley-derived quartzite clasts being present. (iii) The facies comprised chiefly of diamictons are not interbedded with sand and gravel beds which indicates that no major resedimentation occurred after the glacial debris was released from ice (Hartshorn 1958; Boulton 1968). In addition, the internally stratified sand and gravel lenses within the diamicton would not have survived debris flow transport. (iv) Finally, the generally massive nature of the diamicton supports direct deposition from ice. Resedimentation would result in grading (Fisher 1971; Nardin et al. 1979), sorting of the flows (Pierson 1980), or the development of gravel-lag horizons (Lowe 1979; Pierson 1980). Such features are not observed.

The above paragraphs have shown that after the sediment was transported into the study area as glacial debris it was released from the glacier without undergoing resedimentation. This transport and depositional process forms till.

PART 3: INTERPRETATION THAT FACIES 1 WAS DEPOSITED BELOW GLACIAL ICE

Facies 1 is interpreted to have been deposited below glacier ice because the ground surface is smooth above the facies outcroppings. Smooth topography overtop of glacially derived diamicton suggests debris deposition was below glacial ice. If the glacial debris was released supraglacially hummocky topography would form, as was observed by Boulton (1967).

Several properties of the diamicton matrix, in addition to the geomorphic evidence, also suggest till formation occurred below glacier ice (in a basal position). The diamicton matrix is generally massive and has homogeneous, (i) mean grain size (Figure 11), (ii) sorting (Figure 11), and (iii) roundness (Figure 12). Such observed homogeneity is not preserved in a supraglacial environment where the effects of flowing water increases the mean grain size (Sharp 1949; Boulton and Eyles 1979), improves sorting (Boulton and Eyles 1979), and where frost shattering decreases roundness (Sharp 1949; Dreimanis 1976).

FACIES 1 DISCUSSION

It will be argued that facies 1, having properties of both lodgement till and basal till, is composed of sediments formed by a combination of both lodgement and melt-out processes. The facies is interpreted to be basal

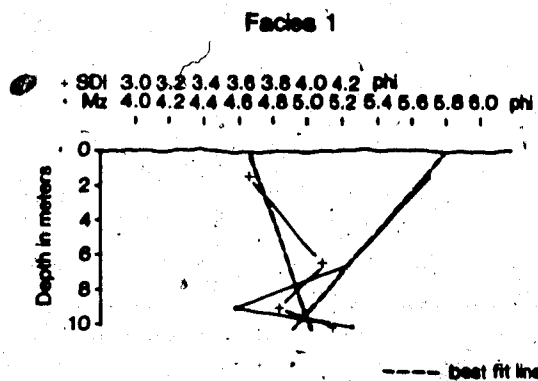


Figure 11. SDI and Mz of diamicton matrix along a vertical column through facies 1.

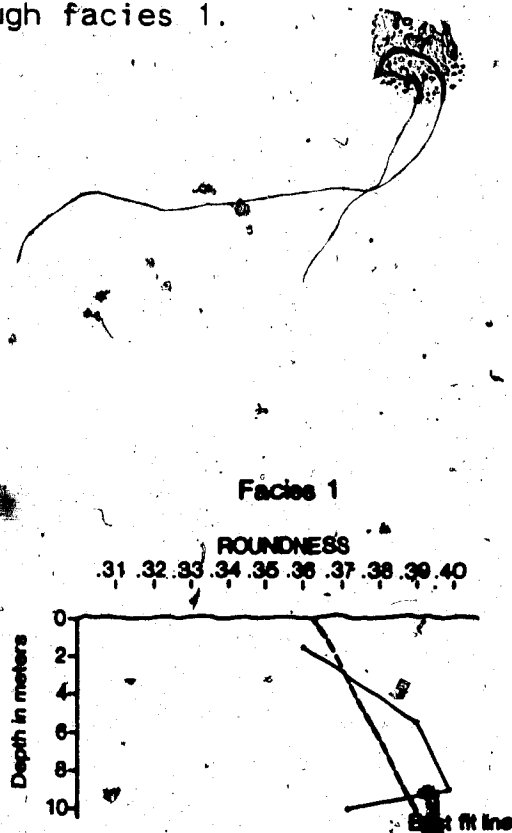


Figure 12. Roundness of 1-2 mm carbonate grains in the diamicton matrix along a vertical column through facies 1.

melt-out till emplaced as a series of successive basally deposited (lodged) glacial-debris layers which melted-out beneath a moving valley glacier.

1a. EVIDENCE WHICH CONTRADICTS LODGEMENT TILL, AND SUPPORTS BASAL MELT-OUT

The presence of abundant lenses filled with unconsolidated sediment indicate that facies 1 was not formed exclusively by lodgement till formation processes. According to Haldorsen and Shaw (1982, p. 261), "unlithified, ~~un~~stratified and stratified sediment", within diamicton does not occur in lodgement till. Additionally, the presence of non-smudged, clasts of soft brown shale within the diamicton eliminates formation by lodgement processes. In lodgement till soft shale clasts are either not preserved intact or are sheared-out (smudged) (Boulton et al. 1974; Kruger 1979). If facies 1 is not lodgement till, then basal deposition of melt-out till is the only basal depositional process remaining to explain the formation of facies 1.

Some attributes of facies 1 directly support a basal melt-out origin. The internally stratified lenses filled with unconsolidated sediment are interpreted as preserved englacial stream channels indicative of basal melt-out deposition (Haldorsen and Shaw 1982). The numerous small

voids in the diamicton also likely formed during basal melt-out when interstitial ice melted within the ice-rich basal debris (Lawson 1979) and the debris did not then completely infill the cavity created by the melted ice.

1b. EVIDENCE WHICH CONTRADICTS A BASAL MELT-OUT TILL ORIGIN, AND SUPPORTS A LODGEMENT TILL ORIGIN

In addition to the characteristics listed above supporting basal melt-out, facies 1 has two characteristics which preclude basal melt-out from a stationary glacier. Firstly, the facies is at least 10 m thick. This thickness is too great to have formed from the melt-out of basal debris-rich ice; basal debris layers in glaciers are usually less than 1 meter thick (Boulton 1972b). The thickness of facies 1 suggests the till was deposited by lodgement processes. Secondly, the petrology of a vertical column of samples does not show an upsection increase in quartzite, a more distantly derived lithology (Figure 13). Basal melt-out till commonly shows such an upsection increase (Hyvarinen *et al.* 1973; Haldorsen 1977).

The evidence indicates that facies 1 has properties which both support and reject formation by basal melt-out processes.

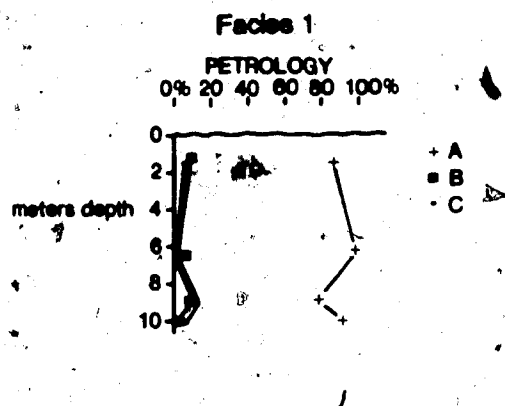


Figure 13. Petrology of 1-2 mm diameter grains along a vertical column through facies 1. A=carbonates, cherty limestone; B=quartzite; C=chert, sandstone, siltstone, shale, and coal.

2. COMPREHENSIVE DISCUSSION

The thickness and homogeneous petrology of facies 1 are interpreted to result from successive layers of basal, debris-laden ice becoming sheared off the base of an active glacier and then becoming stranded below the overriding glacier (Figure 14b). Such a stranding mechanism has been suggested by Muller (1983a). The layers of stranded, debris-laden ice then melt-out and attain characteristics of basal melt-out till. The thickness of facies 1 increases as layers of sheared-off basal debris build up beneath the glacier. During the build-up of layers the petrology remains vertically homogeneous by continually being a petrological subset of the lowermost debris in the glacier.

A bedrock projection extending into the path of the glacier is hypothesized to have acted as an obstacle to ice flow (Plate 1). The bedrock projection is thought to have caused basal shearing to occur above the glacier's base, shown diagrammatically in Figure 14b. This results in the base of the glacier shifting upwards to plane 2 (Figure 14b). When basal shearing occurred at this higher level, the ice and debris stranded below the new shear plane would melt-out, thus, producing basal melt-out till.

Geothermal heat and frictional heat of shearing likely supplied the energy required for basal melting. This melting lowers the plane of shear, i.e. the glacier's base, as shown in Figure 14c. Continued lowering of the active

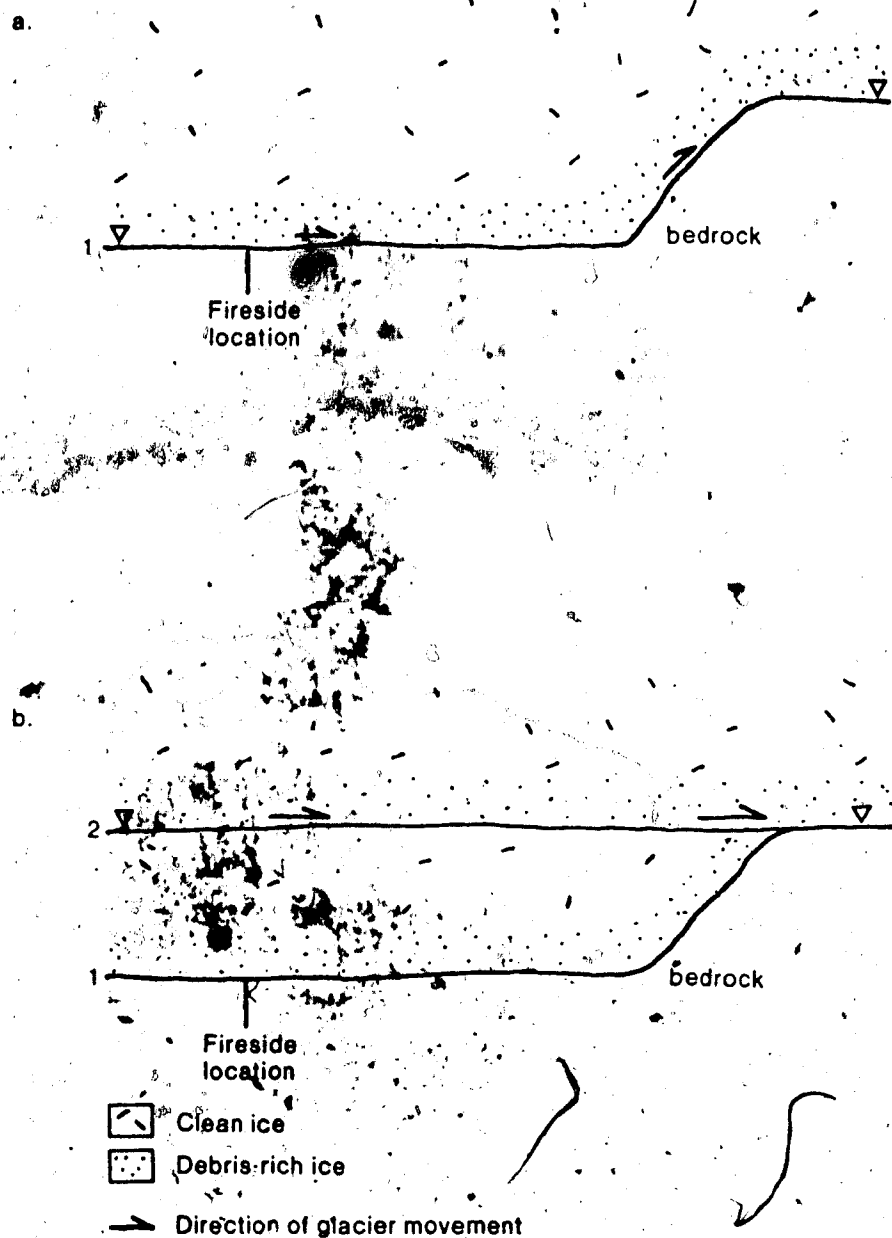
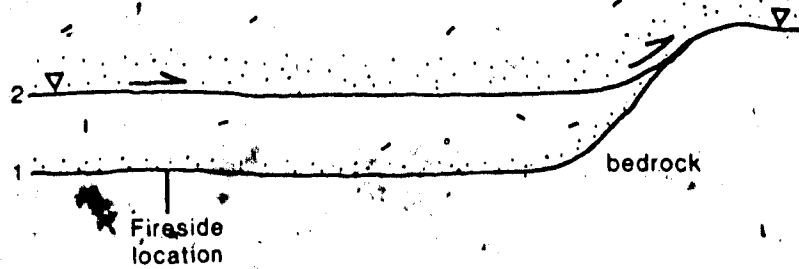


Figure 14. Facies 1 formation. (a.) At start of glaciation, glacier slides over bedrock. (b.) Debris-laden ice is sheared off the base of the active glacier. (c.) This layer of stranded ice melts-out and lowers the plane of basal glacial shear. (d.) A new plane of shear (#3) develops above the lowered shear zones.

c.



d.

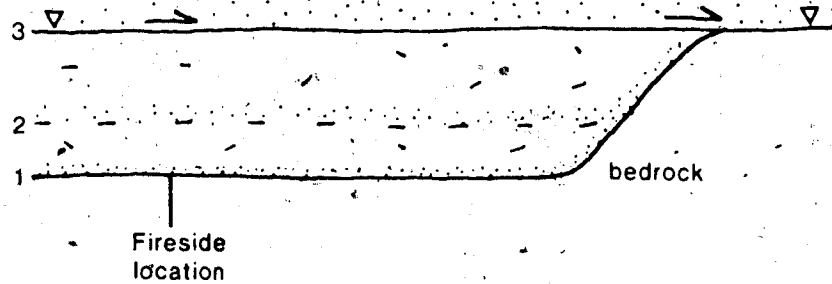




Plate 1. Airphoto of facies 1 and the bedrock protuberance. Dashed line = Facies 1 (Fireside outcrop), solid line = bedrock protuberance into the former glacier's path; glacier movement was downvalley from the Fireside outcrop toward the bedrock protuberance. Energy, Mines and Resources photo # A25671-51.

shear plane leads to increasing amounts of energy becoming expended ascending the bedrock projection. Once too much energy is required by the lower shear zone a new plane of shear develops at a higher elevation above the lower shear zone (Figure 14d). When a new plane develops at a higher elevation the lower shear zone is abandoned and basal melting of all ice below the new active shear (the new base of the glacier) proceeds.

This hypothesis requires ice to be continually melting below the active shear plane. Melting produces water which eventually forms the numerous clay, silt, sand, and gravel lenses. These lenses are products of sedimentation in tunnels developed within ice-rich areas of the stranded basal debris (Haldorsen and Shaw 1982). The ice-rich nature of the basal debris is also manifest in the numerous small voids within the diamicton matrix.

Many of the sand lenses are inclined or have disturbed internal bedding. The attitudes of these features are interpreted to be the result of differential melting of the debris-rich basal ice once it was stranded beneath moving ice. Differential melting is implied because many sand and clay lenses are still horizontal.

The maximum orientations of the diamicton pebble fabrics (Appendix G) reflect an upglacier plunge. This plunge is interpreted to be the preserved englacial pebble fabric of the basal debris. The plunging clasts reflect the

upglacier plunge of flow-lines that ascend the bedrock obstruction situated just down-glacier of facies 1 outcropping.

Traces of the shear planes which were active during formation of facies 1 are not preserved. Shearing was likely situated along horizons of least resistance which most probably would have been ice-rich layers. Evidence for this is not preserved. Pebble fabrics and sediment-filled lenses may have been influenced by differential movement along a shear plane.

Differential movement may have resulted in localised compression caused by non-perfect slip along the shear plane. Possible evidence is the one fabric with a mean orientation transverse to the ice-flow direction and the two oblique fabrics (Figure 9). Compression of ice can align pebble fabrics normal to the direction of flow (Boulton 1971). Compression may also have influenced sediment-filled lenses situated below a shear-plane. These lenses may have been folded as the moving glacier deformed the underlying sediment. A rolled and/or folded silt-filled lens (Plate 2) which probably had a surface in contact with a shear plane shows evidence of such deformation.

It has been shown that even though the initial genetic interpretations arising from the characteristics of facies 1 were contradictory, an understanding of how the facies formed is possible when the processes of lodgement and

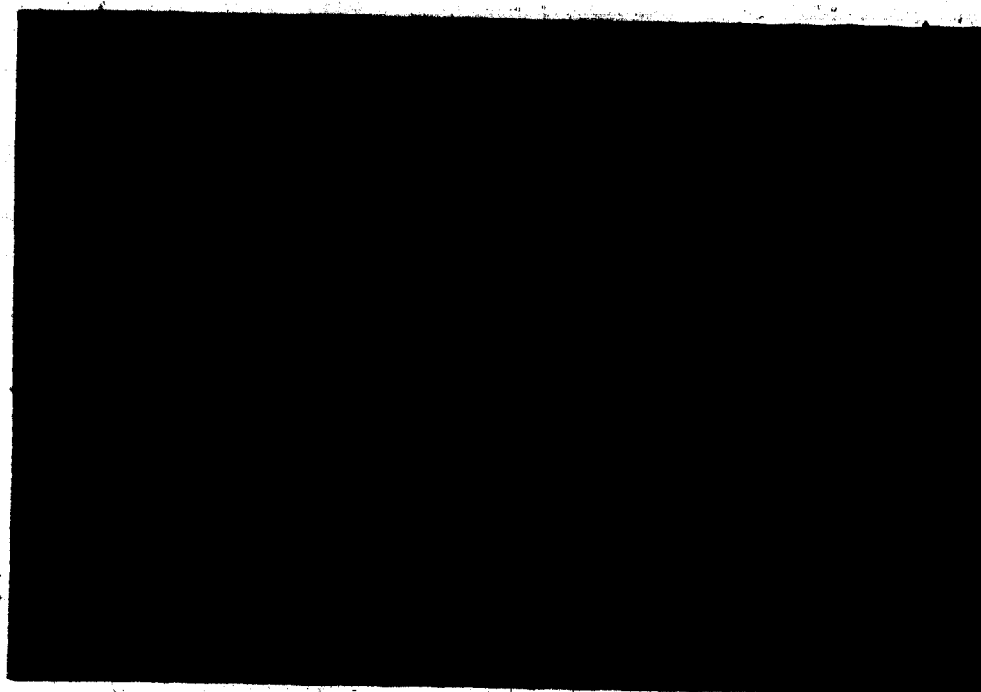


Plate 2. Folded silt-filled lens in facies 1. The lens occupies the middle one third of the plate, diamicton (area without numerous fractures) occupies the upper and lower portion of the plate. Photo width is approximately 1.5 m.

basal melt-out are combined into an interpretation where both processes operated. Dreimanis (1983) calls sediment formed by both processes lodged melt-out till.

B. FACIES 2

FACIES 2 DESCRIPTION

DIAMICTON DESCRIPTION

The diamicton is matrix supported and has an average clast diameter of 2-3 cm; the largest clasts vary from 20 to 40 cm. 5-10% of the diamicton's vertical surface area is composed of clasts larger than 1 cm diameter. Large isolated clasts are homogeneously distributed throughout. Facies 2 is about 24 m thick, and is laterally continuous in two localities (Figures 15a and 16) for 20 m and about 150 m respectively. Two types of inclusions occur within the diamicton; (i) thin gravel layers, and (ii) small sand lenses. Facies 2 overlies a gravel unit (facies 6). Contact between these two facies is distinct, sharp and horizontal; pebbles along the contact are not striated or faceted.

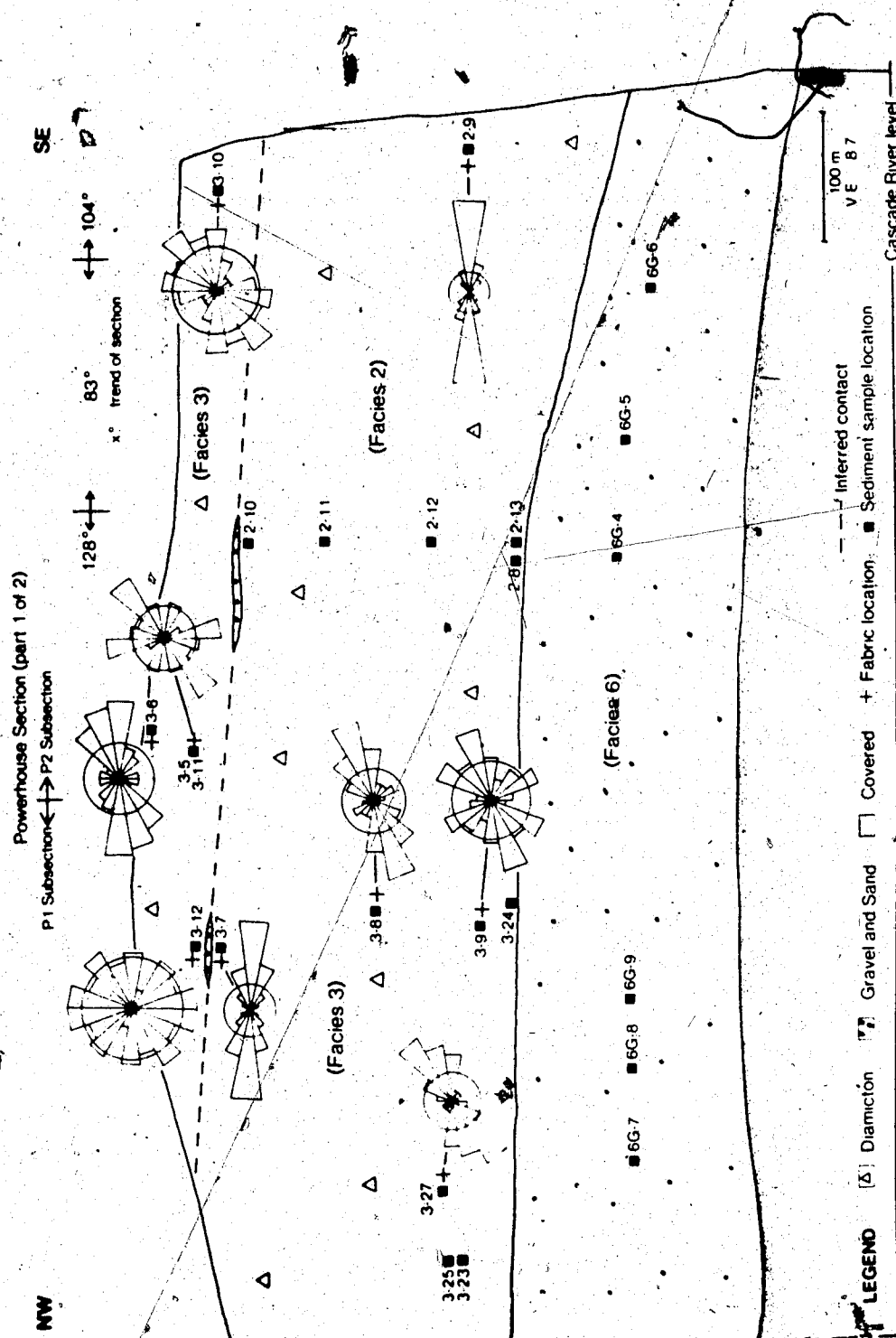


Figure 15a. Powerhouse section, part 1 of 2. Rose histograms are 20° diamicton pebble macrofabrics, N=50. All the rose diagrams in the thesis are diamicton pebble macrofabrics.

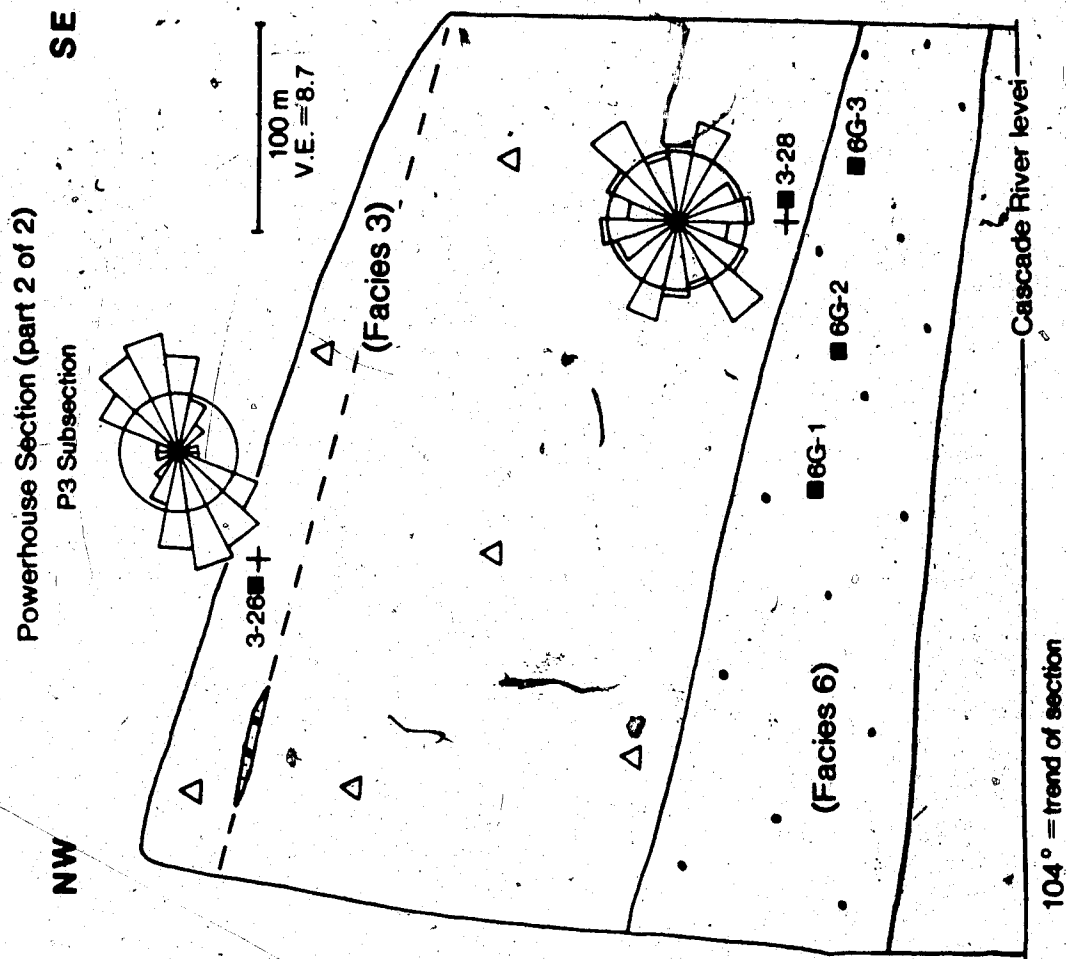


Figure 15b. Powerhouse section, part 2 of 2.

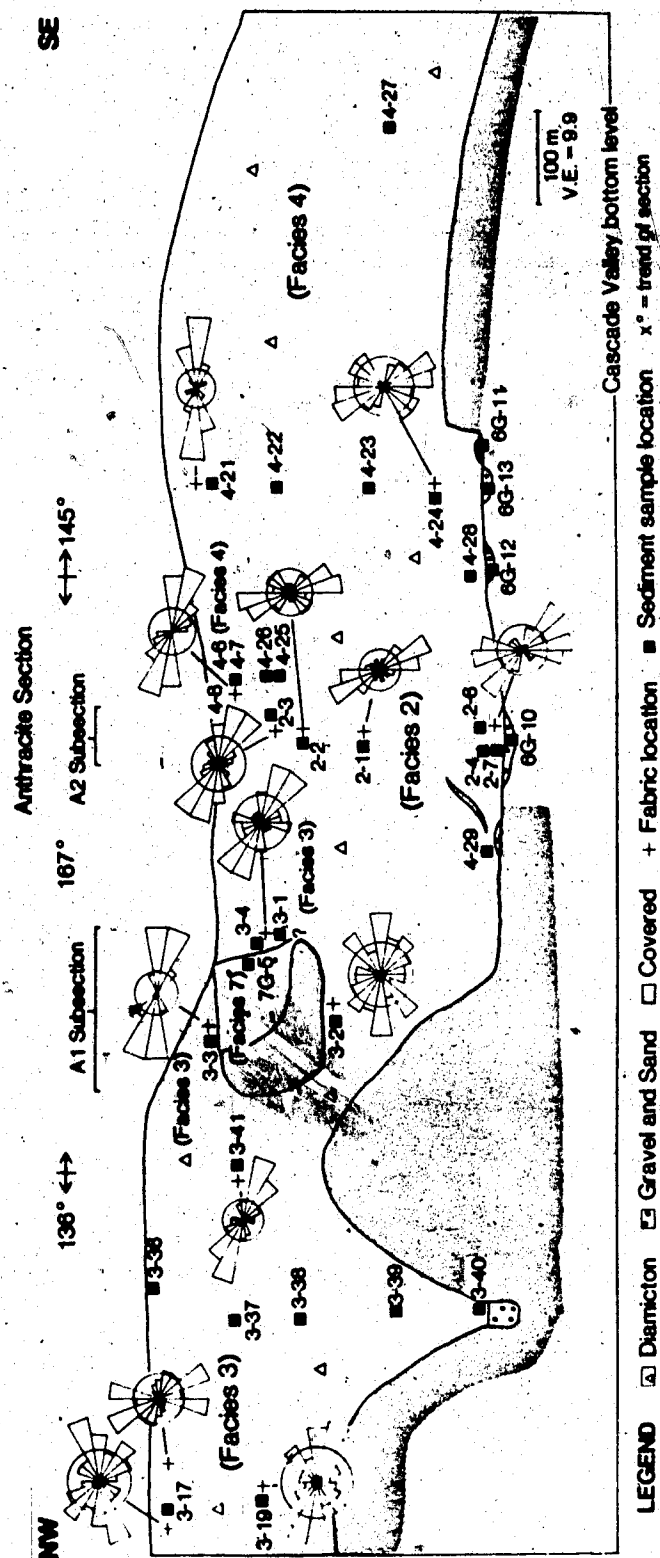


Figure 16. Anthracite section.

Descriptions of inclusions-features within the diamicton

Numerous elongated gravel layers are within the diamicton (Plate 3). They are tens of meters long; 2-10 cm thick, and have an average thickness of 5 cm. They dip to the east, dips vary from 0° to 10° . The layers appear as pebble-rich zones with little fine-grained material or matrix surrounding the clasts inside a zone. Clasts inside a layer vary in diameter from 0.5 to 2 cm. All the layers radiate unidirectionally from the uppermost region of the facies. In the upper regions of the facies and also in an up-valley location at the Powerhouse section the layers are flat lying. The dip and spacing between layers increases in down-valley direction, increasing to a maximum of about 10° . The layers occur in only the upper portions of the facies where the layers start to radiate. Down-valley where maximum dip occurs, the layers are present throughout the entire facies thickness. Vertical spacing between layers near the top of the facies is a few centimeters. Layer-spacing is 10 to 30 cm in the region where layers occupy the entire facies thickness.

Sand-filled lenses are also present. They cover less than 1% of the facies vertical-surface area. The lenses are horizontal and at least 4 times longer than thick.

Dimensions vary from 0.1-30 cm thick by 30-300 cm in length. Contacts between the lenses and diamicton are sharp; lenses pinch out. The sand within the lenses is



Plate 3. Elongated dipping gravel layers in facies 2 at the Powerhouse P2 subsection. Facies 2 is above the dashed line, facies 6 is below. Gravel layers extend the length of the photo and dip downwards from the upper right to the lower left of the outcrop. Downvalley is leftwards.

well- to poorly-sorted, and may contain matrix supported pebbles generally varying from 3 to 30 mm in diameter.

FACIES 2 INTERPRETATION

1. BASAL TILL INTERPRETATION

The sediment of facies 2 is interpreted to have been transported by a valley glacier and then directly deposited from the base of the glacier without any resedimentation occurring after deposition. Thus facies 2 is basal till. The evidence supporting this interpretation is the same as was given for facies 1 (page 64). Additional information supporting a basal till interpretation is the drumlinized topography above the facies (Plate 4). These drumlins indicate the underlying deposits most likely formed beneath a glacier (Muller 1974; Boulton 1976a; Menzies 1979). The type of basal till which makes up facies 2 is discussed in the next section.

2. LODGEMENT TILL INTERPRETATION

Facies 2 is composed of one of the two varieties of basal till, either basal melt-out till or lodgement till. Basal melt-out till is eliminated for the following reasons. (i) Facies 2 is too thick (24 m) to have been

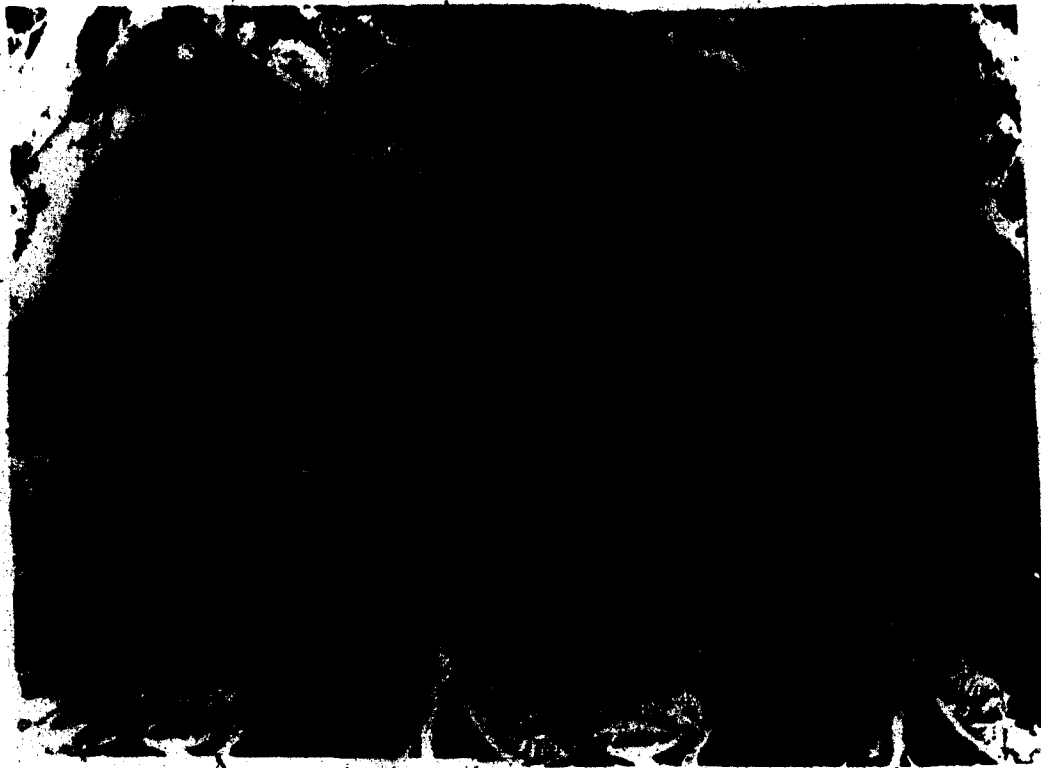


Plate 4. Stereographic airphotos of drumlinoid topography in the Powerhouse outcrops' vicinity. Drumlins trend from the lower left to upper right of photo. Dashed line is the location of the Powerhouse outcrops. Scale bar represents 1 km. Alberta Government photos # AS167 5103 163, 164.

deposited by the process of basal melt-out because melt-out till is usually only a few meters thick (Boulton 1976b; Lawson 1979). The possibility exists that facies 2 is composed of a number of separate tills which collectively add up to 24 meters of till. This is unlikely because only one depositional unit is observed. There are no unconformable internal contacts and the facies possesses homogeneous grain size (Figures 17a and 17b), petrology (Figure 18), and roundness (Figure 19). (ii) The petrology along a vertical column (Figure 18) is homogeneous, a property which basal melt-out tills do not have. Basal melt-out till shows an up-section increase in more distantly derived lithologies (Hyvarinen *et al.* 1973; Haldorsen 1977). (iii) Although not totally diagnostic, facies 2 has too few lenses filled with sorted sediment to be basal melt-out till; basal melt-out till usually has an abundance of such lenses (Lawson 1979; Boulton and Deynoux 1981). (iv) Again, not totally diagnostic, plano-convex lenses (Shaw 1982) are not present along the basal contact of facies 2. Plano-convex lenses are usually present along the lower contact of basal melt-out till (Shaw 1982). Therefore basal melt-out till is eliminated as the type of till composing facies 2. Since lodgement till is the only other possibility it follows, by elimination, that facies 2 is likely composed of lodgement till.

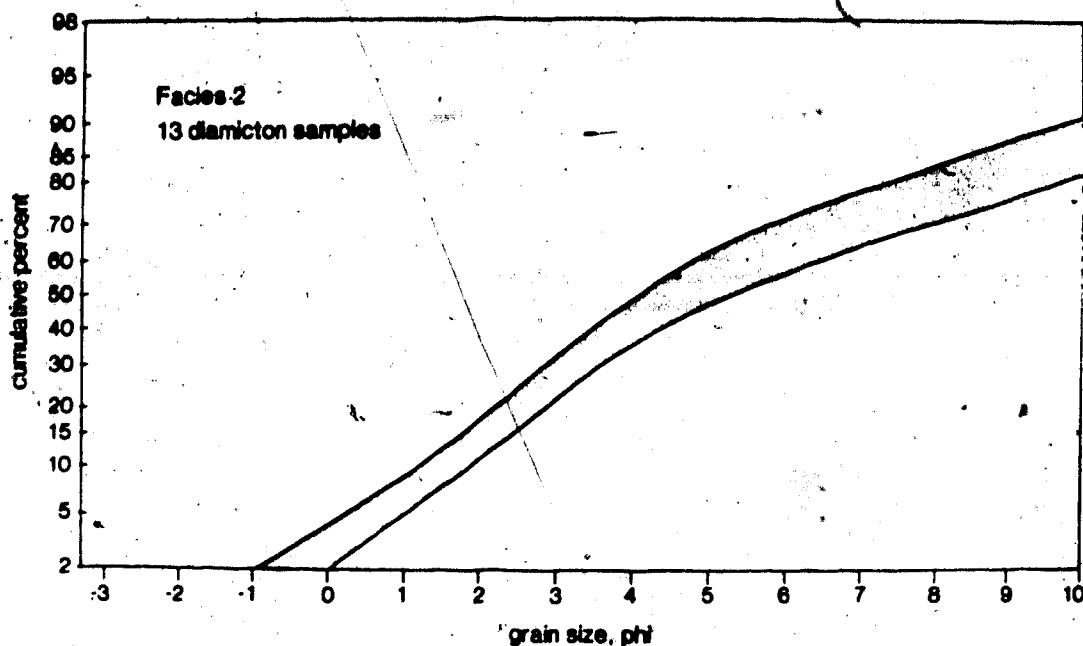


Figure 17a. Facies 2 diamicton matrix cumulative curves. Shaded area represents 13 curves.

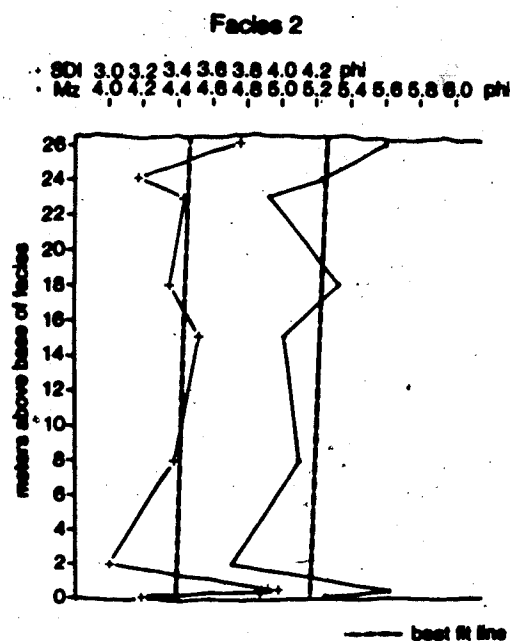


Figure 17b. SDI and Mz of diamicton matrix along a vertical column through facies 2.

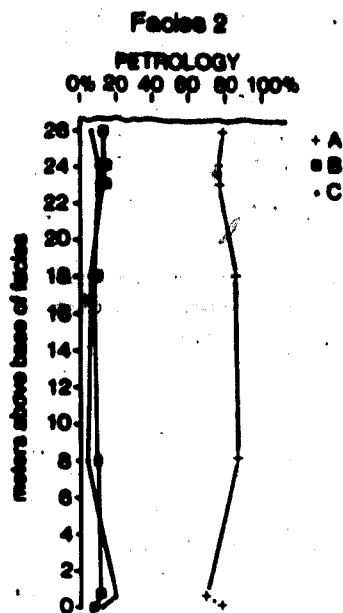


Figure 18. Petrology of 1-2 mm diameter grains along a vertical column through facies 2. A=carbonates, cherty limestone; B=quartzite; C=chert, sandstone, siltstone, shale, and coal.

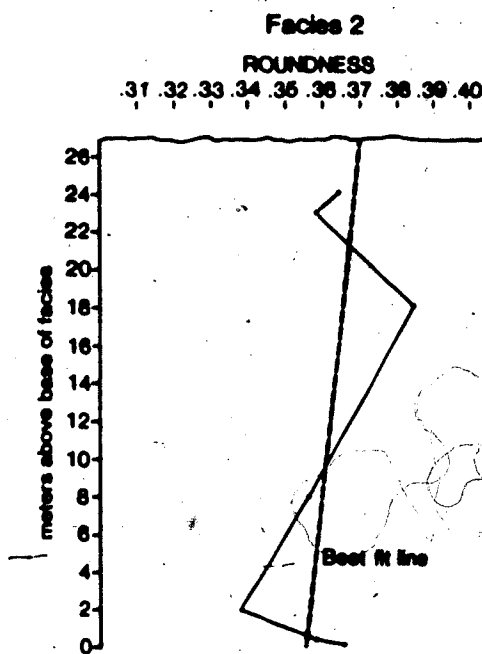


Figure 19. Roundness of 1-2 mm diameter carbonate grains along a vertical column through facies 2.

The following characteristics directly support a lodgement till interpretation. (i) The gravel-rich layers (Plate 3) are interpreted to be horizons of lodged clasts, a common property of lodgement tills (Boulton 1976b; Kruger 1979). These layers could be interpreted as englacial debris stratification preserved by basal melt-out. This is unlikely because englacial debris stratification is usually horizontal (Boulton and Eyles 1979) or dips up-glacier (Boulton 1968). In this case the gravel horizons radiate from one horizon and dip down-glacier. This orientation is interpreted to result from down-glacier accretion of basal debris, a process to be discussed later.

(ii) The gravel layers are contained by a thickness of 24 m of till, this is within the observed thickness range of lodgement tills (Boulton 1976b).

(iii) The petrological composition of a series of samples collected along a vertical column shows homogeneity (Figure 18). This is expected in a lodgement till and is interpreted to be the result of the plastering process during basal debris deposition not preserving petrological stratification from within the glacial ice but instead smearing it out and therefore homogenizing it.

(iv) The shearing process of lodgement deposition will commonly result in soft clasts becoming sheared-out or smudged (Boulton et al. 1974; Kruger 1979). Distorted clasts are not seen in facies 2. The brown colored

shale clasts, observed intact in facies 1, are also not observed. The lack of soft clasts suggests that during lodgement till formation all soft clasts were totally destroyed. Another possibility is that no (or very few) soft clasts were transported into the region.

Other characteristics of facies 2 which are indicative of lodgement till are, (v) the dense voidless nature of the diamicton matrix, (vi) the presence of only a few lens filled with sorted sediment, and (vii) a lower contact which is planar without any convex lenses.

Therefore facies 2 is interpreted to be lodgement till.

FACIES 2 DISCUSSION

Hallet (1981) suggests the debris content of the basal glacial ice partially controls the sliding velocity of the glacier and this velocity in turn partially controls the lodgement process. He suggests glacial debris fragments of all sizes are lodged when the sliding velocity of the glacier equals the rate at which basal-ice melts due to geothermal heating. In facies 2 the diamicton layers located between the gravel-rich horizons are interpreted to have formed by this process (Figure 20a) that is, when the sliding velocity of the glacier equaled the rate of basal ice melting.

Since glacier sliding velocity varies continually (Kamb

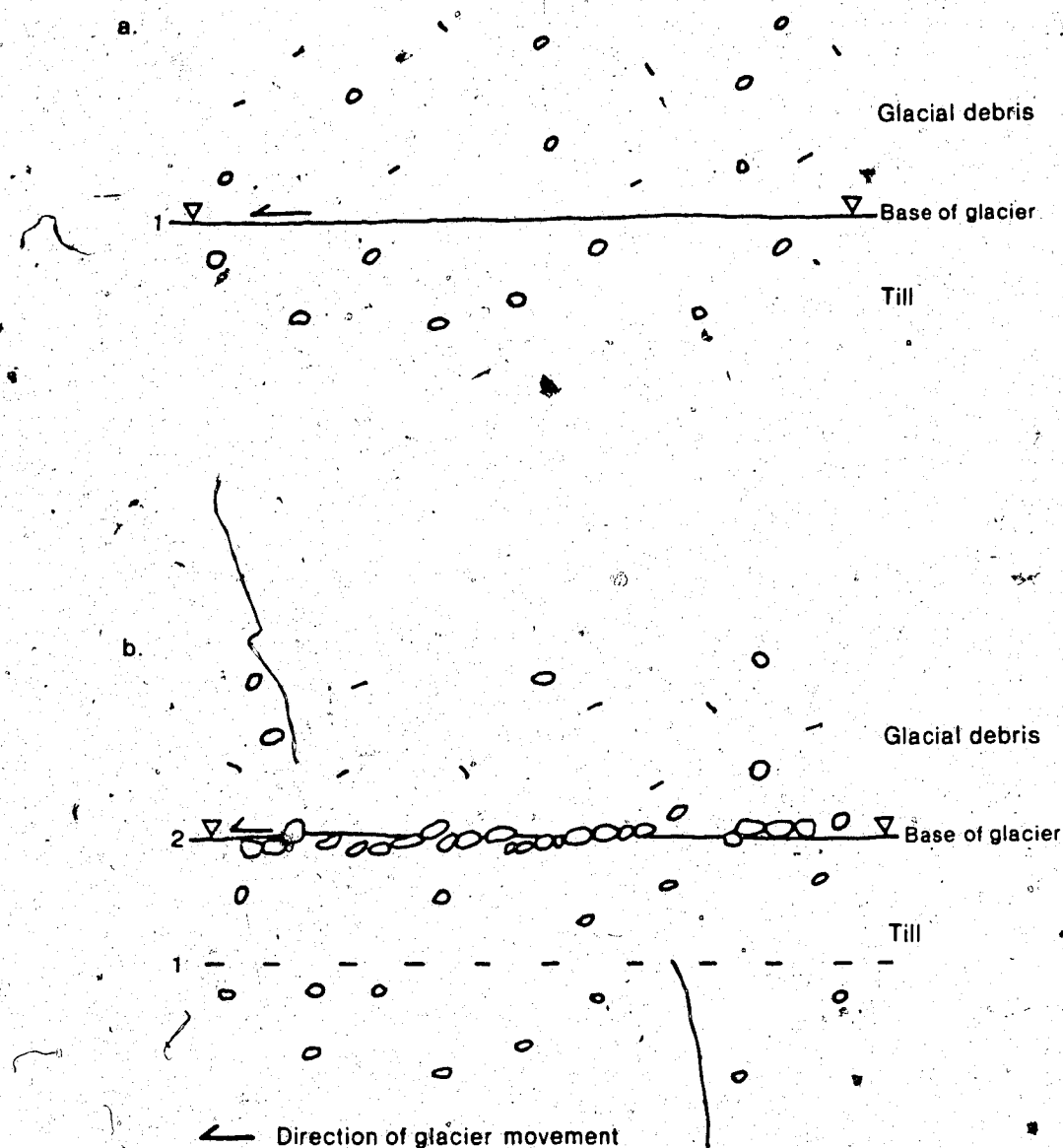


Figure 20. Facies 2 formation. (a.) Lodgement till is forming, glacial debris of all grain sizes is being lodged. Plane 1 is moving upwards at a rate equal to the glacier's basal sliding velocity. (b.) Only gravel-sized clasts are being lodged. Plane 2 is moving upwards at a rate much less

and LaChapelle 1964) the process of lodgement which Hallet (1981) presents becomes inoperative when the sliding velocity of the glacier exceeds the rate at which all grain size-ranges of debris can become dislodged from the ice. It is hypothesized by this author that when this happens (glacier velocity increases) only gravel-sized clasts are lodged against the substrate and that the finer-grained debris is held in the glacier and is carried past the site of lodgement (Figure 20b); this is similar to a lodgement process presented by Muller (1983b). This is how the gravel layers formed.

The alternation of gravel-rich and gravel-poor horizons is interpreted to be a product of jerky glacier motion, a type of motion frequently observed on modern glaciers (Engelhardt et al. 1978). The velocity oscillations may be caused by interstratification within the glacier of basal debris that has differing debris to ice ratios as observed by Lawson (1979). Continual lodgement of alternating gravel-rich horizons and more normal diamicton gradually built up the thick sequence of diamicton which comprises facies 2.

The lack of observable shear-plane traces, which are usually present in lodgement tills (Dreimanis 1976), is interpreted to indicate that the glacial debris lodged without shear continually occurring in the zones of more massive diamicton; shear occurred only at the depositional

interface between the glacier's base and the substrate. This interface would have been located along each gravel-rich plane during the process of lodging each horizon of gravel clasts. Clast orientation, as displayed in till fabric diagrams, adds information about the lodgement process. Three of the five pebble fabrics are oriented obliquely to the former ice flow-lines (Figure 21). The oblique fabrics are interpreted to be a product of clast realignment which occurred during lodgement of an englacial debris clast fabric that was originally parallel to the former ice-flow direction. Johansson (1965) thinks particles become oriented normal to the ice-flow direction when the glacially transported particles make contact with the substrate. This is what likely also happened in facies 2. Not all the fabric sites are reoriented. The parallel fabrics of facies 2 are interpreted to be preserved, non-reoriented englacial fabrics. They were preserved during lodgement because the debris deposition rates were high enough to isolate the clasts from the overlying, moving glacier before realignment of the clasts could take place.

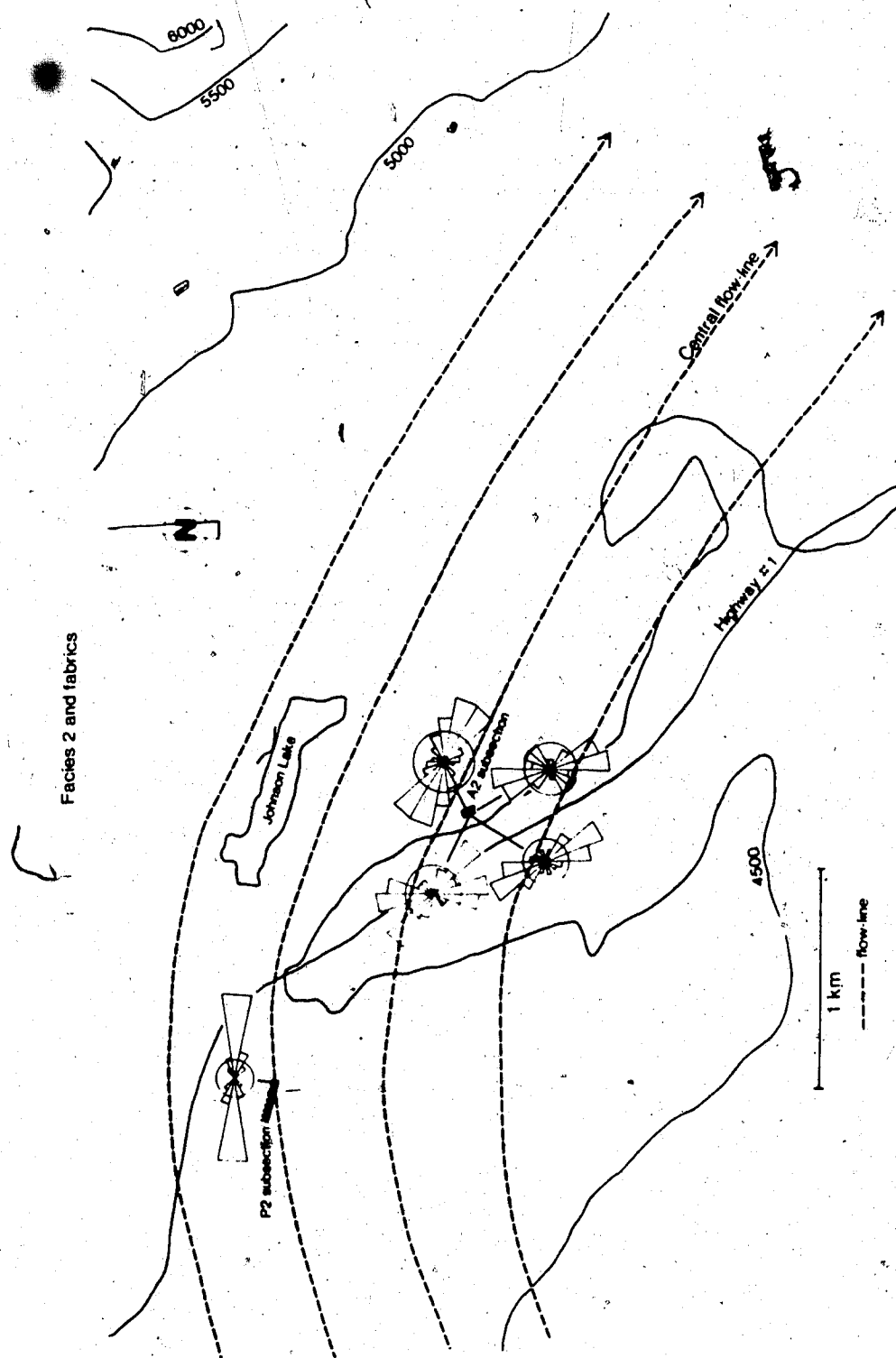


Figure 21. Diamicton pebble fabrics of facies 2 relative to reconstructed glacier flow lines.

C. FACIES 3

FACIES 3 DESCRIPTION.

DIAMICTON DESCRIPTION

The diamicton has two different thicknesses depending on the location of the facies within the study area. The thicker portion of facies 3 is 26-28 meters thick (Figures 15, 16, 22, and 23); the thinner portion of facies 3 is 4-8 meters thick (Figures 24, 25, 26, and 27).

The diamicton is matrix supported. The matrix is massive and dense. The only structures within the diamicton are rare lenses filled with either sand, gravel, or clay. Average clast diameter of the diamicton is 2-3 cm; larger clasts have an average diameter of 10-15 cm and a maximum clast diameter of about 40 cm. Approximately 5-10% of the facies vertical surface exposure is comprised of clasts greater than 1 cm in diameter.

Facies 3 overlies a gravel and sand unit (facies 6) and is also overlain in some places by facies 6. The upper contact of facies 3 is horizontal, sharp, and distinct. The lower contact (or lower surface) of facies 3 is sharp, distinct, nearly planar, and essentially horizontal, undulating by 1-2 cm. The lower surface of facies 3 has a dimpled appearance with no flutes, no flute casts, nor any

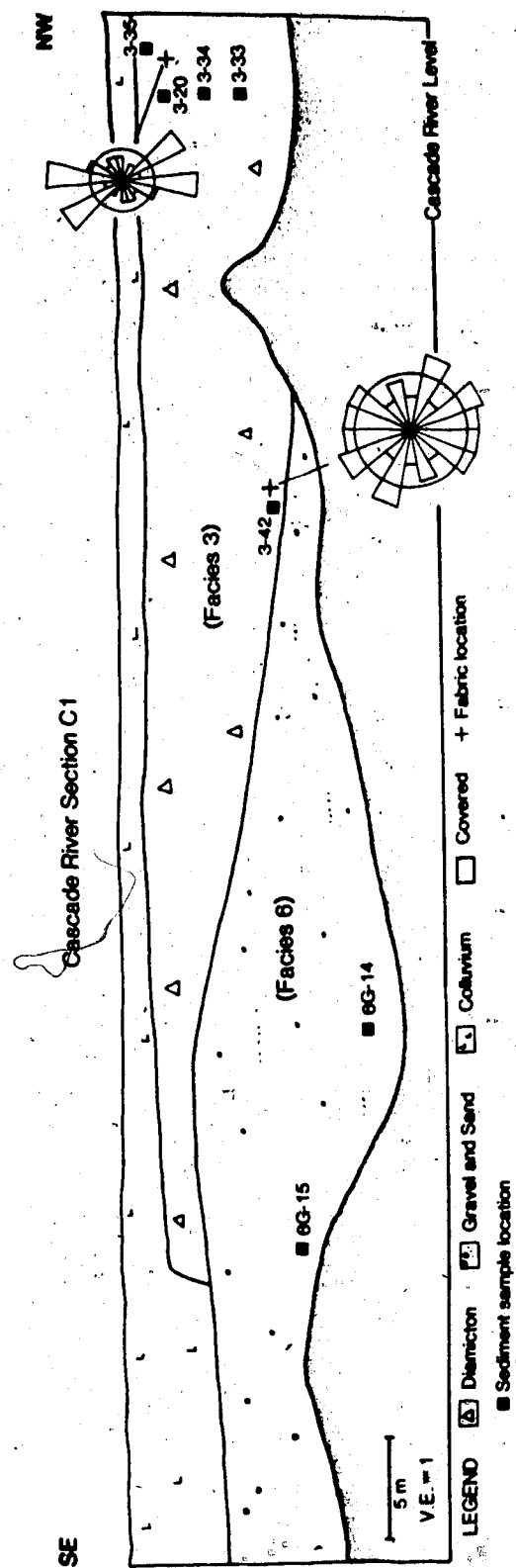


Figure 22. Cascade River section C1.

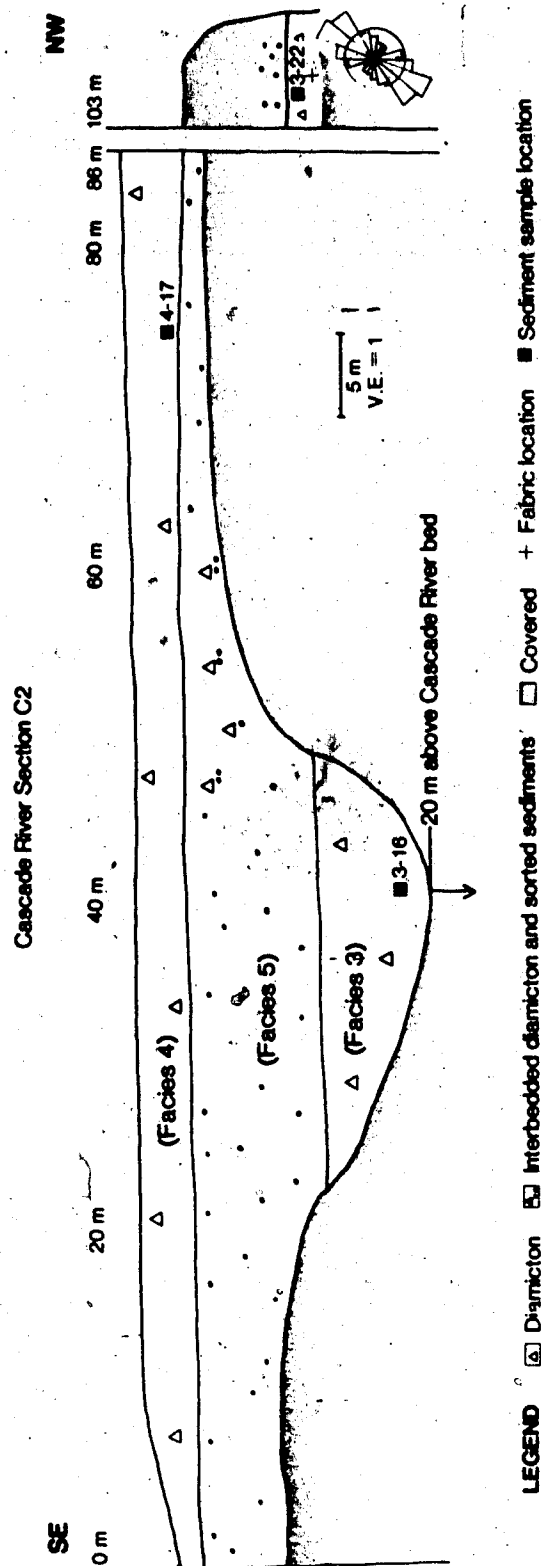


Figure 23. Cascade River section C2.

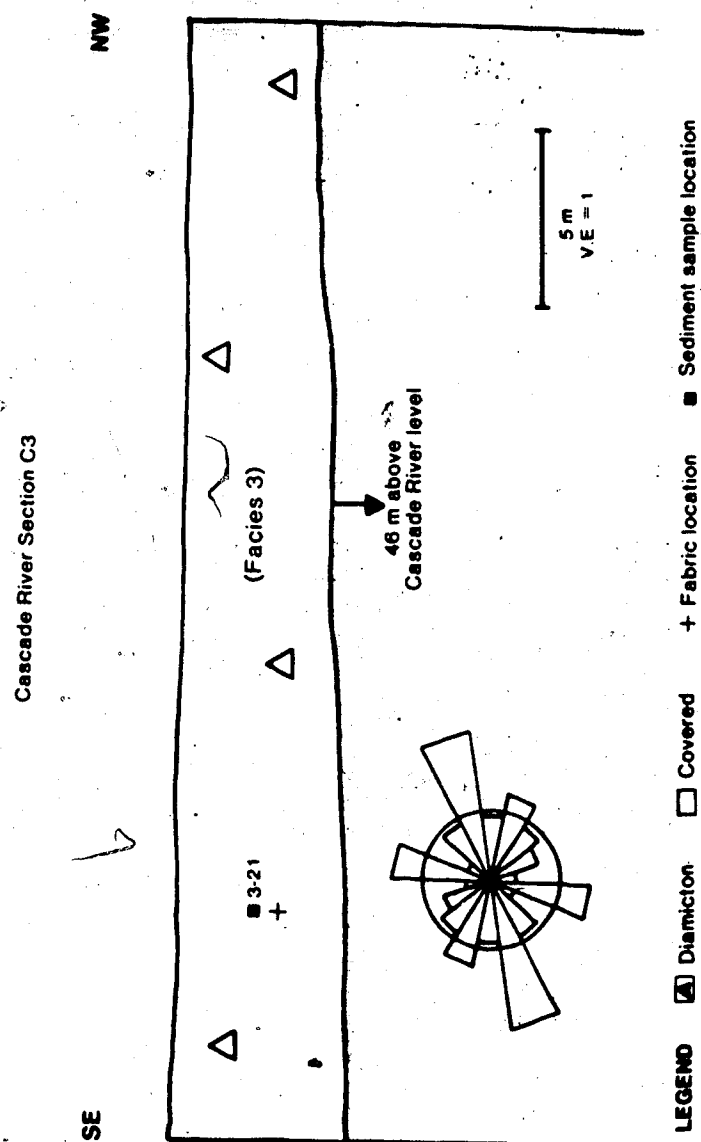


Figure 24. Cascade River section C3.

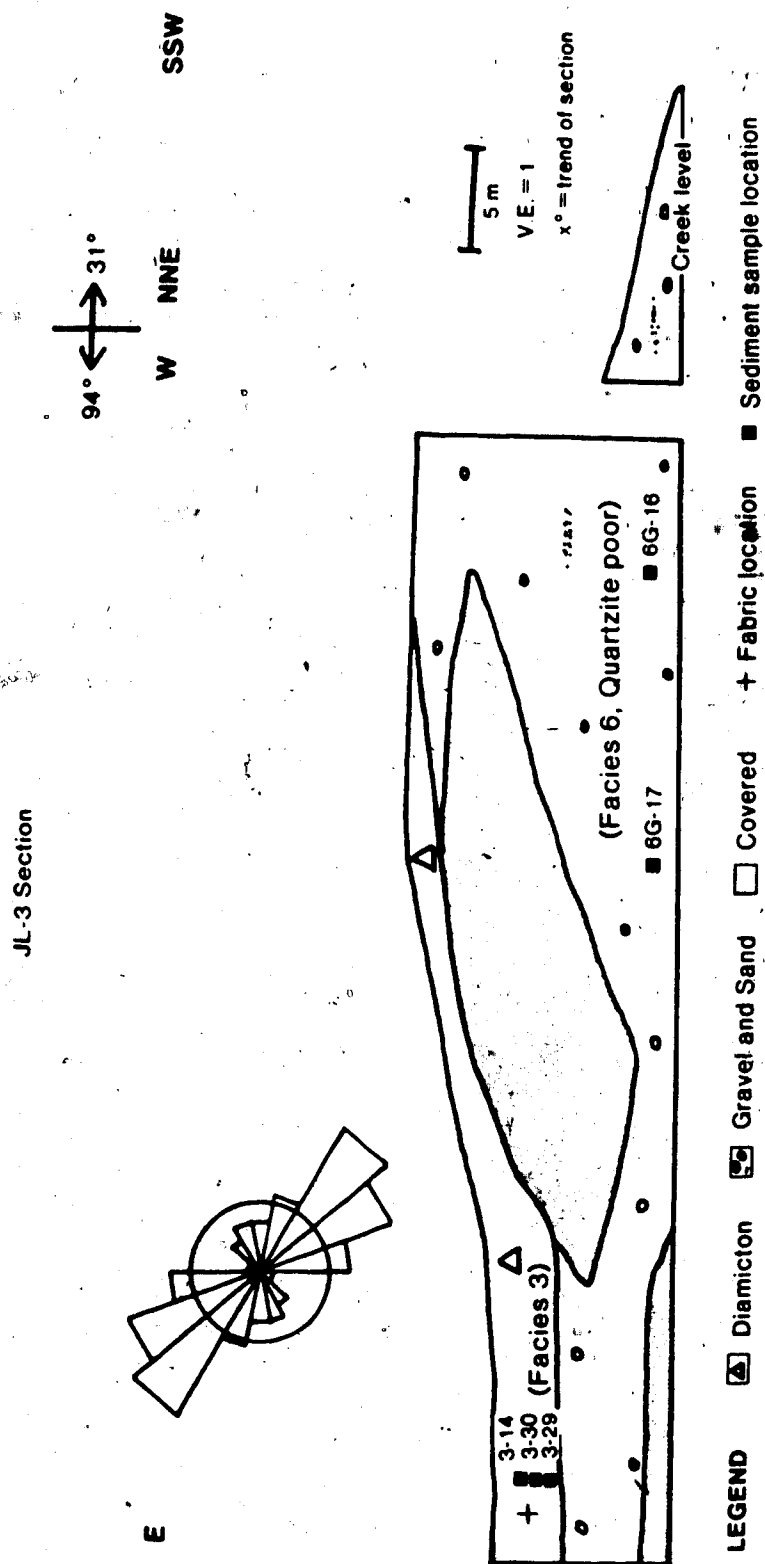


Figure 25. Johnson Lake section JL-3.

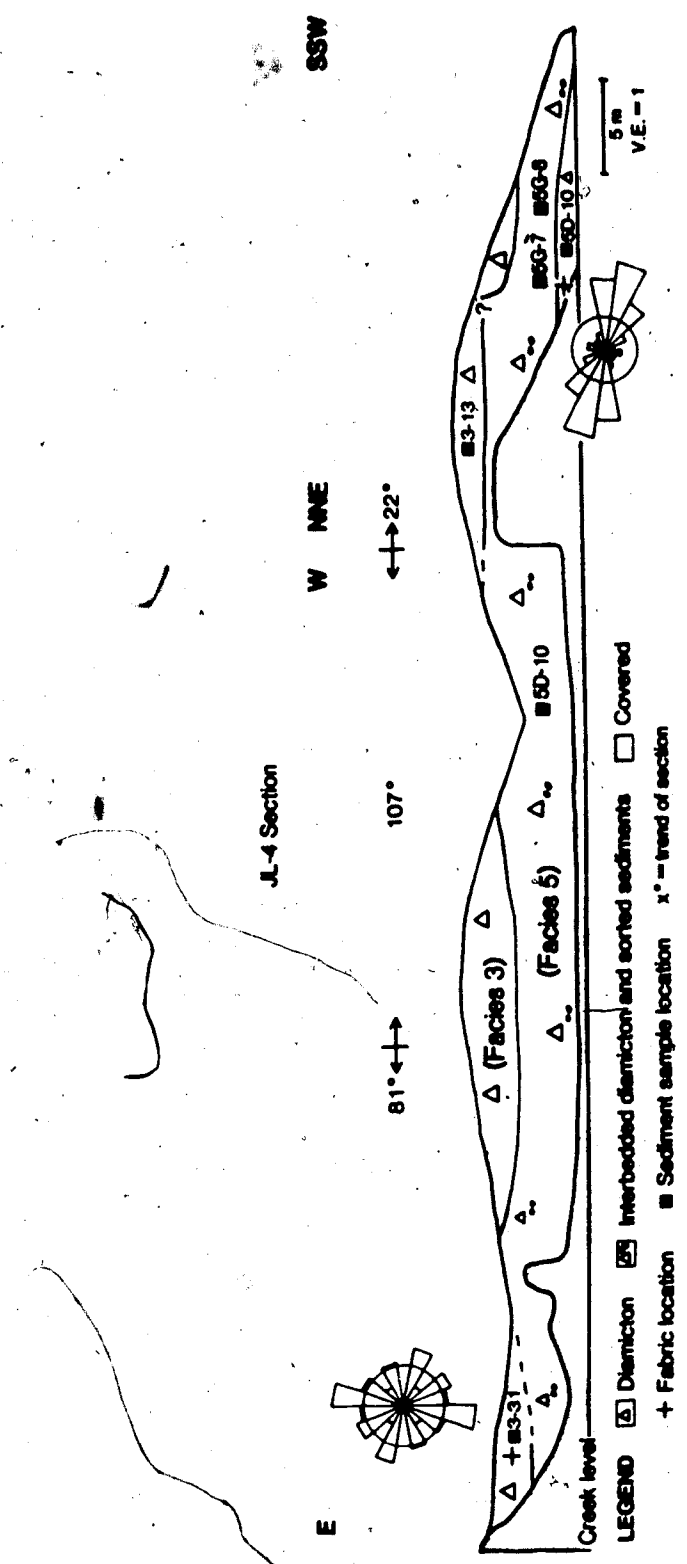


Figure 26. Johnson Lake section JL-4.

other types of directional features. Pebbles straddle this contact; that is, some pebbles are situated in both the overlying diamicton and in the underlying gravel. These pebbles are not striated or faceted.

In one location, the lower surface (lower contact) of facies 3 differs from the preceding description in that, (i) the lower surface undulates by one meter over a 2-3 meter distance, and (ii) pebbles do not cross nor straddle the lower contact; instead the lower (basal) surface of the diamicton conforms to the upper surface of pebbles within the underlying facies.

Description of lenses - features within the diamicton

Features within the diamicton consist of clay laminae, sand bands, sand-filled lenses, and gravel-filled lenses. These inclusions cover less than 1% of the vertical surface area of facies 3.

One horizontal clay layer was observed within facies 3. The layer occurs about 1 m above the base of the facies, it is 3 mm thick and at least 3 m long. This layer makes sharp upper and lower contact with the enclosing diamicton and pinches out at one end, the other end is talus covered.

Two isolated sand bands occur above each other about 6 m above the base of facies 3. Both features are 4-5 cm thick and each extends for 1.5 m and 3 m, respectively, before becoming talus covered at both ends. The bands are

horizontal and have very sharp bases. The upper portion of the bands makes a gradational transition into diamicton over a vertical distance of 1-2 cm. No sedimentary structures occur within these bands aside from the distribution of pebbles. No pebbles occur within 1-2 cm of the bands' lower contact; above this level pebbles with 5-20 mm diameters are randomly distributed.

Sand- and gravel-filled lenses occur rarely in facies 3. Lens dimensions range from 0.5-15 cm thick by 0.2-3 m long. Contact between the lenses and the enclosing diamicton is sharp and distinct. The contacts' shapes range from smooth contacts to wavy contacts with amplitudes up to 3 cm. The lens fill ranges from sand-sized to 1 cm diameter pebbles. The fill of the lenses is horizontally laminated in some lenses and unbedded in other lenses. Most lenses have a horizontally elongated "rectangular" outcrop shape. A very small percentage of the lenses have an irregular round shape which covers about 200 cm² of vertical surface area. Two sand-filled lenses have a L-shape or a contorted spiral shape. Within these, bedding conforms to the lenses' external outline.

FACIES 3 INTERPRETATION

Facies 3 is interpreted as basal till, in greater

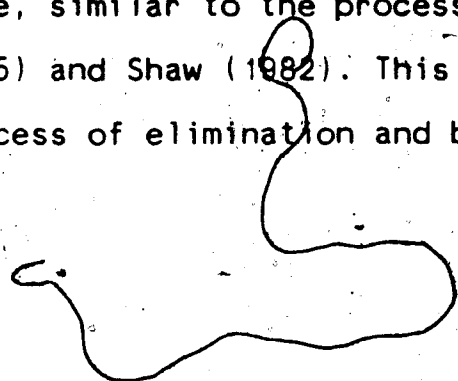
detail, as the lodgement variety of basal till. This more specific interpretation is reached by the process of elimination and using the direct attributes of facies 2.

1. BASAL TILL INTERPRETATION

The sediment of facies 3 is interpreted to have been transported by a valley glacier and then directly deposited from the base of a glacier with no resedimentation occurring after deposition. Evidence to support this interpretation is the same as the information presented for facies 1 (page 64). Additional evidence is the drumlinized topography above facies 3 (Plate 4). The drumlins indicate the underlying deposits most likely formed beneath a glacier (Muller 1974; Boulton 1976a; Menzies 1979). The following section (part 2) determines the type of basal till which makes up facies 3.

2. LODGEMENT TILL INTERPRETATION

Facies 3 is interpreted to be mostly lodgement till formed by the plastering of glacial debris particles onto a subglacial substrate, similar to the process described by Boulton (1972a, 1975) and Shaw (1982). This interpretation is based on the process of elimination and by diagnostic characteristics.



Facies 3 consists of basal till, either basal melt-out till or lodgement till. Basal melt-out till is eliminated because of the following reasons. (i) Both the thick member (26-28 m thick) and the thin member of facies 3 (4-8 m thick) are too thick to have been deposited by basal melt-out because basal melt-out till can only be a few meters thick (Boulton 1976b; Lawson 1979). (ii) Drumlins are situated on portions of the upper surface of facies 3 (Plate 4). Drumlins of this size do not form from the basal melt-out process (Muller 1974); although 20 cm high fluted features can (Lawson 1976). (iii) The petrology along a vertical column is homogeneous (Figure 28) which is not a property of basal melt-out tills. Basal melt-out till shows an up-section increase in more distantly derived lithologies (Hyvarinen et al. 1973; Haldorsen 1977). (iv) The general lack of sorted sediment-filled lenses suggest facies 3 is not basal melt-out till because that type of till usually has many lenses (Lawson 1979; Boulton and Deynoux 1981). (v) The lack of plano-convex lenses along the lower contact of the till suggests it is not basal melt-out till. Such lenses are usually present in basal melt-out till (Shaw 1982).

Eliminating basal melt-out till implies facies 3 is probably lodgement till.

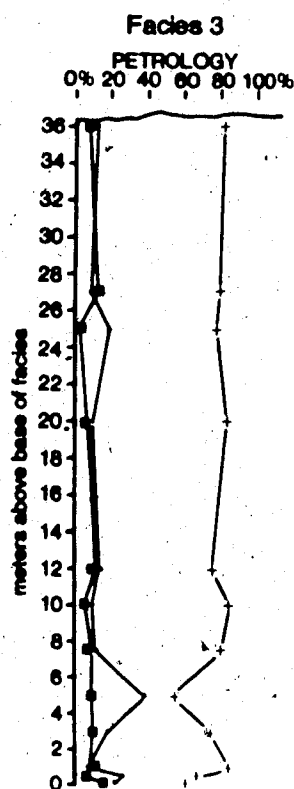


Figure 28. Petrology of 1-2 mm diameter grains along a vertical column through facies 3. A=carbonates, cherty limestone; B=quartzite; C=chert, sandstone, siltstone, shale, and coal.

The drumlinized upper surface of facies 3 indicates it was deposited as lodgement till because this is the only type of till deposited beneath an active, non-eroding glacier (Boulton 1972a; Kruger 1979; Shaw 1983).

Additional properties, characteristic of lodgement till, is facies 3 dense, voidless nature; the presence of very few sediment filled lenses; and the homogeneous petrology or lack of distantly derived lithologies (Figure 28). The sharp, nearly planar lower contact of facies 3 which in places truncates underlying fluvial channels also indicates debris deposition by lodgement processes (Eyles and Sladen 1981).

Therefore facies 3 is lodgement till.

FACIES 3 DISCUSSION

Deposition of facies 3 was preceded by glacial action which removed any preglacial topographic highs. This resulted in the facies having a planar base. As the glacier advanced basal ice conditions resulted in deposition of lodgement till.

Lodgement processes formed the massive nature of facies 3 by simultaneously lodging glacial debris fragments of all sizes from the base of the ice. Hallet (1981) suggests this process takes place when the sliding velocity of the glacier equals the rate at which basal-ice melts due to

geothermal heat. Basal ice has been recorded to melt at a rate which forms 3.2 centimeters of till per year (Mickelson 1973). This thickness is likely equivalent to the minimum approximate basal sliding velocity (0.5-3.2 cm per year) of the valley glacier which deposited facies 3. Only a minimum velocity can be expressed because basal glacial debris has interstitial ice which must be accounted for.

As the glacier moved over the substrate at a minimum velocity of 0.5-3.2 cm per year the mechanisms controlling lodgement till deposition were relatively constant as facies 3 increased in thickness. Evidence for this is the massive nature of facies 3 and also the homogeneity of the grain size (Figures 29a and 29b), petrology (Figure 28), and roundness (Figure 30). Although lodgement till deposition was relatively constant, the sediment-filled lenses indicate that the lodgement process was occasionally interrupted.

The relatively few sediment-filled lenses are interpreted to have formed by the following process. The lowest, thin layer of debris-rich basal ice would occasionally lodge against the substrate and thus be sheared-off from the overlying, moving glacier (Figure 31a and b). This stranded layer would then melt-out beneath the active glacier and form a pod of basal melt-out till (Figure 31c). Sorted sediment would be concentrated in the

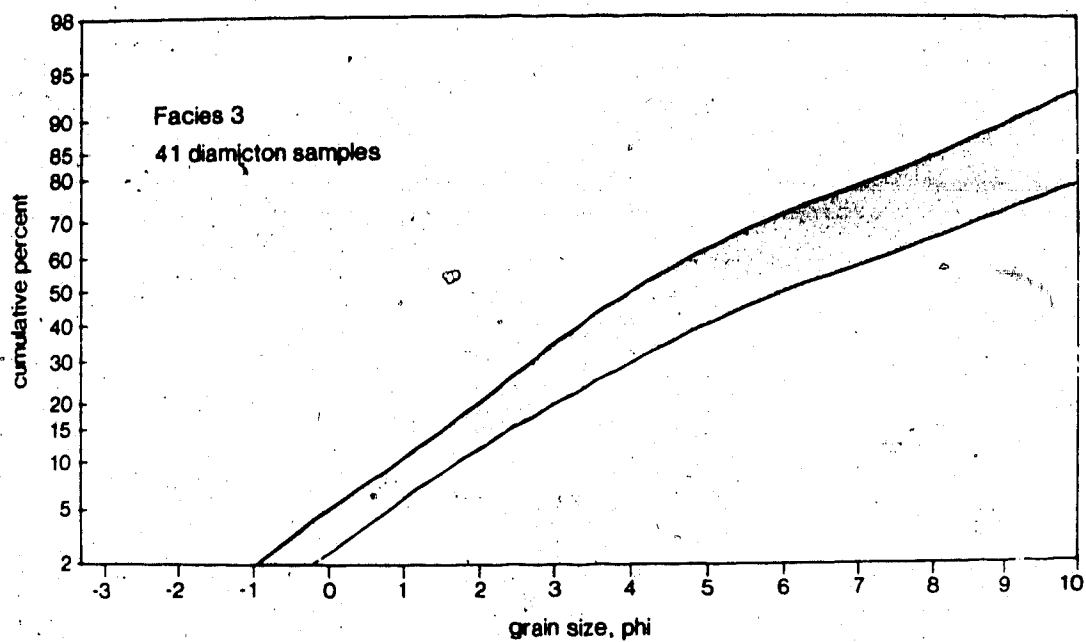


Figure 29a. Facies 3 diamicton matrix cumulative curves. Shaded area represents 41 curves.

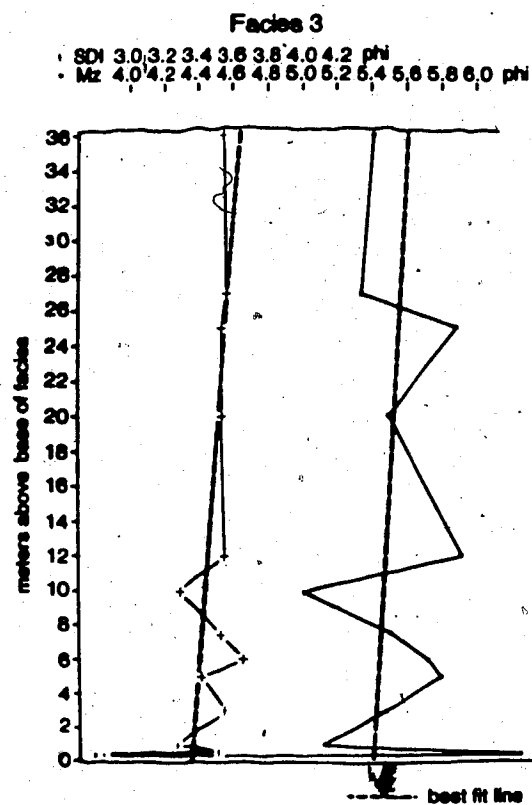


Figure 29b. SDI and Mz of diamicton matrix along a vertical column through facies 3.

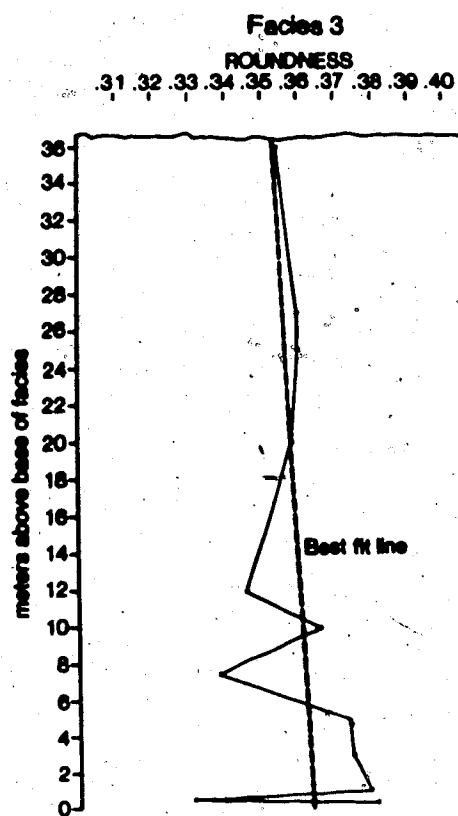
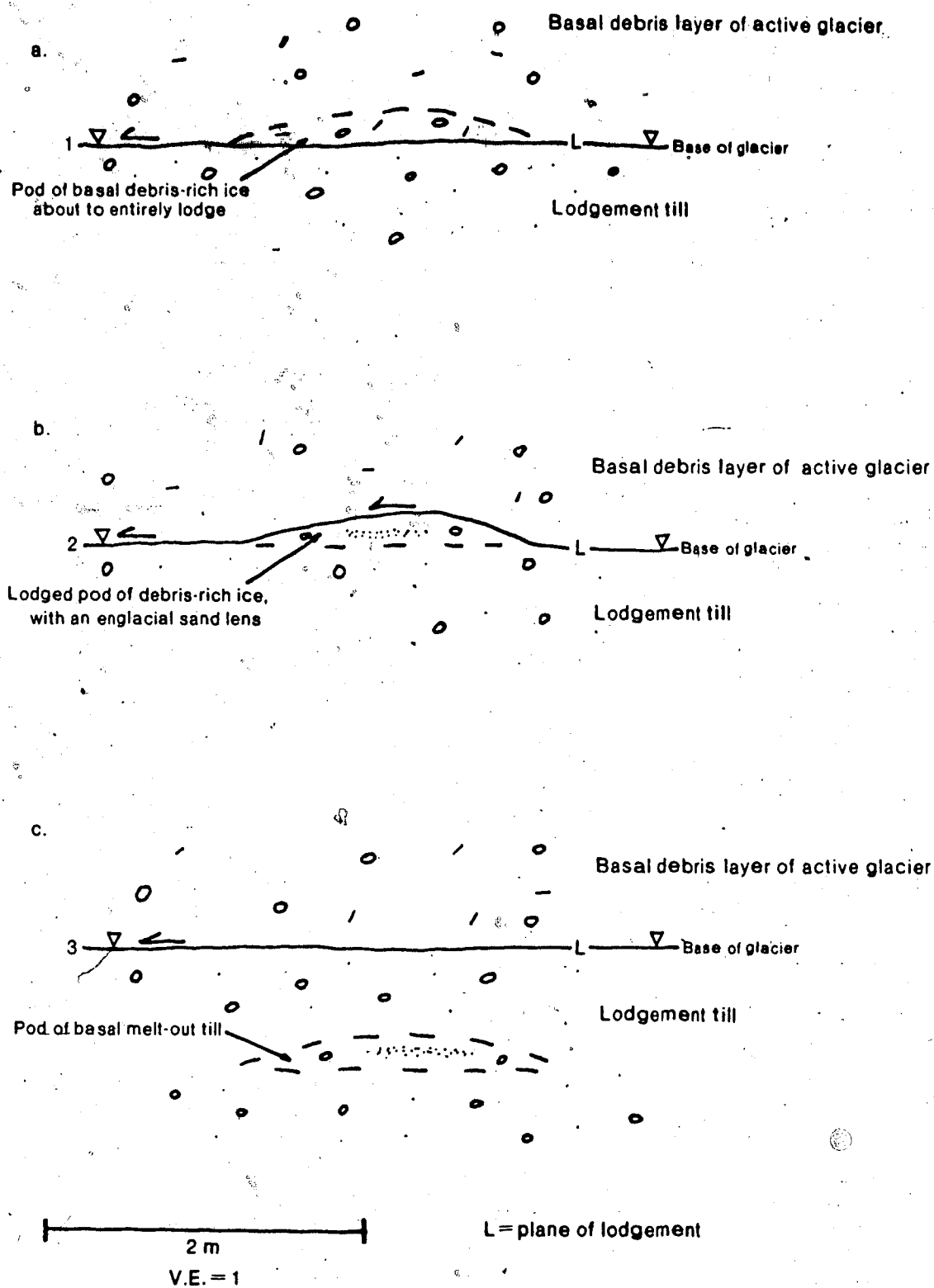


Figure 30. Roundness of 1-2 mm diameter carbonate grains along a vertical column through facies 3.



void space which formed as layers rich in interstitial ice melted. The sharp contacts observed between some of the lenses and the enclosing diamicton may be a result of shearing during emplacement of basal debris layers. Interaction between a recently formed lens of sorted sediment and the overriding glacier may deform the lens; this is believed to have happened to at least one lens (Plate 5). Lodgement would continue above the sheared-off layer of basal debris-rich ice (Figure 31c).

The diamicton pebble fabrics reflect the lodgement process described above. Most of the diamicton pebble fabrics are aligned parallel; with some aligned transverse to the reconstructed former ice flow-lines (Figure 32). Parallel and transverse fabric alignment are observed in lodgement tills. The two chaotic fabrics in facies 3 are located immediately above facies 6 (Figures 15a and 15b). The lack of any preferred fabric alignment in these two particular localities is interpreted to result from the interaction between the glacier and the preglacial topography comprising facies 6.

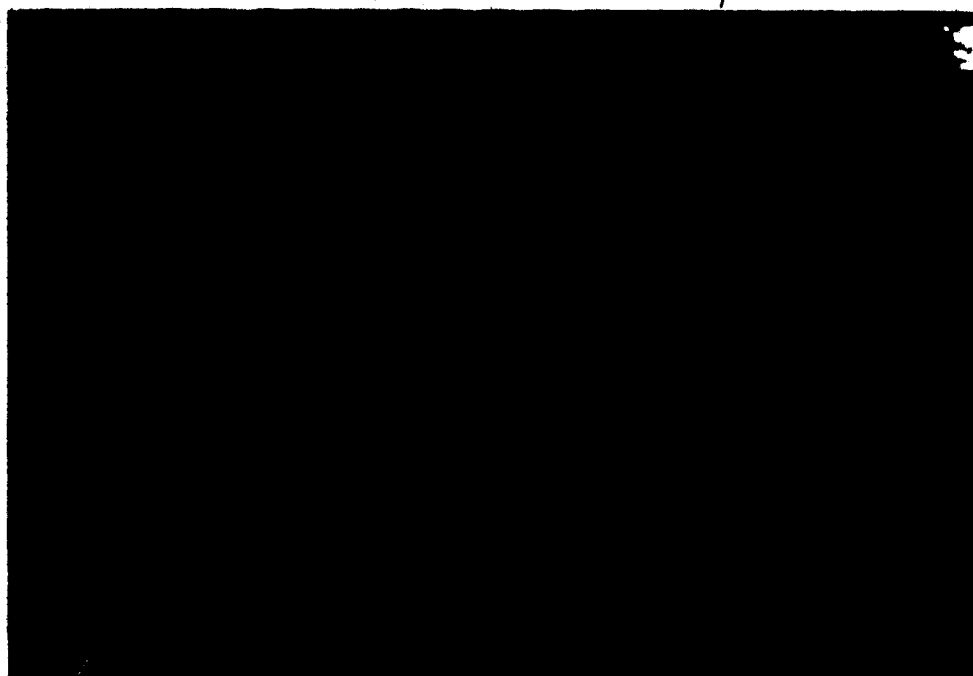


Plate 5. Deformed sand-filled lens in the diamicton of facies 3. Lens occupies right-most portion of plate. (Photograph at Cascade River C2 section).

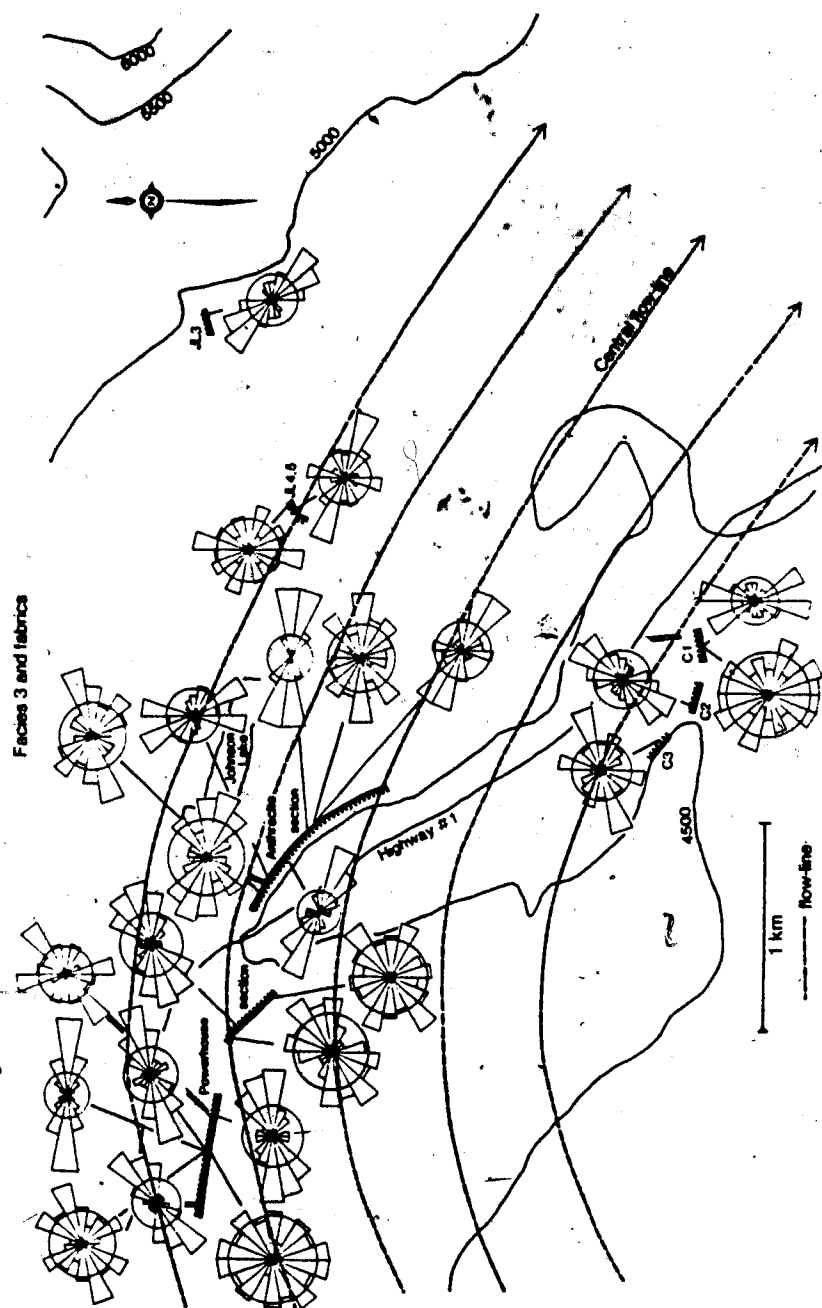


Figure 32. Diamicton pebble fabrics of facies 3 relative to reconstructed glacier flow lines.

D. FACIES 4

FACIES 4 DESCRIPTION

Facies 4 has two different thicknesses. The thicker portion is 30 meters thick and the thinner portion is 3 to 4 meters thick. The outcrops where the facies is exposed are illustrated in Figures 15a (above the gravel lenses near location 2-10), 16, 33, and 34 to 41.

DIAMICTON DESCRIPTION

The diamicton is matrix supported, 99% of the matrix is massive, structureless, and dense. The remaining 1% contains 1 mm^2 void spaces. Voids only occur in one part of facies 4. In this location the voids occur in closely-spaced clusters which collectively form a zone of voids. The zones appear as 1 cm^2 irregularly shaped areas or as 0.5 cm wide by 2 cm long eye-shaped areas. The density of the zones is one zone per 100 cm^2 .

Another feature of the diamicton matrix is an area of near horizontal, curved joints with striated surfaces. (Plate 6). These joints were observed in only one part of the facies. This area covers 2 m^2 immediately above a sand lens.

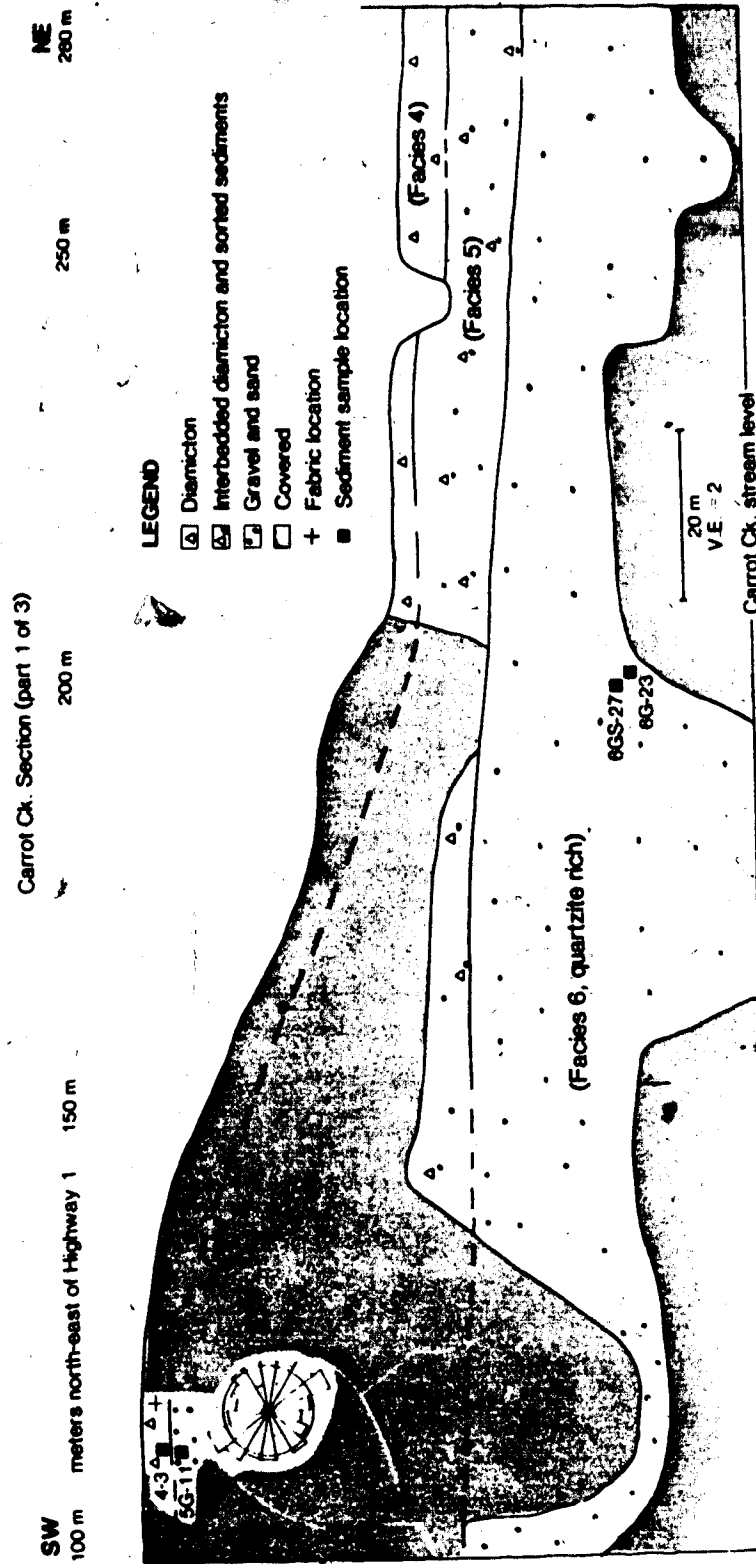


Figure 33a. Carrot Creek section, part 1 of 3.

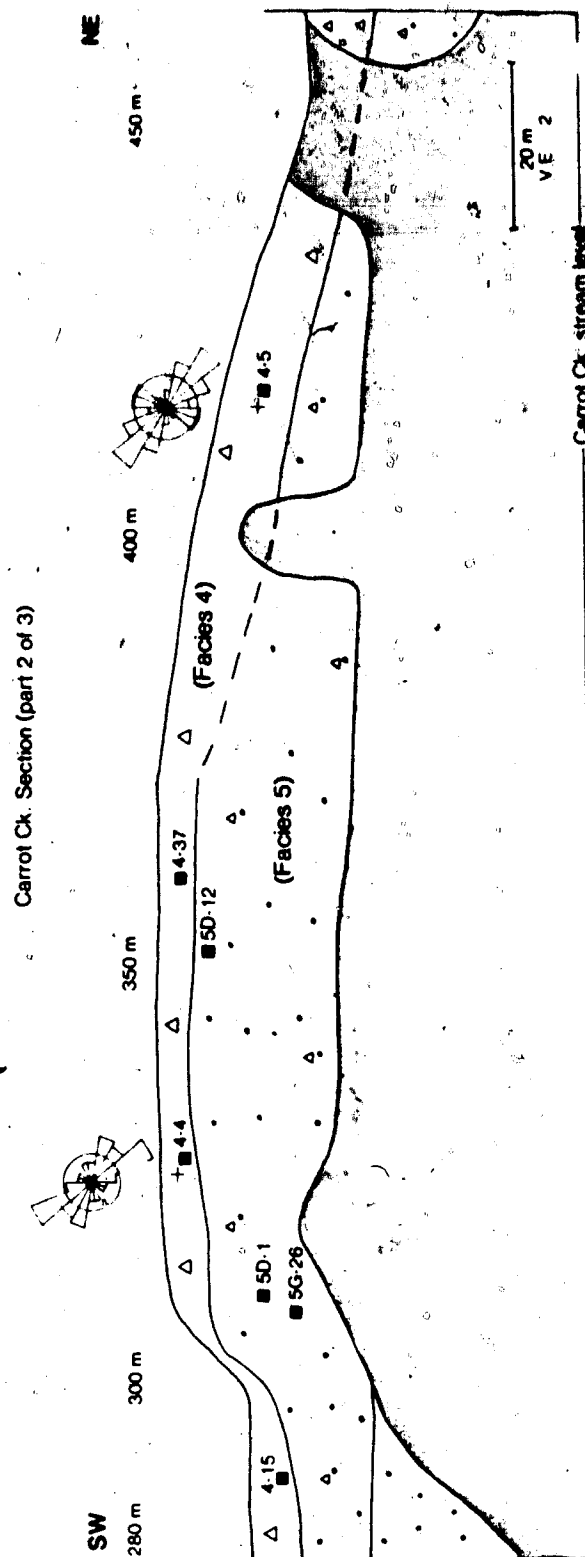


Figure 33b Carrot Creek section, part 2 of 3.

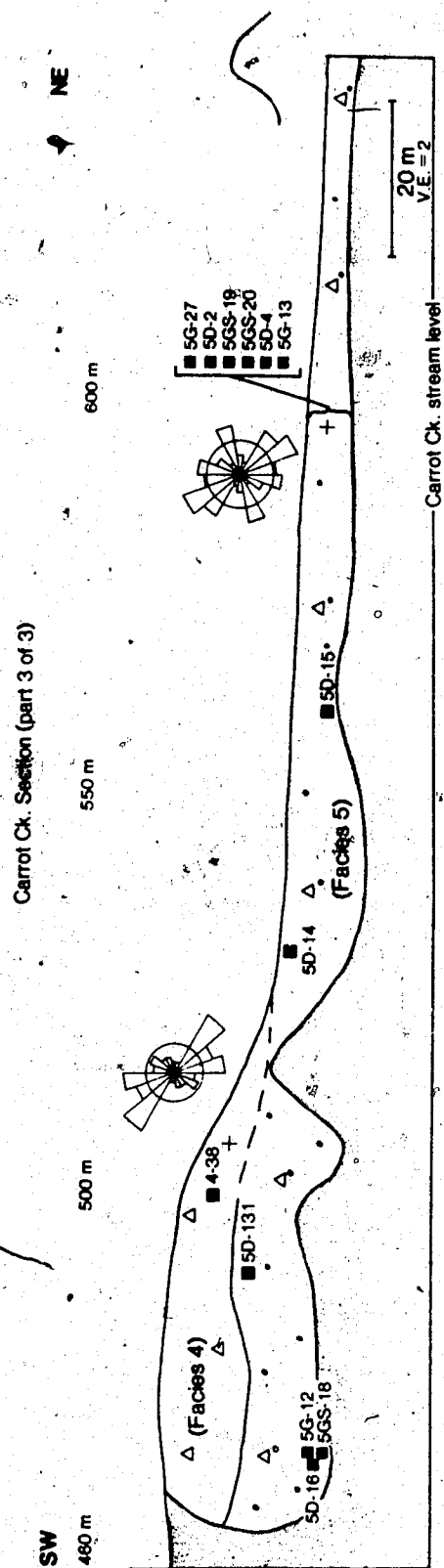


Figure 33c. Carrot Creek section, part 3 of 3.

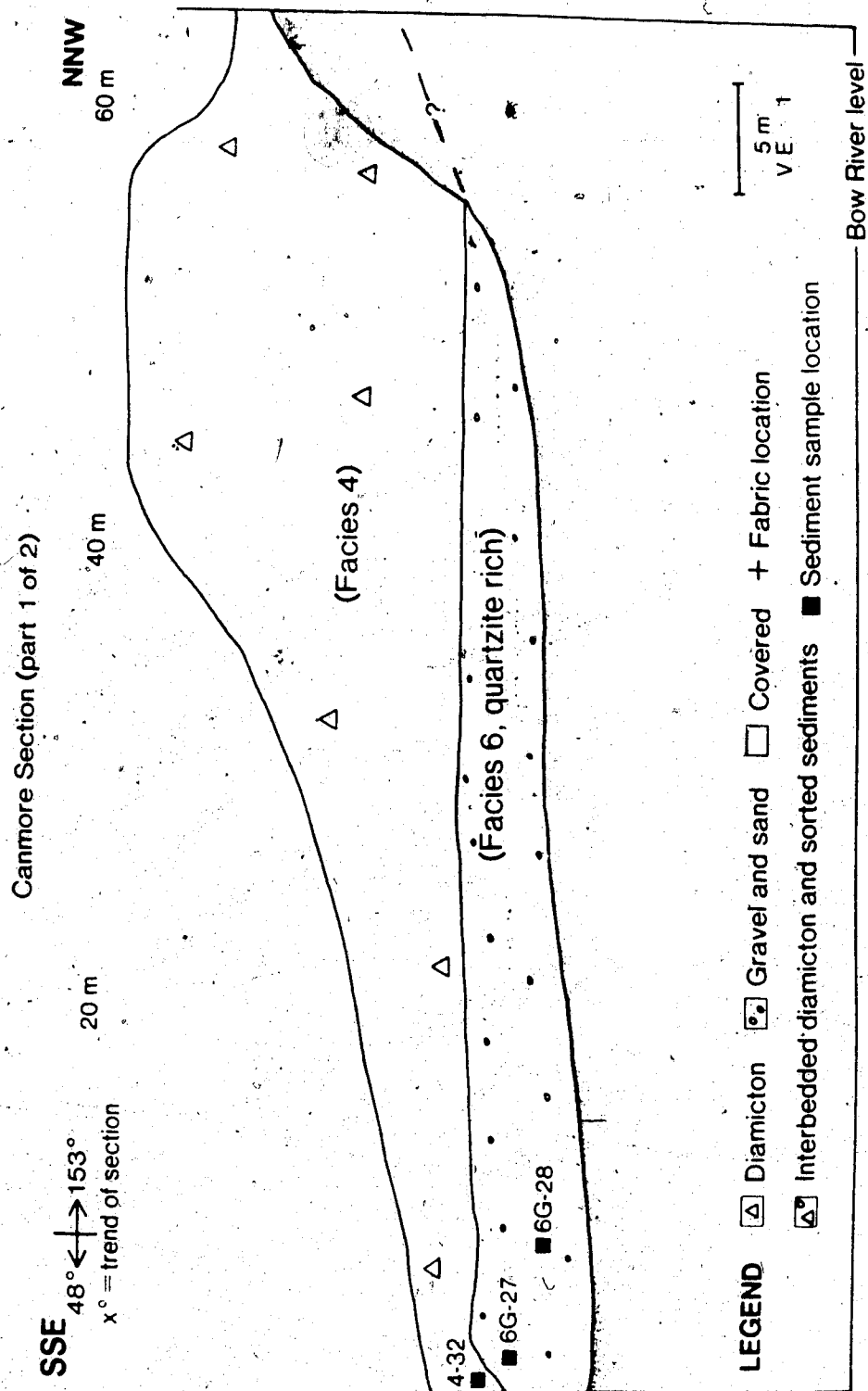


Figure 34a. Canmore section, part 1 of 2.

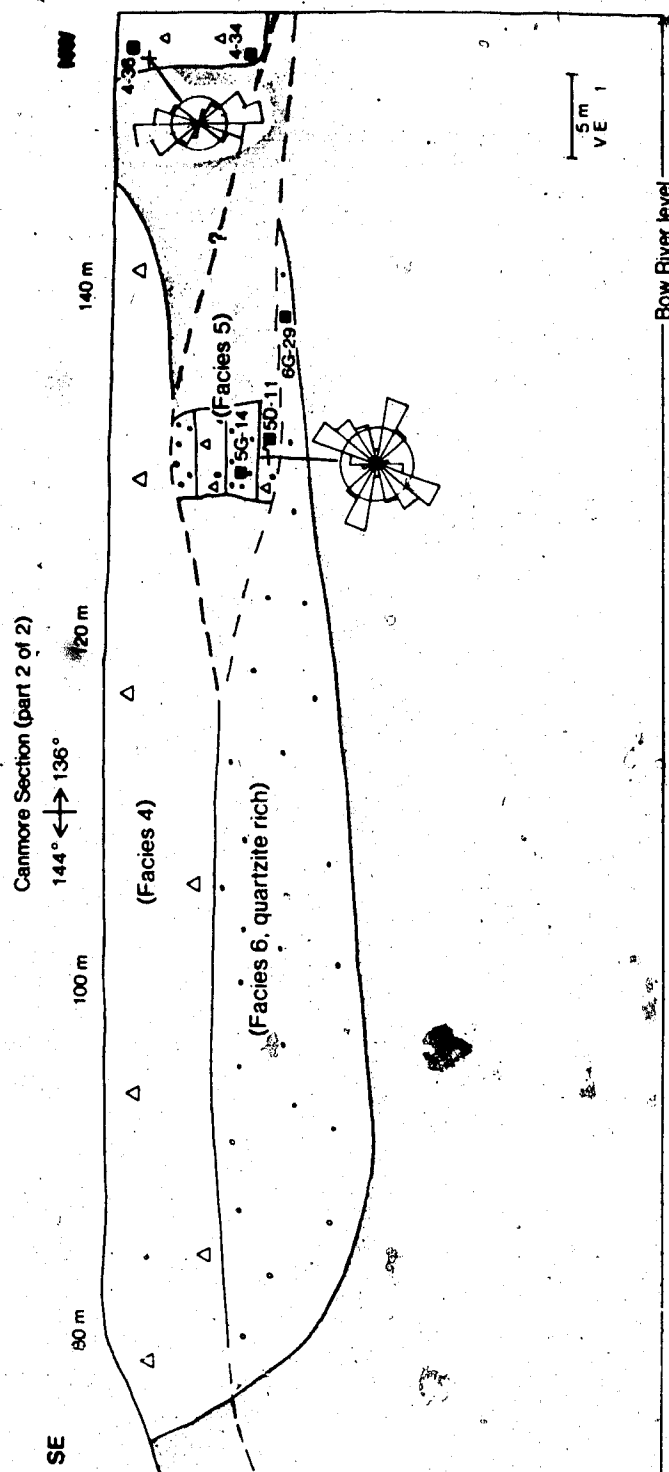


Figure 34b. Canmore section, part 2 of 2.

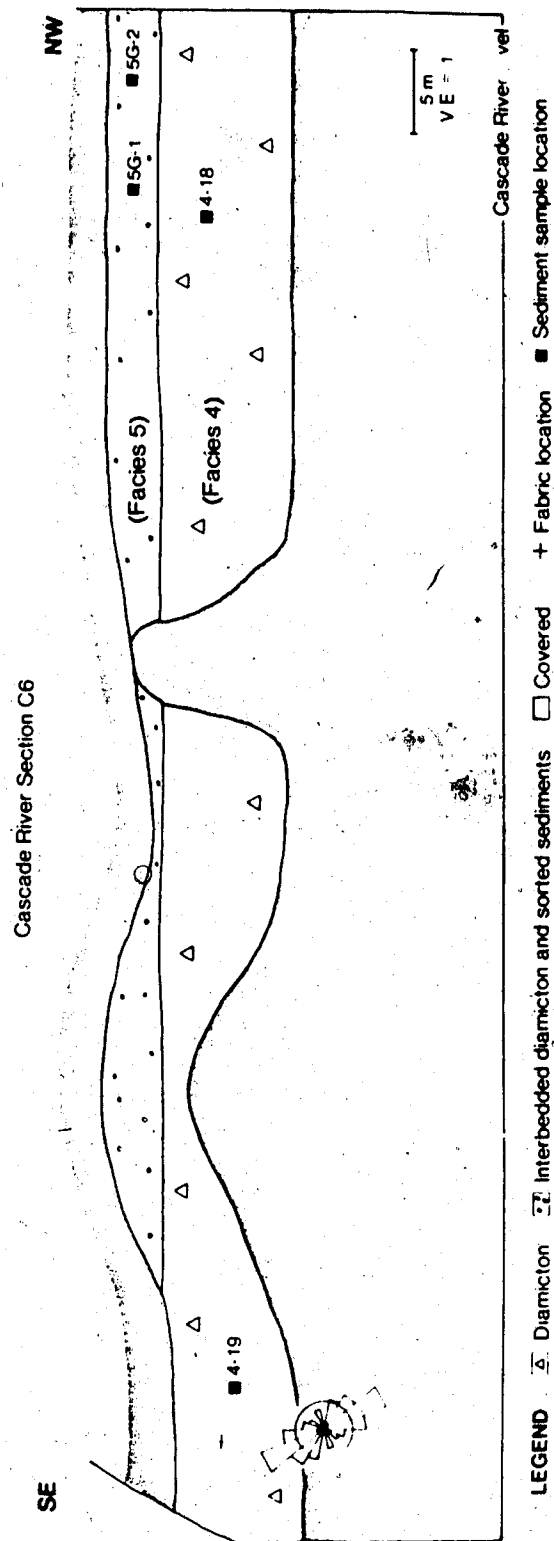


Figure 35. Cascade River section C6.

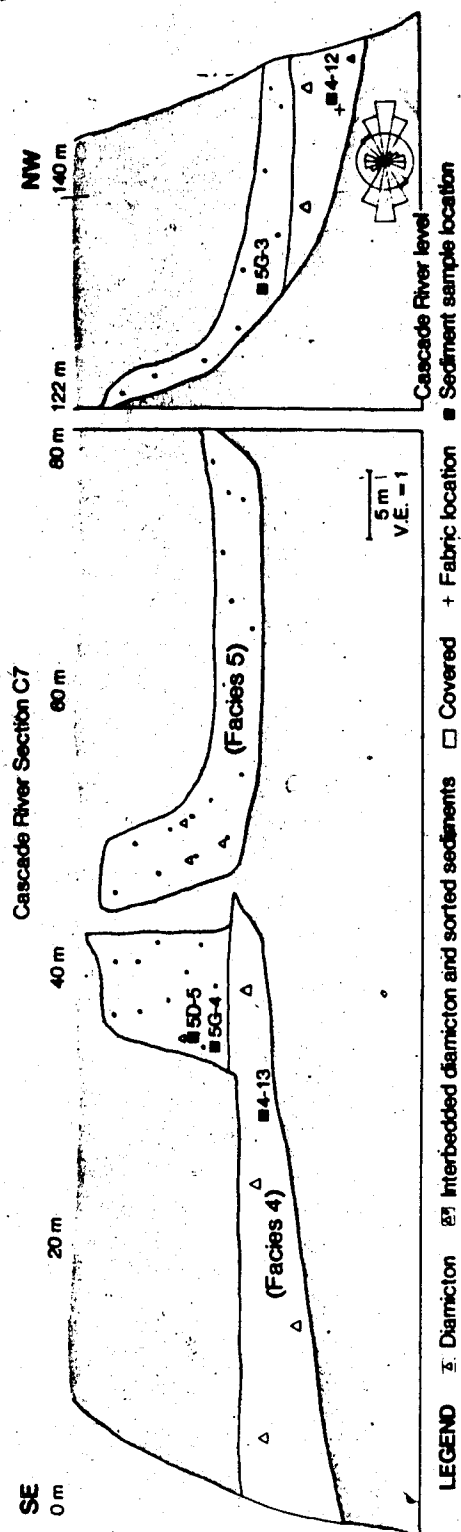


Figure 36. Cascade River section C7.

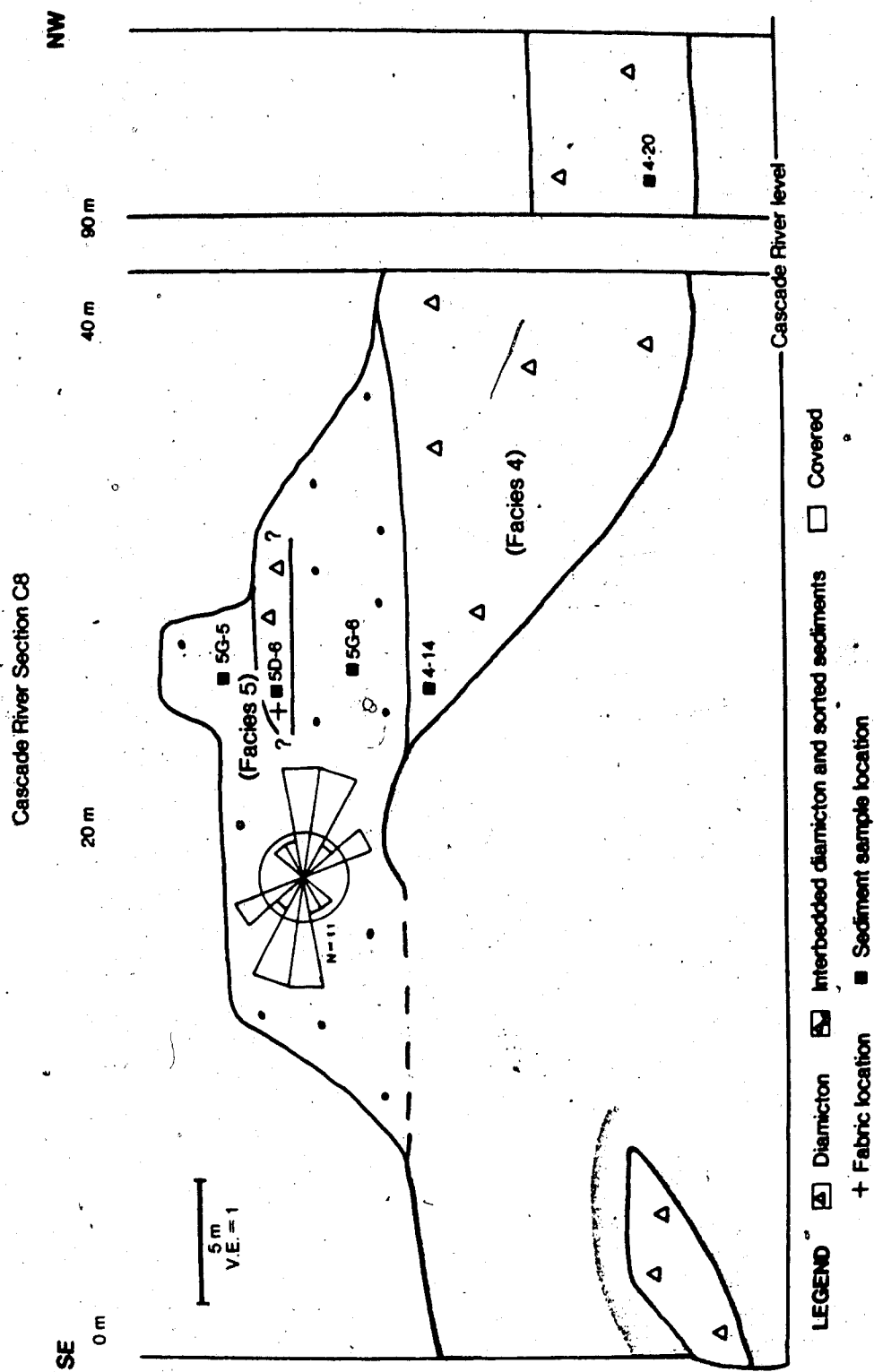


Figure 37. Cascade River section C8.

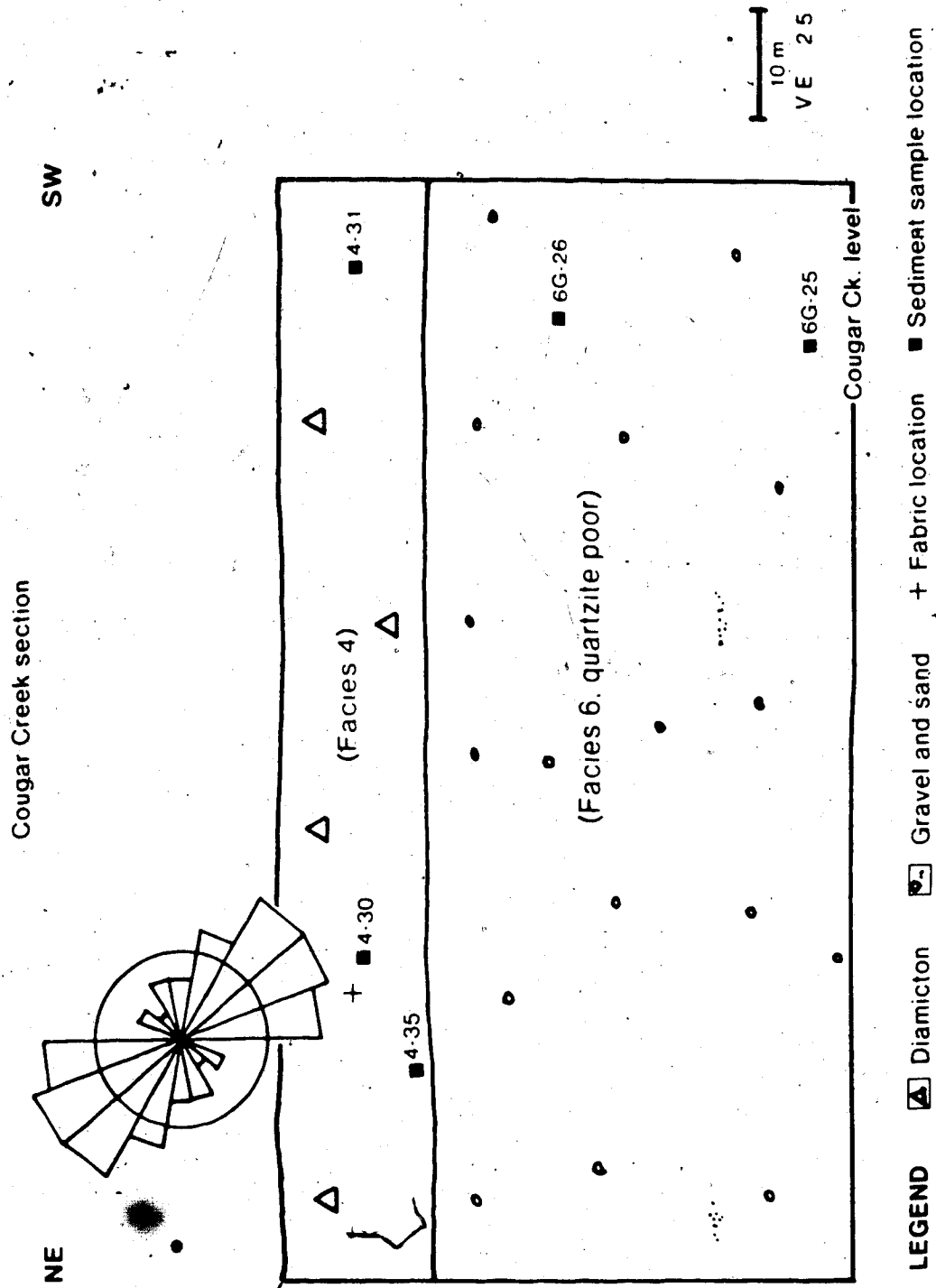


Figure 38. Cougar Creek section.

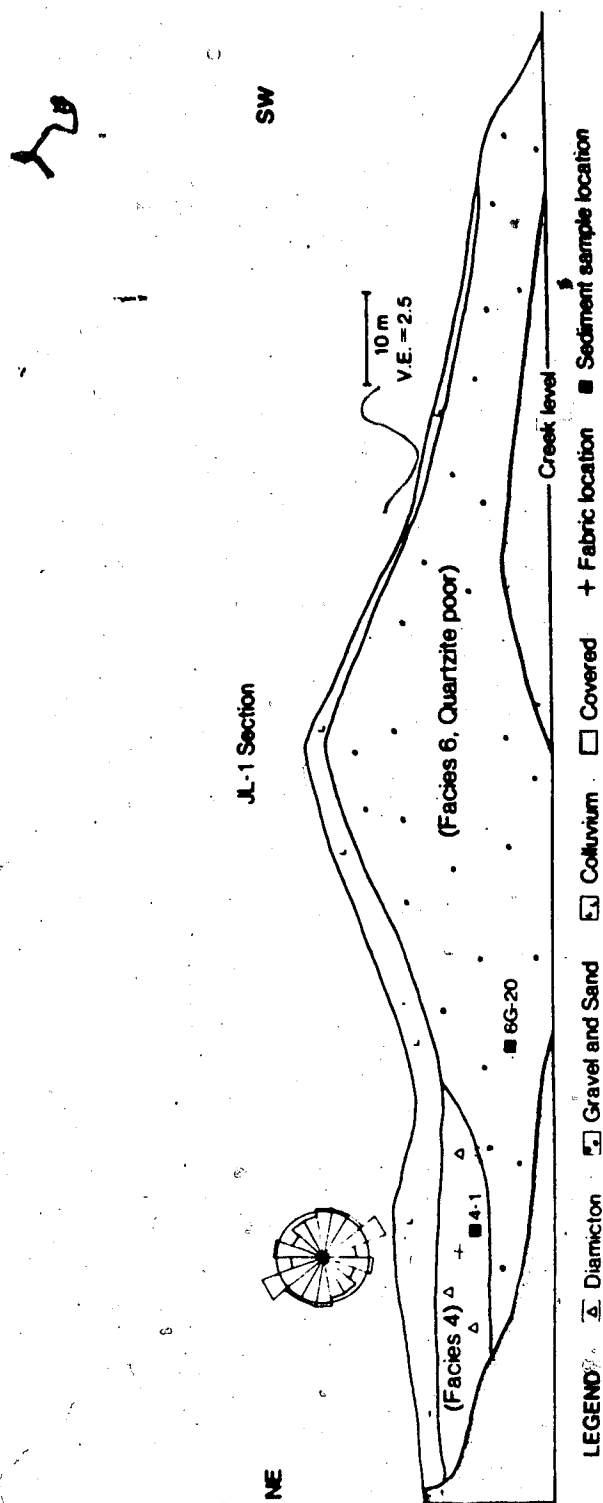


Figure 39. Johnson Lake section JL-1.

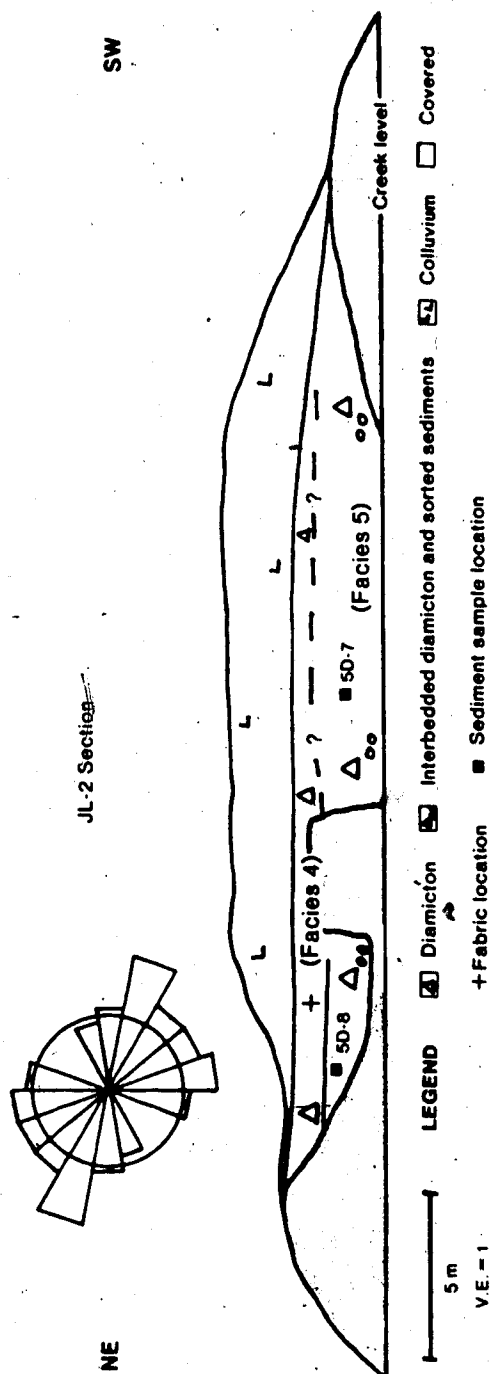


Figure 40. Johnson Lake section JL-2.

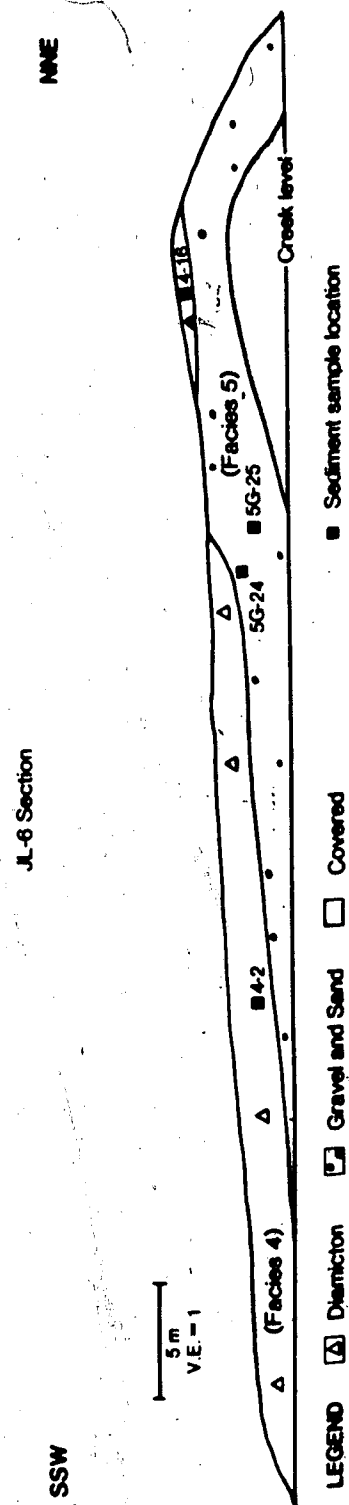


Figure 41. Johnson Lake section JL-6.



Plate 6. Curved joints with striated surfaces in the diamicton of facies 4. (Photograph at the Anthracite section) .--

The diamicton matrix supports clasts. Average clast diameter is 1.5-2.5 cm. The diameter of the largest clasts is about 30 cm; the average diameter of the larger clasts is 6-8 cm. 5-20% of facies 4 vertical surface area is comprised of clasts more than 1 cm in diameter.

The diamicton also contains numerous lenses. The lens-fill widely ranges in both grain size and sorting. Grain sizes are in the clay- to gravel-size range. These lenses are the predominant structures and have a variable distribution both vertically and horizontally throughout.

The sorted-sediment lenses' distribution varies throughout. The thinner portion of facies 4 has abundant lenses near its base. Here, the ratio of lenses to diamicton is 1:1. Moving upwards, the number of lenses decreases markedly. Lens distribution in the thicker portion of facies 4 is more homogeneous; although lens abundance does decrease slightly from lower to upper regions. If the lens-rich area of the thinner member of facies 4 is excluded, 1-2% of the facies is composed of sediment-filled lenses.

Facies 4 forms either the uppermost unit of the sedimentary succession or is overlain by gravels (facies 6). Underlying facies 4 is either a well sorted gravel (facies 6) or an interbedded sequence of poorly-sorted gravels and diamictons (facies 5). Both upper and lower contacts of facies 4 are sharp. The upper contact undulates

by 1-2 cm. The lower contact has a trace which generally passes just below clasts contained in facies 4 and just above clasts contained in underlying units. In addition, some clasts bisect the lower contact. Pebbles situated along both the upper and lower contacts are not faceted or striated. No directional features were observed on the under surface of facies 4.

The upper contact of facies 4 is horizontal along its entire length whereas the lower contact is not. Part of the lower contact (20% of its length) dips 10-20° west or undulates by 1-2 m.

Horizontal, elongated, tabular sediment-filled lenses comprise about 95% of lenses observed within facies 4. They form sharp contacts with the enclosing diamicton and generally pinch out. Average lens dimension is 23 cm thick and 240 cm long (range: 0.5-150 cm thick, 20-1000 cm long).

The horizontal, elongated, tabular lenses form two broad groups. The first group consists of larger lenses which often commonly occur closely spaced in certain areas and vary in size from 10-60 cm thick by 5-8 m long. Vertical separation between the larger lenses is 1-3 m; horizontal separation is 10 m. The second group is comprised of smaller lenses distributed fairly homogeneously throughout the facies. These average 10 cm

thick by 1.5 m long. The lenses of both groups are filled with either clay, silt, sand, or gravel; only rarely do all grainsizes fill a single lens. Most lenses are filled with sand and some pebbles. Sand- or gravel-filled lenses contain very little clay or silt.

About half of the lenses have a structureless fill with the other lenses having very faint, widely spaced, clay and silt, horizontal laminations within the sand fill. Only rarely is this internal bedding deformed or are planar cross beds or climbing ripples observed.

About 5% of the lenses in facies 4 do not have the more common elongated-tabular shape. These less common lenses are categorized into 7 types based upon their shape. Each of the 7 types occurs with about equal frequency. Type 1 inclusions are tabular lenses which are slightly contorted or irregularly shaped with dimensions within the ranges previously given. Type 2 inclusions are 1.5 m² irregularly shaped sand patches within diamicton. Type 3 inclusions are tabular, sand-filled lenses which interfinger with diamicton. Type 4 inclusions occur as numerous thin sand-stringers or sandy wisps within the diamicton; they appear as up to 1 cm thick by 3 cm long sand-filled lenses covering one half of a few 1 m² areas of facies 4. A type 5 inclusion is a mottled zone appearing as interfingering sandier, and less sandy horizontal areas of diamicton covering 3 m². Type 6 inclusions are

vertical lenses, 4 cm wide and 3-4 cm high, filled with fine to coarse well-sorted sand. They also contain a few horizontal clay beds (0.8-1 cm thick) oriented perpendicularly to the height of the lenses. Type 7 lenses are located near, or at the base of, the thick portion of facies 4. These lenses are filled with structureless fine gravel, granules, and coarse sand. The base of the lenses are covered by talus but the proximity of the lenses to the base of the facies (within 1 m) makes it very probable that the lenses' bases are situated along the facies lower contact. Because of this the lens base is likely also horizontal. Type 7 lenses are about 1 m thick and 2-3 m in length.

FACIES 4 INTERPRETATION

BASAL TILL INTERPRETATION

The sediment comprising facies 4 is interpreted to have been transported by a valley glacier and then directly deposited from the base of a glacier with no resedimentation occurring after deposition. The evidence supporting this interpretation is the same as the information presented for facies 1 (page 64). Additional evidence is the drumlinized topography above facies 4 (Plate 4). The drumlins indicate the underlying deposits

most likely formed beneath a glacier (Muller 1974; Boulton 1976a; Menzies 1979).

DETAILED INTERPRETATION OF FACIES 4

Facies 4 has characteristics of both basal melt-out till and lodgement till; it will be shown that facies 4 did not form exclusively from either a basal melt-out process or a lodgement process, but rather formed from a combination of both processes.

Reasons for rejecting the process of basal melt-out for facies 4 are, (i) the homogeneous petrology of facies 4. (Figures 42 and 43 (facies 4 thin)) suggest the facies is not basal melt-out till because basal melt-out till usually has an up-section increase in more distantly derived lithologies (Hyvarinen et al. 1973; Haldorsen 1977). Facies 4 does not show such an increase. In the study area the quartzite percentage would be expected to increase in abundance up a section of basal melt-out till. (ii) The thicker portion of facies 4 has a thickness of 30 meters; this exceeds the observed thickness range of basal melt-out tills which tend to be only a few meters thick (Boulton 1976b; Lawson 1979). (iii) The thinner portion of facies 4 has a drumlinized surface topography (Plate 4) indicating the glacier was moving while the facies was being deposited. A moving glacier during till deposition precludes basal melt-out till deposition since in the

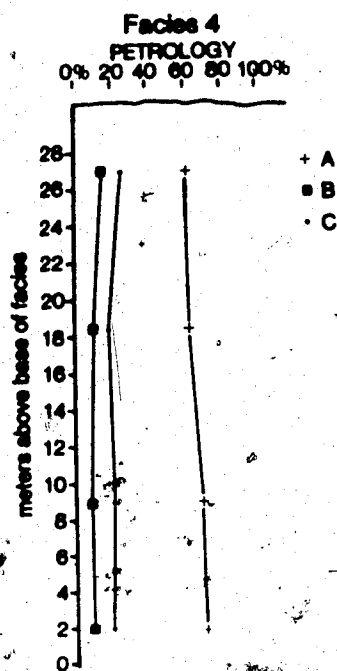


Figure 42. Petrology of 1-2 mm diameter grains along a vertical column through facies 4. A=carbonates, cherty limestone; B=quartzite; C=chert, sandstone, siltstone,

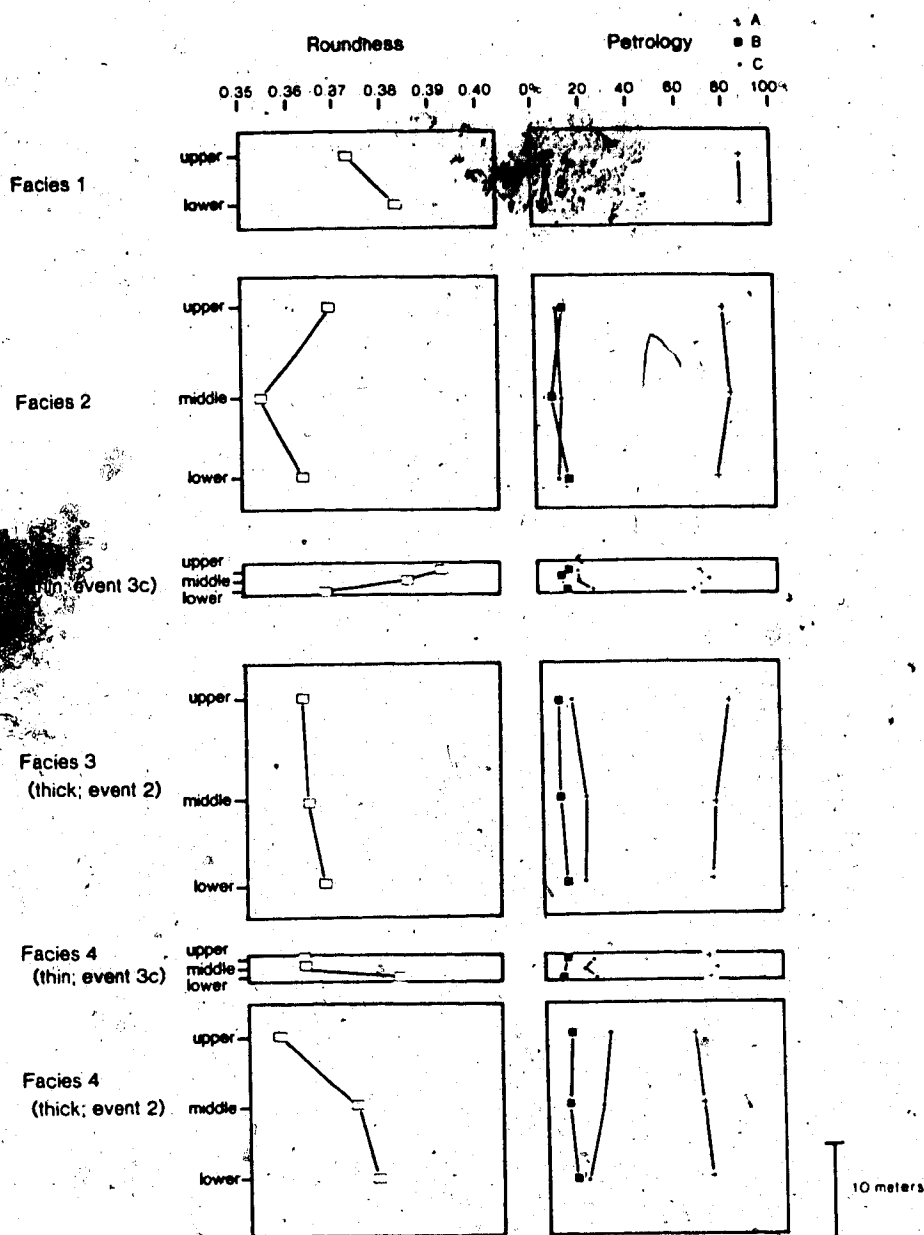


Figure 43. Roundness and petrology of 1-2 mm diameter grains at the upper, middle, and lower portions of each facies. Roundness is of carbonate grains. For petrology: A=carbonates, mostly limestone; B=quartzite; C=chert.

strict sense the basal melt-out process only happens under stationary ice (Shaw 1983).

If facies 4 is not basal melt-out till, it then follows the facies is lodgement till, the other type of basal till. However three characteristics of facies 4 suggest the facies is not lodgement till. Firstly, the facies has more lenses filled with stratified, sorted sediment than is observed or can possibly form in lodgement till (Marcussen 1975; Kruger 1979). Secondly, plano-convex lenses (type 7 lenses) are observed along the base of the facies; these lenses are products of subglacial streams which do not form where lodgement till is forming (Shaw 1982). Thirdly, the undulatory nature of the lower contact of facies 4 (at Carrot Creek, Figure 33) is unlike the planar lower contacts observed in lodgement till (Eyles and Sladen 1981).

It seems, based on the observations listed above, that facies 4 is neither exclusively lodgement till nor basal melt-out till. Instead, the facies has characteristics common to both types of till; this leads to the conclusion that facies 4 was formed in a manner where both lodgement and melt-out processes were operating. The following discussion elaborates on how facies 4 formed from a combination of both processes.

FACIES 4 DISCUSSION

Facies 4 is interpreted to have formed from successive layers or pods of debris-rich basal ice which were lodged beneath a sliding glacier. After a layer of debris-rich ice was lodged against the substrate the interstitial ice melted-out. As the glaciation progressed, layer upon layer of debris-rich ice was plastered against the substrate. Continual lodgement of basal debris layers over time increased the thickness of facies 4 up to 30 meters. This depositional process maintained the upsection homogeneous nature of the diamicton's grainsize (Figure 44), petrology (Figure 42), and roundness (Figure 45).

Lenses or layers of debris-rich basal ice probably became plastered or lodged onto the substrate when the resistance between the base of the glacier and the substrate became greater than the resistance offered above the base of the glacier by an ice-rich layer. This situation could occur when the basal debris-rich ice made contact with a debris-rich substrate, and friction along this contact (the base of the glacier) (Figure 46a) was greater than the resistance of an overlying layer of ice-rich debris. The plane of movement at the base of the glacier would then jump upwards from the base of the glacier to a level of lesser shear resistance (Figure 46b). Once the shear plane jumps upwards a new plane of sliding forms, the new base of the glacier. This effectively

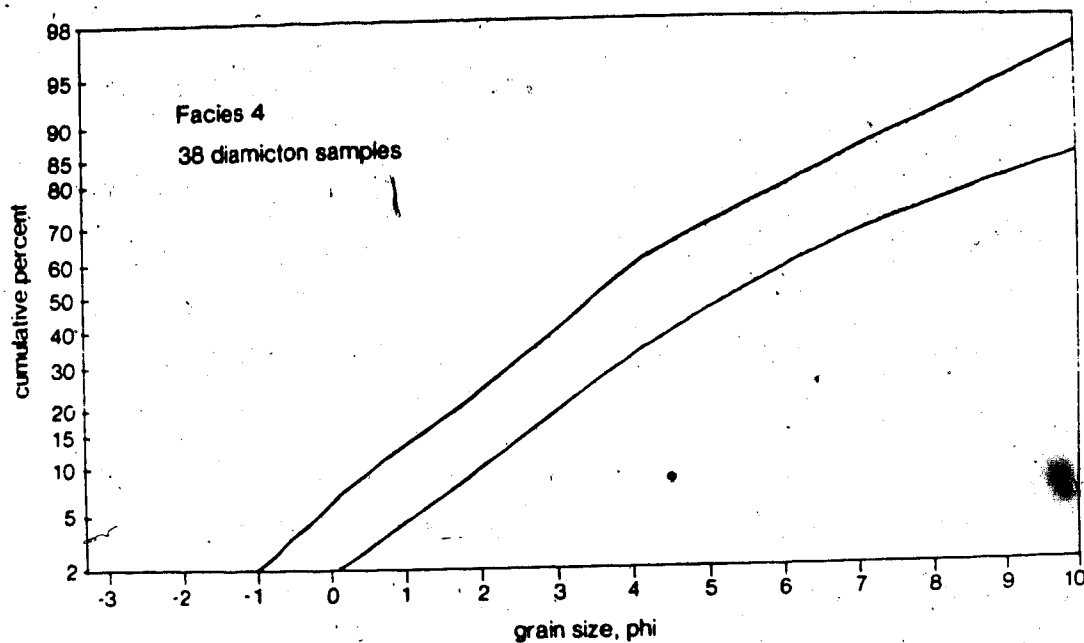


Figure 44a. Facies 4 diamicton matrix cumulative curves.
• Shaded area represents 38 curves.

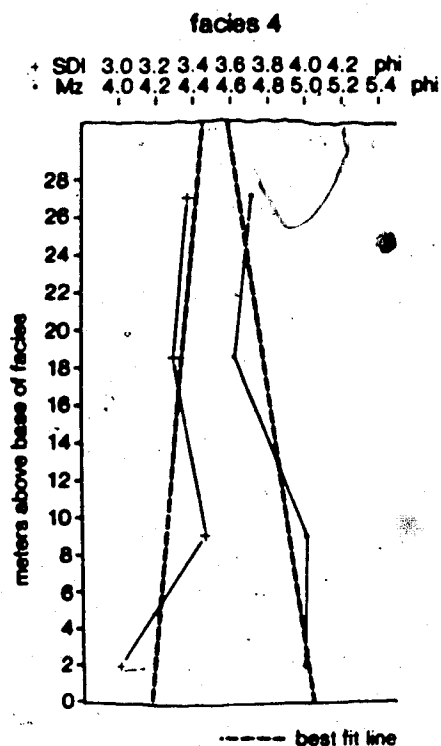


Figure 44b. SDI and Mz of diamicton matrix along a vertical

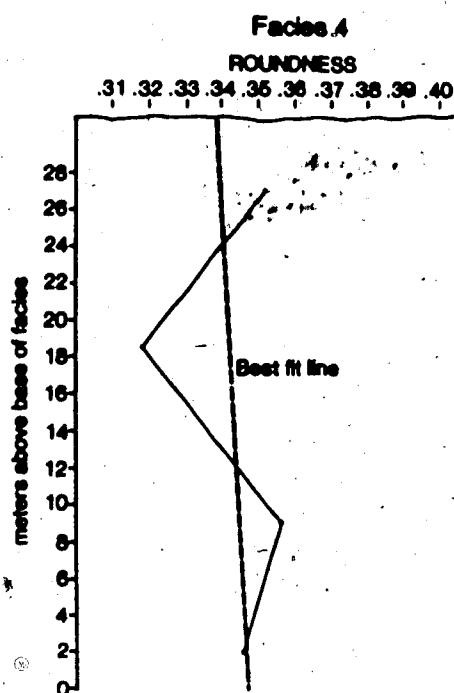


Figure 45. Roundness of 1-2 mm diameter carbonate grains along a vertical column through facies 4.

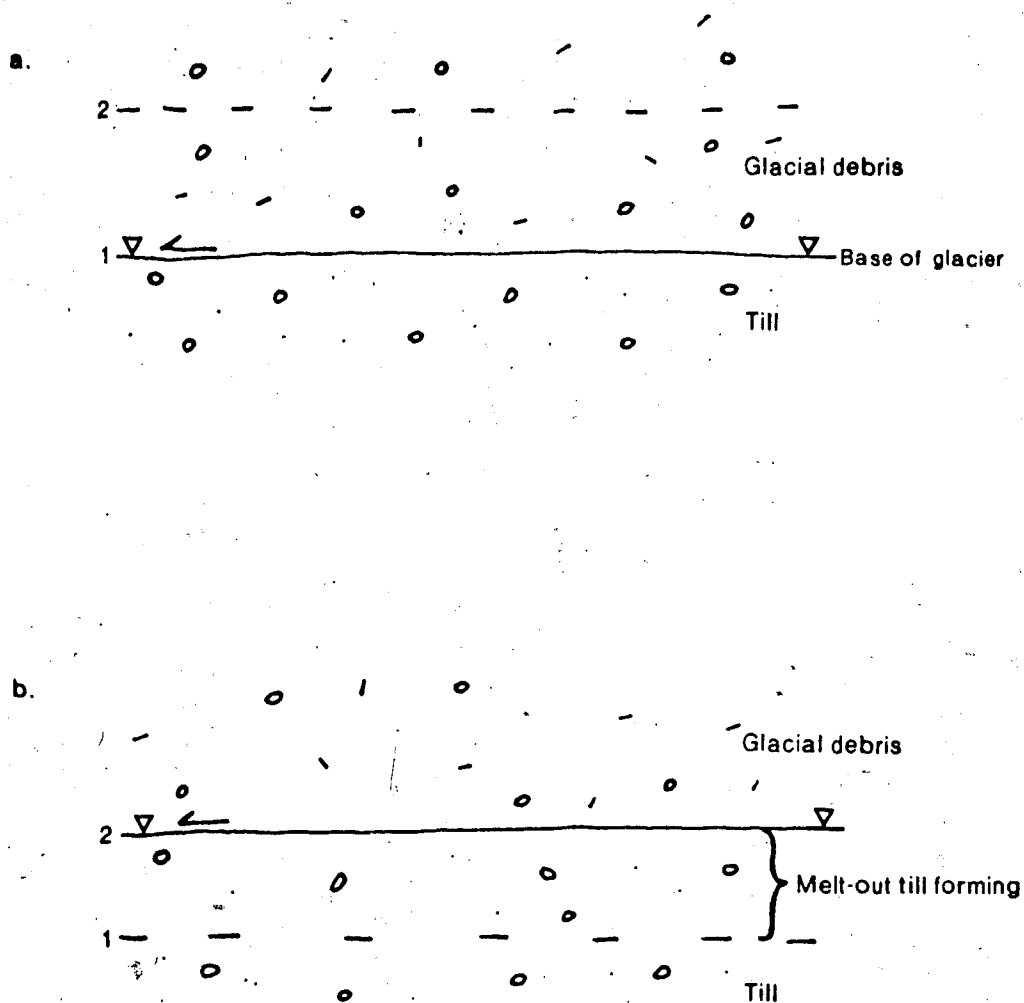
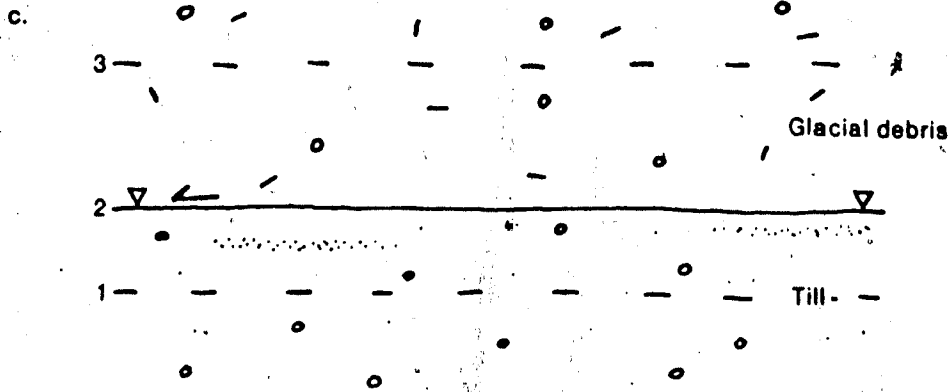


Figure 46. Facies 4 formation. (a.) Basal sliding of glacier along plane 1. When friction along plane 1 exceeds the shear strength of the overlying ice-rich plane 2 the plane of movement or basal sliding is displaced to plane 2. (b.) Plane 2 becomes the glacier's base. Glacier sliding along plane 2 strands a layer of debris-rich ice which then melts-out, figure 44c. Sand fills conduits in the debris-rich ice. (d.) The entire process is repeated.



strands a layer or lens of debris-rich ice below the new plane of sliding. This mode of lodgement is similar to one envisioned by Muller (1983a) where entire layers of debris, instead of individual debris particles, are lodged.

Once a layer of debris-rich ice was lodged it would melt-out (Figure 46b) and the ice-rich zones of the layer would become conduits for meltwater derived from the overlying wet-based glacier and also from melting ice within the layer of lodged debris. These meltwater conduits would become filled with sorted sediment (Boulton 1972a) and become the sediment-filled lenses in facies 4 (Figures 46c and d).

As mentioned, the sediment-filled lenses are interpreted to have developed in lodged basal debris-rich ice and not in the basal debris being actively transported by the glacier. The lenses' generally tabular shape and undisturbed internal stratigraphy indicate that no major deformation of the lenses occurred once they were formed. This preservation could only happen if the lenses formed in stationary ice; in this case developing inside already lodged debris layers. The lenses which have contorted shapes or have no internal stratigraphy may have formed prior to being lodged. The contorted shapes and/or lack of stratigraphy may be a product of active basal transport.

The abundance of non-contorted sand lenses also indicates that ice within the lodged basal debris layers

did not melt differentially since this would have contorted the lenses. Most likely, after a basal debris layer became lodged the glacier continued to slide over this layer without inducing significant deformation within the layer. Some evidence of localised deformation is preserved as fractures.

The curved, sand-lined horizontal fractures with striae on the fracture surfaces (Plate 6) likely delineate a former zone of movement between a lodged basal debris layer and the overriding glacier. Two vertical sediment-filled lenses offer additional evidence of deformation. These lenses may have opened when the till comprising the substrate under a moving glacier was fractured or pulled open and later filled with sediment.

As the glaciation progressed, successive layers of basal debris would become lodged and then melt-out. This action would gradually increase the facies thickness. The rate of increase is partly a function of the thickness and density of the basal debris-rich ice. Thickness of the lodged layers is controlled by the thickness between the glacier's base and the first ice-rich zone. If the basal debris zone lacked ice-rich layers then the entire basal debris zone would probably lodge; in this case, a massive basal zone would have a thickness up to about one meter (Boulton 1972b). If the basal ice is stratified, as observed by Lawson (1979), the lowermost layer of basal

debris only a few centimeters thick may lodge. Pebble fabric orientations retain a record of the clast orientation in this basal debris.

The diamicton pebble fabrics of facies 4 are likely englacial fabrics retained during melt-out of the lodged basal ice layers. The lack of areally significant deformation suggests the fabrics have not been reoriented. Evidence of deformation would be the presence of many contorted sand lenses or more numerous shear planes in the till. Such evidence is not observed.

The preferred orientation of pebble fabrics in the thick portion of facies 4 is both parallel and nearly perpendicular to reconstructed ice-flow lines (Figures 47a and b). The thick portions of facies 4 are located in a bend of the Bow valley where compressive ice-flow may have developed in some localities as the glacier rounded the bend. Perpendicular fabrics represent areas of former compressive ice-flow (Boulton 1971a). All of the pebble fabrics whose principle orientation is parallel to the ice flow-lines are interpreted as representing areas of former extending glacial ice flow.

Facies 4, composed of a diamicton with numerous lenses filled with sorted sediment, has been shown to have formed from a combination of lodgement and basal melt-out processes. The facies was deposited from a series of successively deposited, basal debris layers which melted

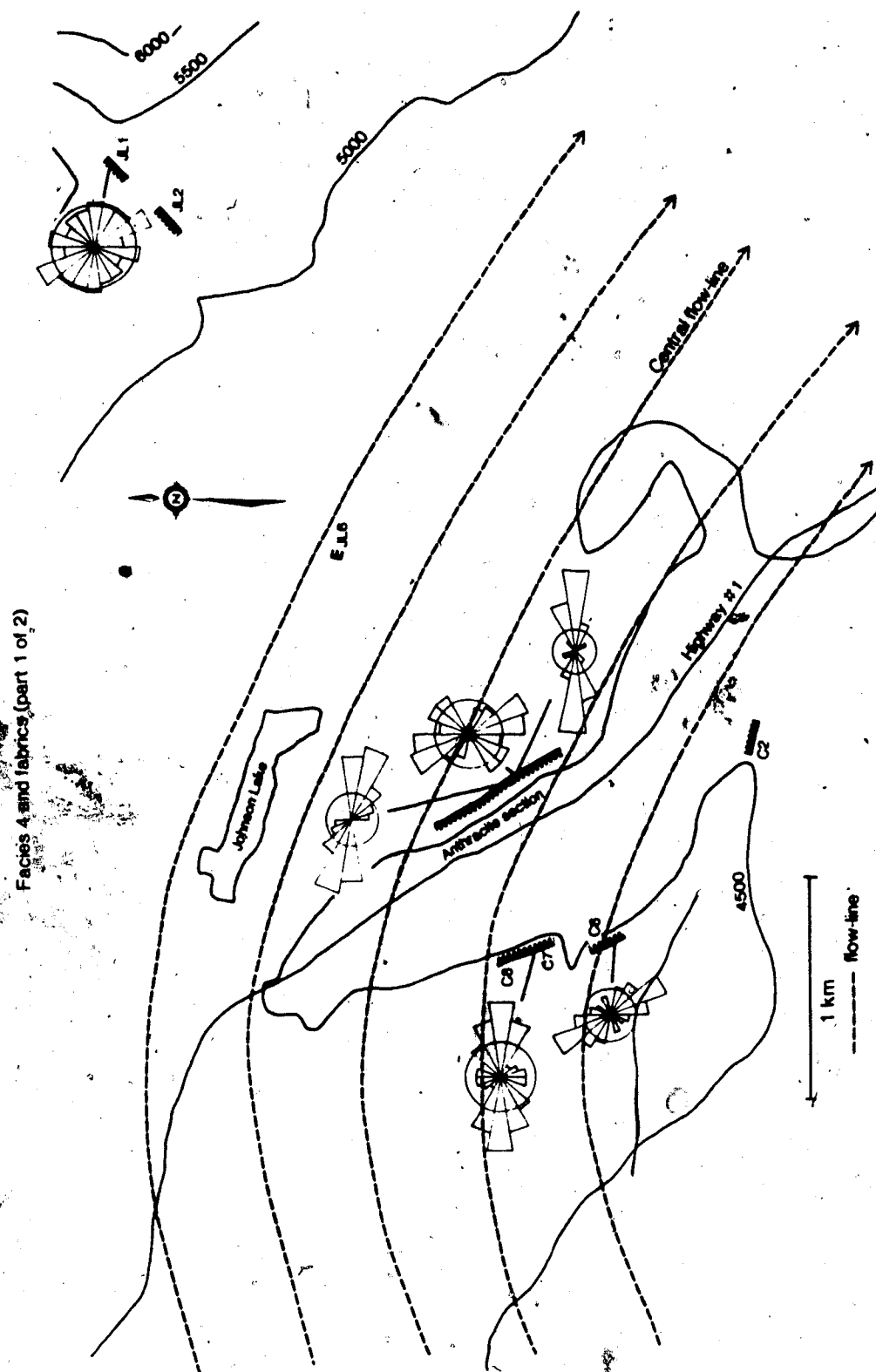


Figure 47a. Diamicton pebble fabrics of facies 4 relative to reconstructed glacier flow lines (part 1 of 2).

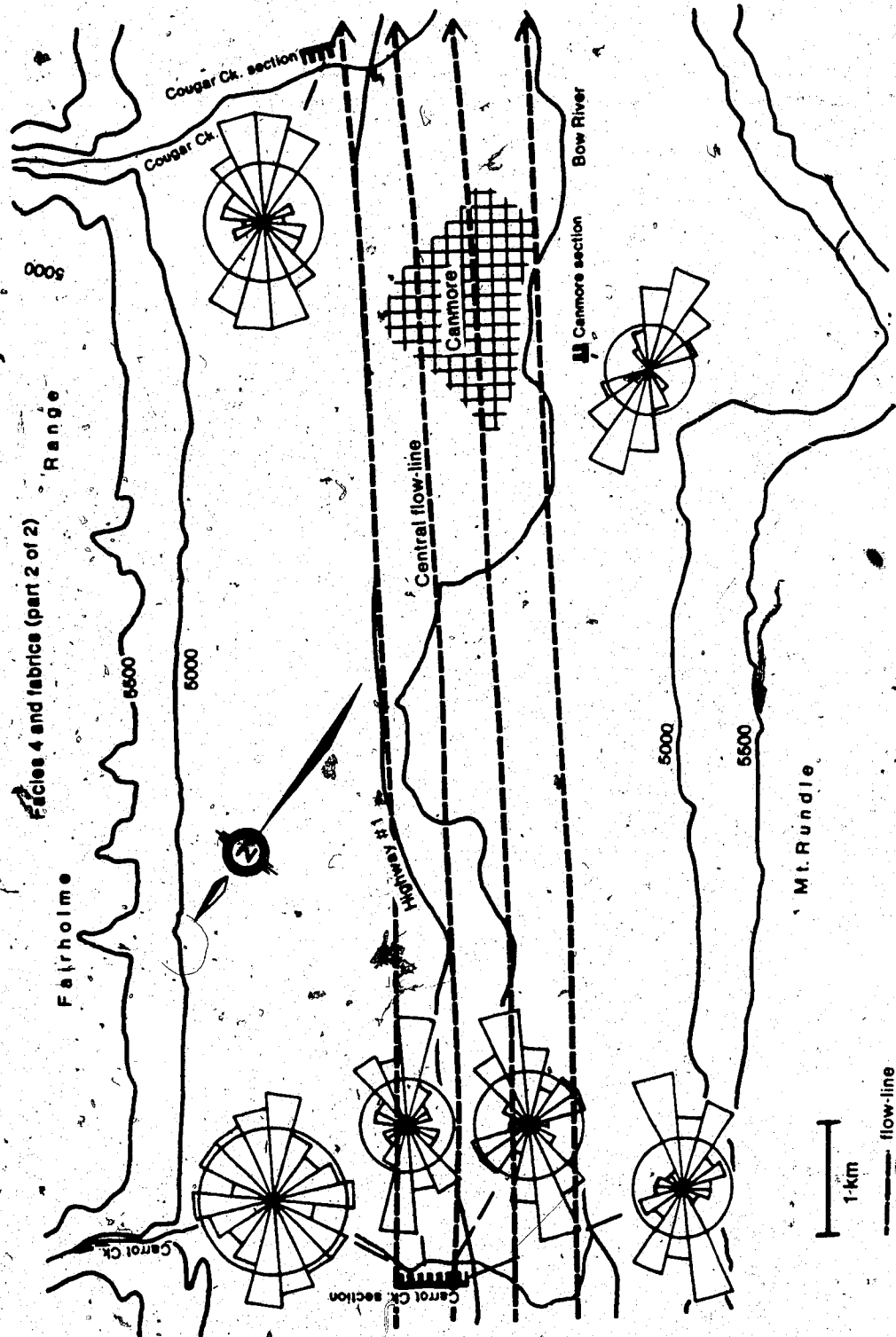


Figure 47b. Diamicton pebble fabrics of facies 4 relative to reconstructed glacier flow lines (part 2 of 2).

out beneath a moving valley glacier.

E. FACIES 5

FACIES 5 DESCRIPTION

Facies 5 consists mainly of an interfingering, interbedded sequence of poorly sorted gravels, diamicton lenses, and diamicton blocks. Also included are poorly sorted gravels which lack diamicton units. The average thickness of facies 5 is 9m (range: 2.5-13 m). The proportion of the facies composed of sand and gravel units to diamicton units ranges from 10:90 to 100:0 (average 50:50). Diamicton lenses generally have tabular shapes, with thicknesses ranging from 5 cm to 2 m and lengths varying from 20 cm to 25 m; average lens thickness is about 75 cm and average length is 6.5 m. Diamicton blocks have diameters ranging from 10-120 cm, averaging 30 cm. The outcrops where facies 5 is exposed are illustrated in Figures 23, 26, 27, 33, 34, 35, 36, and 37.

Two major subfacies make up facies 5. These are (i) diamicton lenses and blocks and (ii) units composed of sorted sediments.

Diamicton lenses are generally horizontal, some have dips up to 15° . Diamicton lenses generally terminate by pinching out, although a few lenses have square-shaped, jagged or serrated ends. Only rarely do the lenses interconnect with one another. Gravel and sand border the diamicton lenses. 99% of all contacts between diamicton and sand-gravel units are sharp and distinct. The contact surfaces between the diamicton units (both diamicton blocks and lenses) and the gravel units are generally smooth; no pebbles straddle the contact surface. About 4% of diamicton lenses' upper and lower contacts have irregular shapes which undulate by 10-15 vertical centimeters; about 1% of the diamicton-lenses' contacts are jagged and have long, thin finger-shaped diamicton projections extending into the surrounding sand and gravel (projections average 5 mm thick by 20-30 mm long).

The diamicton (Figure 48) is matrix supported. Average clast diameter of the diamicton is 3 cm; average diameter of the larger clasts is 8 cm, the maximum clast diameter is about 30 cm. 5-20% of the diamicton's vertical-surface area is comprised of clasts greater than 1 cm diameter. 90% of the diamicton comprising the diamicton lenses and all of the diamicton comprising the diamicton blocks is massive, dense, and structureless. About 9% of the diamicton lenses

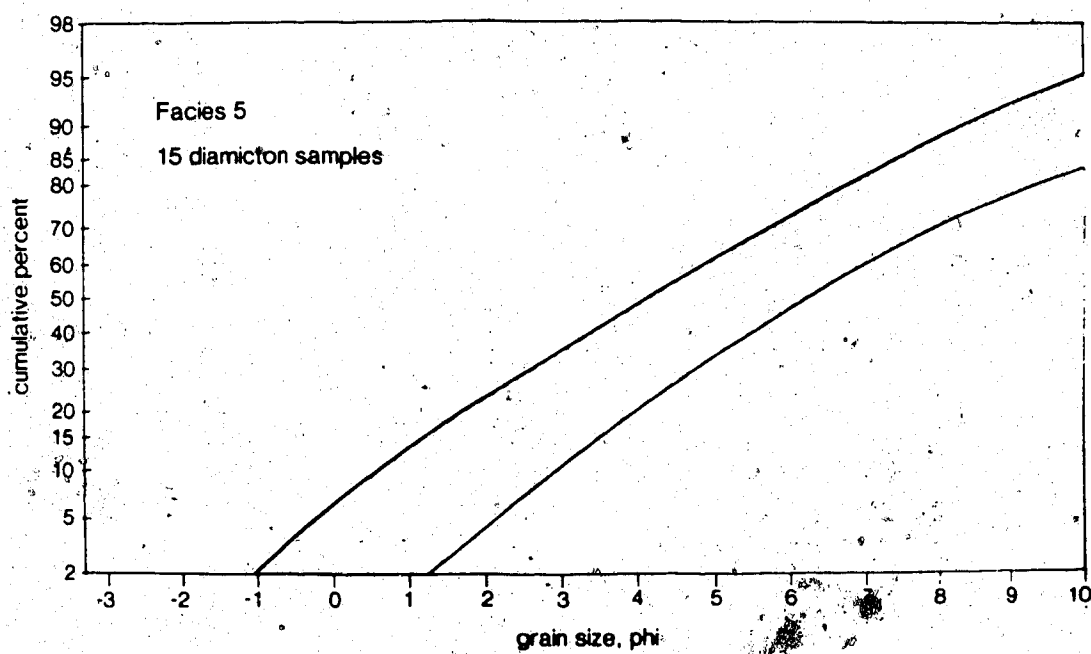


Figure 48. Facies 5, cumulative curves of the 'diamicton lenses' matrix. Shaded area represents 15 curves.

contain well defined sand and granule filled lenses. Fewer than 1% contain small (1-5 mm²) subangular to subrounded shaped voids, or small (3-5.5 cm²) irregularly shaped, poorly defined, pockets filled with fine, structureless sorted sand.

Sand and granule filled lenses are totally enclosed by diamicton. They are generally horizontal, with average thicknesses of 4 cm and average lengths of 50 cm (range: 1-21 cm thick by 0.03-6 m in length). Three lenses are vertical, these are sand-filled and have a width variation of 0.5-20 cm and a height variation of 1-2.5 m.

Individual lenses are usually filled with one grainsize from within the size range of fine sand to open-work granules. Some lenses are filled with matrix supported granules and small pebbles. Sorting of the fill ranges from poor to good. Numerous lenses will commonly occur within an individual diamicton-lens. Each lens within the diamicton will usually have a different grainsize and sorting than other adjacent lenses within the same diamicton lens.

About 60-70% of all horizontal sand- and granule-filled lenses lack sedimentary structures. The only structures within horizontal lenses are thin (0.5-3 mm thick) laminae composed of clay and silt. These laminae are either horizontal or dip slightly; only a couple laminae are

present in any one lens. Two of the three vertical lenses have horizontal or slightly concave-down 1-2 mm thick clay and silt laminae which extend across the lens, and are perpendicular to the outcrop trace of the lens; the other vertical lens is structureless.

The contacts between sand- and granule-filled lenses and the surrounding diamicton are sharp and distinct. Most of these contacts are smooth, although a small number are (i) contorted or undulate with an amplitude of 5 cm over a 30 cm distance, or (ii) are jagged, with the surrounding diamicton and the enclosed sand lens interfingering.

Gravel beds, and to a lesser extent some sand, silt, and clay beds, enclose the diamicton lenses; the contact between the diamicton and better sorted units is sharp and distinct. About 70% of the sorted sediment beds are comprised of horizontal to near horizontal, interbedded, interfingering, tabular, open- and closed-work gravel beds (Figure 49). Only rarely are any of the gravel beds cut into or truncated.

Internally, these beds have horizontal, parallel bedding. Individual gravel beds are differentiated from adjacent gravel beds by differences in both the sorting and grain size of the framework clasts and of the matrix. Contacts between adjacent beds are sharp and distinct. The

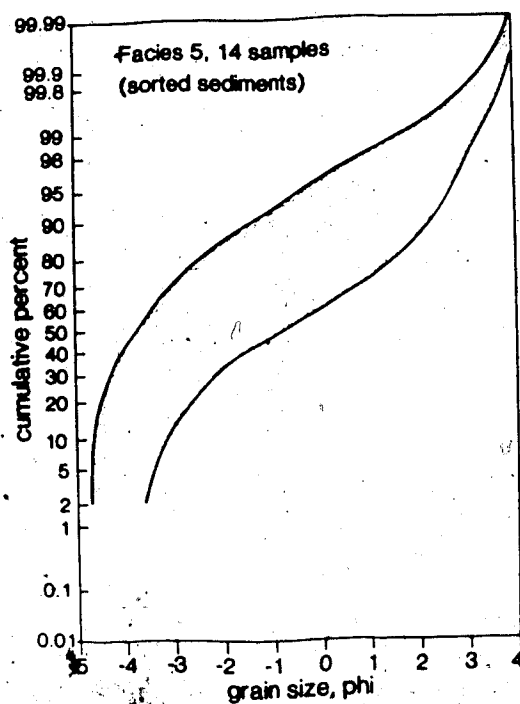


Figure 49. Facies 5, cumulative curves of the sorted sediment's coarser fraction (less than -5 phi fraction). Shaded area represents 14 curves.

sorting and grainsize of the gravel and of the gravel-matrix varies widely between beds. A small number of large clasts with 10-100 cm diameters are randomly distributed throughout.

About 25% of the sorted sediment subfacies consist of structureless gravel, which is characterized by a mixture of gravel and sand. The grainsize and sorting of both the framework-clasts and matrix vary randomly. Some of the matrix is laminated and is described in the following section. Within these gravels are a few groups of 40-100 cm diameter boulders which together cover an area of 4-8 m². The boulders are in contact with one another and have random orientations.

Table 6 gives the dimensions of gravel and sand subfacies and clast sizes within the gravel and sand.

Table 6

Range of clast sizes:			
regular clasts		=	sand-50 cm
random clasts		=	10 - 100 cm
Average clast size :			
regular clasts		=	8 cm
random clasts		=	30 cm
Range of unit thicknesses :			
gravel units		=	0.05-1 m avg = 25 cm
sand units		=	3-90 cm avg = 20 cm
Range of unit lengths :			
gravel units		=	30 cm - 15 m avg = 2.0 m
sand units		=	5 cm - 30 m avg = 12 cm

Pebbles within the gravel beds are usually either flat-lying or lack a preferred orientation; only rarely are the pebbles imbricated. About 60-70% of the gravels are poorly to very poorly sorted. These gravels have a clay- to gravel-sized matrix inclusively. Other beds have a better sorted matrix consisting of only one grain size which is usually sand. About 60% of the gravel beds' matrix is fairly poorly sorted.

About 5% of the sorted sediments are sand lenses (Figure 50). These are elongated, horizontal, and pinch out. About 50% of the sand units are structureless; 40% have horizontal, parallel laminations, and 10% have tabular cross-bedding.

A 2 m long, steeply dipping reverse fault and a 2 m long steeply dipping normal fault, both with displacements of about 20 cm are present in one portion of the gravel and sands.

Fifteen to twenty percent of the gravel's matrix is laminated silt and clay or laminated very fine sandy silt and clay. Rarely is a coarser-grained laminae composed of material as large as granules. The laminated matrix occurs in contiguous areas of clast supported gravel. This matrix consists of alternating finer- and coarser-grained laminae which conform in shape to the lower-surface of the clast

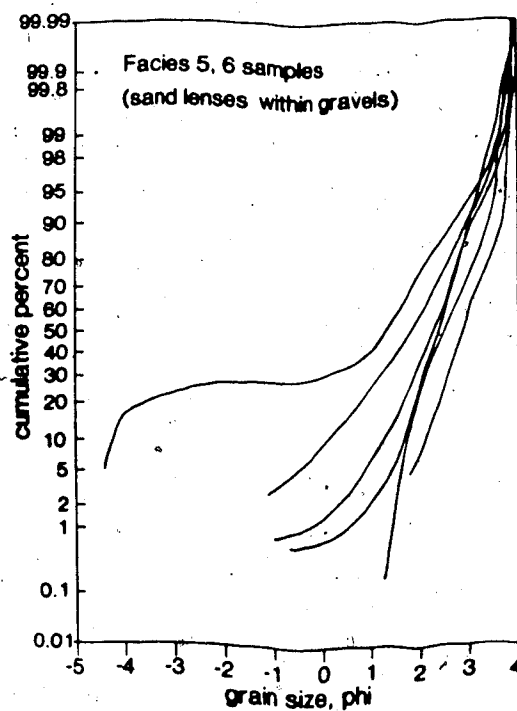


Figure 50. Facies 5, cumulative curves of the sorted sediment's sand lenses.

immediately overlying an interstice between gravel clasts. Laminae terminate against the clasts which form the lateral walls of an interstice (Figure 51). Laminae are from 0.25 to 2 mm thick, and increase in thickness away from their margins, reaching maximum thickness at the lowest point of their curvature. In some cases the lamina is 2-3 times thicker towards the middle than it is near its margins. About 5-10% of the interstices in a zone of laminated-matrix are filled with fine- to medium-grained sand instead of laminated sediment. Forty to seventy percent of the clasts which have a laminated matrix are fractured along 2 or 3 planes.

The nature of the contact that facies 5 makes with other facies varies throughout the study area. The lower contact is distinct and flat. The upper contact is distinct and flat along about 50% of its length; elsewhere it undulates or is uneven. The contact has an amplitude of 50 vertical cm along a 50 cm horizontal distance in areas where the upper contact is undulatory. The uneven portions of the upper contact slope from $6-11^{\circ}$. This unevenness is expressed as a series of ramps, e.g., the contact may be flat, ascend or descend at a $6-11^{\circ}$ angle and then become flat once more (Figure 33).

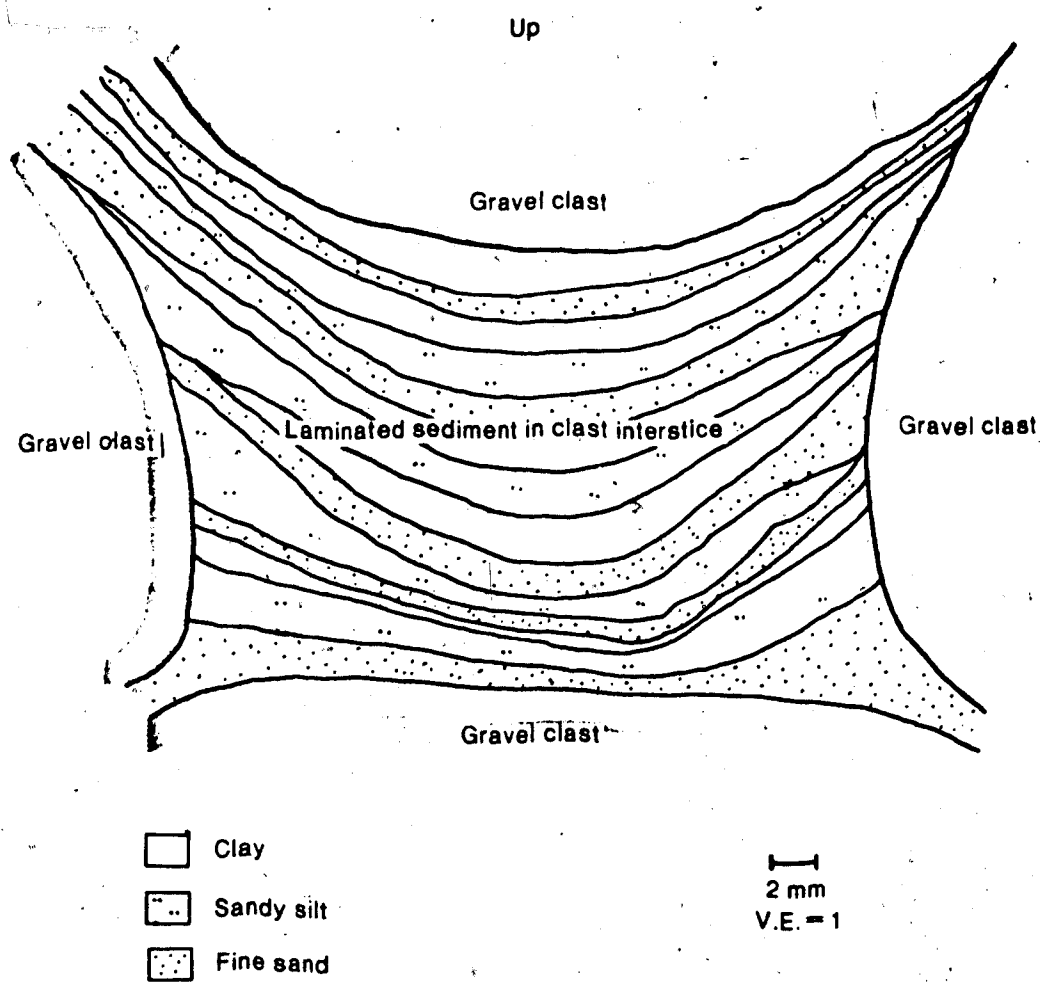


Figure 51. Facies 5; laminated gravel matrix.

FACIES 5 INTERPRETATION

Facies 5 is interpreted to be a group of related sedimentary deposits formed in a proglacial environment. These deposits represent glacial mudflow complexes, dissected till plains, and glacial outwash channel-fill deposits (Figure 52).

GLACIAL MUDFLOW COMPLEX

The interbedded diamicton lenses and sorted sediments, the small diamicton blocks within a sorted sediment matrix, and the sorted silt- to gravel-sized sediment lenses are interpreted to collectively represent a glacial mudflow complex. The lens-shaped diamicton units (and other diamictons in facies 5) are interpreted to be derived from glacial debris on the basis of the similarity between the diamicton of facies 5 and the glacially derived diamicton of facies 1 to 4 (Table 7). In addition, the grain size distribution (Table 7), roundness values (Table 7), petrological distribution (Figure 53), and clast striations of the diamicton comprising facies 1, 2, 3, 4, and 5 are all similar. This similarity also suggests that the diamicton of facies 5 was also derived from glacial debris.

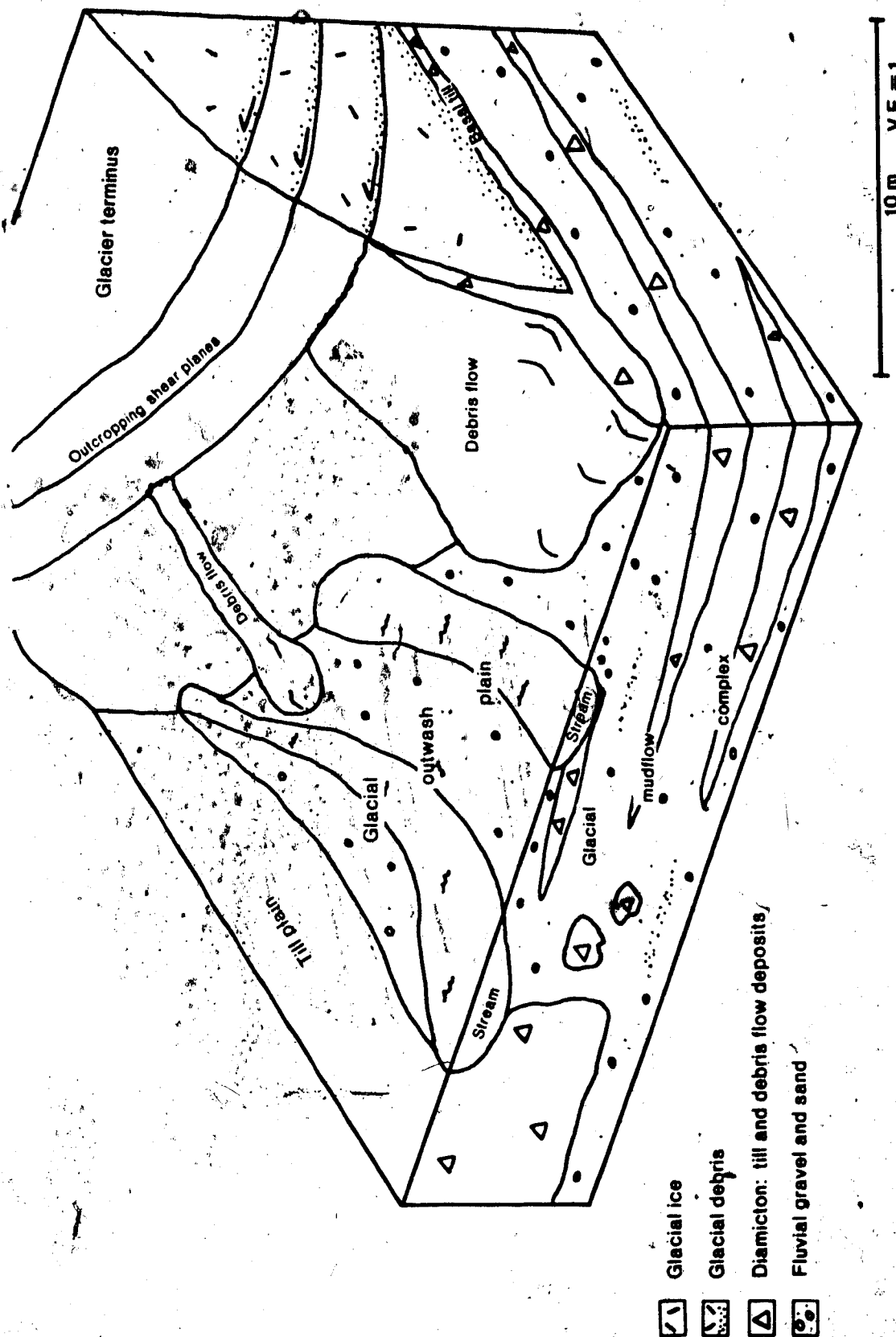


Figure 52. Inferred depositional environment of facies 5.

Table 7. Comparison of properties between facies 1-4 and facies 5 diamicton

Property	Facies 1-4	Facies 5 (diamicton)
Mz (phi)	5.23 ± 0.57 n=110	5.26 ± 0.85 n=16
SDI. (phi)	3.49 ± 0.39 n=110	3.30 ± 0.35 n=16
Roundness	0.369 ± 0.019 n=85	0.367 ± 0.015 n=14

Petrology

A	73.9 ± 9.5 n=80	69.0 ± 6.4 n=15
B	9.8 ± 3.8	9.5 ± 3.2
C	16.3 ± 8.0	21.5 ± 4.4

A = carbonates, cherty limestone; B = quartzite;
C = chert, sandstone, siltstone, shale, and coal.

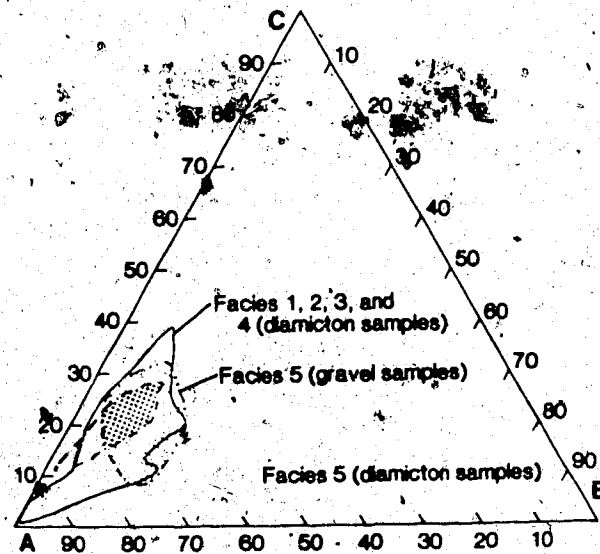


Figure 53. Ternary plot showing that most diamicton samples and the gravel portion of facies 5 all have the same petrological composition. A=carbonates, cherty limestone; B=quartzite; C=chert, sandstone, siltstone, shale, and coal.

The diamicton lenses of facies 5 are interpreted further to be mudflow deposits which flowed down the terminus of a glacier and then became interbedded with small, proglacial outwash streams. This interpretation is based on the similarity between facies 5 and glacial mudflow complexes as observed and described by others (Hartshorn 1958; Boulton 1967, 1968; Marcussen 1975; Dejong and Rappol 1983). The homogeneous clast distribution within the diamicton units (Plate 7) indicates that the mudflows had a yield strength large enough to support the enclosed clasts. A lack of sorted upper horizons within the diamicton lenses indicates the mudflows had either decreased water contents (Pierson 1980) or were not overly fluid.

The mudflows flowed down the glacier's terminus and onto a proglacial outwash plain of shallow braided streams. The horizontal, interbedded, interfingered, tabular, open- and closed-work nature of the gravels of facies 5 (Plate 8) are characteristic of fairly shallow braided streams (Hein and Walker 1977; Steel and Thompson 1983; Smith 1985). Streams active during the deposition of facies 5 flowed over the proglacially deposited, glacially derived mudflow deposits and in many cases covered the mudflows with sorted stream sediments. Later, additional mudflows (diamictons) would cover those same stream sediments; this is how the interbedded nature of the mudflow complex (facies 5)

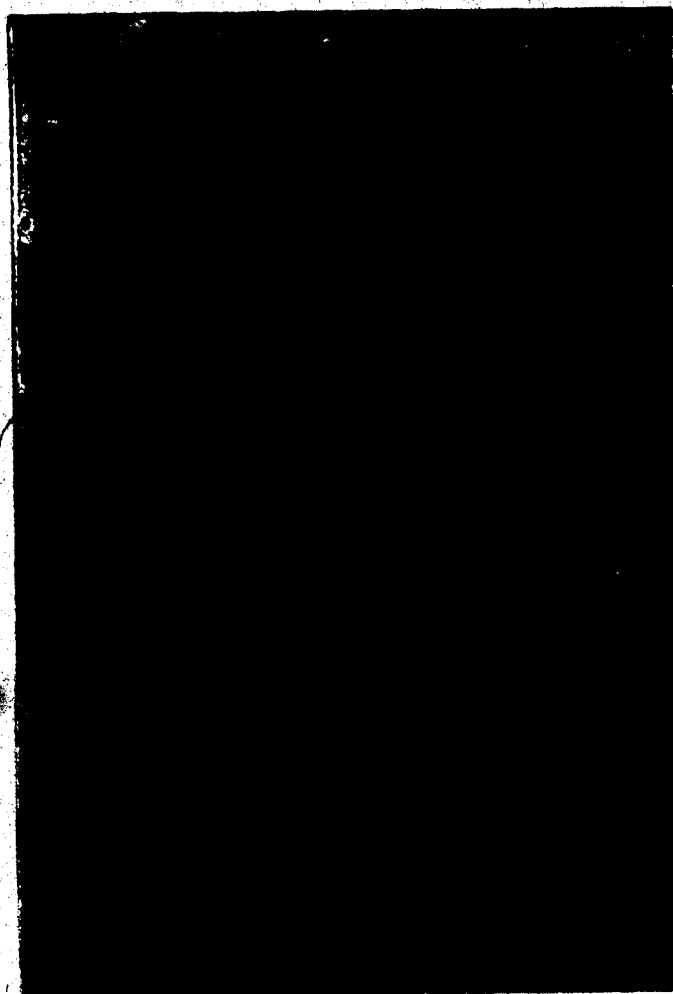


Plate 7. Facies 5. Interbedded diamicton layers/lenses and sorted sediments. The scale bar divisions are in cm. (Photograph at Carrot Creek 598 m mark).

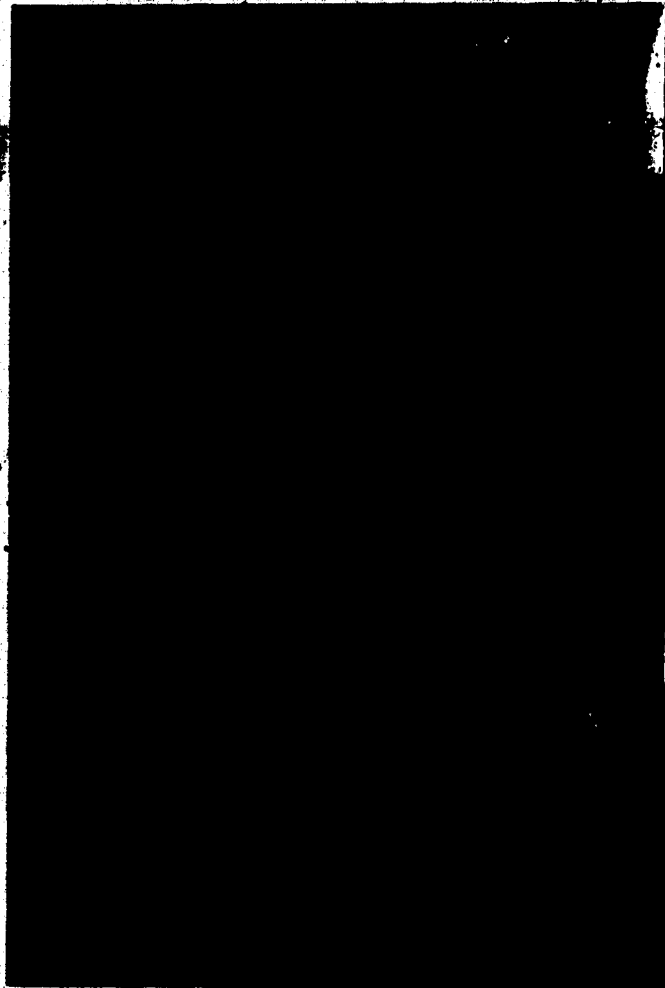


Plate 8. Facies 5. Interbedded diamicton lenses, blocks, and sorted sediments. Blocks are present in the upper right corner of the plate. (Photograph at Carrot Creek 480 m mark).

developed (Plates 7 and 8).

Braided streams would also erode semi-consolidated glacial mudflow deposits and thereby incorporate chunks of mudflow diamictos into the sorted stream sediments (Plate 8). In addition, shallow outwash streams would totally disaggregate mudflow diamictos and incorporate the size fractions of the former diamicton into the stream sediments. This disaggregation results in the braided-stream sands and gravels having the same petrologic sand-sized composition as the glacially derived mudflow diamictos (Figure 53).

Mudflow and stream flow transport of the diamicton also affected the roundness of the diamicton grains. The 1-2 mm diameter carbonate grains in mudflow diamictos are more angular (0.367, Table 7) than the 1-2 mm diameter carbonate grains from the braided stream deposits of facies 5 (0.389, Figure 54). The proglacial braided stream grains of facies 5 are in turn more angular than the 1-2 mm diameter carbonate grains in what are interpreted to be braided stream deposits (facies 6) (Figure 54). Therefore the mudflow complex stream grains have a roundness intermediate between the diamictos (facies 1-5) and the major braided stream deposits (facies 6). The intermediate roundness indicates that slight rounding of the mudflow complex stream grains occurred following derivation of the grains from disaggregated mudflows. As mentioned, the

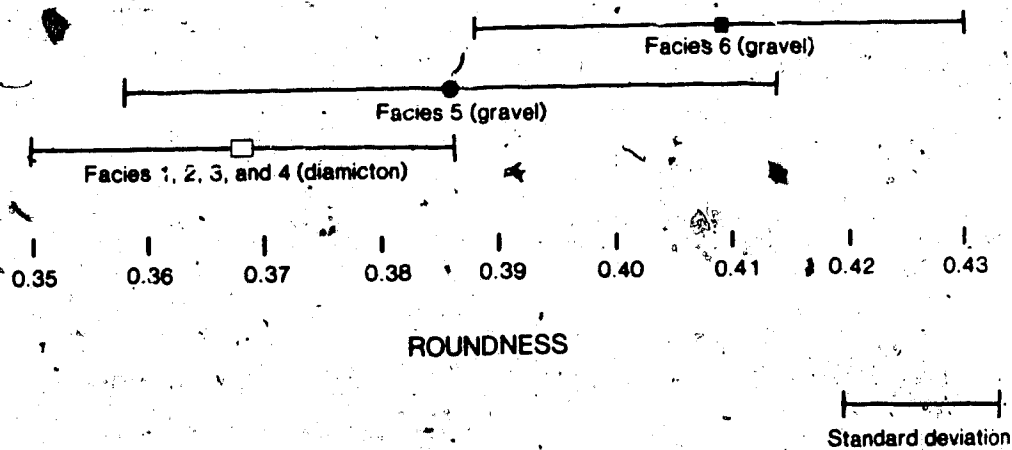


Figure 54. Roundness of 1-2 mm diameter carbonate grains. The population of facies 5 (diamicton) has the same roundness as facies 1-4 (diamicton).

grains were washed out of the mudflows by small, shallow braided streams. The ensuing proglacial stream transport was not extensive enough to abrade the grains to the roundness achieved in a much larger braided stream (facies 6).

DISSECTED TILL PLAIN

The portions of facies 5 containing large blocks (1-10 m²) of diamicton surrounded by sorted sediments are interpreted to be a till plain which was dissected by meltwater streams shortly after the till was deposited (Figure 52). In many cases the larger blocks' pebble fabrics are aligned parallel to the reconstructed ice-flow direction (Figure 55). The diamicton's pebble alignment and massive character are characteristic of basal till (Lawson 1979). The diamicton blocks are therefore interpreted to have been basally deposited by a glacier. Following this, the glacier retreated a short distance and exposed the recently deposited till in front of the ice as has happened in front of the Breidamerkurjökull glacier, Iceland (Boulton 1978). During deposition of facies 5 braided outwash streams issued from the retreated glacier, crossed the till plain, and began to erode the exposed till. Some of the till remained intact as large blocks; these were eventually buried by outwash and thus preserved.

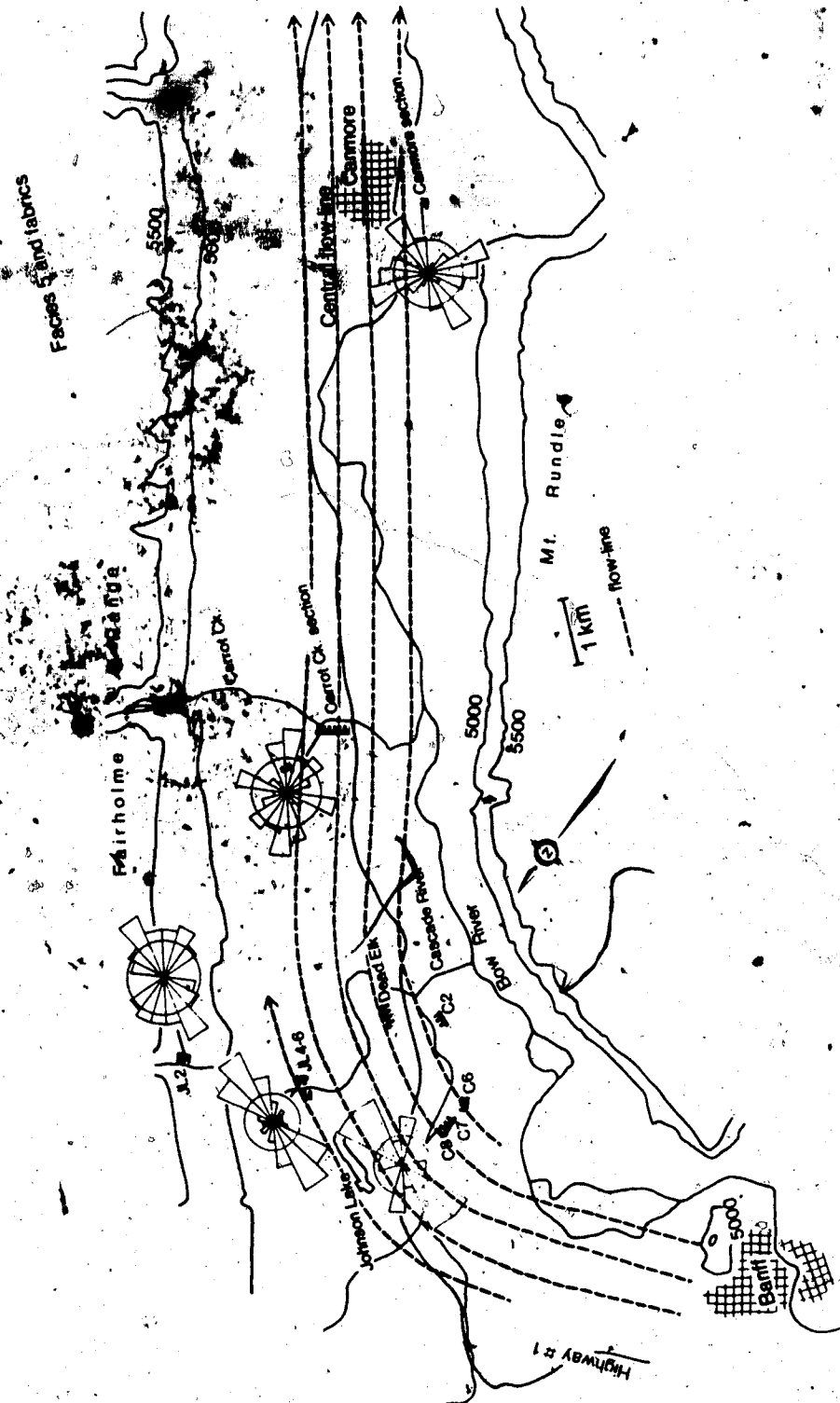


Figure 55. Diamicton pebble fabrics measured in facies 5 diamicton units.

In some areas the till is preserved intact as large blocks, in other areas it is partially disaggregated into smaller blocks of diamicton, or even totally disaggregated. Accumulations of large boulders (up to 1 m in diameter), which are much larger than the gravels they are supported by, indicate regions where the till was totally disaggregated and a very coarse lag left behind.

MAJOR OUTWASH CHANNEL

The cobble- and pebble-sized gravel with a prevalent matrix of laminated silt and clay is interpreted to be a major, filled glacial outwash channel. The unstratified, clast-supported gravel filled the channel during a time of peak water discharge. After the flow subsided, clay and silt gradually infilled the interstices of the gravel deposit and produced the laminated matrix. In addition to the laminated nature of the matrix, the gross mismatch between the grain size of the framework (up to 20 cm diameter cobbles) and the grain size of the matrix (up to 2 mm diameter) indicates the matrix was introduced after the framework clasts were deposited (Harms *et al.* 1982, figure 6-3). The cobble- and pebble-sized gravel unit was likely episodically deposited during a jokulhlaup (large flood of glacially ponded water) and the fine-grained matrix then infilled the clast interstices once more normal outwash conditions returned.

Normal faults present in one region of the gravels indicate where glacial ice was buried by the outwash gravels. Melting of this ice caused settling of the overlying gravels and this resulted in normal faulting (Shaw 1972; McDonald and Shilts 1975).

FACIES 5 DISCUSSION

Facies 5 was deposited proglacially. Glacial mudflow deposition was initiated by compressive ice flow at the glacier's toe. This caused the supraglacial release of glacial debris from inclined shear planes. Supraglacially exposed diamicton then flowed onto a proglacial outwash plain and was likely buried or disaggregated by shallow braided streams. Continual glacial mudflow deposition resulted in the interbedding of the mudflows with shallow braided stream deposits, similar to models presented by Eyles (1979) and Boulton and Deynoux (1981).

In another part of the study area, perhaps at a slightly different time, basal till was exposed in front of the glacier's margin. The exposed basal till was then buried by braided outwash streams in some areas and eroded by outwash streams in other areas. The erosion process envisioned is presently observable in front of the Athabasca Glacier, Alberta (Plate 9). The glacial retreat in the study area, which exposed some till, caused glacial ice to become detached from the main glacier and become






Plate 9. Proglacial stream eroding basal till (diamict) in front of the Athabasca Glacier, Alberta. Till bank is 2 m high.

subsequently buried by braided outwash stream deposits consisting of sand and gravel. As the ice melted, faults were produced in the fluvial deposits.

In order for the deposits of facies 5 to be preserved the major outwash-channels emerging from the glacier had to be incised below the level of the mudflow activity and till plain formation (Boulton 1972a; Eyles 1979). One major outwash channel preserved in facies 5 is filled with cobbles and pebbles which were likely transported onto the outwash plain during a jokulhlaup.

As observed by Boulton (1967), the glacial terminus and proglacial area has a complex pattern of sedimentation. Because of this, proglacial deposits consisting of glacial mudflows, till plains, and outwash channels are all present in the small area represented by facies 5.

F. FACIES 6

FACIES 6 DESCRIPTION

Average thickness of the exposed portion of facies 6 is 13 m (range: 6-24 m). The outcrops where facies 6 is exposed are illustrated in Figures 15, 16, 22, 25, 33, 34, 38, and 39.

The components of facies 6 will be described in order of decreasing abundance. Four types of units make up facies 6, they are (i) stratified gravel units, (ii) unstratified gravel units, (iii) sand and granule lenses, and (iv) silt and clay lenses.

1. GRAVEL UNIT

Facies 6 is comprised mostly of open- and closed-work, horizontal, interbedded, interfingering lens-shaped gravel and granule horizons which laterally terminate by pinching out (Plate 10, Figure 56). Truncated or channelized lenses are rare. Individual lenses are characterized by differences between adjacent lenses in grainsize, sorting, and the presence or absence of matrix. These characteristics change vertically and horizontally throughout the facies, although the general characteristics of the gravels are homogeneous throughout the facies. Contacts between the majority of the lenses is sharp and distinct. Gravel units range in thickness from 0.03 m to 1 m and range in length from 0.3 m to 6 m (average of ranges: 40 cm thick by 2.7 m in length).

The average clast diameter of facies 6 is 8 cm (range: 1-20 cm). Isolated, larger than average-sized clasts occur throughout the gravels and in a few areas large boulders are present in lens-shaped accumulations of 5-10 rocks. Clast diameters range from 10-40 cm; most clasts are in the



Plate 10. Facies 6, quartzite-rich sediments. Downvalley is to the left. (Photograph at Cascade River section C1).

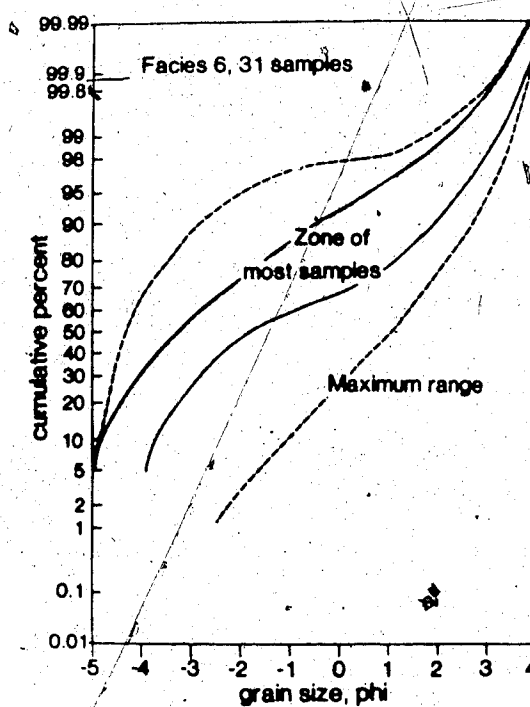


Figure 56. Facies 6, cumulative curves of the less than -5 phi fraction: All 31 curves (or samples) plot within the dashed lines labeled 'maximum range'.

range of 20-30 cm. The major axis of the larger clasts lies within 30° of horizontal (average range: $5-15^{\circ}$).

At one locality (JL-1 section, Figure 39) the gravel clasts are much larger than average; here, 40% of the facies surface area is comprised of 40-120 cm diameter clasts (Plate 11). Many of these large clasts dip at $5-15^{\circ}$ towards the valley side. Some of the smaller clasts are imbricated; they also dip towards the valley's margin. In this area of very large clasts, and in one other area of average-sized gravel, most of the clasts have $1-3 \text{ mm}^2$ white powdery areas on their surfaces, here, termed "peck-marks".

1a. Internal characteristics and structure of gravel units.

Most gravel lenses are comprised of one grainsize and are not internally bedded. Some lenses contain a stacked sequence of poorly developed, horizontal, very thin layers of open-work fine gravel interbedded with 1-3 cm thick layers of coarse sand. Many of these lenses are poorly sorted. For example, open-work units may be filled with particle sizes ranging from 0.1 cm to 15 cm diameter clasts. Non open-work gravel units have clast-interstices partially to totally filled with sediment. Units composed of larger clasts (6-25 cm diameter) are always clast supported and have their clast interstices at least



Plate 11. Large diameter clasts in facies 6, quartzite-poor sediments. View is towards the center of the Bow valley from the base of the Fairholme Range. Large clasts are imbricated towards the Fairholme Range. (Photograph at Johnson Lake section JL-1)

partially to totally filled with sand- to gravel-sized sediment.

The gravel's matrix is usually structureless medium to coarse sand. The matrix is more poorly sorted in areas where larger clasts (20 cm diameter and greater) are present. In this case, the matrix may consist of a combination of grainsizes from sand to 5-10 cm diameter clasts.

Although poorly developed imbrication is observed in some units, clasts in an open-work unit usually lack a preferred orientation. The proportion of open-work to closed-work beds varies throughout facies 6. On average 35% of the beds are open-work (range: 10-50%, depending on locality).

2. DISORDERED GRAVEL AND SAND UNIT DESCRIPTION

These units are exposed in 5-15 m² areas. They lack the interbedded, interfingered, thin, tabular beds of open- and closed-work gravels so prevalent in facies 6. Instead, the units consist of structureless to moderately well bedded, poorly sorted sediment. For example, a typical one square meter area, contains a wide range of clast sizes (from clay-sized to 40 cm diameter). Within this area, the unit is either: (i) a structureless, unsorted combination of sand to medium cobbles, or (ii) composed of poorly to moderately, defined horizontal to slightly dipping gravel

and sand beds.

3. SAND AND GRANULE LENS DESCRIPTION

Sand and granule lenses make up to 1% of facies 6. Sand and granule lenses have an average thickness of 7 cm (range: 1-20 cm) and an average length of 62 cm (range: 23-100 cm). Lenses are filled with well sorted sediment from one distinct portion of the fine sand to granule grain size range. One-third of the lenses also contain sporadically distributed, 1-10 cm diameter pebbles. The lenses have 3 main shapes: (i) tabular (10% of the lenses), (ii) flat-topped with concave base (15% of the lenses), and (iii) lenticular (75% of the lenses). 99% of the sand lenses pinch out; the remainder grade into the gravel. All upper contacts of the sand lenses are sharp and fairly flat. In one place the overlying gravel fills a declivity in the sand. The lower contact of the sand lenses is also sharp except for one gradational contact.

3a. Description of the sand and granule filled lenses' sedimentary structures.

Viewed collectively, the sand and granule filled lenses contain a variety of sedimentary structures. Approximately 35% of the lenses are structureless. The most common sedimentary structures are horizontal or slightly inclined laminations, tabular cross-bedding, and trough

cross-bedding. In most cases, the trough cross-beds have a layer of pebbles and sometimes fragments composed of clay-sized sediment lying along bedding surfaces. The flat topped lenses with concave bases are filled with trough cross-bedding.

4. DESCRIPTION OF THE SILT- AND CLAY-FILLED LENSES

One clay-filled and three silt-filled, lenticular shaped lenses are present in facies 6. The clay horizon is structureless, 2 mm thick and 5 cm long. Average dimensions of a silt horizon are 7 cm thick and 62 cm long. Silt lenses are filled with poorly defined, gently undulating, horizontal laminations.

FACIES 6 INTERPRETATION AND DISCUSSION

Facies 6 is interpreted to represent braided stream deposits. The majority of facies 6 are braided glacial-outwash deposits, a minor part of facies 6 are interpreted as being alluvial fan deposits. Evidence is presented below.

1. THE SEPARATION OF FACIES 6 INTO TWO PETROLOGICAL GROUPS

A ternary plot (Figure 57) of the petrological distribution of all samples from facies 6 illustrates that two petrological populations exist. These two petrological

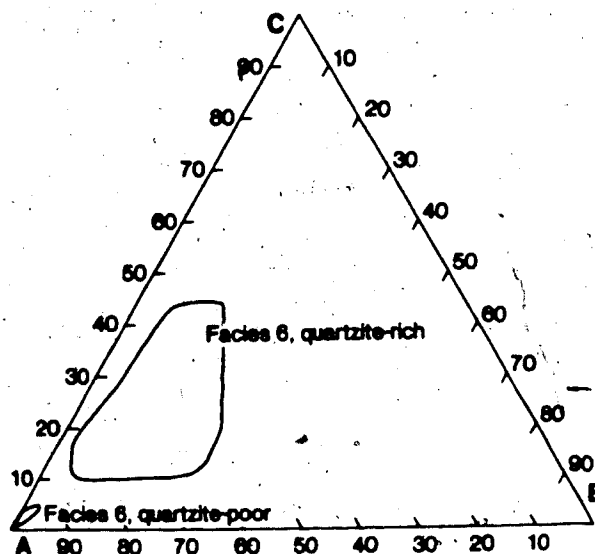


Figure 57. Ternary plot showing the separation between the quartzite-rich and quartzite-poor portions of facies 6. A=carbonates, cherty limestone; B=quartzite; C=chert, sandstone, siltstone, shale, and coal.

groups consist of samples which were collected from two groups of outcrops which occur in two different geographical localities of the study area (Figure 58). The quartzite-rich samples are from outcrops situated near to the center of the Bow Valley (Powerhouse, Anthracite, C2, Carrot Creek, and Canmore outcrops) and the quartzite-poor samples are located near to the valley margin along the base of the Fairholme range (JL1, JL3, and Cougar Creek outcrops). The geographical separation between the two petrological groupings leads to the division of facies 6 into two groups, one quartzite-rich and the other quartzite-poor.

2. INTERPRETATION OF THE QUARTZITE-POOR SEDIMENTS (ALLUVIAL FAN SEDIMENTS)

The quartzite-poor sediments (at JL1, JL3, and Cougar Creek outcrops) are interpreted to be alluvial fan deposits. The alluvial fans formed when side-valley braided streams drained the Fairholme Range and deposited their stream load along the valley margin between the Bow River valley and the Fairholme Range.

The alluvial fan interpretation is based on the following evidence. The 1-2 mm grain-size fraction from the JL1, JL3, and Cougar Creek sections are almost entirely composed of carbonates (Figure 57). The nearest sediment source for this carbonate clast population is the adjacent

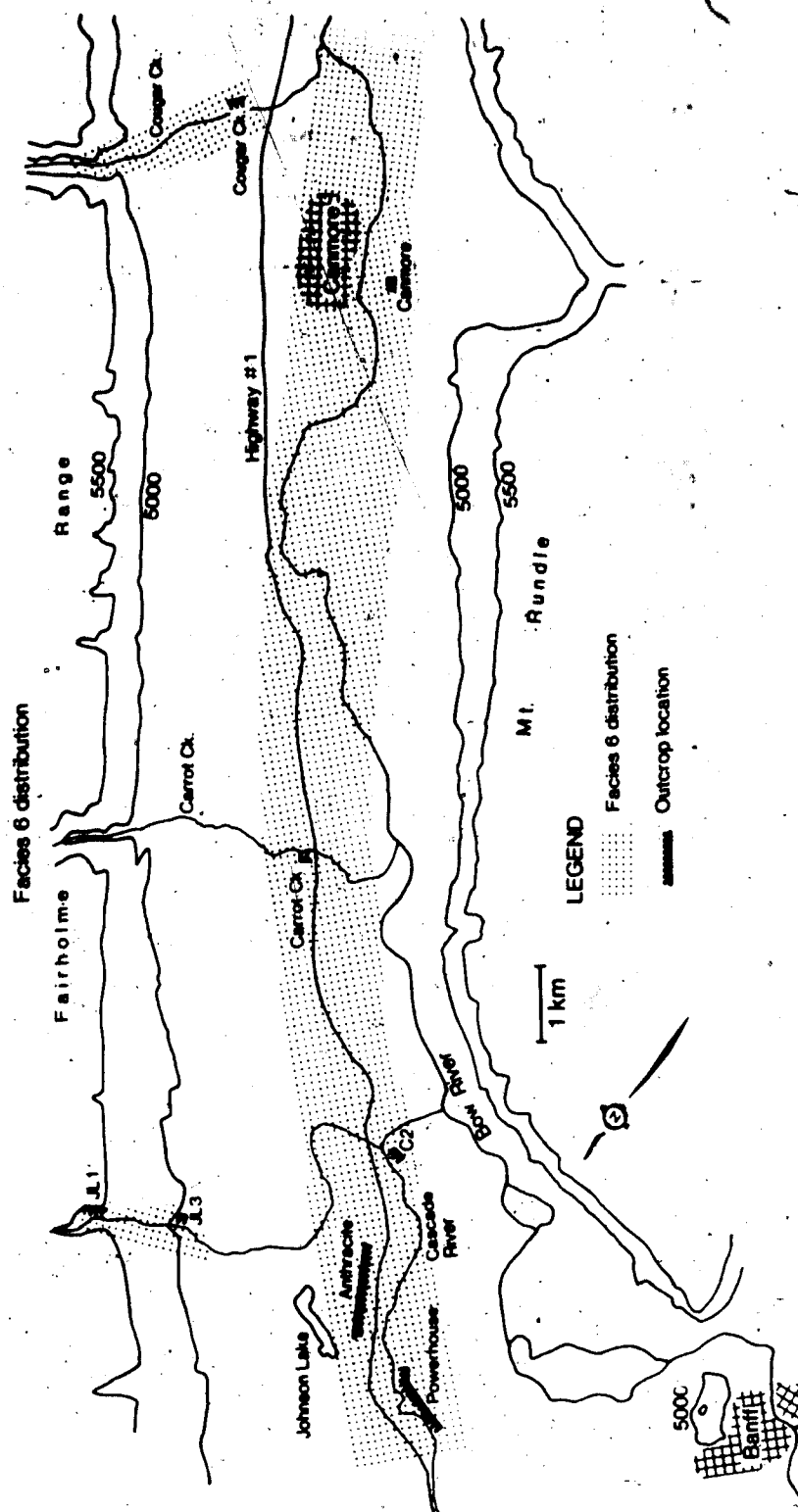


Figure 58. Geographical distribution of facies 6. Facies 6 is present at outcrop locations.

Fairholme Range (Figure 3). Since quartzite is present in the tills at the JL1, JL3, and Cougar Creek outcrops (Figure 59) it seems that the only natural transit path between the local carbonate source, i.e. the Fairholme Range, and the outcrops is through two deeply incised bedrock valleys leading out of the Range.

Additional information which suggests the sediments were derived from the Fairholme Range is contained in the JL-1 outcrop (facies 6). Here, the clasts are imbricated towards the Range (Plate 11). Such imbrication implies the clasts were transported out of the Range and towards the center of the Bow valley. The side valley sediment source of facies 6, combined with the facies location along ancient bedrock-drainage-channels leading out of the Fairholme Range suggests the quartzite-poor sediments belonging to facies 6 are alluvial fan deposits.

Additional properties that suggest an alluvial fan origin are, (i) the facies becomes finer-grained away from the mountains. Bull (1977) and Rust and Koster (1984) found this to be a property of alluvial fans. (ii) The horizontal, interbedded, interfingering lens-shaped open- and closed-work gravel horizons are also characteristic of braided stream sediments deposited in an alluvial fan environment (Bull 1963; Ore 1964; Smith 1970; Steel and Thompson 1983; Kochel and Johnson, 1984; Rust and Koster 1984; Smith 1985). (iii) The abraded, peck-marked clasts at

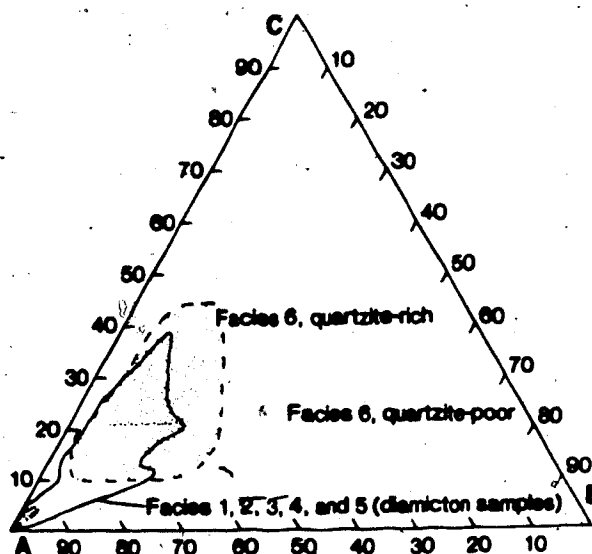


Figure 59. Ternary plot of facies 1 to 6 petrological distribution. A=carbonates, cherty limestone; B=quartzite; C=chert, sandstone, siltstone, shale, and coal.

the JLI and at the Cougar Creek outcrops is a feature observed in alluvial fans by Hooke (1967).

2a. DISCUSSION OF THE ALLUVIAL FAN SEDIMENTS

The alluvial fans were deposited entirely from flowing water without the addition of debris flow sediments which are usually observed in alluvial fan deposits (Bull 1960). The sorted, coarse nature of facies 6 is interpreted to represent sediment deposition from braided streams that had a high discharge energy.

3. INTERPRETATION OF THE QUARTZITE-RICH SEDIMENTS (BRAIDED STREAM SEDIMENTS)

The quartzite-rich sediments of facies 6 (Powerhouse, Anthracite, C2, Carrot Creek, and Canmore outcrops) are interpreted to be shallow braided stream deposits. This interpretation is based on the similarity between the open- and closed-work, horizontal, interbedded, interfingered, lens-shaped gravel and granule beds of facies 6 and the beds produced in shallow braided streams as described by Smith (1985).

Many characteristics of the quartzite-rich sediments provide information which allows more detailed interpretations to be made regarding the exact type of braided stream which deposited the facies. A lack of cross-bedded gravel beds, and the presence of bedding

formed by longitudinal bars, indicates the stream channels were shallow (McDonald and Banerjee 1971; Smith 1974, 1985).

Quartzite is present in facies 6 quartzite-rich beds in the same abundance as in the glacially deposited tills (Figure 60). This petrologic equality is interpreted to result from derivation from a glacial source. The similar petrologies of the glacial tills and the stream sediments also indicates that the stream sediments were not transported to the point where attrition of the less resistant lithologies becomes apparent (Krumbein 1941b; Twenhofel 1945; Sneed and Folk 1958).

The approximate distance of stream transport can be estimated by examining the roundness of the sediments. The average roundness of the braided stream sediments' 1-2 mm carbonate fraction is 0.406; this is rounder than the glacial source (facies 1, 2, 3, and 4 diamicton samples) roundness of 0.368. According to Sneed and Folk (1958) rounding of angular pebbles is achieved after 8-16 km of stream transport. Although the roundness values of very coarse sand can not be reasonably compared to the roundness of pebbles, the subangular nature of the sand fraction suggests the transport distance of the sand grains was of a shorter, rather than a longer distance.

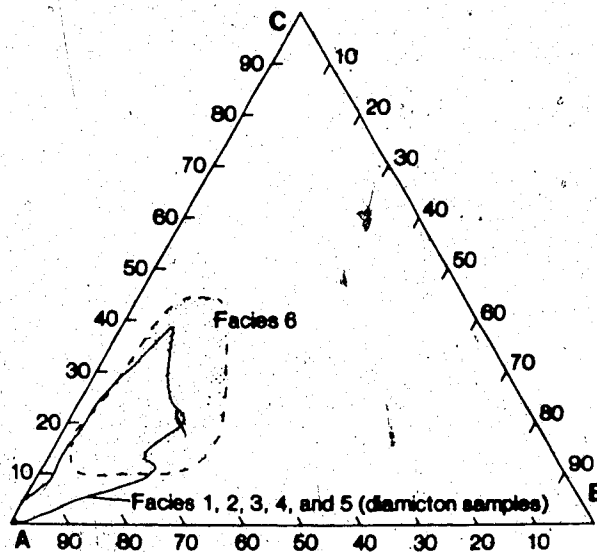


Figure 60. Ternary plot showing that the quartzite-rich portion of facies 6 has the same general petrological composition as the diamicton of facies 1, 2, 3, 4, and 5. A=carbonates, cherty limestone; B=quartzite; C=chert, sandstone, siltstone, shale, and coal.

3a. DISCUSSION OF BRAIDED STREAM SEDIMENT DEPOSITION

The quartzite-rich, braided stream sediments of facies 6 are interpreted to have formed in a proglacial sandur setting. The presence of longitudinal bars which likely formed in shallow, high discharge energy braided-channels support a sandur interpretation. The bars formed from glacially derived sediments which were transported a relatively short distance. The horizontally bedded gravels and lack of significant numbers of sand beds indicate these sediments were deposited by a proximal braided stream (Rust and Koster 1984). The sedimentary characteristics of facies 6 (quartzite-rich samples) place it in the intermediate sandur zone as defined by Smith (1985, p. 97). "The intermediate [sandur] zone is characterized by complex networks of wide, shallow, distinctly braided channels that shift positions frequently. Large mazes of recently abandoned channels are prominent during normal discharges."

Conditions which permit a sandur to cover a valley floor, as is interpreted to have occurred during deposition of these sediments, are referred to as being paraglacial conditions. This term was introduced by Church and Ryder (1972) to characterize conditions where an abundance of unconsolidated sediment is available for stream transport following a glaciation. Here, the sediment source was glacially-derived diamicton exposed by a valley glacier retreating up the Bow River valley.

The distance between the sediment source (the glacier) and the depositional site (the Banff-Canmore area) can be roughly determined using a graph compiled by Boothroyd and Nummedal (1978) (Figure 61). The maximum clast diameter of the proglacial braided stream sediments in the study area is approximately 40 cm. Using this grainsize diameter and Boothroyd and Nummedal's (1978) graph (Figure 61) it is estimated that the glacier's toe was situated about 0.5-3 km upstream of the study area during deposition of the proglacial braided stream sediments.

4. FACIES 6 SUMMARY

The interbedded gravels and sands of facies 6 were found to represent two petrological populations, one quartzite-rich and the other quartzite-poor. The two petrological groups are from two geographically separate sets of outcrops. The geographic setting of the outcrops and the deposits' sedimentary characteristics lead to the interpretation that outcroppings of facies 6 along the base of the Fairholme Range are alluvial fan deposits. Outcrops of the facies located in the main portion of the Bow valley are interpreted to have been deposited by a sandur a short distance from the terminus of a glacier.

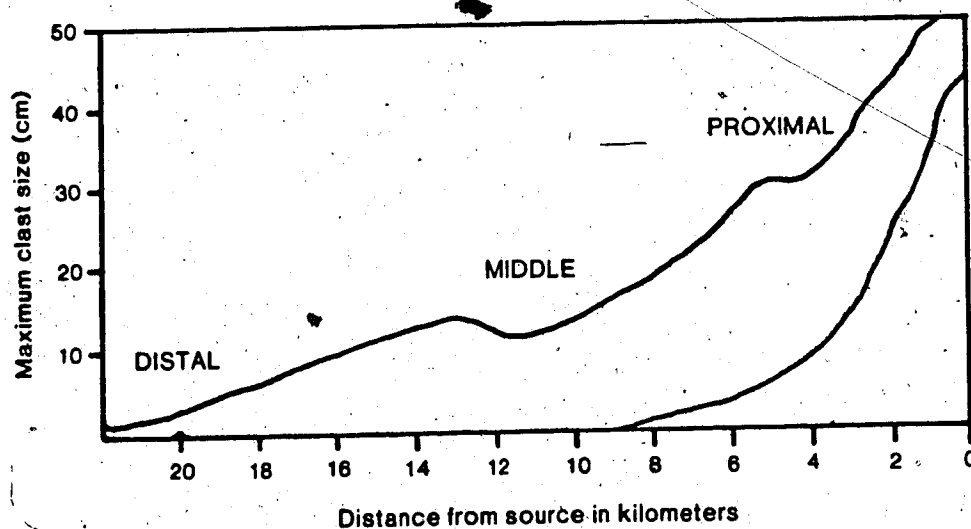


Figure 61. Graph used to indicate the distance between a sediment source (the glacier) and the depositional site (the Banff-Canmore area) along a sandur (after Boothroyd and Nummedal 1978).

G. FACIES 7

FACIES 7 DESCRIPTION

1. INTRODUCTION TO FACIES 7

Facies 7 is exposed at Anthracite subsection A1 (Figure 62). Facies 7 covers over 600 m² of vertical exposure and is subdivided into 6 subfacies based on differences in grainsize, sorting, and sedimentary structures between the major sedimentary units. The six subfacies are:

- Subfacies 7a Interbedded gravel and sand
- " 7b Interbedded gravel, silt, and sand layers
- " 7c Gravel with blocks composed of silt
- " 7d Interbedded gravel and sand with a layer of banded silty clay and blocks of silty clay
- " 7e Silt and sand bed with gravel lenses
- " 7f Banded clay, silt, and diamicton beds

Figure 62 is a map of facies 7; this figure also shows the spatial relationships between the subfacies. Interbedded gravel and sand (subfacies 7a) and silt and sand beds (subfacies 7e) make up the lower half of the section. Layered clay and silt (subfacies 7f) and interbedded gravel, silt and sand layers (subfacies 7b) form the upper part of the facies exposure (Plate 12).

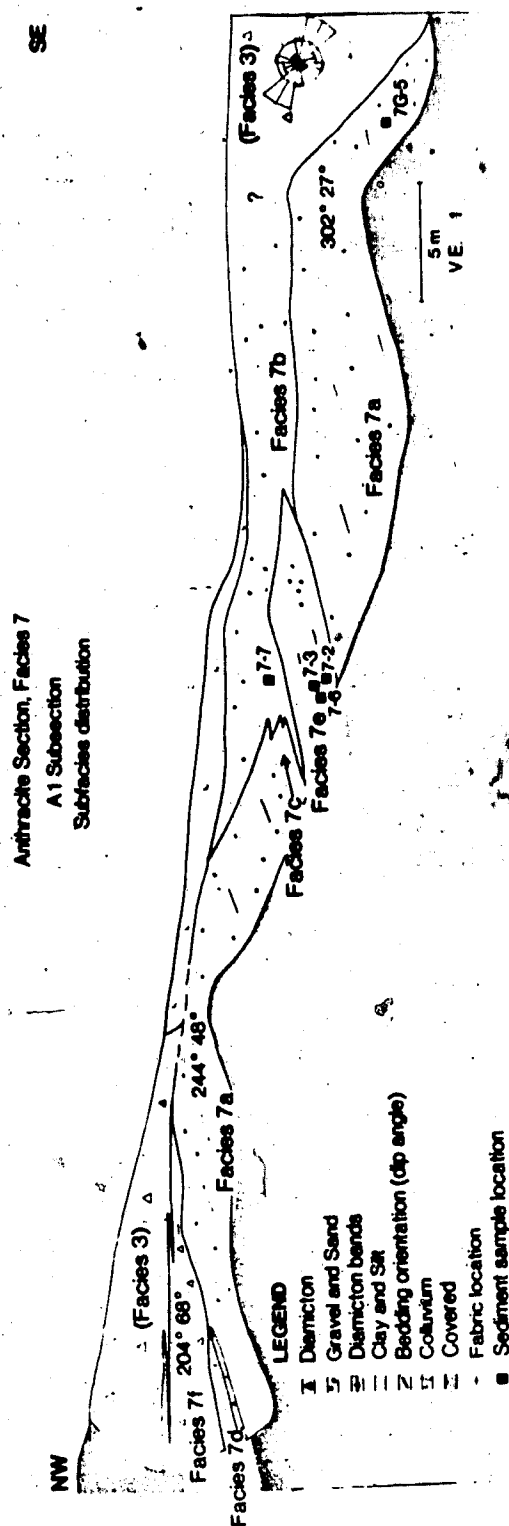


Figure 62. Anthracite subsection A1. Exposure of facies 7.

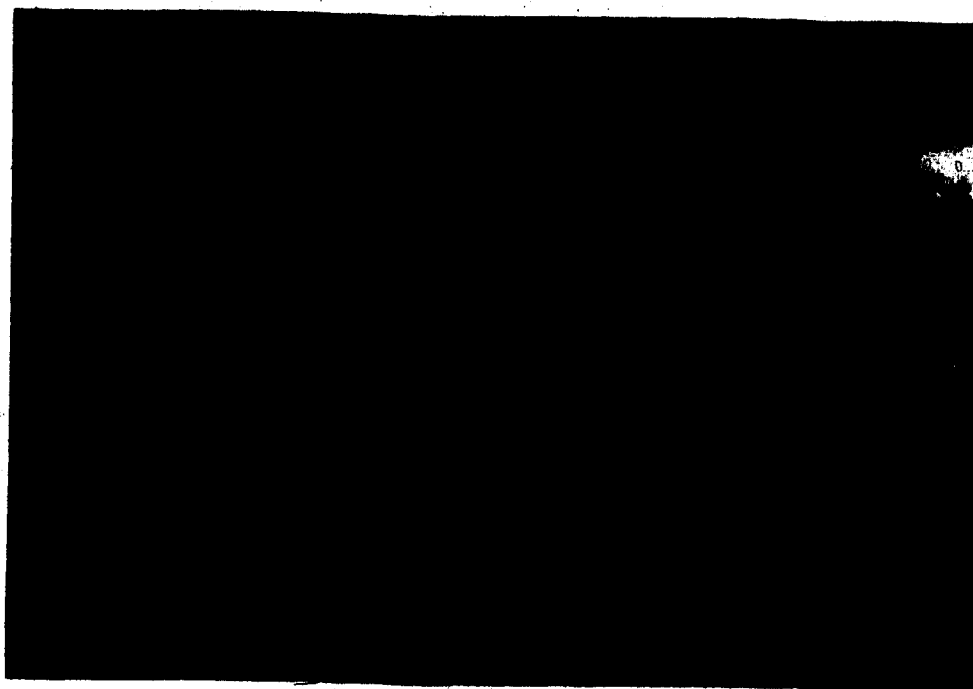


Plate 12. General view of facies 7; downvalley is to the right. (Photograph at Anthracite subsection A1).

2. SUBFACIES DESCRIPTIONS

Each subfacies is described in order of decreasing area of outcrop exposure.

Subfacies 7a: Interbedded gravel and sand

The interbedded gravel and sand subfacies is about 10 m thick, 60 m in length and comprises 71% of facies 7. This subfacies is composed of 4 types of units (types 1-4).

Type 1. 65% of subfacies 7a is comprised of parallel, interbedded, dipping beds of sand to fine gravels that have an average clast diameter of 3 cm (range: sand-sized to 20 cm). These beds have foreset-type crossbedding with true dips of 27° and 48° in the lower and upper portions of the subfacies, respectively. The pebbles' major-axes are aligned parallel to or within 20° of the bedding planes. Individual sand and gravel beds are 5-20 cm thick and extend for 5 to 20 m before terminating along the upper contact of the subfacies. Beds within the gravels are distinguished from one another by slight differences in grainsize, sorting, and the type of matrix between the beds. The gravel-bed matrix is mainly granules and sand, although 5% of the beds have a clay and silt matrix. 20% of the beds are open worked.

Type 2. 25% of subfacies 7a is comprised of horizontal beds and lenses filled with very poorly sorted, sand- to

cobble-sized sediment. These horizontal beds and lenses occur near the base of the type 1 beds. Bed thickness ranges from 30 cm to 100 cm (average: 65 cm). Typical units consist of: (i) A 30 cm X 2 m lens filled with 1-7 cm in length, clast supported, elongated pebbles in a clayey sand matrix. This lens is overlain by a lens of open-work pebbles. (ii) A bed showing faint horizontal bedding of clast supported, 10-25 cm diameter cobbles with a sand matrix. (iii) An 80 cm thick by 5 m long gravel bed. The lower portion of this bed is filled with only structureless sand. Moving upwards in the bed, matrix supported, 8-10 cm diameter clasts occur more frequently; and at the top of the bed the clasts are closely spaced.

Type 3. 8% of subfacies 7a is composed of structureless clast supported gravel which occurs as 1-4 m² zones within the lower portion of subfacies 7a.

Type 4. 2% of subfacies 7a is made up of sand lenses. The sand lenses mainly occur as long, thin horizons within the dipping gravel units. These sand lenses are 3-5 cm thick, and 3-5 m long. Only one lens is not concordant with the dipping gravel units. This lens is horizontal, has dimensions of 0.30 m X 3.5 m, and is filled with structureless sand and some 6-10 cm diameter clasts.

Contacts between the four types of units (1-4) composing subfacies 7a are all fairly sharp and distinct.

Subfacies 7b: Interbedded gravel, silt, and sand layers

Subfacies 7b is 2-3 m thick, 20 m long, and is situated along most of the top of facies 7. The subfacies represents 15% of facies 7 area and consists of gravel beds interbedded with both silt and sand beds. All beds are mainly horizontal and have an average thickness of 10 cm (range 5-30 cm). The beds are 5-10 m long and pinch out. The ratio of gravel to silt and sand layers varies from 40:60 to 90:10. Overall, 65% of subfacies 7b is composed of gravel beds and 35% is composed of silt and sand beds.

Average clast diameter within the gravel layers is 3 cm (range 0.5-8 cm). The gravels are clast supported and have a silt- to granule-sized matrix. Internally, some of the gravel beds have very faint horizontal layering consisting of indistinct layers of finer grained material. The average grain size of an individual gravel layer varies along its length and is different than adjacent gravel layers.

The silt and fine sand layers are very poorly to moderately sorted. No sedimentary structures are observed within these layers and a small number of 1-5 cm diameter pebbles sporadically occur throughout. The contacts between the gravel layers and silt-sand layers are sharp and fairly horizontal.

Subfacies 7e: Silt and sand bed with a gravel lens

One of the silt and sand layers located in the lower


portion of subfacies 7b extends downwards and laterally across the outcrop face into subfacies 7a (Figure 62). Where this layer is totally enclosed by subfacies 7a it is categorized as subfacies 7e.

Subfacies 7e is represented by a 2 m thick and 15 m long lens. Subfacies 7e covers 7% of facies 7. The subfacies is composed of interbedded, moderately well sorted, fine sand beds and thinner, very poorly sorted silt beds which pinch and swell (10 cm vertical displacement over a 200 cm length). A few scattered, 3-5 cm diameter pebbles are in the silt beds. Average thickness of the sand beds is 15 cm (range 8-50 cm); average thickness of the silt beds is 10 cm (range 7-15 cm). 70% of subfacies 7e is composed of sand beds, 20% of silt beds, and 10% of one gravel lens.

The gravel lens is poorly sorted and occurs within the main silt and sand lens. The gravel lens's dimensions are 33 cm X 110 cm. The lens is composed of sediment ranging from sand-sized sediment to large pebbles.

About 50% of the sand beds are structureless. Structures consist of 0.5 mm thick, parallel laminations of coarse sand vertically spaced 0.5-3 cm apart. Some laminations are horizontal, others have apparent dips of 10° to the northwest.

The silt beds consist of 0.5-3 cm thick layers. Within each layer are slightly wavy, parallel, near horizontal



interbeds. The interbeds are differentiated based on grain size. Coarser beds are comprised of silt, finer beds of silty clay. Interbeds make sharp contact with one another. Within interbeds, contacts between coarser and finer layers are gradational. These interbeds can be traced for at least 1 meter. Some interbeds curve upwards and are truncated by an overlying sand layer. All contacts between the sand, silt, and gravel units are sharp and distinct.

Subfacies 7c: Gravel with blocks comprised of silt-sized sediment

Subfacies 7c occurs within an area of gravel representing subfacies 7a. Subfacies 7c consists of two blocks composed of silt- and clay-sized material within the gravel. The two blocks' dimensions are 20 cm X 28 cm and 20 cm X 20 cm. The blocks have the same characteristics as the fine sand beds of subfacies 7e.

Subfacies 7f: Banded clay, silt, and diamicton beds

Subfacies 7f is mainly composed of banded silty clay, sand, and diamicton, all occurring as a wedge-shaped unit with a maximum thickness of 2 m and a length of 15 m. This subfacies comprises 6% of facies 7 total area.

Subfacies 7f's sedimentary characteristics change vertically. The lower 35 cm of the subfacies consists of very distinct, long, thin interbedded layers and lenses of

sand, silty clay, and diamicton (Plate 13). The sand, silty clay, and diamicton comprise 40%, 30%, and 30% of this lower zone respectively. The sand and silty clay layers and lenses have an average thickness of 0.7 cm (range 0.3-4.5 cm); average thickness of diamicton layers and lenses is 2 cm (range 0.5-6 cm). The average clast diameter within the diamicton is 3 cm (range 2-4 cm). Most of the silty clay and sand layers extend for the entire length of the subfacies except for some 10-30 cm long sand lenses and the diamicton lenses which pinch out.

The upper two-thirds of subfacies 7f differs from the lower portion in the following respects. Moving upwards, the silty clay layers gradually decrease in abundance, the sand layers become thicker and contain more pebbles, and the diamicton layers become thicker and contain more sand and less clay. The diamicton layers are massive and lack sedimentary structures; internal sedimentary structures of the other layers will be described below.

Each silty clay layer is subdivided into 1 to 4 zones based on slight changes in grain size within a layer. The zones do not change in thickness lengthwise. 1-3% of the thinner internal zones within silty clay beds are contorted along one portion of the zone. Contortions are manifest by 0.5-1 cm² upward pointing bulbous-shaped features.

About 95% of the sand beds are structureless. 4% of the sand beds have fine parallel, horizontal laminations. 1% of

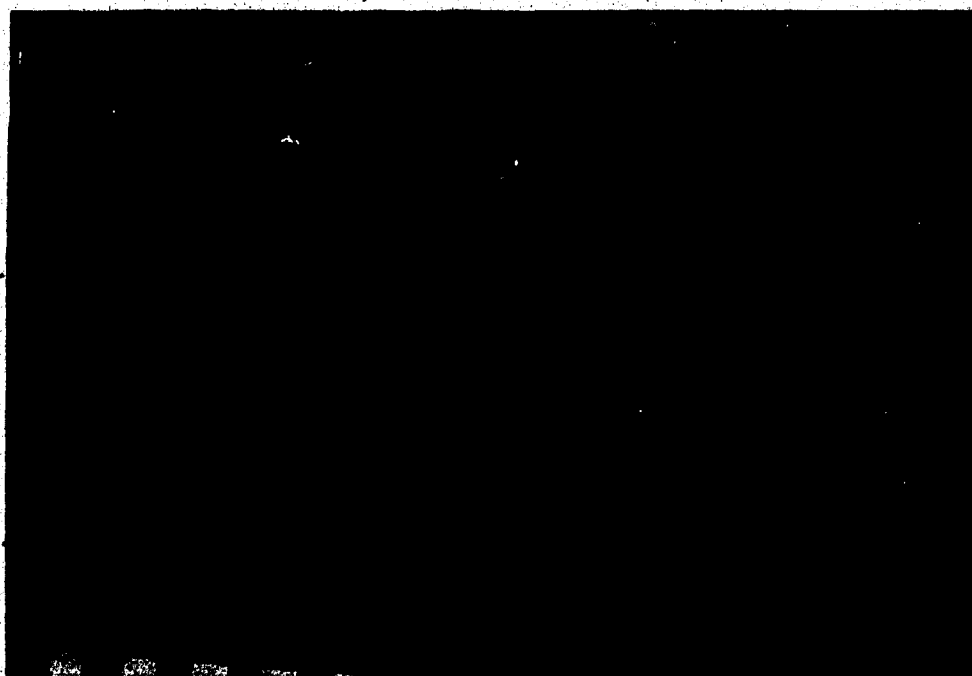


Plate 13. Subfacies 7f.

the sand beds have near tabular crossbeds which are concave upward. The crossbeds are emphasized by very thin, clay-rich laminae.

About 20, 2-6 cm diameter pebbles occur sporadically throughout the lower 35 cm of subfacies 7f. Most of the 2-3 cm diameter pebbles are contained within a layer and do not cross any contacts. A few 4 cm diameter pebbles cross-cut numerous thin layers which extend, undeformed to the pebble margin. In a few cases, the pebbles which interrupt layers are draped by silty clay horizons.

90% of all contacts between the silty clay and sand layers and lenses and the diamicton layers and lenses are sharp, horizontal and parallel. 10% of the upper and lower contacts of the diamicton layers and lenses are wavy and in some cases truncate underlying beds.

Subfacies 7d: Interbedded gravel and sand with a layer of banded silty clay and blocks of silty clay

Subfacies 7d is a wedge-shaped unit 70 cm thick, 7 m long that consists of a gravel with the same general characteristics as subfacies 7a. Subfacies 7d covers 2% of facies 7. Within the gravels is a concordant bed composed of silty clay with characteristics similar to the silty clay layers of subfacies 7f. The silty clay bed in subfacies 7d is 5 cm thick, 2 m long, and pinches-out up dip. It has sharp upper and lower contacts. Within 5 cm of

the top of this gravel unit are numerous rectangular-shaped, 1 cm X 3 cm fragments consisting of silty clay oriented with their long axes parallel to bedding.

3. ORIENTATION OF THE BEDS IN FACIES 7

Dip directions, dip of the trace of the beds, and the strike and dip of the outcrop face were measured. From this data true dip and true dip direction of the beds were calculated using a stereonet (Table 8).

Table 8. Orientation of the beds in facies 7

<u>Subfacies</u>	<u>True dip dirn</u> (w.r.t. true N)	<u>True Dip</u>
7f	204°	68°
7d	204°	68°
7a upper	244°	48°
7a lower	302°	27°

4. DESCRIPTION OF THE CONTACTS BETWEEN FACIES 7 SUBFACIES

The contacts between all subfacies are sharp and distinct. The upper and lower contacts are all smooth and planar except for subfacies 7c. Contact between subfacies 7c and 7a are smooth and curved. Lateral contacts between subfacies 7a and 7b interfinger (in the central portion of the Anthracite A1 subsection).

5. DESCRIPTION OF CONTACTS BETWEEN FACIES 7 AND ADJACENT FACIES

Facies 7 is overlain and bound on both sides by facies 3 (Figure 62). The lower portions and contact of facies 7 is covered. The contact where facies 3 overlies facies 7 is gradational. Subfacies 7f grades up into the overlying diamicton of facies 3. This gradational contact is marked by the amount of diamicton increasing upwards while the abundance of sand and silty clay layers decreases. The lateral contact between facies 7 and facies 3 (at the southeast portion of the A1 subsection) is sharp and straight and has an apparent down-valley dip of 38° .

FACIES 7 INTERPRETATION

Facies 7 is interpreted to be ice proximal, proglacial outwash sediments deposited in a channel cut into previously deposited till. A composite geological column and history of facies 7 deposition is shown in Figure 63.

CHANNEL SETTING

Facies 7 is interpreted to have been deposited in a channel which was cut into a previously deposited glacial till (facies 3). This interpretation is based on the areally restricted exposure of facies 7, its channel-shaped nature, and steeply dipping lateral boundary (Figure 62).

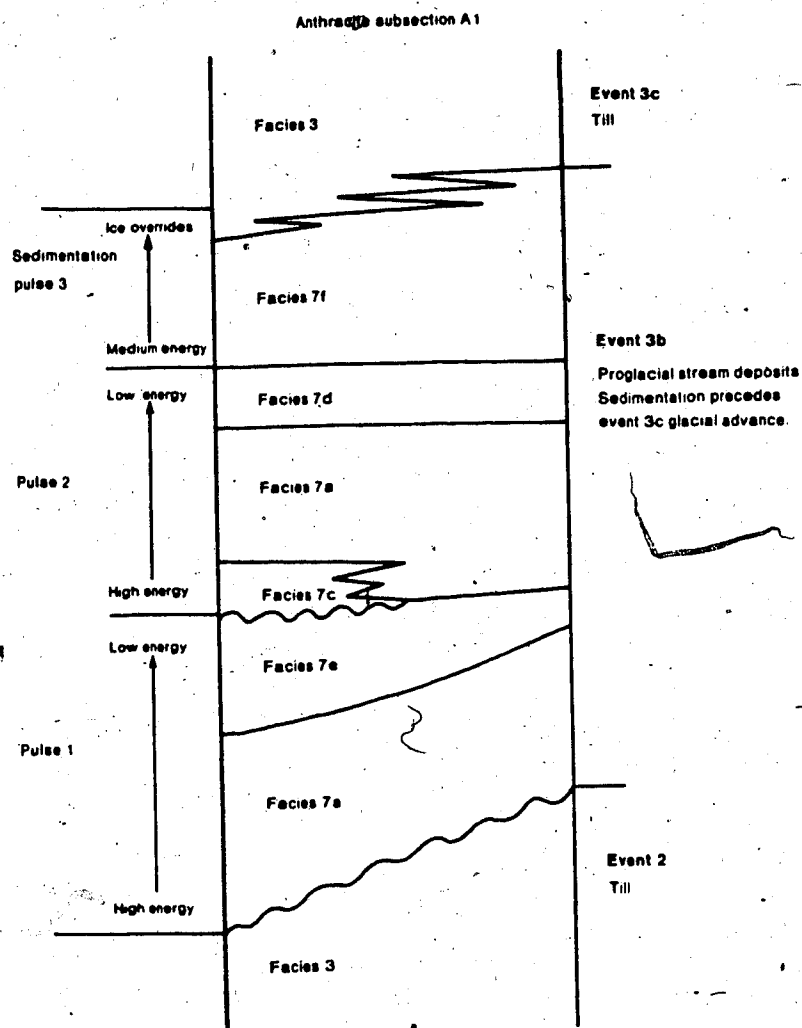


Figure 63. Composite geological column and sedimentation history of facies 7 at Anthracite subsection A1.

The steep contact looks like an undercut channel margin formed by stream incision into an older deposit. The same type of undercutting observed in the study area today likely occurred in the past at the Anthracite subsection A1. One of the overhanging channel banks is preserved adjacent to facies 7. A pebble fabric of the till comprising the overhanging channel margin has a well oriented, parallel to ice-flow alignment (Figure 64) which is interpreted to indicate channel cutting did not affect the till which forms the channel margin.

The lack of faults within facies 7 is another indication that facies 7 was deposited on consolidated till rather than on glacial ice or glacial debris. If the till had consolidated by compaction or if buried ice melted after facies 7 was deposited, the settling of the overlying facies 7 would have been manifest by faults in the facies.

SEDIMENTARY CHANNEL FILL

The channel fill deposit of facies 7 can be subdivided into 3 packages of sediment. Each package consists of a set of internally conformable beds, distinguished from one another by the differences in bedding orientation.

The lowest group of beds (sediment pulse 1, pulse is used here to describe a short-lived period of sedimentation) consists of large scale tabular cross strata (subfacies 7a) interpreted as planar foresets which

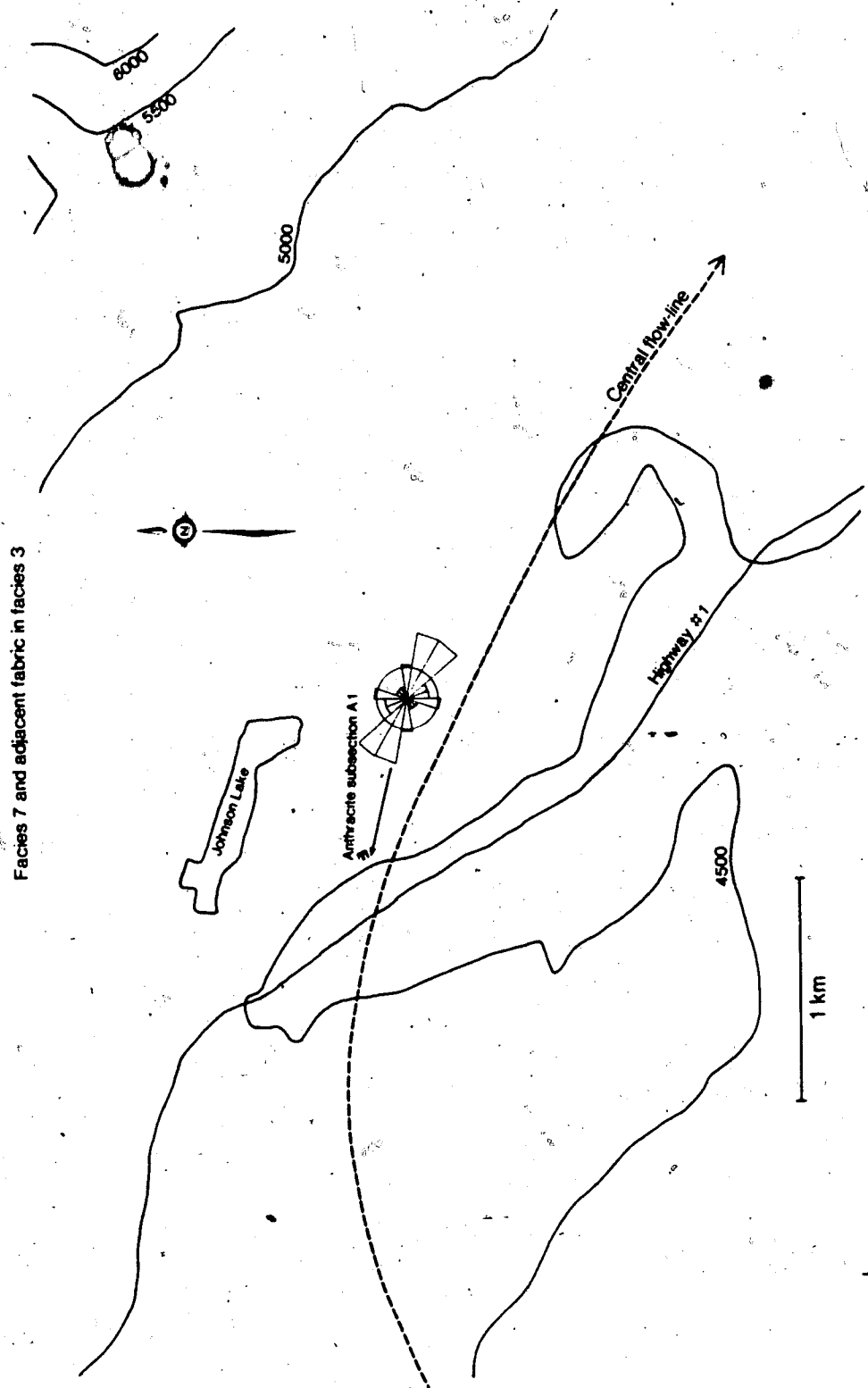


Figure 64. The location and diamictite pebble fabric of facies 3 in the till bank bounding facies 7.

advanced into a water-filled channel. When the water's flow-energy decreased the finer-grained subfacies 7e and 7b were deposited. The fine grained sediments cap the first depositional pulse (302° 27°) of sediments (Figures 63 and 65).

After a period of quiescence a second pulse of tabular cross strata (subfacies 7a) were deposited into the channel. The cross strata have a bedding orientation of 244° 48° . The second pulse of sediment initially eroded some blocks of subfacies 7e which were deposited during the first sedimentation pulse, and incorporated them as intraclasts within the tabular cross-stratified gravels deposited during the second pulse of sedimentation (subfacies 7c). The steeply dipping (48°), planar gravel beds of the second pulse are also interpreted as foresets. The steep nature of the gravel beds of pulses 1 and 2 (27° and 48° respectively) implies the beds were deposited as Gilbert-type delta foresets (Blatt et al. 1980) or as large scale tabular cross strata from large two-dimensional ripples (Harms et al. 1982) which formed in a few meters of water. Towards the top of the second sedimentation pulse flow-energy decreased enough to allow preservation of a diamicton layer (subfacies 7d). The thin, massive, unsorted nature of the layer suggests deposition occurred by mudflow processes.

The third pulse of sediments (subfacies 7f, Plate 13)

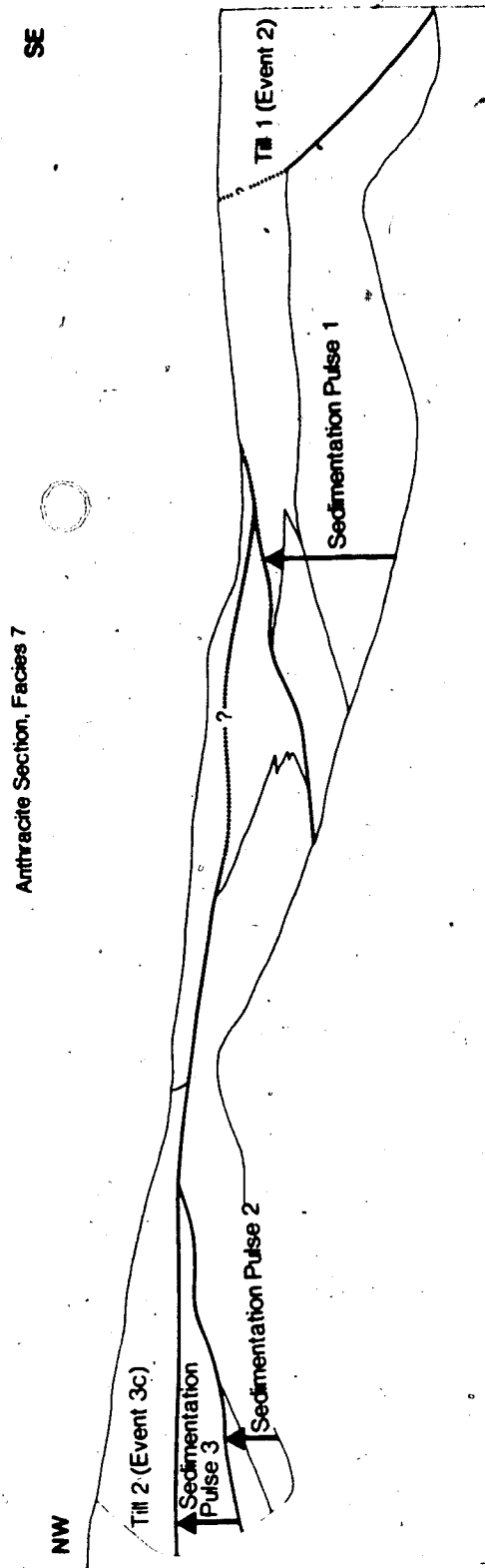


Figure 65. Anthracite subsection A1. Sedimentation infilling history of the channel cut into Till 1 (Event 2). Till 1 is a remnant overhanging channel bank. Sedimentation pulse 3 grades upwards into Till 2 (Event 3c).

is interpreted to be a series of mudflows deposited in standing water. The presence of numerous, thin, conformable diamicton horizons interbedded with some thin, better sorted horizons are indicative of mudflows (Hooke 1967; Johnson 1970; Pierson 1980). Deposition of the flows into water is suggested in order to explain the many graded horizons and the small, sorted, cross-bedded horizons. The bedded horizons are most likely deposited from mudflows. Larger pebbles which cut the sediment layers are interpreted to be from ice-rafted glacial debris.

FACIES 7 DISCUSSION

Facies 7 was deposited in a glacial outwash channel which was cut into previously deposited till. The three sets of sedimentary units comprising facies 7 were each deposited with a different bedding orientation (Figure 66). This indicates the position of the sediment source changed during channel infilling. In addition, depositional discharge energies decreased upwards within each of the first two sediment pulses. These variations in both discharge-energy and sedimentation directions are characteristic of a proglacial depositional environment (Price 1969, 1971; Price and Howarth 1970). Additional evidence for a proglacial setting is facies 7 upwards transition into till.

The foreset cross beds in facies 7 dip obliquely

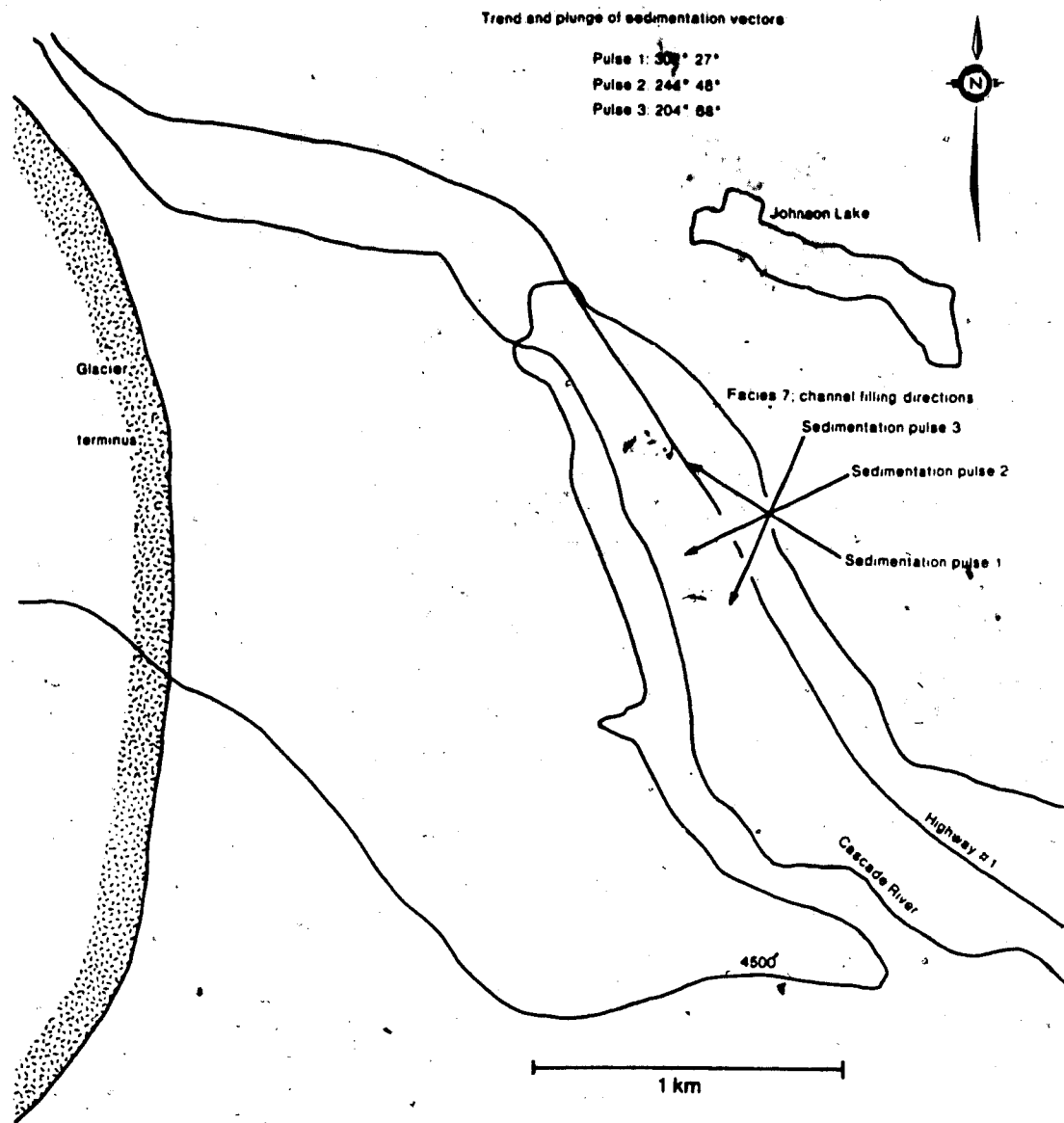


Figure 66. Sediment infilling direction of the channel sediments of facies 7. Arrows point in the dip direction of the foreset beds.

upvalley, towards the former glacier's toe (Figure 66). This probably resulted from a proglacial channel being filled from the north-east. An obstruction, like an end moraine, must have been situated between the glacier, to the west, and the channel to the east.

The sand and gravel foresets (subfacies 7a-7d) are interpreted to be Gilbert-type delta foresets. The delta's sediment source was proglacial outwash deposited under conditions of widely fluctuating discharge and sediment dispersal direction. Foreset deposition was mainly beyond the transport distance of glacial debris flows (subfacies 7f). While the first two sediment packages were being deposited (sedimentation pulse 1 and 2) the glacier was approaching the channel, and then with the third and final sediment pulse glacial debris flows were introduced into the channel. These mudflows eventually grade up into till (facies 3) deposited as the glacier crossed and then covered the channel which by then had totally filled with facies 7.

V. GEOLOGICAL-SEDIMENTATION HISTORY AND CONCLUDING DISCUSSION

A. GEOLOGICAL-SEDIMENTATION HISTORY

This section presents the glacial history of the Banff-Canmore region. The history is based upon sedimentation events discussed in the previous chapter (Figure 67, Tables 9 and 10).

EVENT 1

Braided stream sedimentation in a sandur setting was the first major glacial-depositional event preserved and exposed in the Banff-Canmore area. This sandur was deposited in front of a glacier which was retreating up the Bow valley. The sandur deposits are comprised of facies 6 and are exposed in the localities shown in Figure 68. The sandur deposits (facies 6) were deposited within 0.5 to 3 km of the retreating glacier's toe.

Diamicton deposited from the glacier which preceeded event one is not observed in the study area. This diamicton was likely eroded by the proglacial braided streams of event one. Event one is the same as Rutter's (1972) pre-Bow Valley advance (Table 11).

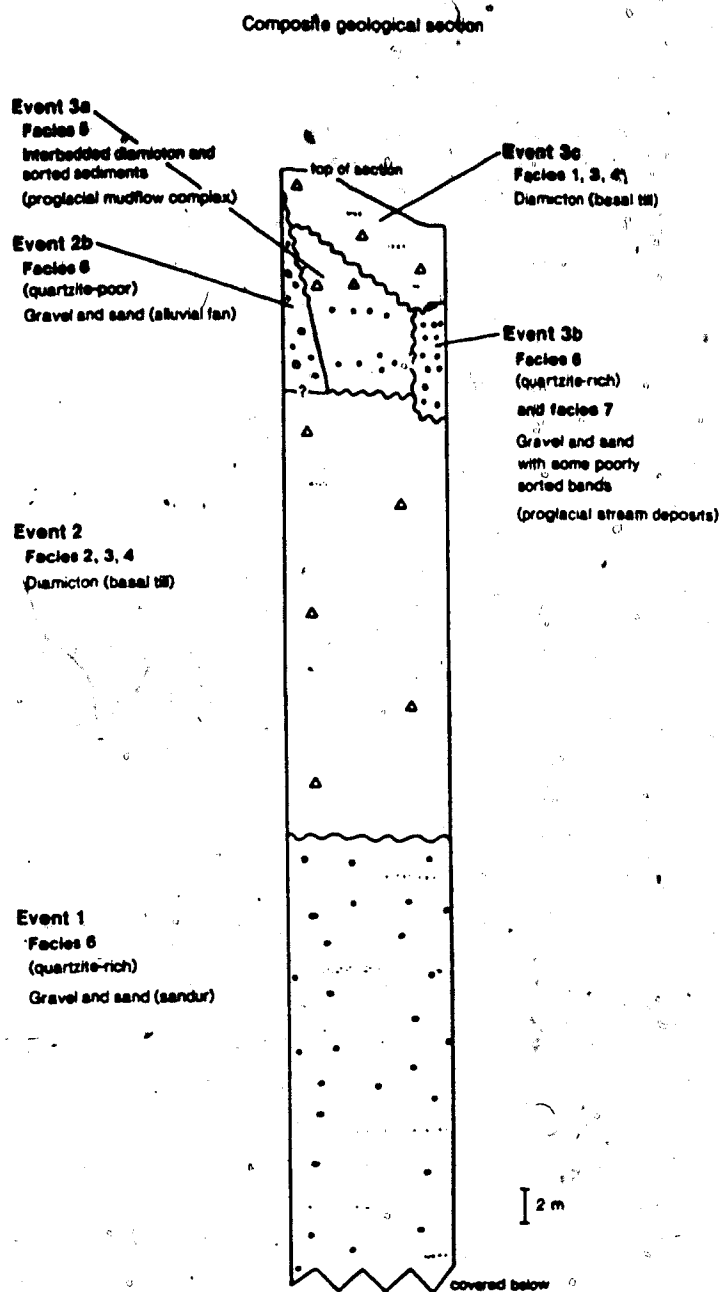


Figure 67. Composite geological section.

Table 9. Facies summaries

Facies	Description	Interpretation	Average thickness (range) in meters
1	Diamicton with numerous lenses filled with clay, silt, sand, and gravel; many lenses inclined. Variable distribution of lenses.	Basal melt-out till, originated from successive basally deposited glacial debris layers which melted-out beneath a moving valley glacier.	at least 10 (-)
2	Diamicton with numerous, long, thin gravel layers. A small number of sand lenses also present.	Lodgement till, formed by plastering glacial debris particles onto a subglacial substrate.	24 (-)
3	Massive diamicton, very few sand- and gravel-filled lenses.	Lodgement till, formed by plastering glacial debris particles onto a subglacial substrate.	6 (4-8) and 27 (26-28)
4	Diamicton with numerous lenses filled with clay, sand, or gravel. Vast majority of lenses are horizontal.	Basal melt-out till, originated from successive basally deposited glacial debris layers which melted-out beneath a moving valley glacier.	3.5 (3-4) and 30 (-)
5	Mainly an interfingered, interbedded sequence of poorly sorted gravels, diamicton lenses, and diamicton blocks. Also some poorly sorted gravels.	Proglacially deposited or situated glacial mud-flow complexes, dissected till plains, and outwash channel-fill deposits.	9 (2.5-13)
6	Mainly horizontal, interbedded, interfingering lens-shaped gravel horizons. Some tabular-, lens-, and trough-shaped sand units are interbedded with the gravel units.	Braided glacial outwash deposits and a lesser amount of fluvially deposited alluvial fan deposits.	13 (6-24)
7	Mainly interbedded gravel and sand layers and lenses. Minor banded clay, silt, and diamicton beds.	Ice proximal, proglacial outwash sediments deposited in a channel cut into previously deposited till.	7 (-)

Table 10. Geological history of the Banff-Canmore area

Event	Facies	Deposits	Event history
3c	1, 3, 4	Diamicton (till)	Valley glacier advanced over study area and deposited basal till. (Event 3c deglaciation by melting of debris-free glacier, no deglacial deposits produced in study area).
3b	6 (quartzite-rich) and 7	Gravels and sands with some poorly sorted bands	Glacier was located at Banff townsite. Proglacial streams cut into event 2 till; glacier advances to begin event 3c.
3a	5	Interbedded diamicton and sorted sediments	Jerky advance of a valley glacier, proglacial mudflow deposits produced, followed by a minor glacial retreat to Banff townsite area.
2b	6 (quartzite-poor)	Gravel and sand	Deglaciation of event 2; alluvial fans formed. (deglacial deposits)
2	2, 3, 4	Diamicton (till)	Valley glacier advanced over study area and deposited basal till.
1	6 (quartzite-rich)	Gravel and sand	Sandur; deposited in front of a retreating glacier.

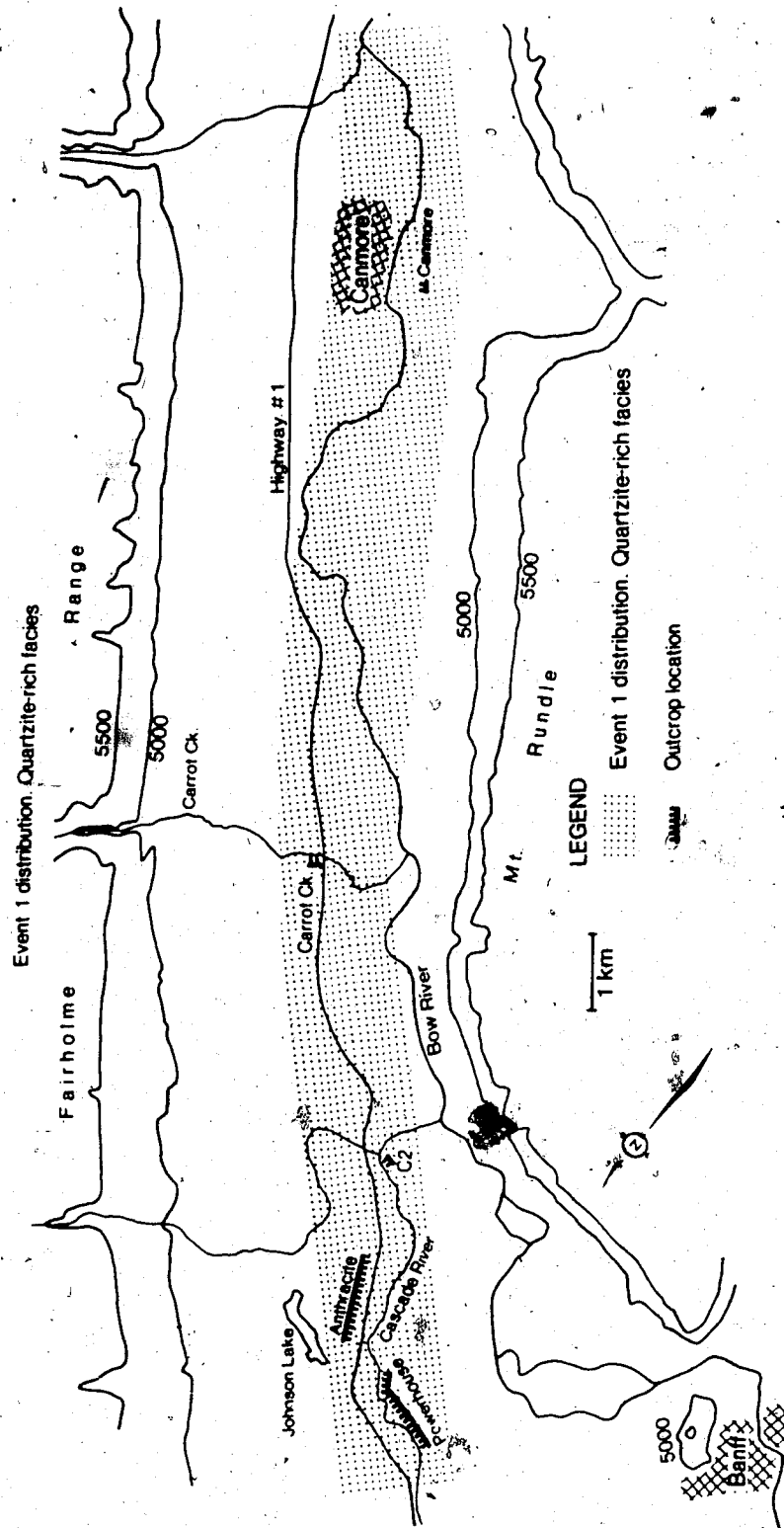


Figure 68. Event 1 sediment distribution. Braided stream sandur sediments.

Table 11. Comparison of Rutter's (1972) chronology to Mandryk's (this study) chronology of the Banff-Canmore area

Rutter (1972)	Mandryk (this study)
pre-Bow Valley advance	Event 1
Bow Valley advance	Event 2
Retreated glacier from Bow Valley advance situated in Banff town area. Readvancing glacier to mark Canmore advance.	Event 3b
Canmore advance	Event 3c

EVENT 2

The first definite evidence of a glacial advance into the study area is the till (facies 2, 3, and 4) located in the regions indicated in Figures 69 and 70. A valley glacier deposited facies 2, 3, and 4 as basal till. This till was deposited as both lodgement till in the strict sense (facies 2 and 3) and as lodged basal debris layers which subsequently melted out (facies 4). Event 2 is equivalent to the Bow Valley advance of Rutter (1972) (Table 11).

The physical nature of till can be used to determine some of the characteristics of the glacier which deposited the till.

THE BASAL THERMAL CONDITIONS OF THE EVENT 2 GLACIER

The basal thermal conditions of the valley glacier which deposited the till of event-2-age can be induced from the type of till deposited. In the regions where facies 2, 3, and 4 were deposited, the base of the glacier had to be at a temperature above the pressure melting point of water (wet- or warm-based) in order for lodgement till (facies 2 and 3) to form (Boulton 1972a; Dreimanis 1982), and in order for the sheared-off basal debris to melt-out (facies 4) (Muller 1983a). Up-valley of the Banff-Canmore area the glacier was mainly cold-based with some local wet-based areas which would later refreeze, incorporating basal

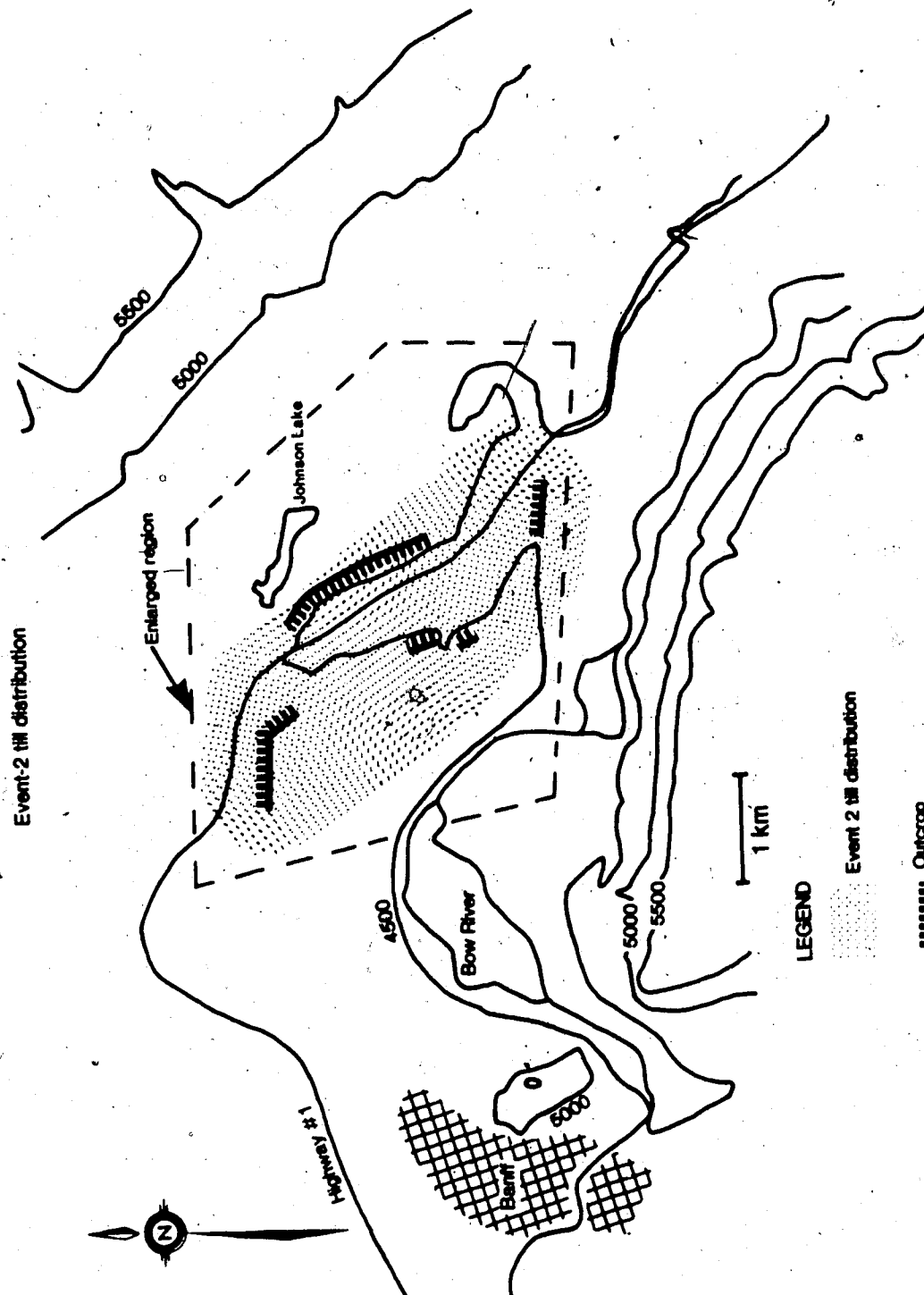


Figure 69a. Event 2 till distribution. Enlarged region in figure 69b.

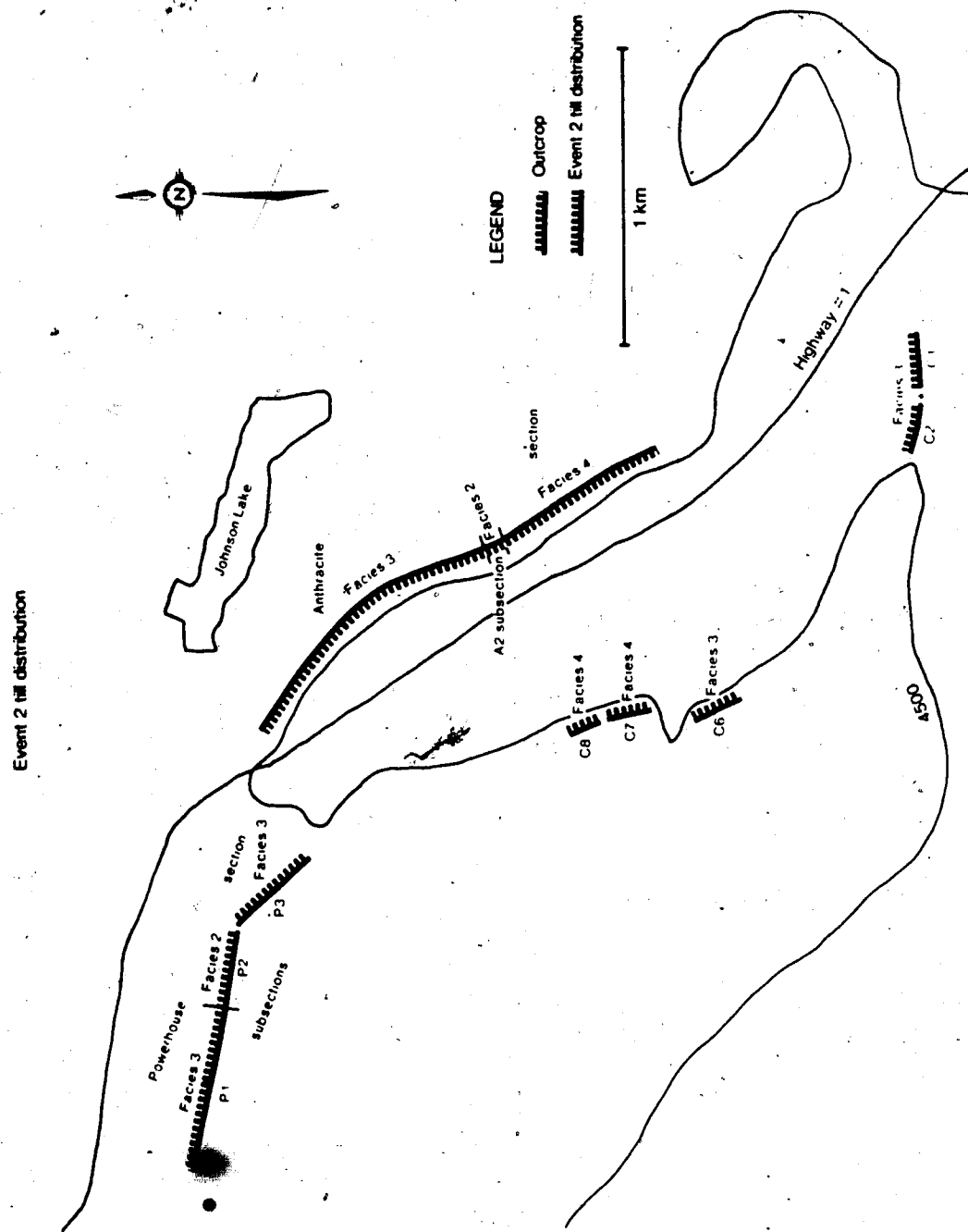


Figure 69b. Event 2 till distribution. Figure 69b shows the enlarged portion of figure 69a.

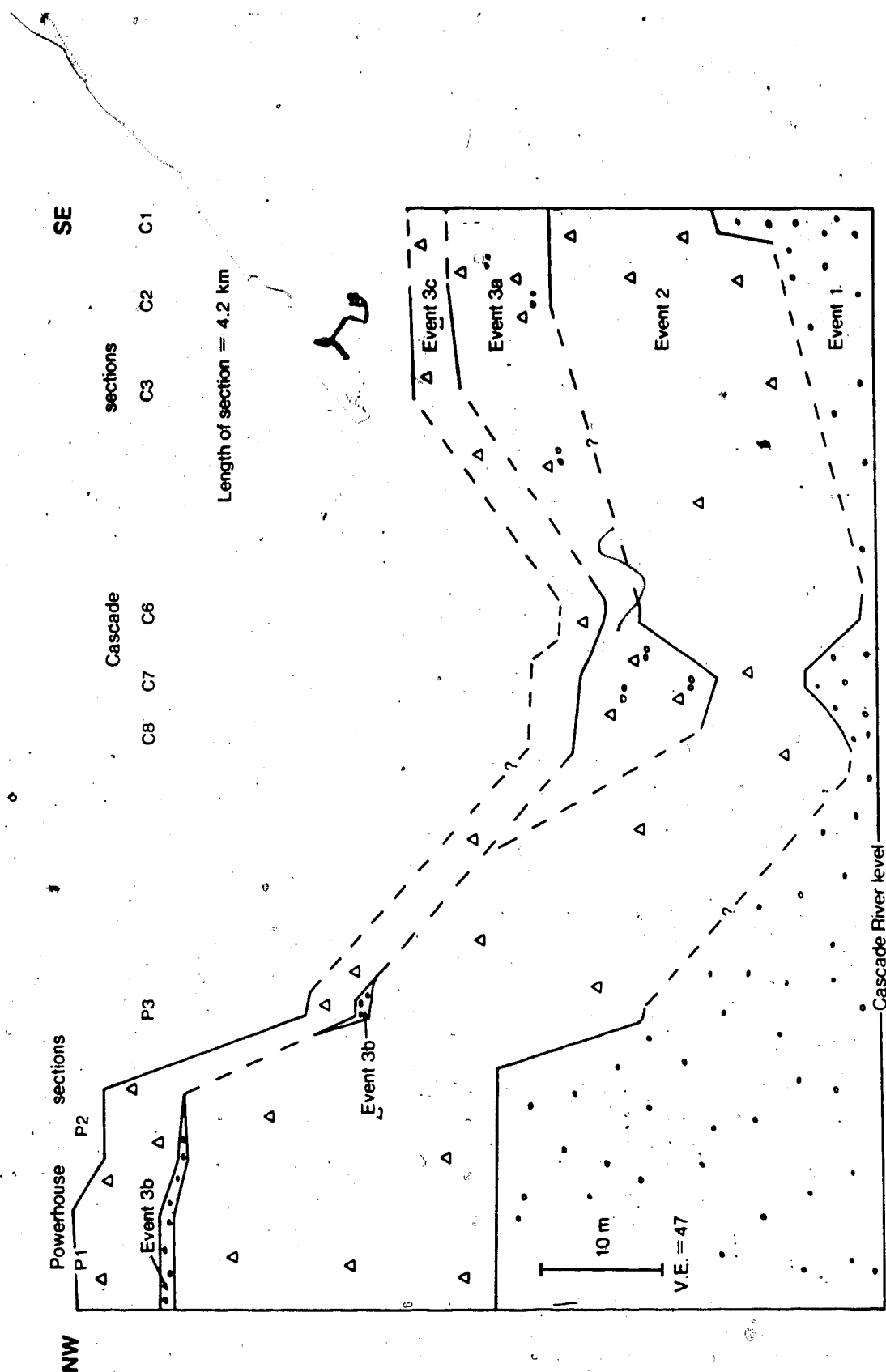


Figure 70a. Correlation chart. NW-SE section from the Powerhouse to Cascade River outcrops, section is parallel to Cascade River and oblique to the ice-flow direction.

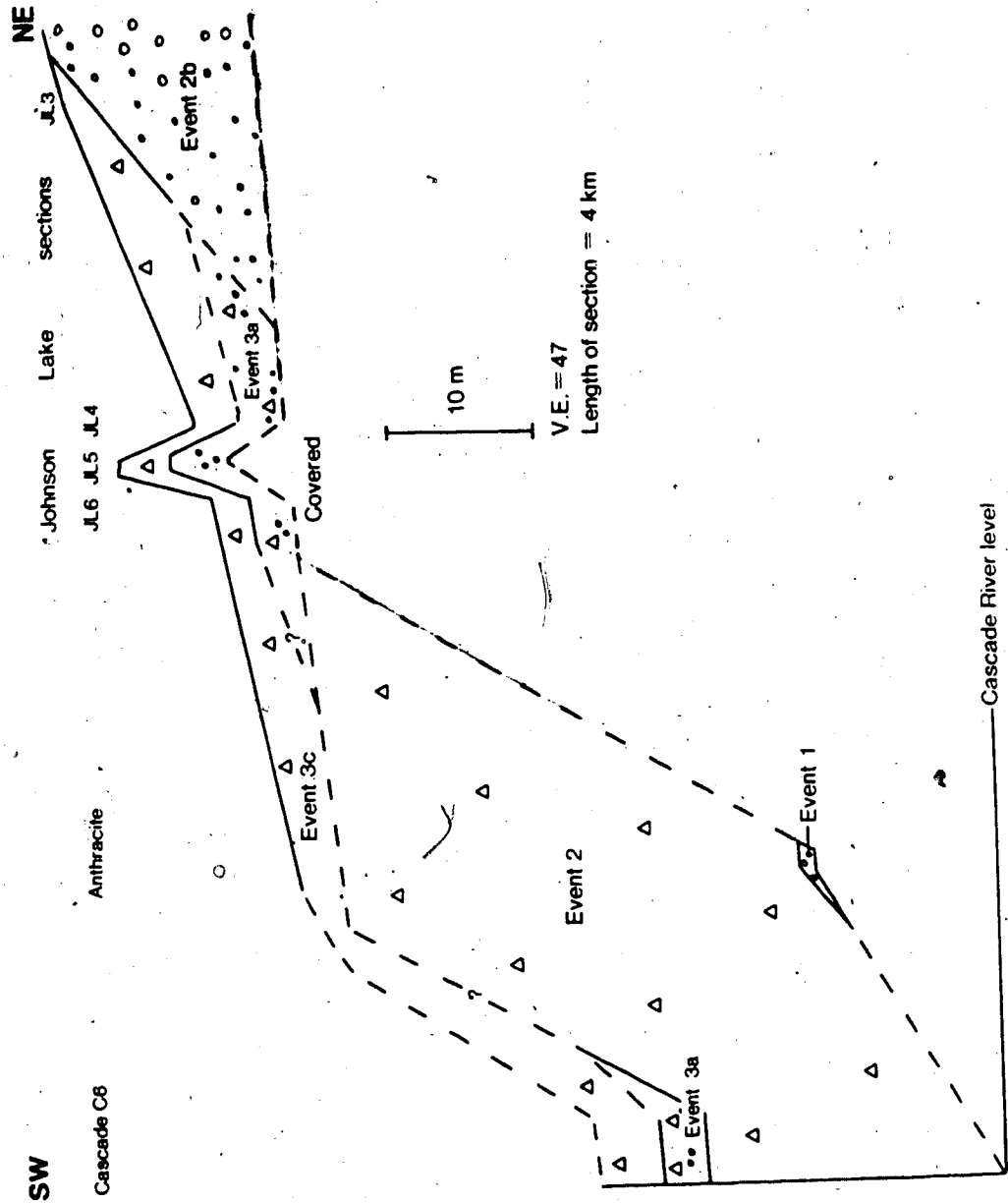


Figure 70b. Correlation chart. SW-NE section from Cascade River section C6 to the Johnson Lake sections. View is upglacier and transverse to the ice-flow direction.

debris by the process of regelation (Boulton 1970a) or the process of basal freeze-on of debris (Weertman 1961). This is how the glacier incorporated the basal debris which was eventually deposited in the study area.

LATERAL ICE CONDITIONS INSIDE THE EVENT 2 GLACIER

Lateral facies changes exist within the event 2 till. These changes are evident along the Powerhouse (Figure 15) and Anthracite (Figure 16) outcrops. In order to attempt an understanding of the lateral facies changes, the direction of facies change relative to the motion of the valley glacier must be known. For example, is the facies change in a direction parallel or perpendicular to the glacier's former flow direction?

To illustrate the relationship between the former valley glacier and the resulting observed facies distribution, a plot of the observed facies distribution is made with respect to reconstructed glacier flow-lines (Figure 71). This map shows that similar facies occur in groups that relate to the trend of the reconstructed glacier flow lines, and that the boundaries between lateral facies changes observed in the field are in fact oriented parallel to reconstructed glacial flow lines (compare Figures 4 and 71). This suggests that the adjacent facies are related in some manner to ice-flow-parallel features in the glacier. It is proposed here, that the lateral facies

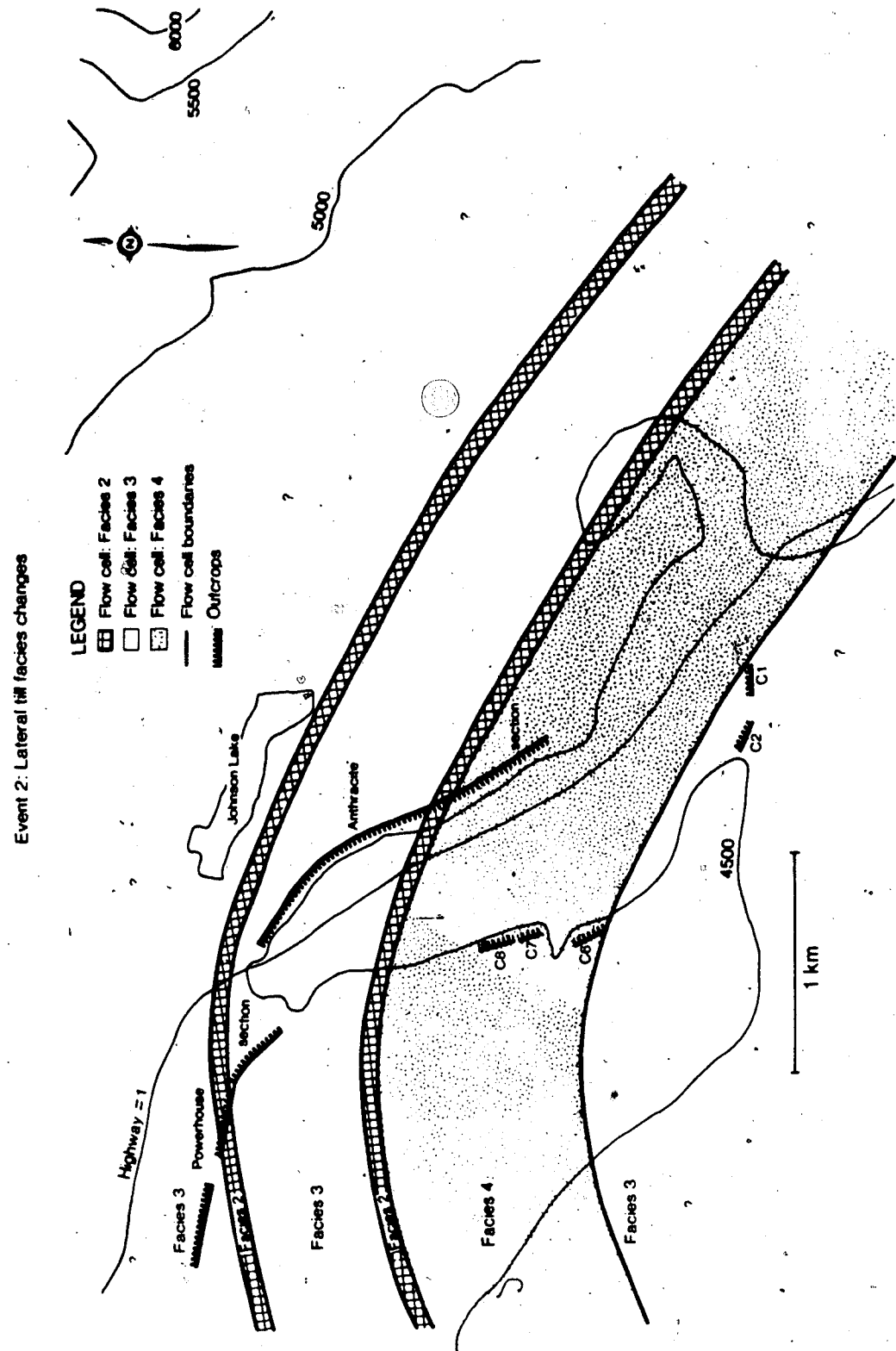



Figure 71. Lateral till facies changes in event 2 till.

changes observed along outcrops are most likely a product of deposition beneath different, adjacent glacier flow cells.

The presence of flow cells within a glacier is a mechanism which accounts for how different facies (facies 2, 3, and 4) are deposited adjacent to one another across the base of a glacier. Each flow cell would have unique glacial debris characteristics and ice flow characteristics. The resulting basally deposited sediment from a flow-cell would inherit characteristics derived from that particular flow-cell's glacial debris and glacial flow properties. This is how three different facies (facies 2, 3, and 4) were simultaneously deposited laterally adjacent to one another in the area of the Powerhouse, Anthracite, and Cascade sections.



More detailed ice-flow information is reconstructed by considering the adjacent nature of facies 2 and 3. As was mentioned in an earlier section, the glacial ice which deposited facies 2 had an oscillating velocity whereas facies 3 was deposited below ice which had a more constant velocity. Facies 2 and 3 were likely simultaneously deposited because of their adjacent setting. Simultaneous, laterally adjacent deposition of these two facies requires that the glacier overtop of facies 2 had an oscillating basal ice velocity; whereas ten's of meters away, across the base of the glacier where facies 3 was being deposited,

the glacier had a more constant basal ice velocity. This suggests that the flow cells which deposited facies 2 and 3 in particular, and perhaps also facies 4, had uncoupled flow-behavior. It follows, therefore, that the event 2 glacier did not have a consistent velocity profile, when viewed normal to the ice flow direction, as has been observed in the Athabasca Glacier (Figure 72) (Raymond 1971).

The above idea suggesting that the event 2 glacier had uncoupled flow cells is not unexpected since modern valley glaciers also seem to have flow cells with differing velocities. This is based on observations of surface foliation patterns, seen for example on the Gulkana glacier, Alaska (Rutter 1965b) and on Greenlandic glaciers (Sugden and John 1976, p. 76). Recognition of lateral, across-valley till facies changes in the Banff-Canmore area strongly suggests that large, ancient valley glaciers also had regions of independent ice flow behavior aligned parallel to the ice flow direction. These regions of independent ice flow produced basal till which retained properties of the various flow cells.

DEGLACIATION OF EVENT 2

Outwash was channeled along the present Bow or Cascade Rivers during the deglaciation of event 2. This channeling prevented the previously deposited glacial till from being

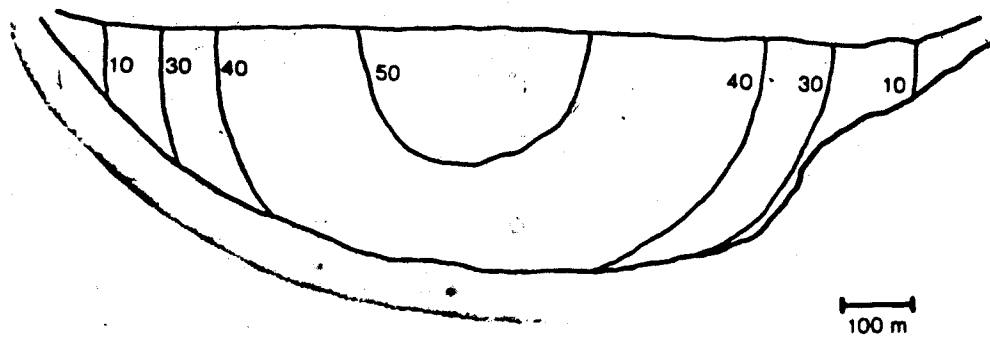


Figure 72. Velocity distribution in Athabasca Glacier, Alberta. Sectioned transverse to valley ice-flow-direction; velocity in meters per year (after Raymond 1971).

eroded in the Powerhouse, Cascade, and Anthracite vicinities.

EVENT 2b

The deglaciation which followed the glacial advance of event 2 was likely accompanied by warmer air temperatures. Warmer temperatures would have melted snow which had accumulated in the Fairholme Range during the event 2 glaciation. This melting would have produced peak water discharges which would flush loose-debris onto the alluvial fans extending out of the Fairholme Range and thereby form the quartzite-poor alluvial fans (facies 6, Figure 73).

EVENT 3a

Event 3a signifies the jerky advance of a valley glacier into the study area after the nonglacial period following event 2. The event 3a glacier deposited proglacial mudflow complexes (facies 5) (Figure 74). The glacier then retreated slightly; this allowed the recently deposited thin basal till, now part of the glacial mudflow complex, to be dissected by outwash streams. This advance and retreat could have occurred entirely within the Banff to Canmore area.

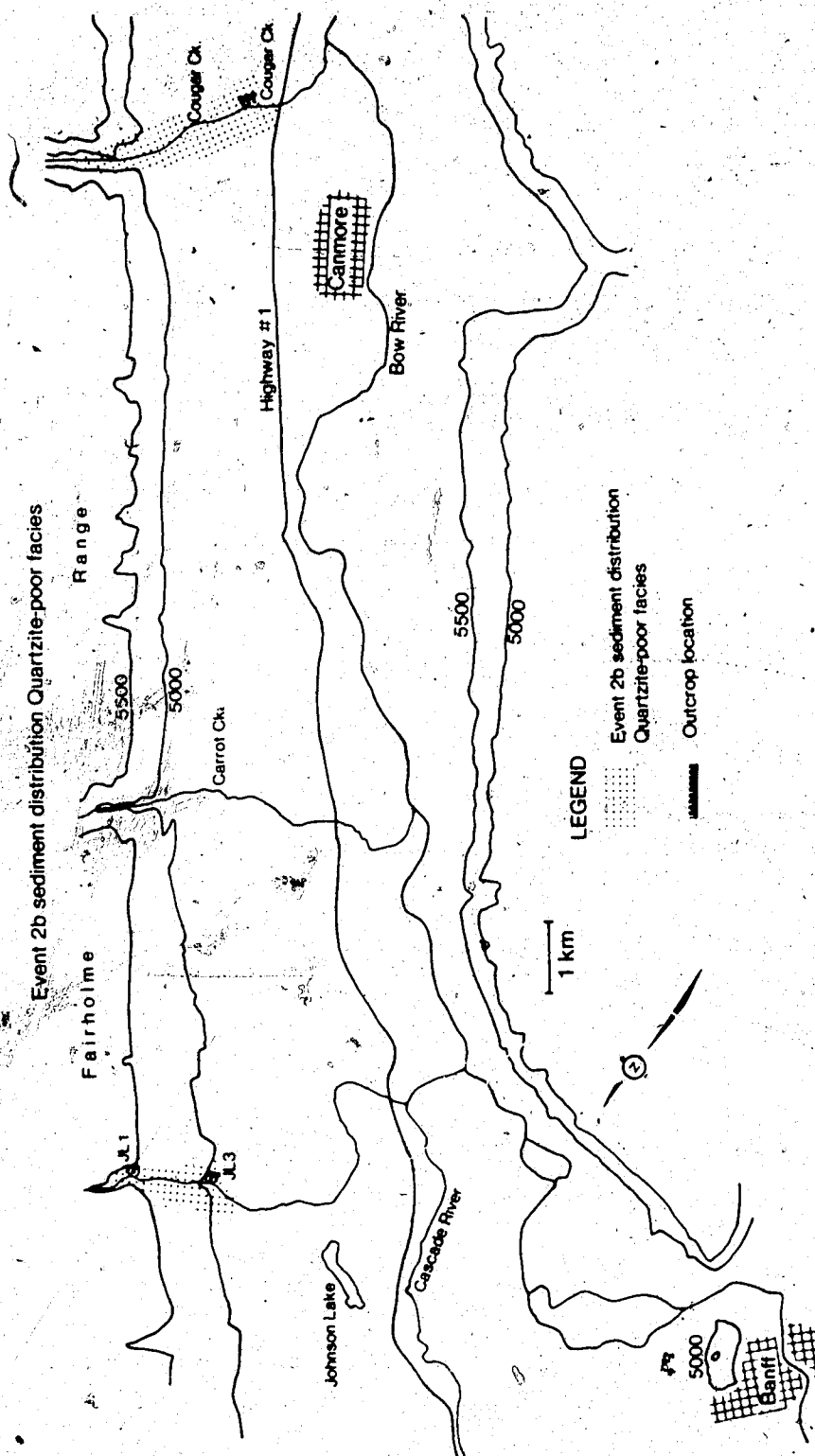


Figure 73. Event 2b sediment distribution; postglacial alluvial fans extending out of the Fairholme Range.

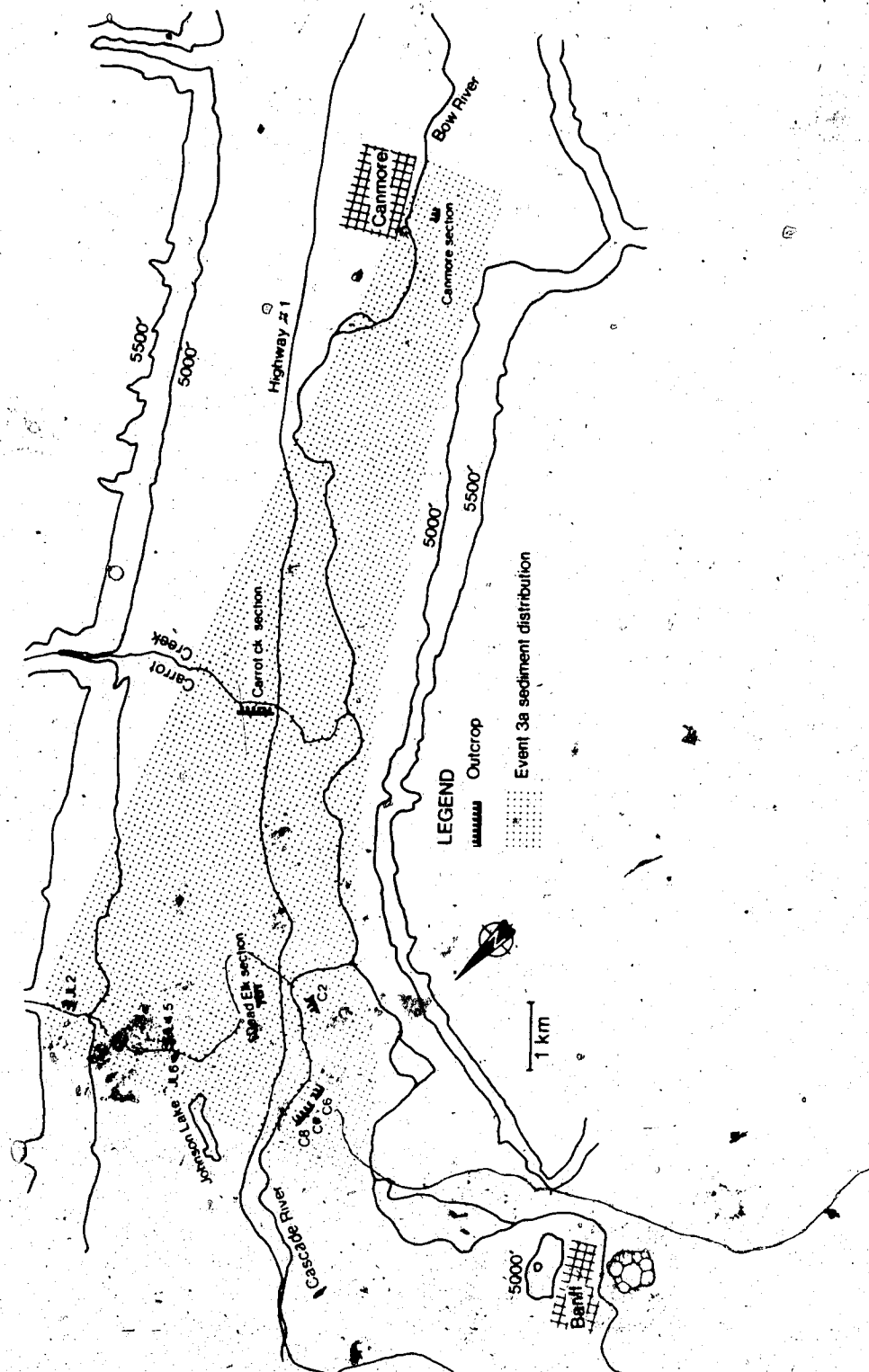


Figure 74. Event 3a sediment distribution; proglacial mudflow complex.

EVENT 3b

Towards the end of event 3a the glacier had retreated up-valley as far as the Banff townsite area. Event 3b began with proglacial streams (facies 6 and 7, Figure 75) cutting into the thicker event 2 till deposits at the Powerhouse (Figure 15) and Anthracite (Figure 16). The uppermost location of facies 6 at the Powerhouse section (Figure 15) was deposited by a proglacial braided stream which had cut into the till of event 2. Facies 7, at the Anthracite A1 subsection (Figure 62), was deposited by an ice proximal, proglacial outwash stream which flowed into a water-filled channel and cut into till of event 2.

Facies 7 grades upwards into the till of the later event 3c at the Anthracite-A1-subsection. This suggests the glacier was advancing while facies 7 was being deposited in the Anthracite area. During early event 3b time this glacier was situated up-valley of Banff but as event 3b progressed the glacier approached the Powerhouse-Anthracite area, and by the end of event 3b had advanced over the area. This glacial advance into the study area signifies the beginning of event 3c.

EVENT 3c

The final glacier which advanced into the study area was the same glacier which deposited the proglacial deposits (facies 6 and 7) of event 3b. The physical

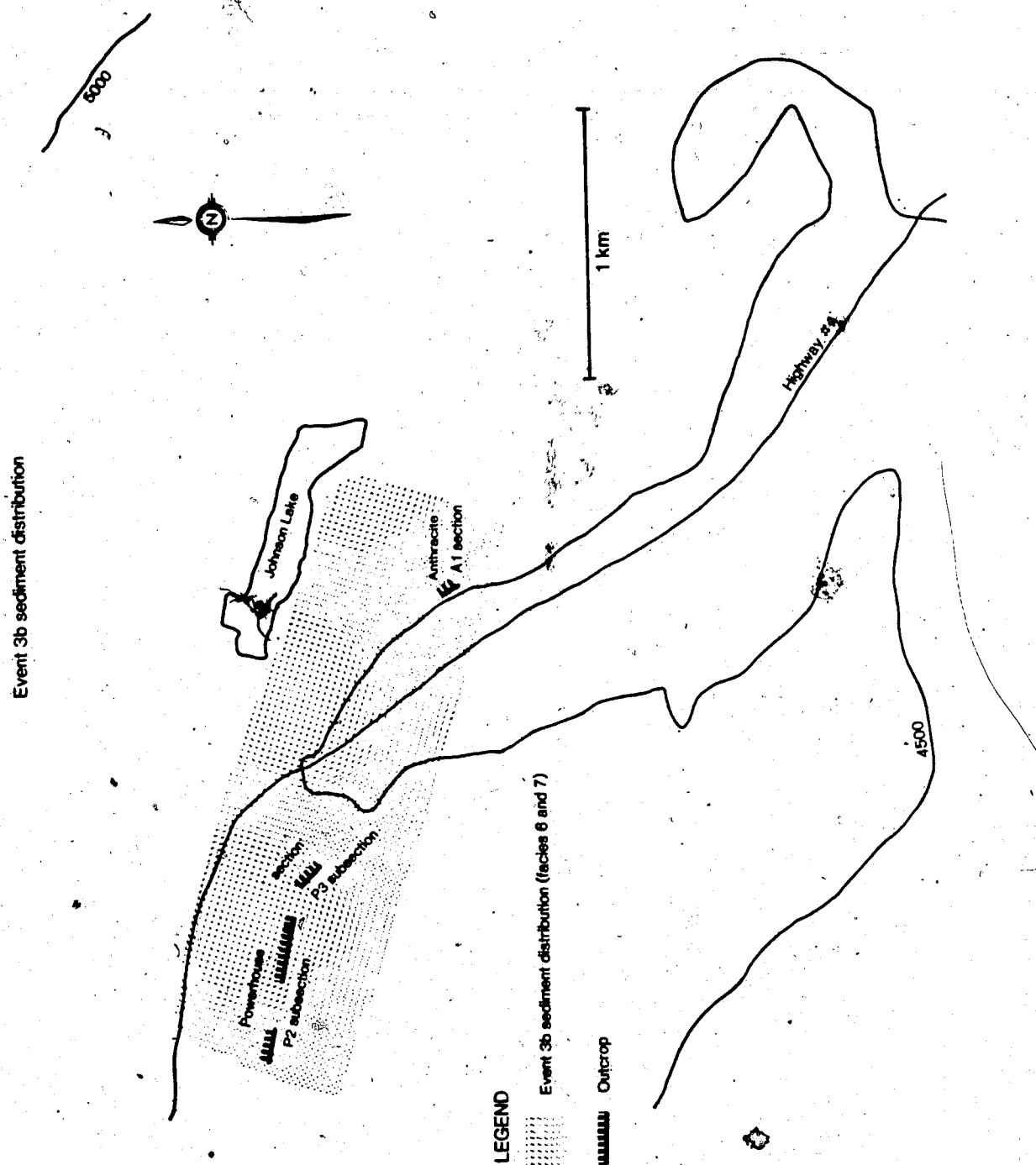


Figure 75. Event 3b sediment distribution; proglacial stream deposits.

connection between event 3b and 3c is established by facies 7 of event 3b grading up into the overlying till of event 3c at Anthracite's A1-subsection.

Event 3c was marked by a valley glacier advancing over the entire study area and depositing an approximately 3 meter thick basal till (Figures 70 and 76). In certain locations in the study area the base of this glacier was erosive prior to till deposition. Figures 15 and 16 show the discontinuous gravel horizons of event 3b (facies 6 at Powerhouse, Figure 15; facies 7 at Anthracite, Figure 16) which separate the underlying till of event 2 and the overlying till of event 3c at the Powerhouse and Anthracite sections. The discontinuous gravel horizons are interpreted to be a result of partial erosion of earlier deposits by the final glacier advance (event 3c).

Event 3c is approximately equivalent to the Canmore advance of Rutter (1972) (Table 11). The difference between event 3c (this study) and Rutter's (1972) Canmore advance is that the till of event 3c is continuous throughout the majority of the study area of this thesis whereas Rutter (1972) observed that the Canmore advance till had a discontinuous, patchy distribution throughout his larger study area.

Detailed interpretations concerning the behavior of the event 3c glacier can be made based on observations of the

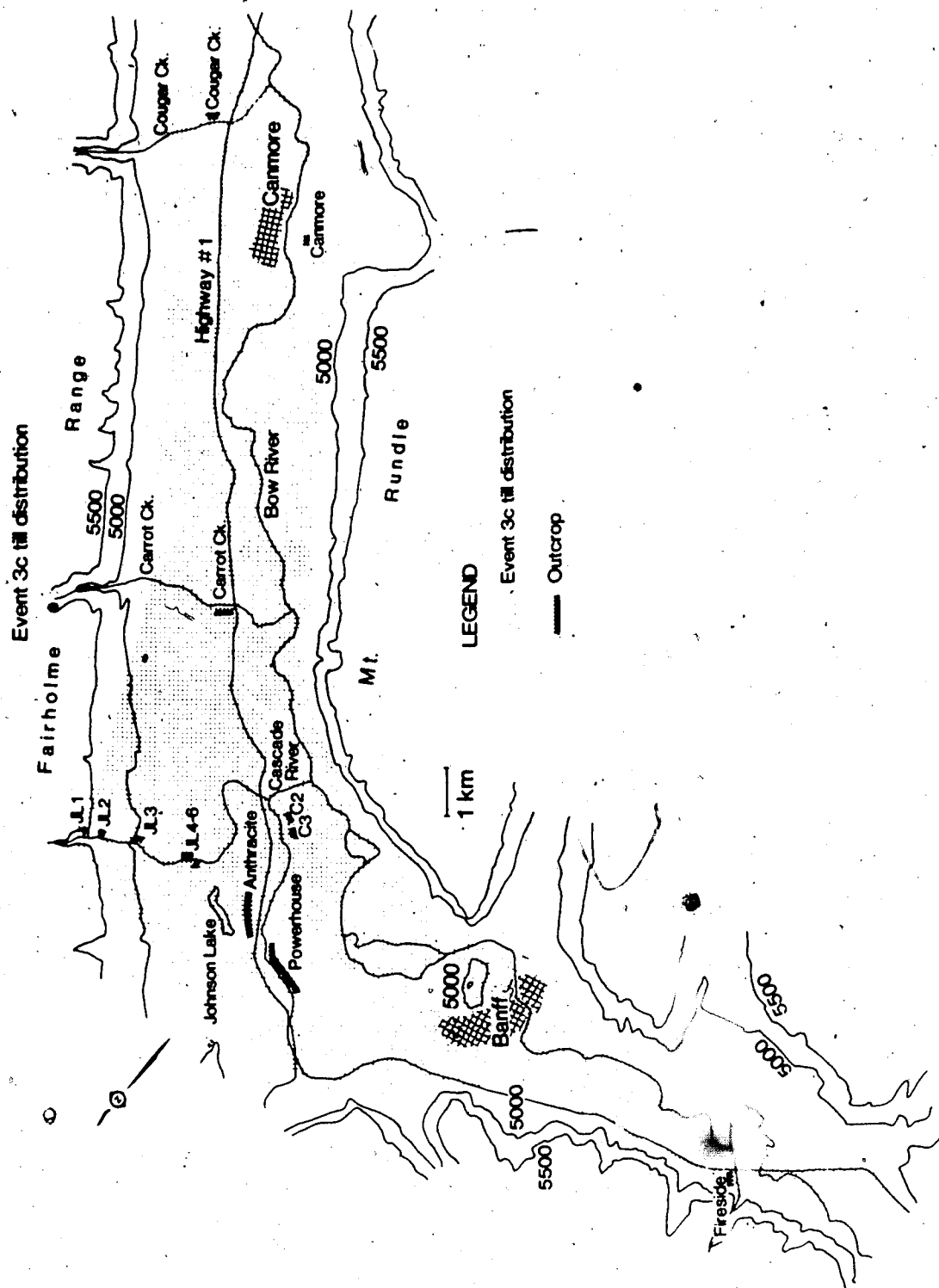


Figure 76. Event 3c till distribution.

resulting event 3c till. The final glacial advance (event 3c) deposited lodgement till (facies 3) and also lodged basal debris layers which then basally melted-out (facies 1 and 4). Facies 2 was not deposited during this final glacial advance. In order for facies 2 to have been deposited a regular fluctuation or oscillation in the basal ice velocity must have existed during the process of lodgement (section IV B). The lack of facies 2 indicates that no part of the glacier, or no flow cell, had an oscillating velocity which would then enable facies 2 to form. It seems that during the last glacial advance (event 3c) the glacier's flow cells all had similar velocities.

The temperature regime of the event 3c glacier can be approximated from its deposits. The event 3c glacier had the same basal temperature regime as the subpolar glacier of event 2. That is, the event 3c glacier had large areas upglacier where the base was frozen (temperatures below the pressure melting point of ice) with pressure melting only occurring at obstacles. Down-glacier, in the study area, the glacier's base was melting (the basal temperature was above the pressure melting point of ice).

Examination of the event 3c till also reveals lateral till facies changes. These lateral facies changes (Figure 77) are interpreted to result from differing depositional

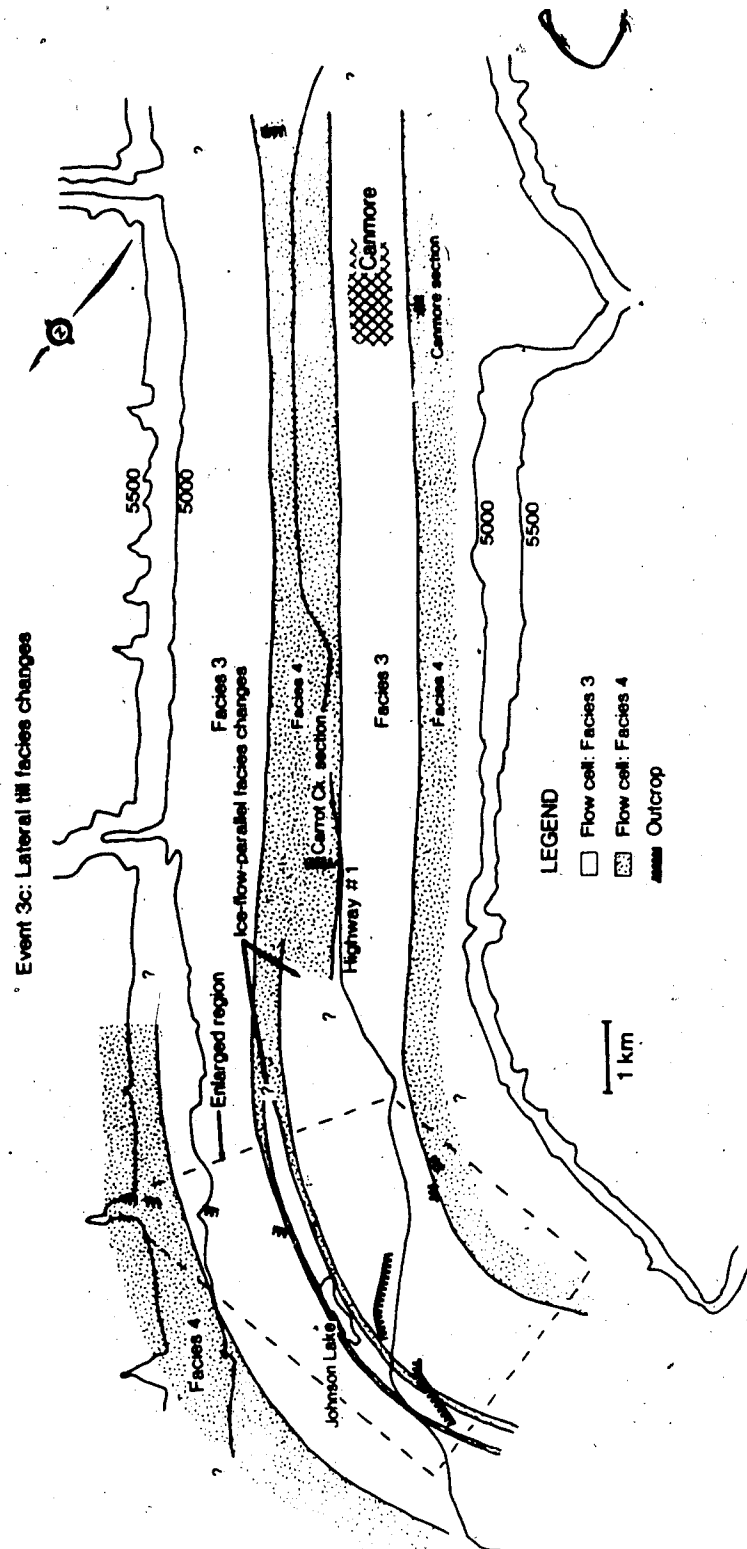


Figure 77a. Lateral till facies changes in event 3c till.
Enlarged region in figure 77b.

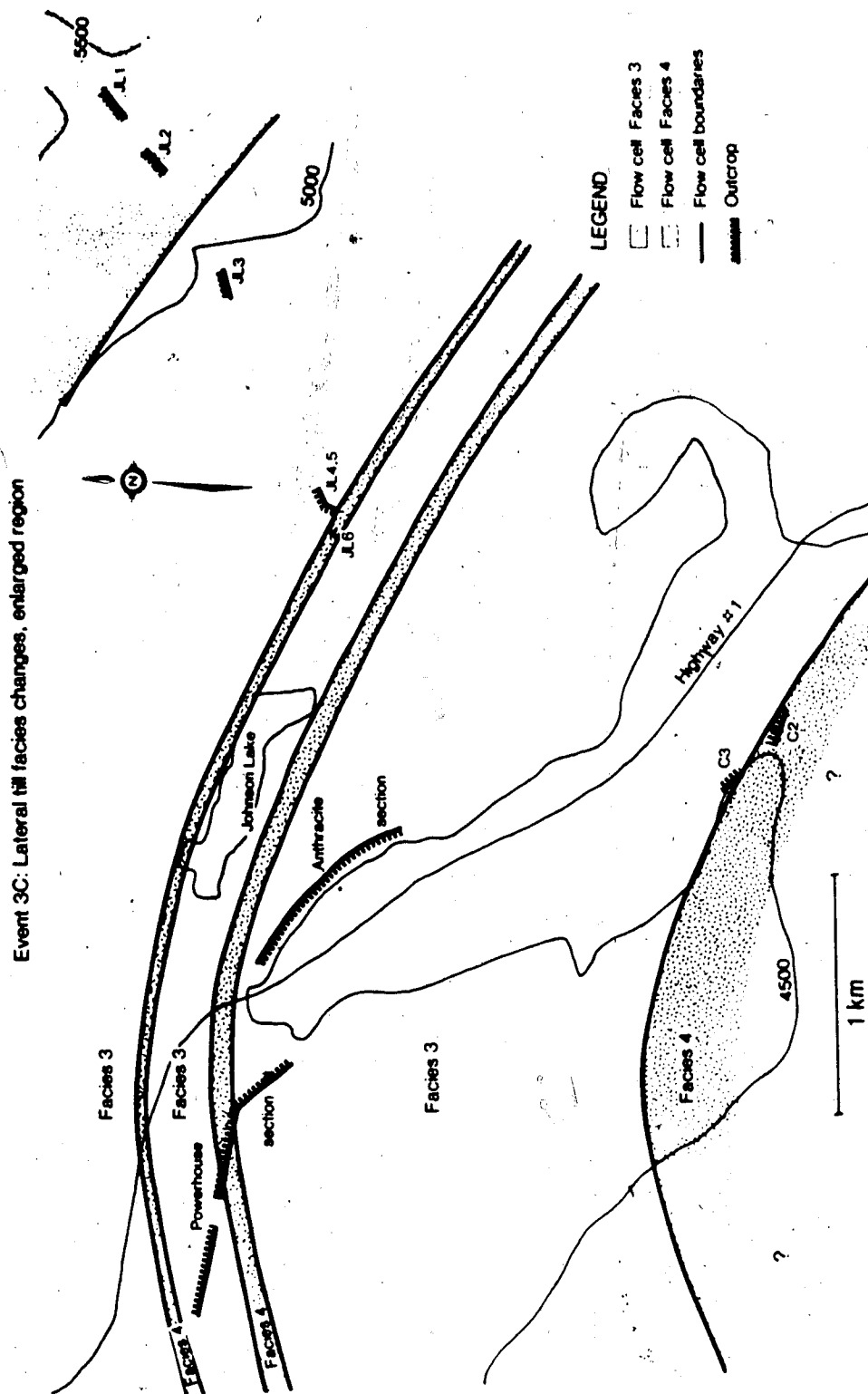


Figure 77b. Lateral till facies changes in event 3c till within the enlarged portion of figure 77a.

processes operating below adjacent glacial flow-cells. Figure 77 shows that facies 3 and 4 were the predominant facies deposited during event 3c. The deposition of facies 3 and 4 continued to the end of event 3c, the last glaciation of the Banff-Canmore area.

DEGLACIATION OF EVENT 3c

It must first be resolved whether any portion of the glacial deposits have been postdepositionally removed by erosion, before the mechanisms and history of deglaciation following the event 3c glaciation can be determined. This is necessary because the deglacial history can only be properly interpreted if the entire deposit is preserved. In the Banff-Canmore area the entire glacial and deglacial sequence of event 3c is apparently preserved unaltered at many locations throughout the study area (for example at the Powerhouse outcrop, Figure 15; at the Carrot Creek outcrop, Figure 33; and at the Fireside outcrop, Figure 5).

The following two characteristics suggest that an unaltered sequence of till is present at the surface. Firstly, the till of event 3c (facies 1, 3, and 4) extends uninterrupted to its upper contact and is then overlain by a silt which is interpreted to be a loess deposit. This stratigraphic sequence implies no postdepositional erosion of the till occurred. Secondly, the preservation of drumlins in the area of the Powerhouse section (plate 4)

indicates that no extensive postdepositional erosion took place.

Since all of the event 3c till was only deposited below active ice, deposition ceased when deglaciation began. This implies that mainly debris-free ice filled the Bow valley during deglaciation. Melting of the ice would have been in a downward direction from the upper, debris-free surface; the toe likely melted concurrently in an upvalley direction.

While the toe retreated up-valley, glacier-flow had already ceased, at least in the study area. If ice flow continued while the toe was retreating, compression near the toe would have emplaced basal debris into a supraglacial position (Boulton 1968). No evidence for supraglacially deposited debris exists during the final glaciation (event 3c). Nothing suggests the style of the earlier event 2 deglaciation was any different than event 3c deglaciation. Deglaciation of the Bow valley therefore consisted of a relatively debris-free glacier with a mainly debris-free surface melting in situ after a period of glaciation.

B. RELATIVE LENGTHS OF GLACIATIONS

Unfortunately no datable materials were found in the

sediments studied in this project. An estimate of the comparative lengths of the event 2 and 3c glaciations is therefore made in this section. The estimates are based on the thicknesses of the two tills.

There is a striking difference in thicknesses between the thicker, event 2 till (24-30 m thick) and the event 3c till (3-10 m thick) (Figure 70). The reason for this difference will be explained below.

A difference in the geothermal heat flux between the two glaciations will affect the relative rates of basal melting. Such a change is possible over a period of a few hundred thousand years in an area with local hot spring activity. Changes in the geothermal heat flux with time in the study area is unknown and will therefore not be considered further.

The till of event 2 and event 3c appear similar to one another and both tills contain generally the same facies (facies 2 and 4). The similarity between these tills therefore suggests that the two glaciers had the same general characteristics. This similarity rules out differences in till deposition rates as a cause for the thickness difference between the till of event 2 and 3c. If anything, during event 2 the thicker facies 2 should have accumulated even more slowly than till did during the final glaciation (event 3c) because at times during event 2 certain flow-cells had elevated velocities which would have

actually decreased the rate of lodgement. (Increased glacier velocity would allow less time for interstitial ice to melt-out from around basal debris as it was about to lodge and would therefore slow the lodging process and thus till accumulation.)

Time, or the duration of a glacial event, is the only obvious variable remaining to explain why till thicknesses differ. Based on the ratio of the till thicknesses from the two events, the duration of glaciation during event 2 is interpreted to have been 2 to 10 times longer than the duration of the final (event 3c) glaciation. The longer period of glaciation during event 2 would have also allowed a thicker mountain snowpack to develop in the Fairholme Range.

C. METHODS EVALUATION

In this section comments will be made on the usefulness of the various field and laboratory methods employed in this study.

FIELD METHODS

Future studies of diamictos or glacial till deposits should investigate, where practical, lateral facies changes in addition to vertical changes.

DIAMICTON (TILL) FABRICS

Diamicton pebble macrofabrics were useful in helping identify the diamictons as being tills.

GRAINSIZE OF THE DIAMICTON (TILL) MATRIX

Provides information useful in making genetic interpretations. Helps determine whether or not vertical facies changes exist within a till.

PETROLOGY

Petrology was useful for, (i) identifying side valley alluvial fans, and (ii) arriving at genetic till interpretations by helping determine whether or not basal melt-out, lodgement, or supraglacial tills were present.

ROUNDNESS

Helped determine the process of glacial deposition and aided in identifying depositional environments.

D. CONCLUSIONS

The three stated objectives of this study were met.

1. The basic stratigraphic framework and geological history determined in this study agrees with Rutter's (1965a). New

information is provided by the recognition of an even alluvial fan sedimentation (event 2b) and events of proglacial sedimentation (events 3a and 3b).

- 2. Facies analysis aided in determining the sedimentological genesis of the deposits. Published observations of modern valley glacier sedimentary processes were found to be useful analogues. Unfortunately, modern glacial observations of basal deposition are lacking in the region up-glacier of the terminus region. As a result, more confidence can be placed on the interpretations of proglacial depositional settings than on settings beneath the glacier.
3. The recognition of lateral facies changes suggest the flow cells (ice streams) within a valley glacier may simultaneously deposit different types of till.

In addition to these findings it appears that the valley glacier which last occupied the Banff-Canmore region transported very little, if any, supraglacial debris. This implies deposition was mainly from the base of the glacier.

VI. REFERENCES

- ALLEN, J.R.L. 1982. Late Pleistocene (Devensian) glaciofluvial outwash at Banc-y-Warren, near Cardigan (west Wales). *Geological Journal*, 17, pp. 31-47.
- AMERICAN SOCIETY FOR TESTING MATERIALS 1964. Standard method for grain size analysis of soils, ASTM D422-63. In *Procedure for testing soils*. American Society for Testing Materials, Philadelphia, U.S.A., pp. 95-106.
- BATES, R.L., AND JACKSON, J.A., editors 1980. *Glossary of Geology*, 2nd edition. American Geological Institute, Falls Church, Virginia, 749 pp.
- BEATT, H., MIDDLETON, G., and MURRAY, R. 1980. *Origin of Sedimentary Rocks*, 2nd edition. Prentice-Hall, New Jersey, 782 p.
- BOOTHROYD, J.C. and NUMMEDAL, D. 1978. Proglacial braided outwash: a model for humid alluvial-fan deposits. In *Fluvial Sedimentology*. Edited by A.D. Miall. Canadian Society of Petroleum Geologists, Memoir 5, pp. 641-668.
- BOULTON, G.S. 1967. The development of a complex supraglacial moraine at the margin of Sorbreen, Ny Friesland, Vestspitsbergen. *Journal of Glaciology*, 6, pp. 717-735.
- BOULTON, G.S. 1968. Flow tills and related deposits on some Vestspitsbergen glaciers. *Journal of Glaciology*, 7, pp. 391-412.
- BOULTON, G.S. 1970a. On the origin and transport of englacial debris in Svalbard glaciers. *Journal of Glaciology*, 9, pp. 213-229.
- BOULTON, G.S. 1970b. On the deposition of subglacial and melt-out tills at the margins of certain Svalbard Glaciers. *Journal of Glaciology*, 9, pp. 231-245.
- BOULTON, G.S. 1971. Till genesis and fabric in Svalbard, Spitsbergen. In *Till: A Symposium*. Edited by R.P. Goldthwait. Ohio State University Press, Columbus, Ohio, pp. 41-72.

- BOULTON, G.S. 1972a. Modern arctic glaciers as depositional models for former ice sheets. *Journal of the Geological Society, London*, 128, pp. 361-393.
- BOULTON, G.S. 1972b. Englacial debris in glaciers: reply to the comments of Dr. J.T. Andrews. *Journal of Glaciology*, 11, pp. 155-156 (letter).
- BOULTON, G.S. 1975. Processes and patterns of subglacial sedimentation: a theoretical approach. In *Ice Ages: Ancient and Modern*. Edited by A.F. Wright and F. Mosley. *Geological Journal, Special Issue* 6, pp. 7-42.
- BOULTON, G.S. 1976a. The origin of glacially fluted surfaces- observations and theory. *Journal of Glaciology*, 17, pp. 287-309.
- BOULTON, G.S. 1976b. A genetic classification of tills and criteria for distinguishing tills of different origin. In *Till, its Genesis and Diagenesis*. Edited by Stankowski. *Seria Geografia*, 12, pp. 65-80.
- BOULTON, G.S. 1978. Boulder shapes and grain-size distributions of debris as indicators of transport paths through a glacier and till genesis. *Sedimentology*, 25, pp. 773-799.
- BOULTON, G.S., DENT, D.L., and MORRIS, E.M. 1974. Subglacial shearing and crushing, and the role of water pressures in till from south-east Iceland. *Geografiska Annaler*, 56A, pp. 135-145.
- BOULTON, G.S. and EYLES, N. 1979. Sedimentation by valley glaciers: a model and genetic classification. In *Moraines and Varves. Origin, Genesis, Classification*. Edited by C. Schluchter. A.A. Balkema, Rotterdam, pp. 11-23.
- BOULTON, G.S. and DEYNOUX, M. 1981. Sedimentation in glacial environments and the identification of tills and tillites in ancient sedimentary sequences. *Precambrian Research*, 15, pp. 397-422.
- BROSTER, B.E. and DREIMANIS, A. 1981. Deposition of multiple lodgement tills by competing glacial flows in a common ice sheet: Cranbrook, British Columbia. *Arctic and Alpine Research*, 13, pp. 197-204.

- BROSTER, B.E., DREIMANIS, A., and WHITE, J.C. 1979. A sequence of glacial deformation, erosion, and deposition at the ice-rock interface during the last glaciation: Cranbrook, British Columbia, Canada. *Journal of Glaciology*, 23, pp. 283-295.
- BULL, W.B. 1960. Types of deposition on alluvial fans in western Fresno County, California. *Bulletin of the Geological Society of America*, 71, p. 2052.
- BULL, W.B. 1963. Alluvial-fan deposits in western Fresno county, California. *Journal of Geology*, 71, pp. 243-251.
- BULL, W.B. 1972. Recognition of alluvial-fan deposits in the stratigraphic record. In *Recognition of Ancient Sedimentary Environments*. Edited by J.K. Rigby and W.K. Hamblin. Society of Economic Paleontologists and Mineralogists, Special Publication 16, pp. 63-83.
- BULL, W.B. 1977. The alluvial fan environment. *Progress in Physical Geography*, 1, pp. 222-270.
- CARTER, R.M. 1975. A discussion and classification of subaqueous mass-transport with particular application to grain-flow, slurry flow, and fluxoturbidites. *Earth Science Reviews*, 11, pp. 145-177.
- CHURCH, M. 1972. Baffin Island Sandurs: A Study of Arctic Fluvial Processes. Geological Survey of Canada, Bulletin 216, 208 p.
- CHURCH, M., and RYDER, J.M. 1972. Paraglacial sedimentation: a consideration of fluvial processes conditioned by glaciation. *Geological Society of America Bulletin*, 83, pp. 3059-3072.
- CHURCH, M., and GILBERT, R. 1975. Proglacial fluvial and lacustrine environments. In *Glaciofluvial and Glaciolacustrine Sedimentation*. Edited by A.V. Jopling and B.C. McDonald. Society of Economic Paleontologists and Mineralogists, Special Publication 23, pp. 22-100.

- CLAGUE, J.J., EVANS, S.G., and BLOWN, I.G. 1985. A debris flow triggered by the breaching of a moraine-dammed lake, Klattasine Creek, British Columbia. *Canadian Journal of Earth Sciences*, 22, pp. 1492-1502.
- CLAPPERTON, C.M. 1975. The debris content of surging glaciers in Svalbard and Iceland. *Journal of Glaciology*, 14, pp. 395-406.
- CURRY, R.R. 1966. Observation of alpine mudflows in the Tenmile Range, Central Colorado. *Geological Society of America Bulletin*, 77, pp. 771-776.
- DEJONG, M.G.G., and RAPPOL, M. 1983. Ice-marginal debris-flow deposits in western Allgäu, southern West Germany. *Boreas*, 12, pp. 57-70.
- DRAKE, L.D. 1972. Mechanisms of clast attrition in basal till. *Geological Society of America Bulletin*, 83, pp. 2159-2166.
- DREIMANIS, A. 1976. Tills: Their origin and properties. In *Glacial till*. Edited by R.F. Legget. The Royal Society of Canada, Special Publication 12, pp. 11-49.
- DREIMANIS, A. 1982. Quaternary glacial deposits: implications for the interpretation of Proterozoic glacial deposits. *Geological Society of America, Memoir* 161, pp. 299-307.
- DREIMANIS, A., and LUNDQVIST, J. 1984. What should be called till? Striae. *Ten Years of Nordic Till Research*, 20, pp. 5-10.
- ENGELHARDT, H.F., HARRISON, W.D., and KAMB, B. 1978. Basal sliding and conditions at the glacier bed as revealed by borehole photography. *Journal of Glaciology*, 20, pp. 469-508.
- ENOS, P. 1977. Flow regimes in debris flow. *Sedimentology*, 24, pp. 133-142.
- EYLES, N. 1979. Facies of supraglacial sedimentation on Icelandic and Alpine temperate glaciers. *Canadian Journal of Earth Sciences*, 16, pp. 1341-1361.

- EYLES, N., and ROGERSON, R.J. 1977. Glacier movement, ice structures, and medial moraine form at a glacier confluence, Berendon Glacier, British Columbia, Canada. *Canadian Journal of Earth Sciences*, 14, pp. 2807-2816.
- EYLES, N., and ROGERSON, R.J. 1978. A framework for the investigation of medial moraine formation: Austerdalsbreen, Norway, and Berendon Glacier, British Columbia. *Journal of Glaciology*, 20, pp. 99-113.
- EYLES, N., and SLADEN, J.A. 1981. Stratigraphy and geotechnical properties of weathered lodgement till in Northumberland, England. *Quarterly Journal of Engineering Geology*, 14, pp. 129-141.
- EYLES, N., SLADEN, J.A., and GILROY, S. 1982. A depositional model for stratigraphic complexes and facies superimposition in lodgement tills. *Boreas*, 11, pp. 317-333.
- FISHER, R.V. 1971. Features of coarse-grained, high concentration fluids and their deposits. *Journal of Sedimentary Petrology*, 41, pp. 916-927.
- FLINT, R.F., SANDERS, J.E., and RODGERS, J. 1960a. Symmictite: a name for nonsorted terrigenous sedimentary rocks that contain a wide range of particle sizes. *Geological Society of America Bulletin*, 71, pp. 507-510.
- FLINT, R.F., SANDERS, J.E., and RODGERS, J. 1960b. Diamictite, a substitute term for Symmictite. *Geological Society of America Bulletin*, 71, pp. 1809-1810.
- FOLK, R.L., and WARD, W.C. 1957. Brazos river bar: a study in the significance of grain size parameters. *Journal of Sedimentary Petrology*, 27, pp. 3-26.
- FRAKES, L.A. 1978. Diamictite. In *The Encyclopedia of Sedimentology*. Edited by R.W. Fairbridge and J. Bourgeois. Dowden, Hutchinson, and Ross, Stroudsburg. pp. 262-263.

- FRYXELL, F.M., and HORBERG, L. 1943. Alpine mudflows in Grand Teton National Park, Wyoming. Geological Society of America Bulletin, 54, pp. 457-472.
- GOW, A.J., EPSTEIN, S., and SHEEHY, W. 1979. On the origin of stratified debris in ice cones from the bottom of the Antarctic ice sheet. Journal of Glaciology, 23, pp. 185-192.
- HALDORSEN, S. 1977. The petrography of tills - a study from Ringsalen, S.E. Norway. Norges Geologiske Undersokelse, 336, 36 p.
- HALDORSEN, S. 1981. Grain-size distribution of subglacial till and its relation to glacial crushing and abrasion. Boreas, 10, pp. 91-105.
- HALDORSEN, S. 1982. The genesis of tills from Astadalen, southeastern Norway. Norsk Geologisk Tidsskrift, 62, pp. 17-38.
- HALDORSEN, S., and SHAW, J. 1982. The problem of recognizing melt-out till. Boreas, 11, pp. 261-277.
- HALLET, B. 1981. Glacial abrasion and sliding: their dependence on the debris concentration in basal ice. Annals of Glaciology, 2, pp. 23-28.
- HARMS, J.C., SOUTHARD, J.B., and WALKER, R.G. 1982. Structures and sequences in clastic rocks. Society of Economic Paleontologists and Mineralogists, Short Course Notes 9.
- HARTSHORN, J.H. 1958. Flow till in southeastern Massachusetts. Geological Society of America Bulletin, 69, pp. 477-482.
- HEIN, F.J., and WALKER, R.G. 1977. Bar evolution and development of stratification in the gravelly, braided Kicking Horse River, British Columbia. Canadian Journal of Earth Sciences, 14, pp. 562-570.

- HERRON, S., and LANGWAY, C. Jr. 1979. The debris-laden ice at the bottom of the Greenland ice sheet. *Journal of Glaciology*, 23, pp. 193-207.
- HOOKE, R. LeB. 1967. Processes on arid-region alluvial fans. *Journal of Geology*, 75, pp. 438-460.
- HUMLUM, O. 1981. Observations on debris in the basal transportation zone of Myrdalsjokull, Iceland. *Annals of Glaciology*, 2, pp. 71-77.
- HYVARINEN, L., KAURANNE, K., YLETTYINEN, V., et al. 1973. Modern boulder tracing in prospection. In *Prospecting in areas of glaciated terrain. Edited by M.J. Jones.* pp. 87-95.
- JOHANSSON, C.E. 1965. Structural studies of sedimentary deposits. *Geologiska Foreningens I Stockholm Forhandlingar*, 87, pp. 3-61.
- JOHNSON, A.M. 1970. *Physical Processes in Geology*. Freeman, Cooper and Company, San Francisco, CA, 577 p.
- KAMB, B., and LaCHAPELLE, E. 1964. Direct observation of the mechanism of glacier sliding over bedrock. *Journal of Glaciology*, 5, pp. 159-172.
- KEMMIS, T.J. 1981. Importance of the regelation process to certain properties of basal tills deposited by the Laurentide ice sheet in Iowa and Illinois, U.S.A. *Annals of Glaciology*, 2, pp. 147-152.
- KOCHEL, R.C., and JOHNSON, R.A. 1984. Geomorphology and sedimentology of humid-temperate alluvial fans, central Virginia. In *Sedimentology of Gravels and Conglomerates. Edited by E.H. Koster and R.J. Steel.* Canadian Society of Petroleum Geologists, Memoir 10, pp. 109-122.
- KRUGER, J. 1979. Structures and textures in till indicating subglacial deposition. *Boreas*, 8, pp. 323-340.
- KRUGER, J. 1984. Clasts with stoss-lee form in lodgement tills: A discussion. *Journal of Glaciology*, 30, pp. 241-243.
- KRUMBEIN, W.C. 1941a. Measurement and geological significance of shape and roundness of sedimentary particles. *Journal of Sedimentary Petrology*, 11, pp. 64-72.

- KRUMBEIN, W.C. 1941b. The effect of abrasion on the size, shape and roundness of rock fragments. *Journal of Geology*, 49, pp. 482-520.
- LAWSON, D.E. 1976. Observations on flutings at Spencer Glacier, Alaska. *Arctic and Alpine Research*, 8, pp. 289-296.
- LAWSON, D.E. 1979. Sedimentological analysis of the western terminus region of the Matanuska Glacier, Alaska. U.S. Army Corps of Engineers Cold Regions Research and Engineering Laboratory Report 79-9, 122p.
- LAWSON, D.E. 1981a. Sedimentological characteristics and classification of depositional processes and deposits in the glacial environment. U.S. Army Corps of Engineers Cold Regions Research and Engineering Laboratory Report 81-27, 22p.
- LAWSON, D.E. 1981b. Distinguishing characteristics of diamictons at the margin of the Matanuska Glacier, Alaska. *Annals of Glaciology*, 2, pp. 78-84.
- LAWSON, D.E. 1982. Mobilization, movement and deposition of active subaerial sediment flows, Matanuska Glacier, Alaska. *Journal of Geology*, 90, pp. 279-300.
- LOWE, D.R. 1979. Sediment gravity flows: their classification and some problems of application to natural flows and deposits. In *Geology of continental slopes*. Edited by L.J. Doyle and O.H. Pilkey. Society of Economic Paleontologists and Mineralogists, Special Publication 27, pp. 75-82.
- MARCUSSEN, I. 1973. Studies on flow till in Denmark. *Boreas*, 2, pp. 213-231.
- MARCUSSEN, I. 1975. Distinguishing between lodgement till and flow till in Weichselian deposits. *Boreas*, 4, pp. 113-123.
- MCDONALD, B.C., and BANERJEE, I. 1971. Sediments and bed forms on a braided outwash plain. *Canadian Journal of Earth Sciences*, 8, pp. 1282-1301.
- MCDONALD, B.C., and SHILTS, W.W. 1975. Interpretation of faults in glaciofluvial sediments. In *Glaciofluvial and Glaciolacustrine Sedimentation*. Edited by A.V. Jopling and B.C. McDonald. Society of Economic Paleontologists and Mineralogists, Special Publication 23, pp. 123-131.

- MENZIES, J. 1979. A review of the literature on the formation and location of drumlins. *Earth Science Reviews*, 14, pp. 315-359.
- MIALL, A.D. 1978. Lithofacies types and vertical profile models in braided river deposits: a summary. *In* *Fluvial Sedimentology*. Edited by A.D. Miall. Canadian Society of Petroleum Geologists, Memoir 5, pp. 597-604.
- MICKELSON, D.M. 1973. Nature and rate of basal till deposition in a stagnating ice mass, Burroughs Glacier, Alaska. *Arctic and Alpine Research*, 5, pp. 17-27.
- MIDDLETON, G.V., and HAMPTON, M.A. 1976. Subaqueous sediment transport and deposition by sediment gravity flows. *In* *Marine Sediment Transport and Environmental Management*. Edited by D.J. Stanley and D.J.P. Swift. John Wiley, N.Y., pp. 197-218.
- MIDDLETON, G.V. 1978. Facies. *In* *The Encyclopedia of Sedimentology*. Edited by R.W. Fairbridge and J. Bourgeois. Dowden, Hutchinson and Ross, Inc. Stroudsburg, Pa. 901 p.
- MILLS, H.H. 1977. Differentiation of glacial environments by sediment characteristics: Athabasca glacier, Alberta, Canada. *Journal of Sedimentary Petrology*, 47, pp. 728-737.
- MILLS, H.H. 1978. Some characteristics of glacial sediments on Mount Rainier, Washington. *Journal of Sedimentary Petrology*, 48, pp. 1345-1356.
- MORTON, D.M., and CAMPBELL, R.H. 1974. Spring mudflows at Wrightwood, southern California. *Quarterly Journal of Engineering Geology*, 7, pp. 377-384.
- MULLER, E.H. 1974. Origin of drumlins. *In* *Glacial Geomorphology*. Edited by D.R. Coates. SUNY, Binghamton, pp. 187-204.
- MULLER, E.H. 1983a. Dewatering during lodgement of till. *In* *Tills and Related Deposits*. Edited by pp. 13-18.
- MULLER, E.H. 1983b. Till genesis and the glacier sole. *In* *Tills and Related Deposits*. Edited by pp. 19-22.

- NARDINE, T.R., HEIN, F.J., GORSLINE, D.S., and EDWARDS, B.D. 1979. A review of mass movement processes, sediment and acoustic characteristics and contrasts in slope and base-of-slope systems versus canyon-fan-basin floor systems. In *Geology of Continental Slopes*. Edited by L.J. Doyle and O.H. Pilkey. Society of Economic Paleontologists and Mineralogists, Special Publication 27, pp. 61-73.
- ORE, H.T. 1964. Some criteria for recognition of braided stream deposits. *Wyoming University Contributions to Geology*, 3, pp. 1-14.
- PIERSON, T.C. 1980. Erosion and deposition by debris flows at Mt Thomas, New Zealand. *Earth Surface Processes*, 5, pp. 227-247.
- PIERSON, T.C. 1981. Dominant particle support mechanisms in debris flows at Mt Thomas, New Zealand, and implications for flow mobility. *Sedimentology*, 28, pp. 49-60.
- PRICE, R.J. 1969. Moraines, sandur, kames and eskers near Breidamerkurojokull, Iceland. *Institute of British Geographers Transactions*, 46, pp. 17-43.
- PRICE, R.J. 1971. The development and destruction of a sandur, Breidamerkurjokull, Iceland. *Arctic and Alpine Research*, 3, pp. 225-237.
- PRICE, R.J., and HOWARTH, P.J. 1970. The evolution of the drainage system (1904-1965) in front of Breidamerkurjokull, Iceland. Joekull (Joeklarannsoknafelag Islands, Arsrit), Reykjavik, 20, pp. 27-37.
- RAYMOND, C.F. 1971. Flow in a transverse section of Athabasca glacier, Alberta, Canada. *Journal of Glaciology*, 10, pp. 55-84.
- REHEIS, M.J. 1975. Source, transportation and deposition of debris on Arapaho Glacier, Front Range, Colorado, USA. *Journal of Glaciology*, 14, pp. 407-420.
- ROBIN, G. de Q., and MILLAR, D.H.M. 1982. Flow of ice sheets in the vicinity of subglacial peaks. *Annals of Glaciology*, 3, pp. 290-294.

- RODINE, J.D., and JOHNSON, A.M. 1976. The ability of debris, heavily freighted with coarse clastic materials, to flow on gentle slopes. *Sedimentology*, 23, pp. 213-234.
- ROSE, J. 1974. Small-scale spatial variability of some sedimentary properties of lodgement till and slumped till. *Geologists' Association (London), Proceedings, Colchester*, 85, pp. 239-258.
- RUST, B.R., and KOSTER, E.H. 1984. Coarse alluvial deposits. In *Facies Models*, 2nd edition. Edited by R.G. Walker. *Geoscience Canada*, pp. 53-69.
- RUTTER, N.W. 1965a. Surficial geology of the Banff area, Alberta. Ph.D. dissertation, University of Alberta, Edmonton, Alberta, 105p.
- RUTTER, N.W. 1965b. Foliation pattern of Gulkana glacier, Alaska range, Alaska. *Journal of Glaciology*, 5, pp. 711-718.
- RUTTER, N.W. 1972. Geomorphology and multiple glaciation in the area of Banff, Alberta. *Geological Survey of Canada, Bulletin* 206, 54p.
- RYDER, J.M. 1971. The stratigraphy and morphology of paraglacial alluvial fans in south-central B.C. *Canadian Journal of Earth Sciences*, 8, pp. 279-298.
- SHARP, R.P. 1949. Studies of superglacial debris on valley glaciers. *American Journal of Science*, 247, pp. 289-315.
- SHAW, J. 1972. Sedimentation in the ice-contact environment, with examples from Shopshire (England). *Sedimentology*, 18, pp. 23-62.
- SHAW, J. 1977. Till body morphology and structure related to glacier flow. *Boreas*, 6, pp. 189-201.
- SHAW, J. 1979. Genesis of the Sveg tills and Rogen moraines of central Sweden: a model of basal meltout. *Boreas*, 8, pp. 409-426.
- SHAW, J. 1982. Melt-out till in the Edmonton area, Alberta, Canada. *Canadian Journal of Earth Sciences*, 19, pp. 1548-1569.

- SHAW, J. 1983. Forms associated with boulders in melt-out till. In Till and Related Deposits. Edited by pp. 3-12.
- SHAW, J. 1985. Subglacial and ice marginal environments. In Glacial sedimentary environments. Edited by G.M. Ashley, J. Shaw, N.D. Smith. Society of Economic Paleontologists and Mineralogists, Short Course Notes 16, pp. 7-84.
- SMALL, R.J., and CLARK, M.J. 1974. The medial moraines of the lower Glacier de Tsidjiore Nouve, Valais, Switzerland. Journal of Glaciology, 13, pp. 255-263.
- SMALL, R.J., CLARK, M.J., and CAWSE, T.J.P. 1979. The formation of medial moraines on Alpine glaciers. Journal of Glaciology, 22, pp. 43-52.
- SMALL, R.J., and GOMEZ, B. 1981. The nature and origin of debris layers within Glacier de Tsidjiore Nouve, Valais, Switzerland. Annals of Glaciology, 2, pp. 109-113.
- SMITH, N.D. 1970. The braided stream depositional environment: comparison of the Platte River with some Silurian clastic rocks, north-central Appalachians. Geological Society of America Bulletin, 81, pp. 2993-3014.
- SMITH, N.D. 1974. Sedimentology and bar formation in the upper Kicking Horse River, a braided outwash stream. Journal of Geology, 82, pp. 205-223.
- SMITH, N.D. 1985. Proglacial fluvial environment. In Glacial Sedimentary Environments. Edited by G.M. Ashley, J. Shaw, and N.D. Smith. Society of Economic Paleontologists and Mineralogists, Short Course Notes 16, pp. 85-134.
- SNEED, E.D., and FOLK, R.L. 1958. Pebbles in the lower Colorado River, Texas, a study in particle morphogenesis. Journal of Geology, 66, pp. 114-150.
- STEEL, R.J., and THOMPSON, D.B. 1983. Structures and textures in Triassic braided stream conglomerates (Bunter pebble beds) in the Sherwood sandstone group, North Staffordshire, England. Sedimentology, 30, pp. 341-367.

SUGDEN, D.E., and JOHN, B.S. 1976. Glaciers and landscape. A geomorphological approach. Edward Arnold, publisher, 376p.

TWENHOFEL, W.H. 1945. The rounding of sand grains. Journal of Sedimentary Petrology, 15, pp. 59-71.

WEERTMAN, J. 1961. Mechanism for the formation of inner moraines found near the edge of cold ice caps and ice sheets. Journal of Glaciology, 3, pp. 965-978.

WIT, R. de. 1975. Geological highway map of Alberta. Geological highway map series, The Canadian Society of Petroleum Geologists, 1 sheet.

VII. APPENDICES

Appendix A. Sand-silt-clay percentages of diamicton samples.

Sample Sand Silt Clay
Number

1-1	33.0	39.5	27.5
1-2	33.0	39.5	27.5
1-3	41.5	34.5	24.0
1-4	51.5	33.0	15.5
1-5	38.5	37.5	24.0
1-6	36.5	41.0	22.5
1-7	30.5	45.0	24.5
1-8	35.5	39.5	25.0
1-9	48.0	33.5	18.5
1-10	37.5	36.5	26.0
1-11	39.5	39.0	21.5
1-12	48.5	34.0	17.5
1-13	47.5	34.5	18.0
1-14	44.5	40.5	15.0
1-15	36.5	42.0	21.5
1-16	44.5	35.5	20.0
1-17	38.0	40.5	21.5
1L-18	04.0	50.5	45.5
1L-19	00.5	54.0	45.5
1L-20	05.0	46.0	49.0
2-1	44.5	35.0	20.5
2-2	50.0	34.5	15.5
2-3	40.0	32.0	28.0
2-4	39.0	36.5	24.5
2-5	41.0	36.0	23.0
2-6	41.0	44.5	14.5
2-7	46.0	33.5	20.5
2-8	37.0	32.0	31.0
2-9	45.0	33.0	22.0
2-10	36.5	43.5	20.0
2-11	36.5	40.5	23.0
2-12	39.5	39.0	21.5
2-13	42.0	37.0	21.0
3-1	36.5	34.0	29.5
3-2	37.4	31.2	31.4
3-3	39.0	39.0	22.0
3-4	36.5	35.5	28.0
3-5	45.0	30.0	25.0
3-6	45.0	29.5	25.5
3-7	33.5	33.5	33.0
3-8	35.0	32.5	34.5
3-9	42.0	25.5	32.5
3-10	40.0	38.5	21.5
3-11	44.0	30.5	25.5

Sample Number	Sand	Silt	Clay
3-12	47.0	25.5	27.5
3-13	40.0	36.0	24.0
3-14	29.5	36.0	34.5
3-15	45.5	32.5	22.0
3-16	34.0	32.5	33.5
3-17	33.0	36.0	31.0
3-18	33.0	37.0	30.0
3-19	30.0	34.0	36.0
3-20	35.5	37.5	27.0
3-21	46.0	35.0	19.0
3-22	29.0	37.5	33.5
3-23	45.0	32.0	23.0
3-24	63.0	25.0	12.0
3-25	47.5	32.0	20.5
3-26	44.0	37.5	18.5
3-27	41.5	33.0	25.5
3-28	34.5	42.0	23.5
3-29	33.5	37.5	29.0
3-30	31.5	38.0	30.5
3-31	48.0	36.0	16.0
3-32	42.5	37.5	20.0
3-33	38.5	41.5	20.0
3-34	33.5	41.5	25.0
3-35	33.5	41.0	24.5
3-36	37.0	39.0	24.0
3-37	38.0	39.0	23.0
3-38	36.5	38.5	25.0
3-39	37.5	42.0	20.5
3-40	41.0	38.5	20.5
3-41	39.5	39.0	21.5
3-42	22.5	35.5	42.0
4-1	44.0	37.0	19.0
4-2	42.0	34.5	23.5
4-3	43.0	35.0	22.0
4-4	49.5	31.0	19.5
4-5	33.0	46.0	21.0
4-6	54.5	30.5	15.0
4-7	35.0	38.0	27.0
4-8	55.0	28.5	16.5
4-9	32.5	41.0	26.5
4-10	56.0	28.5	15.5
4-11	30.5	46.5	23.0
4-12	39.0	36.5	24.5
4-13	34.5	33.5	32.0
4-14	46.0	31.5	22.5
4-15	52.0	38.0	10.0
4-16	42.0	36.5	21.5
4-17	35.5	47.0	17.5
4-18	40.0	39.5	20.5
4-19	46.5	35.0	18.5

Sample Number	Sand	Silt	Clay
4-20	31.5	41.0	27.5
4-21	48.0	34.0	18.0
4-22	48.5	34.5	17.0
4-23	43.5	35.5	21.0
4-24	42.5	38.5	19.0
4-25	57.0	35.0	08.0
4-26	55.5	34.0	10.5
4-27	28.0	58.5	13.5
4-28	41.5	43.0	15.5
4-29	43.0	35.0	22.0
4-30	37.5	42.5	20.0
4-31	35.0	42.0	23.0
4-32	49.0	40.0	11.0
4-33	42.0	39.5	18.5
4-34	45.5	40.0	14.5
4-35	43.0	37.5	19.5
4-36	41.5	38.0	20.5
4-37	47.0	34.5	18.5
4-38	26.5	56.0	17.5
5D-1	20.0	51.5	28.5
5D-2	40.5	37.5	22.0
5D-3	18.0	48.5	33.5
5D-4	37.5	39.5	23.0
5D-5	27.5	43.5	29.0
5D-6	49.0	28.0	23.0
5D-7	56.0	36.5	07.5
5D-8	48.0	38.0	14.0
5D-9	36.5	40.5	23.0
5D-10	46.0	38.0	16.0
5D-11	46.5	37.5	16.0
5D-12	36.5	48.5	15.0
5D-16	15.5	62.5	22.0
5D-13	33.5	36.0	30.5
5D-14	37.5	41.5	21.0
5D-15	40.0	42.5	17.5
7-2	00.0	52.5	47.5
7-3	94.0	06.0	00.0
7-6	14.0	36.0	50.0
7-7	34.0	35.5	30.5

Appendix B. Grain size phi values at various cumulative percentages.

Numbers below 5 to 95 are phi values
5 to 95 are cumulative percentiles

Sample#	5	10	16	25	30	50	70	75	84	90	95
1-1	-14	16	1.00	2.55	3.64	5.72	7.73	8.38	10.97	12.02	12.02
1-2	-23	56	1.37	2.69	3.40	5.39	7.70	8.38	9.97	10.97	12.02
1-3	-10	56	1.22	2.10	2.59	4.70	7.14	7.86	9.83	10.97	12.02
1-4	-12	69	1.29	1.94	2.29	3.68	5.76	6.42	7.89	9.04	10.29
1-5	-58	15	1.09	2.43	3.15	4.72	7.16	7.86	9.37	10.97	12.02
1-6	-46	36	1.22	2.59	3.20	4.98	7.04	7.65	9.19	10.97	12.02
1-7	-10	1.12	2.06	3.28	3.76	5.55	7.29	7.91	9.48	10.97	12.02
1-8	-63	12	1.02	2.46	3.10	5.01	7.32	8.02	9.70	10.97	12.02
1-9	-28	34	1.97	1.78	2.20	3.97	6.24	6.91	8.84	10.29	12.02
1-10	-72	1.01	2.35	3.04	4.96	7.67	8.16	9.85	10.97	12.02	
1-11	-58	1.22	2.42	3.02	4.78	6.78	7.42	9.23	10.97	12.02	
1-12	-26	1.98	1.69	2.08	3.88	6.15	6.81	8.29	10.97	12.02	
1-13	-21	51	1.13	1.89	2.29	4.04	6.28	6.91	8.48	10.97	12.02
1-14	-55	18	1.88	1.83	2.32	4.49	6.36	6.89	7.88	9.48	12.02
1-15	03	94	1.76	2.86	3.28	4.88	6.97	7.53	8.97	10.29	12.02
1-16	-36	25	1.94	1.84	2.38	4.10	6.63	7.25	8.76	10.97	12.02
1-17	-58	29	1.26	2.68	3.18	4.86	6.55	7.51	9.03	10.97	12.02
1L-18	4.21	4.97	5.43	6.06	6.38	7.69	9.46	9.97	10.97	12.02	12.02
1L-19	4.59	4.98	5.39	5.99	6.30	7.64	9.48	10.29	10.97	12.02	12.02
1L-20	4.04	4.60	5.14	5.88	6.31	7.90	9.48	9.94	10.97	12.02	12.02
2-1	46	1.27	1.89	2.64	3.00	4.32	5.21	7.00	9.00	10.97	12.02
2-2	52	1.24	1.83	2.47	2.79	3.98	5.61	6.27	7.83	9.59	12.02
2-3	45	1.35	1.93	2.64	3.05	4.92	7.73	8.52	9.97	10.97	12.02
2-4	1.00	1.76	2.29	2.94	3.28	4.78	6.86	7.83	9.59	10.97	12.02

Sample#	5	10	16	25	30	50	70	75	84	90	95
2-5	47	1.34	1.94	2.62	3.00	4.52	6.60	7.64	9.48	10.97	12.02
2-6	84	1.67	2.27	2.94	3.32	4.35	5.44	5.90	7.53	10.97	12.02
2-7	64	1.38	1.89	2.49	2.82	4.04	6.18	7.00	10.97	10.97	12.02
2-8	29	1.18	1.79	2.95	3.41	5.38	8.16	8.90	10.97	12.02	12.02
2-9	22	1.14	1.79	2.47	2.81	4.44	6.47	7.31	9.42	10.97	12.02
2-10	1.06	1.92	2.56	3.21	3.51	4.57	6.59	7.22	8.59	9.66	12.02
2-11	75	1.76	2.40	3.18	3.49	4.65	6.86	7.67	8.97	9.80	12.02
2-12	61	1.36	2.18	2.92	3.21	4.32	6.96	7.59	8.83	10.97	12.02
2-13	49	1.41	2.05	2.77	3.12	4.30	6.73	7.48	8.62	9.85	8.70
3-1	74	1.54	2.13	2.91	3.40	5.29	7.83	8.84	9.83	10.97	12.02
3-2	75	1.63	2.18	2.87	3.29	5.47	8.22	8.97	10.29	10.97	12.02
3-3	58	1.47	2.13	2.89	3.25	4.49	6.35	7.10	9.42	10.97	12.02
3-4	43	1.38	2.06	2.84	3.28	5.08	7.67	8.59	10.97	12.02	12.02
3-5	58	1.35	1.89	2.51	2.87	4.11	6.72	7.97	10.97	12.02	12.02
3-6	34	1.19	1.72	2.36	2.74	4.32	7.02	8.10	9.97	10.97	12.02
3-7	69	1.56	2.32	3.12	3.59	5.68	8.38	8.83	9.63	10.97	12.02
3-8	86	1.79	2.51	3.28	3.68	5.32	8.59	9.08	9.97	10.97	12.02
3-9	58	1.39	2.00	2.74	3.08	4.61	8.33	8.59	9.97	10.97	12.02
3-10	34	1.27	2.00	2.80	3.20	4.56	6.14	7.06	8.86	9.12	10.97
3-11	51	1.38	1.93	2.56	2.92	4.54	7.08	8.10	9.52	10.97	12.02
3-12	40	1.16	1.66	2.20	2.51	4.21	7.51	8.38	9.48	9.97	10.97
3-13	32	1.24	1.99	2.79	3.18	4.94	7.08	7.86	9.61	10.97	12.02
3-14	20	1.35	2.40	3.51	3.97	5.89	8.68	9.55	10.97	12.02	12.02
3-15	17	1.08	1.74	2.46	2.82	4.11	6.38	7.31	9.07	10.97	12.02
3-16	08	1.98	1.84	2.88	3.51	5.64	8.43	9.04	10.97	12.02	12.02
3-17	49	1.42	2.18	3.18	3.64	5.38	8.20	8.91	9.97	10.97	12.02
3-18	62	1.51	2.25	3.18	3.70	5.59	7.97	8.71	10.97	12.02	12.02
3-19	79	1.64	2.45	3.41	3.92	5.98	8.73	9.32	10.97	12.02	12.02
3-20	32	1.38	2.20	3.07	3.52	5.29	7.59	8.27	9.73	10.97	12.02

Sample#	5	10	16	25	30	50	70	75	84	90	95
3-21	23	1.04	1.75	2.54	2.92	4.21	6.05	6.83	8.64	9.97	12.02
3-22	86	1.86	2.65	3.61	4.08	6.01	8.45	9.08	10.97	12.02	12.02
3-23	39	1.23	1.89	2.62	2.98	4.04	6.84	7.69	8.98	10.97	12.02
3-24	36	1.09	1.58	2.08	2.28	3.08	3.94	4.49	6.91	8.41	9.51
3-25	36	1.17	1.74	2.36	2.68	3.86	6.28	7.14	8.97	10.29	12.02
3-26	48	1.32	1.98	2.72	3.08	4.24	6.11	6.90	8.38	9.82	12.02
3-27	65	1.43	1.99	2.62	2.97	4.38	7.28	8.10	9.69	10.97	12.02
3-28	80	1.80	2.50	3.21	3.51	4.88	7.20	7.81	9.16	10.97	12.02
3-29	18	1.32	2.27	3.18	3.47	5.20	7.20	8.46	9.38	13.29	12.02
3-30	15	1.32	2.40	3.47	3.84	5.47	8.04	8.57	9.48	10.97	12.02
3-31	18	1.12	1.83	2.61	2.98	4.06	5.75	6.47	8.00	9.09	10.97
3-32	09	.91	1.62	2.52	3.00	4.32	6.66	7.33	8.62	9.79	12.02
3-33	45	1.30	1.99	2.85	3.23	4.50	6.63	7.36	8.62	10.12	12.02
3-34	77	1.69	2.44	3.22	3.50	5.11	7.30	7.97	9.29	10.97	12.02
3-35	47	1.49	2.26	3.10	3.51	4.92	7.33	7.92	9.38	10.97	12.02
3-36	25	1.34	2.18	3.00	3.45	4.79	7.31	7.92	9.25	10.97	12.02
3-37	43	1.32	1.99	2.81	3.18	4.80	8.48	8.48	9.24	10.97	12.02
3-38	42	1.45	2.24	3.10	3.46	4.90	3.93	7.37	10.97	12.02	
3-39	60	1.59	2.35	3.18	5.70	4.44	6.84	7.60	9.84	12.02	
3-40	39	1.10	1.84	2.82	3.18	4.37	6.84	7.54	9.46	10.97	
3-41	57	1.45	2.12	2.86	3.21	4.58	6.84	7.73	9.75	10.97	
3-42	1.40	2.41	3.20	4.27	4.84	7.08	9.24	10.97	12.02	12.02	
4-1	21	.54	1.21	2.13	2.63	4.29	6.53	7.45	8.59	10.29	12.02
4-2	09	.97	1.71	2.48	2.87	4.71	6.93	7.72	9.97	10.97	12.02
4-3	89	1.74	2.64	3.06	4.36	6.53	7.38	9.29	10.97	12.02	
4-4	64	1.33	2.08	2.45	3.92	5.98	6.86	8.97	10.97	12.02	
4-5	86	1.94	2.71	3.44	3.72	4.88	6.63	7.31	9.59	10.97	12.02
4-6	38	1.17	1.74	2.32	2.56	3.56	5.21	5.72	7.80	9.52	12.02
4-7	93	1.71	2.36	3.17	3.49	5.11	7.45	8.27	9.97	10.97	12.02

Sample#	5	10	16	25	30	50	70	75	84	90	95
4-8	22	.97	1.33	2.13	2.40	3.58	5.27	5.84	8.16	9.59	12.02
4-9	67	1.69	2.26	3.18	3.64	5.21	7.43	8.24	9.90	10.97	12.02
4-10	1.30	1.79	2.18	2.56	2.76	3.59	5.11	5.79	7.76	9.75	12.02
4-11	85	1.89	2.74	3.59	3.92	5.11	6.84	7.64	9.48	10.97	12.02
4-12	1.07	1.89	2.47	3.07	3.38	4.72	7.04	7.93	9.38	10.97	12.02
4-13	58	1.47	2.15	2.06	3.41	5.47	8.24	8.97	10.97	12.02	12.02
4-14	36	1.22	1.79	2.37	2.68	4.24	6.64	7.56	9.12	10.97	12.02
4-15	11	.81	1.55	2.32	2.65	3.72	5.27	5.82	6.97	7.97	9.30
4-16	60	1.43	2.06	2.77	3.16	4.29	6.51	7.48	8.78	9.92	12.02
4-17	73	1.74	2.52	3.25	3.56	4.64	6.51	7.04	8.12	9.46	12.02
4-18	53	1.47	2.15	2.89	3.27	4.37	6.51	7.30	8.64	9.78	12.02
4-19	58	.31	1.09	2.05	2.56	4.11	6.47	7.18	8.34	9.68	10.97
4-20	85	1.79	2.54	3.32	3.54	5.32	7.66	8.32	9.62	10.97	12.02
4-21	37	1.21	1.86	2.51	2.83	3.98	6.07	6.88	8.29	9.52	12.02
4-22	63	1.38	1.89	2.47	2.76	3.84	5.73	6.51	8.17	9.38	12.02
4-23	56	1.83	2.01	2.72	3.07	4.21	6.51	7.43	8.94	10.97	12.02
4-24	71	1.62	2.21	2.80	3.08	4.32	6.20	6.95	8.53	9.49	10.29
4-25	80	1.51	2.00	2.51	2.74	3.47	4.36	4.82	5.96	7.44	8.80
4-26	77	1.41	1.88	2.40	2.67	5.71	4.38	5.00	6.67	8.07	9.30
4-27	1.78	2.74	3.43	3.87	4.06	4.52	5.63	6.14	7.56	8.65	9.58
4-28	83	1.69	2.33	3.05	3.35	4.72	5.97	6.62	7.90	9.05	10.97
4-29	57	1.47	2.13	2.85	3.13	4.21	6.51	7.55	8.95	13.29	10.97
4-30	14	1.10	1.99	3.04	3.41	4.54	6.76	7.38	8.54	9.58	10.97
4-31	36	1.31	2.11	3.06	3.44	4.94	7.27	7.78	8.97	9.95	10.97
4-32	89	1.73	2.26	2.82	3.05	3.88	5.04	5.58	6.97	8.28	9.88
4-33	15	.94	1.69	2.64	3.16	4.45	6.36	7.03	8.38	9.18	9.97
4-34	1.36	2.25	2.73	3.18	3.35	3.88	4.91	5.45	7.60	8.90	9.97
4-35	03	.94	1.70	2.60	3.04	4.36	6.55	7.27	8.45	9.42	10.97
4-36	09	.98	1.74	2.64	3.10	4.43	6.75	7.41	8.71	9.79	10.97
4-37	43	1.43	2.13	2.84	3.13	4.04	5.97	6.81	8.59	9.83	12.02

Sample	5	10	16	25	30	50	70	75	84	90	95
4-38	1.69	2.85	3.38	3.81	4.01	4.88	6.28	6.91	8.18	9.39	10.97
5D-1	2.17	2.97	3.46	4.10	4.44	5.88	7.83	8.52	9.97	10.97	12.02
5D-2	2.29	1.20	1.94	2.82	3.24	4.57	6.28	7.27	9.20	10.97	12.02
5D-3	2.40	3.21	3.72	4.39	4.79	6.37	8.45	9.25	10.97	12.02	12.02
5D-4	2.17	2.63	3.02	3.47	3.68	4.43	6.36	7.51	9.21	10.97	12.02
5D-5	1.40	2.38	3.06	3.78	4.06	5.41	7.88	8.54	9.66	10.97	12.02
5D-6	.66	1.32	1.86	2.47	2.75	3.92	6.48	7.56	9.32	10.97	12.02
5D-7	-.46	.15	.79	1.59	2.00	3.56	5.10	5.71	6.66	7.48	9.12
5D-8	-.12	.69	1.43	2.36	2.82	4.01	5.55	6.17	7.60	8.76	9.97
5D-9	-.14	.81	1.67	2.71	3.21	4.88	7.14	7.78	9.04	10.29	12.02
5D-10	.20	1.06	1.76	2.51	2.88	4.04	5.95	6.57	7.98	9.16	10.97
5D-11	-.03	1.00	1.87	2.81	3.15	4.06	5.49	6.25	8.04	9.20	10.97
5D-12	-.08	1.08	2.00	2.98	3.32	4.56	6.22	6.80	7.88	8.86	12.02
5D-13	-.32	.29	.97	2.18	3.20	5.73	8.04	8.54	9.47	10.29	12.02
5D-14	-.26	.56	1.40	2.63	3.21	4.79	6.86	7.47	8.78	9.97	12.02
5D-15	.53	1.56	2.31	3.04	3.27	4.31	6.20	6.86	8.34	9.92	12.02
5D-16	2.94	3.56	4.05	4.57	4.85	5.94	7.29	7.70	8.78	9.64	12.02

7-2	4.64	5.11	5.59	6.20	6.51	7.79	9.97	10.97	12.02	12.02	12.02
7-3	1.37	1.56	1.71	1.89	1.96	2.28	2.64	2.76	3.01	3.18	3.47
7-7	.47	1.49	2.20	3.11	3.63	5.51	8.04	8.93	10.97	12.02	12.02

N	5	10	16	25	30	50	70	75	84	90	95
5G-1	-3.72	-3.42	-3.13	-2.7	-2.46	-1.15	1.04	1.39	1.88	2.21	2.61
5G-2	-4.6	-4.41	-4.2	-3.42	-2.75	0.38	1.58	1.78	2.14	2.41	2.72
5G-3	-4.61	-4.5	-4.37	-4.16	-4.03	-3.65	-3.11	-2.91	-2.32	-1.63	-0.49
5G-4	-4.58	-4.42	-4.27	-4.0	-3.8	-2.81	-1.64	-1.18	-0.21	0.6	1.51
5G-5	-4.56	-4.43	-4.31	-4.15	-4.05	-3.42	-2.51	-2.18	-1.47	-0.87	-0.11
5G-6	-4.48	-4.31	-4.13	-3.84	-3.66	-2.89	-1.8	-1.45	-0.62	0.09	0.99
5G-7	-4.64	-4.52	-4.4	-4.2	-4.08	-3.48	-2.75	-2.5	-1.88	-0.97	1.08
5G-8	-4.62	-4.49	-4.32	-4.08	-3.91	-3.25	-2.43	-2.14	-1.19	-0.12	1.0
5G-9	-3.38	-3.17	-2.9	-2.47	-2.26	-1.36	0.09	0.5	1.51	2.04	2.55
5G-10	-4.4	-4.21	-4.0	-3.67	-3.51	-2.98	-2.32	-2.1	-0.3	0.74	1.49
5G-11	-4.68	-4.6	-4.51	-4.36	-4.3	-3.79	-2.61	-2.15	-0.7	0.12	0.97
5G-12	-4.68	-4.58	-4.48	-4.33	-4.24	-3.79	-3.0	-2.65	-0.98	1.28	1.99
5G-13	-4.32	-4.23	-4.13	-3.97	-3.89	-3.49	-2.72	-2.37	-1.0	0.6	1.89
5G-14	-4.31	-4.08	-3.72	-3.29	-3.08	-2.2	-1.2	-0.94	-0.43	-0.1	0.61
5G-15	-4.4	-4.22	-4.05	-2.55	-0.35	1.25	1.73	1.9	2.28	2.63	3.11
5G-16	1.30	1.59	1.77	1.97	2.08	2.49	2.97	3.09	3.32	3.46	3.55
5G-17	-0.61	0.06	0.5	0.95	1.12	1.75	2.28	2.42	2.7	2.98	3.30
5G-18	1.81	2.06	2.22	2.42	2.51	2.83	3.19	3.28	3.49	3.62	3.73
5G-19	0.84	1.2	1.46	1.73	1.84	2.25	2.61	2.7	2.88	3.02	3.21
5G-20	1.59	1.72	1.88	2.06	2.12	2.38	2.62	2.71	2.9	3.1	3.4
5G-21	-4.18	-4.09	-3.97	-3.8	-3.7	-3.16	-1.7	-0.95	0.39	1.1	1.77
5G-22	-4.58	-4.45	-4.31	-4.1	-3.96	-3.02	-1.79	-1.35	-0.29	0.7	1.86
5G-23	-4.2	-4.0	-3.8	-3.54	-3.4	-2.75	-1.59	-0.93	0.75	1.39	1.85
5G-24	-0.59	-0.2	-0.1	0.45	0.6	1.17	1.76	1.95	2.32	2.68	3.03
5G-25	-4.66	-4.55	-4.42	-4.25	-4.12	-3.32	-2.29	-1.91	-0.86	0.53	1.91
5G-27	-4.73	-4.63	-4.54	-4.39	-4.31	-3.81	-2.72	-2.26	-0.61	1.27	2.87
6G-1	-4.08	-3.95	-3.82	-3.65	-3.56	-3.1	-2.32	-2.0	-1.2	-0.43	0.51

<u>N</u>	<u>5</u>	<u>10</u>	<u>16</u>	<u>25</u>	<u>30</u>	<u>50</u>	<u>70</u>	<u>75</u>	<u>84</u>	<u>90</u>	<u>95</u>
6G-2	-4.12	-3.93	-3.47	-2.78	-2.3	-0.91	-0.07	0.13	0.56	0.98	1.5
6G-3	-4.11	-3.93	-3.74	-3.5	-3.34	2.63	-0.95	-0.47	0.43	1.11	2.0
6G-4	-4.41	-4.28	-4.09	-3.76	-3.6	-2.86	-1.21	-0.16	1.11	1.72	2.28
6G-5	-4.8	-4.48	-4.12	-3.55	-3.27	-2.05	-0.08	0.55	1.2	1.63	2.45
6G-6	-4.97	-3.82	-3.58	-3.46	-3.31	-2.69	-1.55	-1.13	-0.12	0.85	1.94
6G-7	-4.64	-4.49	-4.51	-4.04	-3.85	-2.99	-1.77	-1.4	-0.56	0.21	1.09
6G-8	-4.64	-4.31	-4.03	-3.82	-3.38	-1.86	0.5	0.92	1.5	1.91	2.35
6G-9	-4.44	-3.92	-3.42	-2.25	-1.39	0.68	1.68	1.9	2.32	2.65	3.0
6G-10	-4.9	-4.72	-4.52	-4.25	-4.08	-3.15	-2.15	-1.84	-1.15	-0.41	0.67
6G-11	-4.8	-4.61	-4.44	-4.22	-4.08	-3.42	-2.59	-2.28	-1.49	-0.16	1.79
6G-12	-1.72	-1.14	-0.66	-0.1	0.15	1.0	1.71	1.9	2.29	2.61	3.01
6G-13	-4.34	-4.11	-3.91	-3.62	-3.46	-2.56	-0.7	-0.2	0.97	1.58	2.19
6G-14	-4.9	-4.81	-4.68	-4.48	-4.38	-3.95	-3.29	-3.04	-2.45	-1.63	1.09
6G-15	-4.69	-4.62	-4.56	-4.48	-4.43	-4.26	-3.93	-3.72	-3.28	-2.28	2.11
6G-16	-4.61	-4.46	-4.3	-4.08	-3.9	-3.14	-2.1	-1.75	-0.96	-0.18	0.9
6G-17	-4.5	-4.34	-4.18	-3.94	-3.78	-2.96	-1.61	-1.12	-0.1	0.74	1.71
6G-20	-4.41	-4.21	-4.0	-3.6	-3.4	-2.58	-1.46	-1.06	-0.2	0.6	1.68
6G-23	-4.46	-4.32	-4.19	-3.97	-3.85	-3.29	-2.21	-1.66	0.21	1.13	1.68
6G-24	-4.19	-3.81	-3.51	-3.14	-2.9	-2.34	-1.61	-1.38	-0.87	-0.39	0.29
6G-25	-4.51	-4.32	-4.11	-3.74	-3.5	-2.82	-1.95	-1.7	-1.11	-0.61	0.06
6G-26	-4.2	-4.0	-3.83	-3.5	-3.51	-2.95	-1.81	-1.37	-0.33	0.57	1.44
6G-27	-4.6	-4.43	-4.25	-4.0	-3.79	-3.06	-1.95	-1.5	-0.22	1.2	2.32
6G-28	-4.6	-4.49	-4.37	-4.06	-3.89	-2.89	-0.21	0.37	1.17	1.62	2.08
6G-29	-4.58	-4.43	-4.31	-4.11	-3.96	-2.79	-0.32	0.24	0.93	1.39	1.89
6G-30	-4.29	-4.1	-3.92	-3.69	-3.55	-2.72	0.37	0.98	1.52	1.85	2.25
6G-31	-4.8	-4.73	-4.68	-4.61	-4.55	-4.34	-3.96	-3.77	-3.21	-0.72	2.09
6GS-33	0.90	1.18	1.34	1.51	1.58	1.81	2.08	2.18	2.41	2.68	3.03
7G-4	-4.9	-4.61	-4.36	-4.02	-3.82	-2.99	-1.74	-1.25	0.45	1.47	2.25
7G-5	-4.9	-4.66	-4.46	-4.18	-4.04	-3.41	-2.67	-2.42	-1.8	-1.05	0.2

Appendix C.
Graphic statistical results in phi units

Sample#	SDI	KG	MZ
1-1	.04	.85	5.90
1-2	.07	.88	5.58
1-3	.24	.86	5.25
1-4	.27	.95	4.29
1-5	.14	.95	5.06
1-6	.08	1.01	5.13
1-7	.05	1.06	5.70
1-8	.09	.93	5.24
1-9	.27	.98	4.59
1-10	.11	.90	5.27
1-11	.13	1.03	5.08
1-12	.21	.98	4.38
1-13	.26	1.00	4.55
1-14	.16	1.02	4.31
1-15	.16	1.05	5.20
1-16	.24	.94	4.60
1-17	.10	1.07	5.05
1-18	.15	.82	8.03
1-19	.25	.71	8.00
1-20	.04	.81	8.00
2-1	.32	1.09	5.07
2-2	.34	1.24	4.55
2-3	.24	.81	5.61
2-4	.32	.92	5.55
2-5	.31	.94	5.31
2-6	.29	1.55	4.72
2-7	.46	1.03	5.63
2-8	.18	.81	6.05
2-9	.30	1.00	5.22
2-10	.35	1.12	5.24
2-11	.31	1.03	5.34
2-12	.35	1.00	5.11
2-13	.19	.71	4.99
3-1	.19	.81	5.75
3-2	.18	.76	5.98
3-3	.33	1.11	5.35
3-4	.26	.83	6.04

Sample #	SK	SDI	KG	MZ
3-5	.45	4.00	.86	5.66
3-6	.34	3.83	.83	5.34
3-7	.10	3.54	.81	5.88
3-8	.22	3.56	.79	5.93
3-9	.32	3.73	.80	5.53
3-10	.23	3.33	1.02	5.14
3-11	.31	3.64	.85	5.33
3-12	.31	3.56	.70	5.12
3-13	.22	3.68	.95	5.51
3-14	.11	3.93	.80	6.42
3-15	.34	3.63	1.00	4.97
3-16	.11	4.12	.81	6.15
3-17	.17	3.69	.82	5.84
3-18	.18	3.91	.84	6.27
3-19	.12	3.83	.78	6.47
3-20	.16	3.66	.92	5.74
3-21	.31	3.51	1.13	4.87
3-22	.13	3.77	.84	6.54
3-23	.38	3.53	.94	4.97
3-24	.42	2.72	1.56	3.86
3-25	.41	3.57	1.00	4.86
3-26	.32	3.35	1.13	4.87
3-27	.36	3.65	.85	5.35
3-28	.28	3.37	1.00	5.51
3-29	.16	3.57	.92	5.62
3-30	.12	3.57	.95	5.78
3-31	.28	3.18	1.15	4.63
3-32	.26	3.56	1.02	4.85
3-33	.27	3.41	1.05	5.04
3-24	.22	3.42	.97	5.61
3-25	.24	3.53	1.00	5.52
3-36	.25	3.55	1.01	5.41
3-37	.24	3.57	.97	5.34
3-38	.24	3.54	.98	5.50
3-39	.33	3.29	1.09	5.13
3-40	.25	3.28	.94	4.92
3-41	.24	3.23	.91	5.14
3-42	.03	3.55	.78	7.08
4-1	.21	3.70	1.00	4.70
4-2	.24	3.89	.94	5.46
4-3	.28	3.73	1.05	5.13
4-4	.32	3.76	1.05	4.74
4-5	.32	3.41	1.18	5.73

Sample#	SKI	SDI	KG	MZ
4-6	.43	3.30	1.40	4.40
4-7	.26	3.58	.89	5.81
4-8	.39	3.50	1.29	4.36
4-9	.21	3.63	.92	5.79
4-10	.53	3.02	1.36	4.51
4-11	.27	3.38	1.13	5.78
4-12	.34	3.39	.92	5.52
4-13	.20	3.94	.79	6.20
4-14	.33	3.60	.92	5.05
4-15	.19	2.78	1.10	4.08
4-16	.35	3.41	.09	5.04
4-17	.28	3.11	1.22	5.09
4-18	.32	3.36	1.07	5.05
4-19	.18	3.56	.92	4.51
4-20	.21	3.46	.92	5.83
4-21	.36	3.37	1.09	4.71
4-22	.41	3.30	1.16	4.63
4-23	.36	3.47	1.00	5.05
4-24	.29	3.03	.95	5.02
4-25	.30	2.20	1.42	3.81
4-26	.38	2.49	1.34	4.75
4-27	.38	2.21	1.41	5.17
4-28	.19	2.93	1.16	4.98
4-29	.35	3.28	.91	5.10
4-30	.20	3.28	1.02	5.02
4-31	.16	3.32	.92	5.34
4-32	.32	2.54	1.33	4.37
4-33	.15	3.16	.92	4.84
4-34	.47	2.52	1.55	4.74
4-35	.21	3.35	.96	4.84
4-36	.22	3.39	.93	4.96
4-37	.39	3.37	1.20	4.92
4-38	.34	2.61	1.23	5.48
5D-1	.25	3.12	.91	6.44
5D-2	.27	3.59	1.08	5.24
5D-3	.22	3.27	.81	7.02
5D-4	.14	3.04	1.00	5.55
5D-5	.17	3.26	.91	6.04
5D-6	.14	3.59	.91	5.03
5D-7	.11	2.92	.95	3.67
5D-8	.17	3.07	1.09	4.35
5D-9	.15	3.68	.98	5.20
5D-10	.28	3.19	1.09	4.59

Sample#	SKI	SDI	KG	MZ
5D-11	.27	3.21	1.31	4.66
5D-12	.18	3.30	1.30	4.81
5D-13	.05	3.99	.80	5.39
5D-14	.13	3.71	1.04	4.99
5D-15	.34	3.25	1.23	4.99
5D-16	.27	2.56	1.19	6.26
7-2	.23	2.73	.63	8.47
7-3	.13	.64	.99	2.33
7-7	.19	3.94	.81	6.23

Sample#	SMI	SDI (phi)	KG	MZ (phi)
5G-1	.20	2.21	.63	-2.80
5G-2	.40	2.69	.58	-2.56
5G-3	.42	1.14	1.35	-3.45
5G-4	.35	1.94	.89	-2.43
5G-5	.43	1.38	.93	-3.07
5G-6	.36	1.71	.94	-2.55
5G-7	.43	1.50	1.38	-3.25
5G-8	.41	1.63	1.19	-2.92
5G-9	.31	2.00	.82	-2.92
5G-10	.48	1.82	1.54	-2.43
5G-11	.65	1.79	1.05	-3.03
5G-12	.67	1.89	1.63	-3.08
5G-13	.66	1.72	1.59	-2.87
5G-14	.11	1.57	.86	-2.12
5GS-15	.59	2.72	.69	-2.17
5GS-16	.01	.73	.82	2.53
5GS-17	.17	.14	1.09	1.65
5GS-18	.01	.61	.90	2.85
5GS-19	.15	.71	1.00	2.20
5GS-20	.07	.53	1.14	2.39
5G-21	.64	1.99	.86	-2.25
5G-22	.44	1.98	.96	-2.54
5G-23	.53	2.05	.95	-1.93
5G-24	.03	1.10	.99	-1.20
5G-25	.49	1.89	1.15	-2.87
5G-27	.69	2.13	1.46	-2.99
6G-1	.51	1.35	1.14	-2.71
6G-2	.21	1.86	.79	-1.27
6G-3	.49	1.97	.83	-1.98
6G-4	.53	2.31	.76	-1.95
6G-5	.22	2.38	.69	-1.66
6G-6	.51	1.79	1.04	-2.16
6G-7	.36	1.81	.88	-2.62
6G-8	.21	2.44	.63	-1.46
6G-9	.40	2.58	.73	-2.44
6G-10	.28	1.69	.95	-2.94
6G-11	.44	1.74	1.39	-3.12
6G-12	.14	1.45	.97	-2.88
6G-13	.45	2.21	.78	-1.83
6G-14	.51	1.47	1.70	-3.69
6G-15	.60	.71	1.39	-4.03

Sample#	SKI	SDI (phi)	KG	MZ (phi)
6G-16	.39	1.67	.97	-2.80
6G-17	.45	1.96	.90	-2.41
6G-20	.33	1.87	.98	-2.26
6G-23	.60	2.03	1.09	-2.42
6G-24	.14	1.34	1.04	-2.24
6G-25	.20	1.44	.92	-2.68
6G-26	.53	1.73	1.02	-2.37
6G-27	.48	2.06	1.15	-2.51
6G-28	.48	2.40	.60	-2.03
6G-29	.43	2.29	.61	-2.06
6G-30	.54	2.35	.57	-1.71
6G-31	.70	1.41	3.36	-4.08
6GS-33	.13	.59	1.30	1.85
7G-4	.45	2.29	1.06	-2.30
7G-5	.31	1.44	1.19	-3.22

Appendix D. Roundness values of each sample per facies.

Facies Sample# Roundness Std. Dev.

1	1-1	0.373	0.083
	1-3	0.352	0.091
	1-4	0.384	0.098
	1-5	0.378	0.068
	1-6	0.382	0.066
	1-7	0.360	0.083
	1-8	0.390	0.079
	1-9	0.398	0.100
	1-10	0.372	0.076
	1-11	0.390	0.076
	1-13	0.372	0.090
	1-14	0.358	0.067
	1-15	0.362	0.088
	1-16	0.382	0.092
	1-17	0.360	0.081

2	2-4	0.370	0.104
	2-5	0.358	0.107
	2-6	0.338	0.097
	2-7	0.358	0.121
	2-8	0.360	0.103
	2-9	0.368	0.104
	2-10	0.364	0.090
	2-11	0.384	0.096
	2-12	0.356	0.086
	2-13	0.362	0.119

3thin	3-5	0.324	0.102
	3-6	0.368	0.117
	3-10	0.384	0.091
	3-11	0.378	0.104
	3-12	0.368	0.110
	3-14	0.416	0.102
	3-15	0.378	0.095
	3-21	0.380	0.105
	3-26	0.370	0.091
	3-29	0.402	0.110
	3-30	0.370	0.091
	3-32	0.404	0.245

3thick	3-7	0.360	0.105
	3-8	0.346	0.093
	3-9	0.392	0.112

Factes Sample# Roundness Std. Dev.

3thick 3-22 0.346 0.095
3-24 0.382 0.096
3-27 0.392 0.105
3-28 0.350 0.102
3-33 0.358 0.086
3-34 0.374 0.063
3-35 0.338 0.081
3-36 0.354 0.086
3-37 0.360 0.093
3-38 0.358 0.099
3-39 0.366 0.110
3-40 0.380 0.099
3-41 0.396 0.095
3-42 0.332 0.084

4thin 4-1 0.366 0.092
4-2 0.368 0.100
4-3 0.340 0.103
4-4 0.336 0.110
4-5 0.362 0.097
4-6 0.342 0.095
4-8 0.356 0.088
4-15 0.384 0.082
4-16 0.366 0.092
4-17 0.392 0.094
4-30 0.382 0.087
4-33 0.360 0.101
4-34 0.368 0.102
4-35 0.380 0.076
4-36 0.376 0.112
4-37 0.348 0.095
4-38 0.370 0.105

4thick 4-12 0.378 0.115
4-13 0.352 0.086
4-14 0.360 0.103
4-18 0.396 0.103
4-19 0.384 0.082
4-20 0.364 0.085
4-21 0.352 0.095
4-22 0.318 0.116
4-23 0.356 0.113
4-24 0.346 0.111
4-25 0.382 0.098
4-26 0.396 0.105
4-28 0.394 0.074
4-29 0.400 0.111

Facies Sample# Roundness Std. Dev.

5 dia. 5D-1 0.358 0.111
 5D-2 0.360 0.097
 5D-3 0.370 0.104
 5D-4 0.352 0.089
 5D-5 0.358 0.095
 5D-6 0.360 0.099
 5D-7 0.394 0.087
 5D-8 0.384 0.095
 5D-9 0.390 0.093
 5D-11 0.363 0.099
 5D-12 0.350 0.104
 5D-13 0.386 0.111
 5D-14 0.356 0.088
 5D-15 0.354 0.073

5 gvl 5G-1 0.384 0.108
 5G-5 0.398 0.104
 5G-6 0.376 0.113
 5G-8 0.398 0.130
 5G-9 0.428 0.114
 5G-11 0.354 0.123
 5G-13 0.344 0.091
 5G-14 0.406 0.091

5 5GS-19 0.364 0.078
 sand lenses from within 5 gvl

6 6G-10 0.396 0.083
 6G-11 0.398 0.094
 6G-15 0.392 0.124
 6G-17 0.378 0.082
 6G-23 0.398 0.138
 6G-24 0.422 0.140
 6G-26 0.448 0.105
 6G-29 0.402 0.127
 6G-30 0.416 0.135

Appendix E. Petrology of each sample per facies..

A = carbonates, cherty limestone; B = quartzite; C = chert, sandstone, siltstone, shale, and coal.

Facies	Sample Number	A	B	C
1	1-2	94.9	2.8	2.3
	1-3	83.0	10.2	6.8
	1-4	80.0	12.8	7.3
	1-5	92.5	2.5	5.0
	1-6	93.1	1.3	5.6
	1-7	86.5	8.1	5.4
	1-8	98.2	0	1.8
	1-9	78.2	9.0	12.8
	1-10	92.2	1.7	6.1
	1-11	90.3	3.5	6.2
	1-12	78.1	11.5	10.4
	1-13	82.0	10.5	7.5
2	2-2	78.0	12.9	9.1
	2-3	79.1	13.7	7.2
	2-4	74.3	14.5	11.2
	2-5	75.6	12.8	11.7
	2-7	69.8	19.0	11.2
	2-8	80.7	10.8	8.5
	2-9	77.0	10.5	12.6
	2-10	76.2	12.7	11.1
	2-11	86.0	6.1	7.9
	2-12	86.6	4.1	9.3
	2-13	80.6	11.2	8.2
3 thin	3-5	69.9	14.5	15.6
	3-6	63.9	14.2	21.9
	3-10	78.5	9.4	12.0
	3-11	68.4	16.4	15.2
	3-12	60.8	15.1	24.1
	3-14	74.1	12.4	13.5
	3-15	77.0	10.5	12.5
	3-21	64.5	9.6	25.9
	3-26	75.4	9.3	15.3
	3-29	60.9	8.4	30.7
	3-30	61.8	6.5	31.8
	3-32	65.1	13.2	21.7
3 thick	3-7	77.1	3.3	19.5
	3-8	74.7	11.8	13.5
	3-9	74.2	11.6	14.3
	3-16	77.8	10.6	11.6
	3-22	62.4	8.7	28.9

Facies	Sample Number	A	B	C
	3-24	61.8	15.1	23.0
	3-28	68.9	11.8	19.3
	3-33	72.8	7.6	19.6
	3-34	53.6	8.3	38.1
	3-35	80.1	9.0	10.9
3 thick	3-36	81.4	7.1	11.4
	3-37	79.0	12.5	8.6
	3-38	82.9	7.5	9.5
	3-39	84.6	5.7	9.7
	3-40	85.9	7.7	6.4
	3-41	77.2	7.9	14.9
	3-42	67.0	5.6	27.4
4 thin	4-1	82.9	8.8	8.3
	4-2	70.7	12.9	16.4
	4-3	71.1	10.1	18.8
	4-4	73.2	11.1	15.7
	4-5	62.7	11.4	25.9
	4-15	61.3	12.0	26.7
	4-16	66.5	9.3	24.3
	4-17	62.9	9.7	27.4
	4-30	73.9	7.4	18.7
	4-33	75.2	7.0	17.8
	4-34	77.3	6.8	15.9
	4-35	78.6	4.4	17.0
	4-36	71.5	10.1	18.4
	4-37	66.5	12.8	20.7
	4-38	65.0	9.8	25.2
4 thick	4-12	65.4	12.9	21.8
	4-13	65.2	10.0	24.9
	4-14	61.9	8.6	29.5
	4-18	66.5	9.6	23.9
	4-19	62.2	8.9	29.0
	4-21	60.8	14.6	24.6
	4-22	62.2	10.6	27.2
	4-23	71.2	8.5	20.3
	4-24	71.3	9.3	19.3
	4-25	60.7	19.7	19.7
	4-26	63.8	11.2	25.0
	4-28	68.8	14.1	17.2
	4-29	77.1	8.3	14.6
5 dia	5D-1	67.6	12.9	19.5
	5D-2	66.0	9.7	24.3
	5D-3	69.1	5.8	25.2
	5D-4	63.8	11.7	24.5

Facies	Sample Number	A	B	C
	5D-5	67.8	7.6	24.6
	5D-6	60.5	12.0	27.6
	5D-7	86.4	2.0	11.6
	5D-8	77.2	5.4	17.4
	5D-9	68.3	10.6	21.1
	5D-10	72.1	9.7	18.1
	5D-11	74.0	8.9	17.2
	5D-12	66.7	10.5	22.9
	5D-13	68.0	12.4	19.7
5 dia	5D-14	64.9	13.5	21.6
	5D-15	62.7	10.0	27.3
5 gvl	5G-1	60.3	20.1	19.6
	5G-2	68.3	11.8	19.9
	5G-3	75.9	9.2	14.9
	5G-4	71.7	18.9	9.4
	5G-5	64.0	17.5	18.5
	5G-6	75.6	16.1	8.2
	5G-8	63.9	15.7	20.4
	5G-9	71.4	4.6	24.0
	5G-10	65.0	6.2	28.9
	5G-11	67.5	6.3	26.3
	5G-12	74.7	7.1	18.1
	5G-13	58.6	10.4	31.1
	5G-14	64.8	5.6	29.6
	5GS-19	57.3	10.9	31.9
	5G-21	62.9	18.2	18.8
	5G-24	65.0	9.3	25.8
6	6G-1	82.3	4.4	13.3
	6G-3	68.1	7.1	24.8
	6G-4	74.7	7.6	17.7
	6G-6	79.1	7.1	13.8
	6G-7	83.5	6.2	10.4
	6G-9	73.9	3.6	22.6
	6G-10	72.8	13.0	14.1
	6G-11	62.7	25.4	11.8
	6G-12	54.1	26.0	19.9
	6G-13	69.0	16.9	14.1
	6G-14	79.1	2.7	18.2
	6G-15	78.8	2.7	18.5
	6G-23	64.4	7.5	28.1
	6G-24	72.3	9.3	18.5
	6G-28	42.2	14.4	43.4
	6G-29	50.4	14.1	35.5
	6G-30	49.8	6.8	43.4
	6G-31	54.9	9.8	35.3

Facies	Sample Number	A	B	C
6a	6G-16	93.8	2.3	3.9
	6G-20	99.3	0.0	0.7
	6G-25	96.8	0.7	2.6
	6G-26	95.7	0.5	3.8
7	7G-4	78.9	3.8	17.3
	7G-5	67.7	12.0	20.3

Appendix F. Facies locations throughout study area.

Facies	Outcrops where facies is present
1	Fireside
2	Anthracite subsection A2, Powerhouse subsection A1
3	Anthracite; Cascade outcrops C1, C2, C3; Johnson Lake outcrops JL3, JL4, JL5; Powerhouse.
4	Anthracite; Canmore; Carrot Creek; Cascade outcrops C2, C6, C7, C8; Cougar Creek; Johnson Lake outcrops JL1, JL2, JL6; Powerhouse.
5	Canmore; Carrot Creek; Cascade outcrops C2, C6, C7, C8; Dead Elk; Johnson Lake outcrops JL2, JL4, JL5.
6	Anthracite; Canmore; Carrot Creek; Cascade outcrop C1; Cougar Creek; Johnson Lake outcrops JL1, JL3; Powerhouse.
7	Anthracite subsection A1.

Appendix G.

Diamicton Pebble Fabrics


50 clasts were sampled at each site, N=50.

Facies	Upper, Middle, Lower posi- tion	Meters above lower contact	Meters below upper contact	Eigenvectors		Eigenvalue N	Plunge directions column
				Trend	Plunge		
1	M	?	2	16.7	36.7	0.6507	U
				335.1	32.6	0.2450	
				93.3	36.5	0.1043	
1	M	?	6.5	265.6	27.6	0.5230	U
				166.0	17.6	0.3028	
				47.5	56.4	0.1742	
1	M	?	6.5	262.0	12.7	0.5604	U
				353.2	5.1	0.2958	
				104.5	76.3	0.1438	
1	M	?	6.5	241.5	20.4	0.5190	U
				148.1	9.0	0.2496	
				35.5	67.5	0.2314	
1	M	?	6.5	149.5	4.7	0.4815	T to
				243.3	38.9	0.3074	
				53.8	50.8	0.2111	
2	U	26	-1	291.9	12.8	0.6818	U
				23.8	8.3	0.2457	
				146.2	74.7	0.0725	
2	U	22	-1	349.1	18.4	0.6297	T away
				254.9	12.5	0.2492	
				132.6	67.5	0.1211	
2	M	13	-12	92.5	2.2	0.7658	D
				183.7	29.0	0.1363	
				358.4	60.9	0.0979	
2	M	15	-8	337.6	28.8	0.7164	T away
				75.6	14.2	0.1935	
				188.8	57.3	0.0901	
2	L	1	-22	158.3	20.4	0.6949	T to
				249.8	3.9	0.2208	
				350.2	69.2	0.0842	

3	U	6	THIN 1	256.3 166.2 49.2	4.2 2.1 85.3	0.6609 0.2644 0.0747	U
3	U	2	-2	68.0 161.0 320.9	7.3 22.2 66.5	0.6123 0.2014 0.1863	D
3	M	-4	THIN -4	279.8 23.0 176.0	13.9 42.8 43.9	0.7830 0.1423 0.0747	U
3	M	5	3	56.3 146.3 325.3	0.1 7.8 82.2	0.5851 0.3155 0.0993	Chaos (to)
3	M	3	6	131.1 28.8 222.1	3.5 74.0 16.6	0.5879 0.2157 0.1964	D
3	M	2.5	1.5	291.9 24.8 172.3	9.8 16.5 70.6	0.5290 0.2894 0.1816	U
3	M	7	2.5	255.5 151.6 5.5	17.4 37.3 47.3	0.5042 0.3151 0.1807	T away
3	L	1	2*	178.5 268.6 65.0	1.0 2.4 87.4	0.5153 0.3548 0.1299	T to
3	L	2	5	211.8 121.8 24.2	3.1 0.4 86.9	0.5567 0.3080 0.1353	T to
3L	I	6	6	206.0 299.4 66.6	15.4 12.4 70.0	0.5403 0.3865 0.0732	U (chaos)

3	U	25	THICK		271.2	5.9	0.7635	U
			1		181.1	1.1	0.1687	
					81.1	84.0	0.0678	
3	U	34	2		279.5	1.5	0.5843	U
					9.7	8.8	0.3102	
					177.3	83.0	0.1055	
3	U	34	2		338.2	10.3	0.5624	T away
					70.5	12.7	0.2777	
					210.4	73.5	0.1599	
3	U	25	6		123.3	0.9	0.5948	U girdle
					214.2	45.9	0.3293	
					32.4	44.0	0.0759	
3	M	12	THICK 14		251.7	16.3	0.6329	U
					346.7	16.6	0.2263	
					119.7	66.4	0.1408	
3	M	7	1		35.5	21.4	0.6526	T to
					301.2	10.8	0.2812	
					186.2	65.7	0.0662	
3	M	6	16		62.0	15.7	0.7109	D
					330.7	4.4	0.2120	
					225.3	73.7	0.0771	
3	M	24	12		284.1	14.5	0.5806	U
					16.8	10.7	0.2917	
					142.0	71.9	0.1276	
3	M	26	10		299.7	9.1	0.7452	U
					31.0	7.8	0.1879	
					160.7	78.0	0.0668	
3	M	18	12		98.8	1.9	0.4727	D
					8.5	8.9	0.3462	
					200.4	80.9	0.1811	
3	M	7	1.5		2.3	12.5	0.5856	T to
					94.2	8.8	0.3153	
					218.5	74.7	0.0991	
3	L	1	22		59.3	12.1	0.5110	D (chaos)
					327.8	6.9	0.4008	
					208.7	76.1	0.0882	
3	L	3	23		252.5	10.8	0.5340	U (chaos)
					345.5	15.3	0.3645	
					128.5	71.1	0.1016	
3	L	1	5		160.5	1.6	0.4944	D (chaos)
					70.5	13.1	0.3665	
					257.7	76.8	0.1391	

THIN							
4	U	0.5	1	140.2 49.7 257.5	3.9 7.5 81.6	0.5098 0.3803 0.1099	D
4	U	1.5	1.5	349.4 259.4 84.2	0.6 6.9 83.1	0.6547 0.2370 0.1082	H
4	M	1	1.3	296.4 29.5 132.7	25.6 6.5 63.4	0.4982 0.3345 0.1673	U
4	M	1.5	1.5	136.7 228.7 33.0	5.4 21.0 68.3	0.6236 0.2726 0.1039	D
4	M	2	2	141.0 50.5 234.6	1.3 20.3 69.6	0.5619 0.3091 0.1289	D
4	M	2	2	151.6 61.1 243.4	1.0 28.9 61.0	0.5816 0.2702 0.1482	D
4	M	3	3	348.9 52.8 202.2	10.7 19.8 67.3	0.6113 0.2602 0.1285	U

THICK							
4	U	29	3	269.4 1.1 159.9	5.9 16.1 72.8	0.7879 0.1257 0.0865	U
4	U	28	2.5	295.0 32.5 194.8	8.9 39.9 48.7	0.7056 0.1880 0.1064	U
4	M?	?	?	271.6 180.7 49.2	7.6 6.8 79.8	0.7353 0.1969 0.0678	U
4	M?	?	?	264.6 3.9 160.2	11.8 37.7 49.9	0.5555 0.3099 0.1347	U
4	M?	?	?	278.5 34.6 167.5	25.7 42.5 36.6	0.7174 0.1685 0.1141	U
4	M?		3	329.1 61.4 182.6	14.2 8.9 73.1	0.6192 0.2701 0.1106	U oblique
4	M?	?	4	87.8 180.3 313.3	12.0 11.7 73.1	0.6049 0.2915 0.1036	D
4	L	1	28	173.4 264.0 74.8	2.3 15.0 74.8	0.6002 0.3256 0.0742	T to

5	M	5	5	105.5	16.2	0.8019	D
				199.9	14.8	0.1763	
				330.1	67.2	0.0218	
5	?	2	1	308.2	8.1	0.5482	U
				213.8	27.7	0.3059	
				53.0	60.9	0.1459	
5	M	7	4	286.7	13.3	0.6696	U
				17.8 4.4	0.1846		
				125.8	76.0	0.1458	
5	M	1.5	1	154.7	1.8	0.5364	D
				244.9	6.2	0.9421	
				48.8 83.5	0.1214		
5	?	2	6	78.2 11.6	0.4678	T to	
				174.7	28.6	0.3651	
				328.6	58.7	0.1671	
5 GRAVEL				205.4	18.3	0.5094	
				307.4	32.1	0.2797	
				90.4 51.9	0.2109		
7	U			248.3	4.0	0.5846	??
				157.7	8.2	0.2943	
				4.2 80.9	0.1211		

Explanations to plunge directions column

Plunge direction of major alignment.

U = Upvalley plunge

D = Downvalley plunge

T = Transverse to valley trend, either toward (to) or away (away) from valley center

Chaos = no predominant trend (low S values)

H = No plunge.